UNIVERSIDAD DE MURCIA

ESCUELA INTERNACIONAL DE DOCTORADO

Study of Inflammasome Activation in Autoinflammatory Diseases and Tendinopathies

Estudio de la Activación del Inflamasoma en Enfermedades Autoinflamatorias y Tendinopatías

D. Alejandro Eleazar Peñín Franch

2022

AGRADECIMIENTOS

En primer lugar, me gustaría a agradecerle a mi director Pablo Pelegrín, la confianza depositada en mí, tanto al comienzo seleccionándome de entre los demás candidatos para la realización de este proyecto, como a lo largo de estos años. Gracias por enseñarme tanto, en una etapa que seguro no olvidaré.

A las empresas Prim y MVClinics, por financiar parte de mi contrato y darme la posibilidad de desarrollar esta tesis. En concreto, agradecer a Fermín Valera y Francisco Minaya de MVClinics, su dedicación en este proyecto y su consejo durante las diferentes reuniones desarrolladas.

A mis tutores, Pedro Aparicio al comienzo, y Trinidad Hernández en este último año, por su ayuda a lo largo del desarrollo de esta tesis doctoral.

A mis compañeros de laboratorio, a los que estáis, Ana I., Laura, Cristina M., Julio, Adrián, Malvina, Mari Carmen, Diego, Curro, Alberto y Santi, y a los que no, Carlos, Ana T., Cristina A., Helios, y Fernando, gracias por vuestra ayuda, consejo y apoyo durante estos años.

A la plataforma de patología del IMIB, en especial a Carlos Manuel, por su ayuda, sus consejos, y por siempre recibirme con una sonrisa. Gracias por todos esos momentos tan divertidos que hemos pasado.

A todos los colaboradores que han participado en el desarrollo de este proyecto. Primero, a los miembros del grupo de Fisioterapia y Discapacidad del IMIB, en concreto a José Antonio García, Pilar Escolar y Francesc Medina, por su implicación, su ayuda y su guía a lo largo del proyecto. También al Dr. Juan Manuel Bueno y a Rosa María Martínez del Laboratorio de Óptica de la Universidad de Murcia, por su ayuda en las medidas de microscopia de segundo armónico. Al Dr. Antonio José Ortiz, vicedecano de Odontología de la Universidad de Murcia, por su ayuda con las medidas de tensión del tendón de Aquiles de ratón. Por último, al Dr. Juan Ignacio Arostegui por la colaboración establecida con su laboratorio durante el análisis de muestras de pacientes con enfermedades autoinflamatorias, permitiéndome involucrarme en diversos trabajos centrados en el estudio de NLRC4.

Al profesor Sahil Adriouch de la Universidad de Rouen (Francia) por permitirme trabajar y formar parte de un grupo maravilloso, además de realizar un proyecto que me

aportó muchos nuevos conocimientos. Gracias por acogerme de una manera tan afectiva, especialmente fuera del laboratorio.

Gracias a todos los miembros del grupo, Romain Hardet, Mélanie Demeules, Marine Blandin, Henri Gondé, Gaétan Riou, y Allan Scarpitta, por ayudarme cada día en el laboratorio, y, sobre todo, por integrarme como uno más de vosotros. Gracias a todos, junto a Élise y Audrey, por tantos momentos felices y por todas esas tardes que nos hicieron sentir como en casa.

En especial, gracias Romain por tu disponibilidad y tu paciencia para cada cosa que he necesitado durante mi estancia, has sido un gran apoyo durante esta etapa. También gracias a Allan, mi “gasdermin couple”, por tu ayuda a lo largo del proyecto y por tantos momentos divertidos que hemos compartido.

A Laura, Cristina M. y Julio, por formar un grupo de “predocs” que nos hemos ayudado y apoyado en todo momento, dentro y fuera del laboratorio.

A Cristina A., Carlos, Ana T. y Ana I. por ayudarme a adaptarme en el laboratorio y acogerme cuando llegué. Gracias por incluirme como uno más de vosotros, aunque fui el último en llegar, y en especial por vuestro apoyo, consejo y cariño.

A mis amigos de Crevillente, Elche, Murcia y Rouen por hacer que estos años de esfuerzo y sacrificio hayan sido más fáciles y más llevaderos.

A mi familia, por todo el apoyo y el cariño que me habéis dado desde siempre, y en especial en esta etapa. A mi hermano, que hasta en los momentos más difíciles ha conseguido sacarme una sonrisa.

Finalmente, quiero dar las gracias a Inmaculada, por haberme aguantado en los momentos de estrés, por haberme aconsejado en los momentos de incertidumbre, por haberme querido en los momentos difíciles, y por haberme apoyado y animado en los momentos de debilidad. Sin ti esta tesis no habría sido posible.

“Estudia las frases que parecen ciertas y ponlas en duda.”

David Riesman

INDEX

INDEX OF FIGURES

INDEX OF TABLES

ABBREVIATIONS

2-APB	2-aminoethyl diphenyl borinate
ADCC	Antibody-dependent cellular cytotoxicity
AGS	Aicardi-Goutières syndrome
AIDs	Autoinflammatory diseases
AIM2	Absent in melanoma 2
ALR	AIM2-like receptor
AP-1	Activator protein-1
APCs	Antigen presenting cells
APLAID	Autoinflammation and PLCG2- associated antibody deficiency and immune dysregulation
APP	Acute phase proteins
ASC	Apoptosis-associated speck-like protein containing a caspase-recruitment domain
ATP	Adenosine triphosphate
BIR	Baculovirus inhibitor of apoptosis repeat
BRCC3	Lys63-specific deubiquitinase BRCC36
BRET	Bioluminescent resonance energy transfer
BSA	Bovine serum albumin
CANDLE	Chronic atypical neutrophilic dermatosis with lipodystrophy and elevated temperature
CAPS	Cryopyrin-associated periodic syndrome
CARD	Caspase recruitment domain
CCL	Chemokine ligand
cDCs	Conventional dendritic cells
CIITA	MHC-class II transactivator
CLRs	C-type lectin receptors
COVID-19	Coronavirus disease 2019
COX	Cyclooxygenase
CRP	C-reactive protein
CXCL	C-X-C motif chemokine ligand
DAB	3-3'-diaminobenzidine
DADA2	Deficiency of adenosine deaminase 2
DAMPs	Damage-associated molecular patterns

DD	Death domain
DEAD	Asp-Glu-Ala-Asp
DIRA	Deficiency of IL-1Ra
DITRA	Deficiency of IL-36Ra
DMSO	Dimethyl sulfoxide
DPP	Dipeptidyl peptidase
DUBs	Deubiquitinase enzymes
ECL	Enhanced chemiluminescence
ECM	Extracellular matrix
EDTA	Ethylenediaminetetraacetic acid
ELISA	Enzyme-linked immunosorbent assay
EP4	Prostaglandin E2 receptor 4
ERK	Extracellular signal regulated kinase
ESCRT	Endosomal sorting complexes required for transport
ESWT	Extracorporeal shockwave therapy
FCAS	Familial cold autoinflammatory syndrome
FCS	Fetal calf serum
FIIND	Functional-to-find domain
FMF	Familial Mediterranean fever
GM-CSF	Granulocyte-macrophage colony-stimulating factor
GoF	Gain-of-function
GPCRs	G-protein-coupled receptors
GSDMB	Gasdermin-B
GSDMD	Gasdermin-D
$GSDMD^{NT}$	N-terminal domain of gasdermin-D
HA20	Haploinsufficiency of A20
HAMPs	Homeostasis-altering molecular processes
HD	Helical domain
HIN	Hematopoietic interferon-inducible nuclear
HMGB1	High mobility group box 1
HSP	Heat shock protein
HSR	Heavy slow resistance
IFN	Interferon
IG	Immunoglobulin
IKK	IκB kinase

IL	Interleukin
IL-10R1	IL-10 receptor 1
IL-18BP	IL-18 binding protein
IL-1R6	IL-36 receptor
IL-1Ra	IL-1 receptor antagonist
IL-1RAcP	IL-1 receptor accessory protein
IL-36Ra	IL-36 receptor antagonist
IL-6R	IL-6 receptor
ILCs	Innate lymphoid cells
ILRs	IL-1 receptors
INT	Iodotetrazodium chloride
IPS-1	IFN-β-promoter stimulator 1
IRAK	IL-1R-associated kinase
IRF	IFN-regulatory factor
JNK	c-Jun N-terminal kinase
LAP	Latency-associated peptide
LB	Luria-Bertani
LDH	Lactate dehydrogenase
LFn-FlaA	Flagellin A lethal factor
LPS	Lypopolysacharide
LRRK2	LRR kinase-2
LRRs	Leucine-reach repeats
LTA	Lipoteichoic acid
MAPKs	Mitogen-activated protein kinases
MAS	Macrophage activation syndrome
M-CSF	Macrophage colony-stimulating factor
MD-2	Myeloid differentiation factor-2
MDA5	Melanoma differentiation-associated gene 5
MDP	Muramyl-dipeptide
MHC	Major histocompatibility complex
MKD	Mevalonate kinase deficiency
MMPs	Metalloproteinases
MNS	3,4-methylenedioxy-beta-nitrostyrene
MWS	Muckle-Wells syndrome
NACHT	NAIP, CIITA, HET-E, and TP-1

NAIP	NLR family apoptosis inhibitory protein
NBD	Nucleotide-binding and oligomerization domain
NEK7	NIMA-related kinase 7
NEMO	NF-κB essential modulator
NETs	Neutrophilic extracellular traps
NF-κB	Nuclear factor kappa B
NIK	NF-κB inducing kinase
NIMA	Never in mitosis gene a
NK	Natural killer
NLRC	NLR CARD-containing
NLRP	NLR protein
NLRs	NOD-like receptors
NOD	Nucleotide binding oligomerization domain
NOMID	Neonatal-onset multisystem inflammatory disease
NSAIDs	Non-steroidal anti-inflammatory drugs
oxPAPC	Oxidized phospholipids
P/S	Penicillin and streptomycin
PA	Protective antigen
PAAND	Pyrin-associated autoinflammation with neutrophilic dermatitis
PAMPs	Pathogen-associated molecular patterns
PAPA	Pyogenic arthritis with pyoderma gangrenosum and acne
PBMCs	Peripheral blood mononuclear cells
PBS	Phosphate-buffered saline
pDCs	Plasmacytoid dendritic cells
PG	Prostaglandin
PKCδ	δ isoform of protein kinase C
PLAID	PLCG2- associated antibody deficiency and immune dysregulation
PLCG2	Phospholipase C gamma 2
PMNs	Polymorphonuclear neutrophilic leucocytes
PRAAS	Proteasome-associated autoinflammatory syndrome
PRP	Platelet-rich plasma
PRRs	Pattern recognition receptors
PYD	Pyrin domain

RIG	Retinoic-acid inducible gene
RIP	Receptor interacting protein
RLRs	Retinoic acid-inducible gene (RIG)-I-like receptors
RLR-3	Rig-I-like receptor 3
ROS	Reactive oxygen species
RT	Room temperature
SAA	Serum amyloid A
SAP130	Spliceosome-associated protein 130
SAVI	STING-associated vasculopathy of infancy
SpeB	*Streptococcal pyrogenic* endotoxin B
SPF	Specific pathogen free
T3SS	Type III secretion system
TACE	TNF-alpha converting enzyme
TAK1	TGF-β-activated kinase 1
TBS	Tris-buffered saline
TEMED	Tetramethylethylenediamine
TGF	Tumor growth factor
TGF-βR	TGF-β receptor
TIR	Toll/IL-1R homology
TIRAP	TIR adaptor protein
TLRs	Toll-like receptors
TMB	3,3',5,5'-tetramethybenzidine
TNF	Tumor necrosis factor
TNFR	TNF receptor
TRADD	TNFR-associated death domain
TRAF	TNFR-associated factor
TRAIL	Tumor necrosis factor-related apoptosis-inducing ligand
TRAM	TRIF-related adaptor molecule
TRAPS	TNF receptor-associated periodic syndrome
TRIF	TIR domain-containing adaptor inducing IFN-β
TXNIP	Thioredoxin-interacting protein
USP	Ubiquitin specific protease
VbP	Val-boro-Pro
VEGF	Vascular endothelial growth factor
WHD	Winged helix domain

INTRODUCTION

1. Innate immune system and the inflammatory response

1.1. General introduction

Defense against injury and pathogens are primary mediated by the innate immune system by inducing an acute inflammatory response triggered by the presence of microbes or molecules derived from tissue damage (Akira et al., 2006; Beutler et al., 2006). The innate immune system is composed of several specific cells that recognize pathogens and molecules associated to damaged tissues by cell-associated receptors and release a number of signaling proteins called cytokines. Besides these specific cells, three additional primary innate immune defenses are present in mammals, grouped in (i) mechanical barriers like skin and epithelial cells joined by tight junctions, movements of cilia or tears; (ii) chemical barriers like low pH, lysozymes or fatty acids; and (iii) microbiological barriers with the normal host-related microbiota that competes against microbial pathogens (Murphy & Weaver, 2017; Yeretssian et al., 2008).

After the action of these immediate innate barriers, the induced innate immune response begins. The induced immune innate defenses are composed of the complement system and the activation of innate immune cells, lead to the release of cytokines and chemokines (Brubaker et al., 2015). The release of pro-inflammatory cytokines and chemokines are responsible of the migration, the recruitment and the activation of more immune cells to the site of the infection or tissue injury, that will amplify the innate immune response and will initiate the adaptative immune response (Said-Sadier & Ojcius, 2012).

1.2. Innate immune cells

Innate immune cells are mainly white blood cells that mediate innate immunity and include mainly cells with phagocytic activity that are able to engulf damaged cells and microbes to trigger inflammatory responses. The main classes of phagocytic cells are macrophages and monocytes, granulocytes and dendritic cells, being the macrophages the major phagocytic population resident in tissues at homeostasis. The second major family of phagocytes are the granulocytes, also known as polymorphonuclear neutrophilic leucocytes (PMNs). The third class of phagocytes are the dendritic cells that can be divided into two main functional types, conventional dendritic cells (cDCs) and plasmacytoid dendritic cells (pDCs). But there are also another kind of innate immune cells without phagocytic activity such as Langerhans cells, mast cells, innate lymphoid cells (ILCs), and natural killer cells

(Murphy & Weaver, 2017; Newton & Dixit, 2012). Next, we will describe the main different innate immune cells:

Natural killer cells

Natural killer (NK) cells belong to a specific and reduced group of lymphocytes called ILCs that are considered to be members of innate immune system. NK cells are cytotoxic cells that induce the cell death of compromised cells first by receptors recognition of molecules on the surface of infected or malignant cells and after, by the releasing of their cytotoxic granules, including granzymes and perforins. In order to distinguish between healthy and infected or damaged cells, NK cells express activating and inhibitory receptors. The overall balance between these receptors determines whether an NK cell engages and kills a target cell (Murphy & Weaver, 2017).

The activating receptors on the NK cells are able to detect changes in expression of a various surface proteins on a target cell. These changes can be induced by cellular stress signals like metabolic stress or DNA damage. Once NK cell recognizes an infected cell expressing activating receptors, perforins are released to induce membrane pores in the target cell and after, granzymes released enter into the cell to induce its death. This mechanism is dependent on the binding of antibodies to the Fc receptor present in NK cells, and this known as antibody-dependent cellular cytotoxicity (ADCC) (Ochoa et al., 2017; Prager et al., 2019). Also, NK cells or cytotoxic T lymphocytes can induce pyroptotic cell death of gasdermin B (GSDMB)-positive cells. The induction of pyroptosis results from the cleavage of GSDMB by lymphocyte-derived granzyme A, triggering its pore-forming activity. Interestingly, interferon (IFN)-γ up-regulates GSDMB expression and promotes granzyme A induced pyroptosis (Zhou et al., 2020).

On the other hand, inhibitory receptors on NK cells identify surface molecules that are constitutively expressed at high levels by most healthy cells, like major histocompatibility complex (MHC)-class I molecules. The higher the number of MHC-class I molecules present in the surface of the cell, the better is the cell protected against NK cells attack. MHC-class I molecules can be downregulated in cells that are infected by virus or other intracellular pathogens (Ganesan & Hoglund, 2021; Karre, 2002).

Dendritic cells

The discovery of dendritic cells supposed the Nobel Prize in 2011. After their discovery several studies have stablished a correlation between DCs and immune responses against

allografts, pathogens, or cancer cells, as well as in the maintenance of self-tolerance (Cabeza-Cabrerizo et al., 2021). The main function of these cells is to phagocyte particulate matter present on the tissues and ingest high amounts of the extracellular fluid and its contests by micropinocytosis (Swanson & Watts, 1995), and to perform their function DCs need to be activated mainly by the recognition of pathogen-associated molecular patterns (PAMPs) or damage-associated molecular patterns (DAMPs) through PRRs (Kratky et al., 2011). After their activation, DCs process ingested particles in order to generate peptide antigens to act like antigen-presenting cells (APCs) inducing the adaptive immune response by activating several kinds of specific lymphocytes such as T cells or B cells by cell-cell interactions (Cabeza-Cabrerizo et al., 2021; Pasqual et al., 2018). DCs have also an important role as regulators of the innate immune system, due to their ability for example to induce NK cell cytotoxicity and proliferation by a combination of cell-cell interactions and the release of soluble cytokines (Viaud et al., 2009).

Normally, immature DC migrate through the bloodstream from the bone-marrow to the tissues, but immature dendritic cells are not the unique cells that can differentiate to mature DCs. Human monocytes cultured *in vitro* with granulocyte-macrophage colony-stimulating factor (GM-CSF) and IL-4 can give rise to DC-like cells and also mouse monocytes can result in DC-like cells during inflammation *in vivo* (Randolph et al., 1998).

Granulocytes

Granulocytes cells include basophils, eosinophils and neutrophils, being the neutrophils the cells with the greatest phagocytic activity, more abundant and the cells most immediately involved in innate immunity. Granulocytes are characterized by densely stained granules that can be released to the extracellular space upon stimulation, and these granules contain both molecules to kill microorganisms and soluble mediators such as cytokines. Their maturation occurs in the bone-marrow and they are released fully differentiated into the bloodstream during their short life (Farahi et al., 2012; Pillay et al., 2010). Granulocytes migrate from the circulation into the tissues in response to chemoattractants, and become fully active after stimulation by cytokines and/or molecules derived from pathogens or damaged cells (Mantovani et al., 2011). Under physiological conditions granulocytes die by both intrinsic or extrinsic apoptosis. Intrinsic apoptosis occurs in the absence of pro-survival factors and by activation of caspase-8 (Conus et al., 2008), and extrinsic apoptosis by the cross-linking of death receptors such as Fas ligation (Simon, 2009). Apoptotic granulocytes are cleared by phagocytosis from macrophages, but also apoptotic granulocytes that are not cleared by macrophages at the right time undergo

secondary necrosis and can trigger inflammatory responses. Under pathological conditions granulocytes may undergo secondary necrosis due to the exposure to bacterial or other toxins (Geering et al., 2013).

Basophils and eosinophils are less abundant compared with neutrophils, but they can also induce inflammatory responses through the release of their granules. Basophils and eosinophils are important mainly in the defense against parasites that are too big to be engulfed by macrophages or neutrophils (Murphy & Weaver, 2017). Eosinophils are effector cells implicated in the protection against helminth infections and, after activation eosinophils degranulates and release pro-inflammatory mediators and toxic proteins which might cause tissue damage, but also commit the viability of helminths (Kobayashi et al., 2010). Basophils can also contribute to the Th2 response through the production of IL-4 (Nadif et al., 2013).

Neutrophils are the most abundant granulocytes and have a main role in the innate immune response against infection. They differentiate in the bone-marrow and migrate to the site of inflammation through the blood. Neutrophils recruitment on injured or infected sites is triggered by the secretion of chemokines by activated tissue-resident macrophages. In response to these chemokines, permeability of local blood vessels increases and there is also an induction of the expression of adhesion molecules, such as L-selectin, in the cell surface of endothelial cells, which help neutrophils to extravasate from the circulation (Kolaczkowska & Kubes, 2013). Once they extravasate, neutrophils participate in the resolution of infections or tissue injury by three main mechanisms: phagocytosis, degranulation and NETosis. The phagocytosis is the main function of the neutrophils and is used to engulf and destroy microorganisms in intracellular vesicles using degradative enzymes and other antimicrobial molecules stored in their cytoplasmic granules. Degranulation is the secretion of the cytoplasmic granules into the extracellular space to kill pathogens, and the main enzymes that are present in the neutrophil granules are myeloperoxidase and neutrophil elastase (Kolaczkowska & Kubes, 2013). NETosis is the release of neutrophil extracellular traps (NETs) to trap and neutralize pathogens (**Figure 1**¡Error! No se encuentra el origen de la referencia.). NETs are composed by decondensed chromatin that forms web-like DNA structures coated with nuclear proteins, granule proteins, and cytosolic proteins (Chapman et al., 2019; Petretto et al., 2019). NETosis initiation requires neutrophil activation as resting neutrophils in non-inflammatory conditions do not undergo NETosis (Yipp et al., 2012). In addition, NETosis can be also induced by the presence of cytosolic bacterial lipopolysaccharide (LPS). LPS can activate non-canonical inflammasome activation through its recognition by caspase-11, triggering gasdermin-D

(GSDMD) dependent neutrophil death. GSDMD-dependent death, induces neutrophils to extrude antimicrobial NETs. In addition, caspase-11 and GSDMD are required both for neutrophil plasma membrane rupture during the final stage of NET extrusion, and also for early features of NETosis, including nuclear delobulation and DNA expansion (Chen et al., 2018). Between the receptors that are involved into activation of neutrophils, ligands of G-protein-coupled receptors (GPCRs) (Gupta et al., 2014), tumor necrosis factor (TNF) receptors (Keshari et al., 2012), and Fc receptors (Rossaint et al., 2014) can be found.

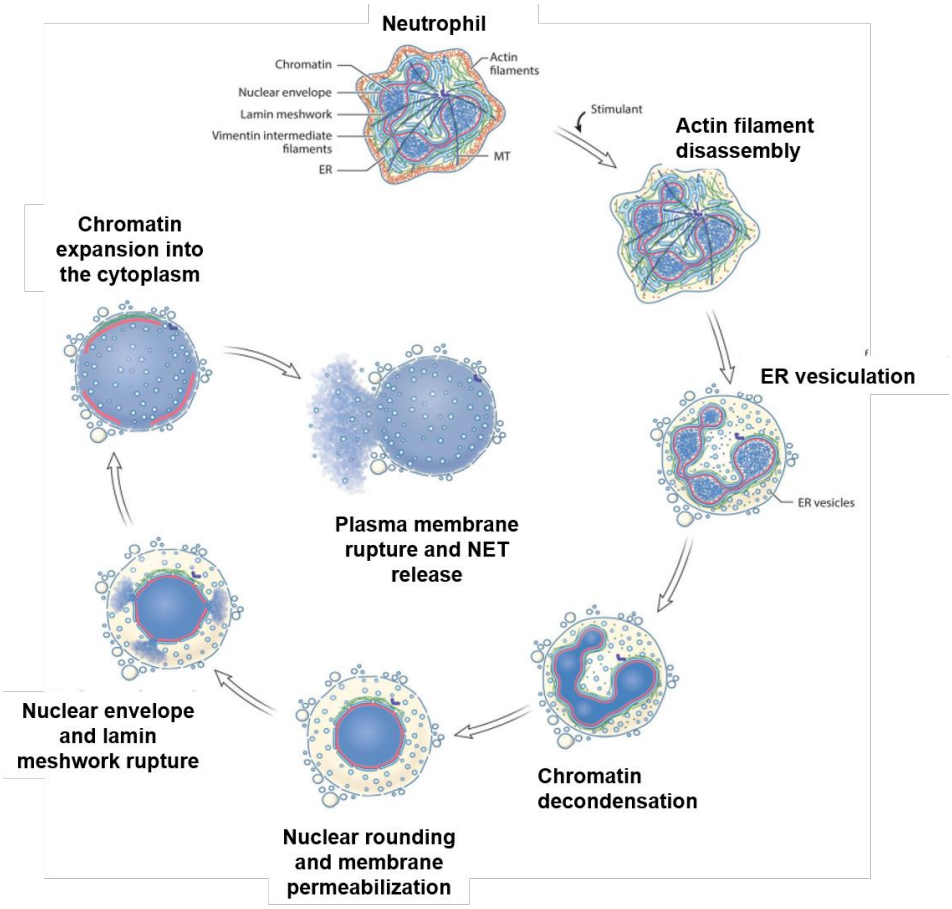

Figure 1. Diagram of cellular events and molecular regulators involved in NETosis. Neutrophil activation leads to plasma membrane rupture and NET formation and release. Adapted from: (Thiam et al., 2020).

After performing their function, neutrophils die by caspase-dependent apoptosis and apoptotic neutrophils are cleared by macrophage phagocytosis, switching the phenotype of the macrophages from pro-inflammatory phenotype to anti-inflammatory phenotype (Rowe et al., 2002).

Monocytes and macrophages

Monocytes are the main population of myeloid cells that circulates in the blood, but are also present in the bone-marrow and the spleen. Monocytes can be subdivided, according

to the expression of CD14 and CD16 present on their surface, into three groups that are: classical ($CD14^{++}CD16^{-}$), intermediate ($CD14^{++}CD16^{+}$), and non-classical ($CD14^{+}CD16^{++}$) monocytes (Hijdra et al., 2013). Monocytes are immune effector cells equipped with chemokine receptors and PRRs and migrate from blood to tissues during inflammation, but also during non-inflammatory conditions to patrol homeostasis of the tissues. During tissue damage, classical monocytes migrate to the injured or infected site to produce cytokines, phagocytose microbes and damaged cells, and after they are able to present antigens through MHC-class II from phagocytosed pathogens to lymphocytes. However, there is controversy regarding the function of non-classical monocytes, is not clear if these cells have an anti-inflammatory or a pro-inflammatory role (Chiu & Bharat, 2016). After extravasation, they differentiate to DCs and macrophages (Serbina et al., 2008; Zaslona et al., 2009).

Tissue-resident macrophages are resident phagocytic cells in lymphoid and non-lymphoid tissues, such as heart, skin, bone, lung, liver, connective tissue, or peritoneum, that have an embryonic origin (Epelman et al., 2014). They are involved in maintaining steady-state tissue homeostasis via the clearance of apoptotic cells, and the production of growth factors. Macrophages possess a broad range of PRRs that make them efficient into the recognition and killing of invading pathogens as well as the recognition of DAMPs (Gordon, 2002). Moreover, macrophages also initiate inflammatory responses by maturation and release of pro-inflammatory cytokines (Shapouri-Moghaddam et al., 2018). Also, they represent around 10 and 15% of the total cell number of quiescent cells, and this number can increase considerably in response to inflammatory stimuli (Italiani & Boraschi, 2014). Two mainly subsets of macrophages can be found regarding its activation, classical activated macrophages or pro-inflammatory macrophages (M1 macrophages) and alternatively activated macrophages or anti-inflammatory macrophages (M2 macrophages), although nowadays is well recognized that a continuum state of macrophages exists from M1 to M2. Exposure of macrophages to IFN-γ, TNF and/or bacterial PAMPs, such as LPS promotes M1 development, whereas exposure to IL-4 and/or IL-13 polarizes macrophages to M2 macrophages (Biswas & Mantovani, 2010; Gundra et al., 2014) (**Figure 2**¡Error! No se encuentra el origen de la referencia.).

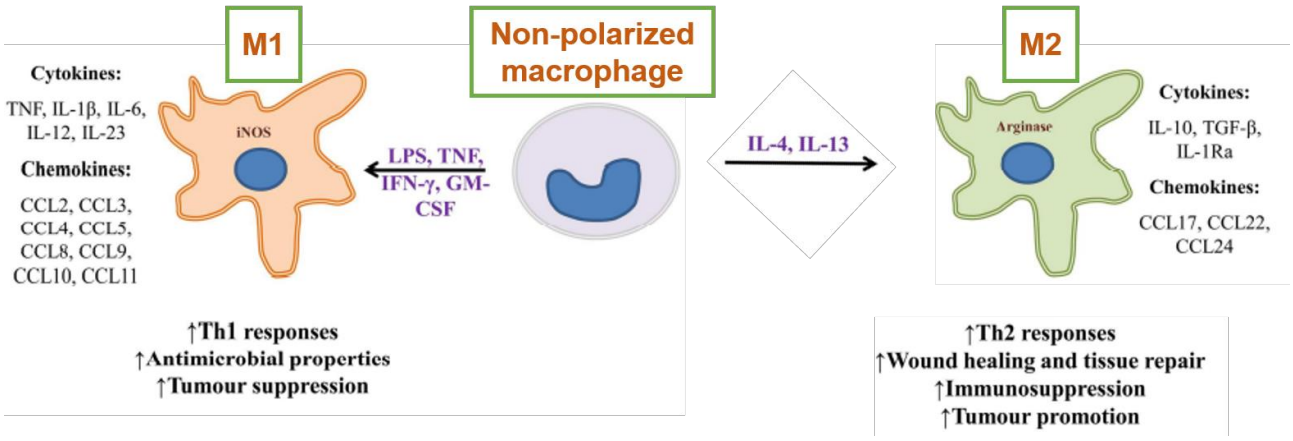

Figure 2. Diagram of macrophage M1 and M2 polarization. In presence of IFN-γ, TNF, LPS or GM-CSF macrophages are polarized to M1 macrophages that induce pro-inflammatory responses, but in presence of IL-4 and/or IL-13 naïve macrophages are polarized to M2 macrophages that induce anti-inflammatory responses. Adapted from: (Arango Duque & Descoteaux, 2014).

M1 macrophages mediate host response against tissue damage and infection after pathogen recognition and their function includes antigen presentation via MHC-class II, initiate the inflammation and recruit other immune cells like granulocytes to the injured or infected site (Chiu & Bharat, 2016). After being activated, M1 macrophages secrete different kinds of pro-inflammatory cytokines being the interleukin (IL)-6, TNF-α, IL-1β and IL-18 the more studied, and also chemokines such as C-X-C motif chemokine ligand (CXCL)-10, chemokine ligand (CCL)-13, CCL-14 or CCL-24 (Martinez et al., 2009).

M2 macrophages mediate anti-inflammatory functions and promote resolution of inflammation. In contrast with M1 macrophages, M2 macrophages release anti-inflammatory cytokines such as IL-10, IL-1 receptor antagonist (IL-1Ra) or tumor growth factor (TGF)-β, and chemokines such as CXCL-1 or IL-8 (Arango Duque & Descoteaux, 2014).

1.3. Pattern recognition receptors

Germline-encoded PRRs are specific receptors of the innate immune system that are responsible for sensing the presence of microorganisms, by sensing PAMPs or endogenous molecules released from damaged cells, called DAMPs. The sensing of this PAMPs and DAMPs by PRRs leads to an upregulation of genes involved in the inflammatory responss such as pro-inflammatory cytokines, type I interferons, chemokines and antimicrobial proteins, as well as proteins involved in the modulation of PRR signaling (Takeuchi & Akira, 2010).

Four different families of PRRs have been identified, including transmembrane receptors as Toll-like receptors (TLRs) and C-type lectin receptors (CLRs), and also

cytoplasmic receptors as Retinoic acid-inducible gene (RIG)-I-like receptors (RLRs) and nucleotide binding oligomerization domain (NOD)-like receptors (NLRs).

TLR receptors

The TLR family is one of the best characterized PRR families with ten members identified in humans and twelve in mice. TLRs are composed by three domains, the N-terminal leucine-rich repeats (LRRs), a central transmembrane region, and a cytoplasmatic C-terminal Toll/IL-1R homology (TIR) domain. TLRs are expressed in a wide variety of cells including innate immune cells such as macrophages and dendritic cells, adaptive immune cells as B cells or some T cells, and also in non-immune cells such as fibroblasts or epithelial cells. TLRs can be located both in the plasma membrane and in endolysosome membrane, being TLR1, TLR2, TLR4, TLR5, TLR6 and TRL11 in the plasma membrane, and TLR3, TLR7, TLR8, TLR9 and TRL10 in the endolysosome membrane.

TLR2 is able to sense components from bacteria, mycoplasma, fungi, and viruses. TLR2 forms a heterodimer with TLR1 or TLR6 to recognize its ligands by forming M-shaped structures that are able to interact with the ligands in its internal pockets (Jin et al., 2007). The activation of TLR2 by its ligands lead to the production of pro-inflammatory cytokines in macrophages or dendritic cells in response to bacterial ligands, and to type I IFNs in response to viral infection (Barbalat et al., 2009).

TLR4 can be activated by a wide variety of ligands. Some DAMPs has been described to activate TLR4, such as heat shock protein (HSP)60 or HSP70 (Asea et al., 2002; Vabulas et al., 2001), heparan sulfate (Brennan et al., 2012), or fibrinogen (Motojima et al., 2010). Furthermore, different PAMPs are also described to activate TLR4, such as mannan (Tada et al., 2002), or flavolipin (Gomi et al., 2002). In addition, TLR4 can also be activated after viral infections, by recognition of viral envelope proteins or DAMPs related with viral infections, as shown for H5N1 avian influenza virus (Imai et al., 2008). However, between all the ligands described to activate this receptor, TLR4 mainly recognize LPS from the outer membrane of Gram-negative bacteria. To recognize LPS, TLR4 forms a heterodimer with myeloid differentiation factor-2 (MD-2) and LPS to induce the formation of an m-shaped receptor homodimer composed of two TLR4/MD-2/LPS complexes that interact symmetrically (Park et al., 2009).

Some TLRs including TLR3, TLR7, TLR8 and TLR9 are able to recognize nucleic acids derived from viruses and bacteria, as well as endogenous nucleic acids in pathogenic conditions (Akira et al., 2006).

There are two different pathways that can be triggered by TLRs, the MyD88-dependent signaling pathway and the TRIF-dependent signaling pathway. MyD88 is composed of a death domain (DD) in addition to a TIR domain, and is essential for the downstream signaling of the major part of the TLRs. TIR domain-containing adaptor inducing IFN-β (TRIF) is also included in the same family of MyD88. Almost every TLR is able to induce MyD88 dependent pathway, being TLR3 the only TLR that induce only TRIF-dependent pathway (Vidya et al., 2018). Interestingly, TLR4 is able to induce both MyD88 or TRIF-dependent signaling pathways. TLR4 requires TIR adaptor protein (TIRAP) for binding to MyD88; and TRIF-related adaptor molecule (TRAM) to bind to TRIF. After activation of MyD88, the pathway involving proteins such as IL-1R-associated kinase (IRAK)-4 and TNFR-associated factor (TRAF) 6, induces the translocation of NF-kB into the nucleus and activates the expression of pro-inflammatory cytokines (Kawagoe et al., 2008). Also, the activation of TRIF triggers the activation of TRAF6, but in this case, to activate IFN-regulatory factor (IRF) 3. IRF3 once phosphorylated translocate to the nucleus resulting in an induction of type I IFNs and expression of IFN-inducible genes (Tenoever et al., 2007) (**Figure 3**).

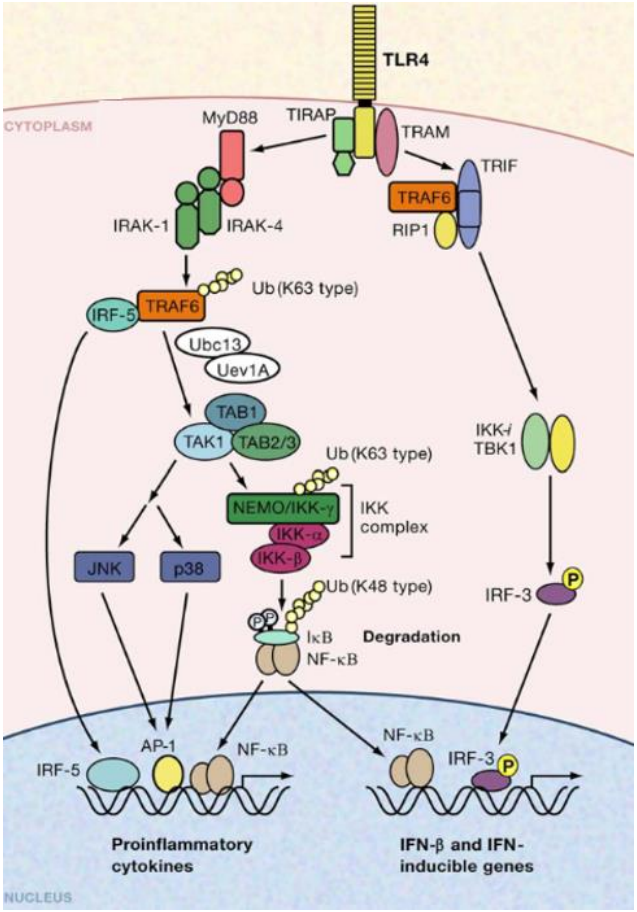

Figure 3. Activation of MyD88 or TRIF-dependent pathway by TLR4. TLR4 is able to activate MyD88-dependent pathway leading to NF-kB translocation into the nucleus and inducing pro-inflammatory cytokines expression, and also, to activate TRIF-dependent pathway leading to IRF-3

translocation into the nucleus and inducing IFN-β and IFN-inducible genes expression. Adapted from: (Akira et al., 2006).

TLRs activation triggers the translocation of the nuclear factor kappa B (NF-kB) into the cell nucleus after its activation. NF-κB activation can be induced by canonical and non-canonical pathways. Canonical activation of NF-κB is normally produced in response to TNF-α and IL-1 signaling, and is also known as NF-κB essential modulator (NEMO)-dependent pathway. This pathway is mediated by kinase complexes that contain NEMO protein (also known as IκB kinase (IKK)γ), IKKα and IKKβ. All these three kinases are members of the mitogen-activated protein kinases (MAPKs) family, and are activated by the phosphorylation of serines in the activation T-loop (Adhikari et al., 2007; Cheong et al., 2006; Iwai, 2012). Once activated, the complex binds to and phosphorylates IκB proteins that acts as inhibitors of NF-κB. Phosphorylation of these proteins leads to their ubiquitination and proteasomal degradation, triggering the release of NF-κB dimers associated with them and allowing it to translocate to the nucleus (Hoffmann et al., 2002). On the other site, non-canonical activation of NF-κB is not dependent on NEMO, but is dependent on NF-κB inducing kinase (NIK) and IKKα proteins. Once activated, NIK complex is able to phosphorylate and activate IKKα, leading to phosphorylation of p100 protein and activation of NF-κB (Ling et al., 1998; Sun, 2017). After its activation and translocation to the nucleus, NF-κB increases the expression of hundreds of biologically important genes that regulate cell function, cell death and survival, and proliferation. In concrete and interestingly for this Thesis, NF-κB is able to increase the expression of other PRRs like *Nlrp3* (Bauernfeind et al., 2009), in addition to the expression of pro-inflammatory cytokines such as *Tnfa* (Shakhov et al., 1990), *Il6* (Libermann & Baltimore, 1990), and *Il1b* (Hiscott et al., 1993), among many others.

CLR receptors

CLRs comprise a transmembrane receptor family characterized by the presence of one or more domains that are homologous to carbohydrate recognition domains but do not always bind carbohydrate structures (Zelensky & Gready, 2005). CLRs can be divided into two groups: group I CLRs belong to the mannose receptor family and group II CLRs belong to the asialoglycoprotein receptor family. CLRs through recognition of carbohydrates on microorganisms like bacteria, virus and fungi, are able to stimulate the production of pro-inflammatory cytokines or inhibit TLR-mediated immune complexes (Geijtenbeek & Gringhuis, 2009). As an example, the macrophage C-type lectin MINCLE is able to sense

infection by fungi such as Malassezia and Candida, and also to detect an endogenous protein, spliceosome-associated protein 130 (SAP130), which is present in necrotic host cells (Yamasaki et al., 2008).

RLR receptors

RLR family is composed of RIG-I, melanoma differentiation-associated gene 5 (MDA5), and RIG-I-like receptor 3 (RLR-3) (Yoneyama & Fujita, 2008). RLRs are composed of two N-terminal caspase activation and recruitment domains (CARD), a central Asp-Glu-Ala-Asp (DEAD) box helicase/ATPase domain, and a C-terminal regulatory domain. RLRs have a cytoplasmic localization and are able to recognize the genomic RNA of dsRNA viruses and dsRNA formation during ssRNA virus replication. In this sense, mouse fibroblasts lacking RIG-I are not able to produce type I IFNs or inflammatory cytokines in response to different RNA viruses (Kato et al., 2006). The CARDs of RLRs are able to trigger signaling cascades by direct interaction with the N-terminal CARD-containing adaptor IFN-β-promoter stimulator 1 (IPS-1). After, IPS-1 activates TRAF3 and the TNFR-associated death domain protein (TRADD) to induce IFN-inducible genes expression through the same downstream signaling molecules than TRIF-dependent signaling pathway (Koyama et al., 2008).

NLR receptors

The NLR family consists of sensors that recognize cytoplasmic pathogens, PAMPs and DAMPs, and are mainly composed by a LRR domain, a central nucleotide-binding and oligomerization domain (NBD) and a N-terminal domain that differs between four different NLR subfamilies (Inohara et al., 2005). If a pyrin (PYD) domain is present in the N-terminal of the protein the family is called NLRP and includes 14 members (NLRP1-14) (Bertin & DiStefano, 2000). When a CARD domain is present the family is called NLRC and is composed by five members (NOD1, NOD2, NLRC3-5) (Tschopp et al., 2003). Also, if a baculovirus inhibitor of apoptosis repeat (BIR) domain is present on the N-terminal of the protein the family is called NLRB or NLR family apoptosis inhibitory protein (NAIP). In other NLRs, between the CARD and the NBD domain an acidic activation domain is present and is known as MHC-class II transactivator (CIITA) complex, and is present in NLRA subfamily (Said-Sadier & Ojcius, 2012). Finally, the receptors which N-terminal domain has no homology to other NLR subfamily members, are included in the NLRX subfamily (Ting et al., 2008).

The NLRs family is comprised of 22 genes in humans and 33 genes in mice (Reed et al., 2003). NLRs could signal via two different pathways, forming complexes called NOD-signalosomes (NOD-1/2) or inflammasomes (NLRP1/2/3/6/10/12 and NLRC4) (Martinon et al., 2009).

The NOD-signalosomes are associated with the receptor interacting protein (RIP) 2 and TGF-β-activated kinase 1 (TAK1) to activate NF-κB and MAPKs such as extracellular signal regulated kinase (ERK)1/2, p38 and c-Jun N-terminal kinase (JNK) inducing the expression of several pro-inflammatory genes (Said-Sadier & Ojcius, 2012). The activation of one pathway or other, depends on the accessory proteins attached to the NOD-signalosomes. NOD receptors are able to bind to the pro-apoptotic BH3-only BCL2 family member BID to activate NF-κB and ERK1/2, or to CARD9 to activate JNK and p38 (Yeretssian et al., 2011).

The inflammasomes are mostly formed in innate immune cells and their formation can be modulated by DAMPs, PAMPs or cytokines, however, immune cells are not the only type of cells that present inflammasomes. Also, non-immune cells could form NLR-related inflammasomes and they can modulate the immune response to specific characteristics of the tissue, this is the case for example of hepatocytes and the activation of stellate cells during hepatic fibrosis (Gaul et al., 2021) or keratinocytes in the development of psoriasis (Zhang et al., 2018). The major part of the NLRs act as pro-inflammatory molecules, but there are some NLRs that repress the inflammatory response. NLRP10 present important anti-inflammatory effects in murine cutaneous leishmaniasis (Clay et al., 2017), and NLRP11 represses NF-κB and type I interferon responses (Ellwanger et al., 2018).

1.4. Cytokines

The production and release of cytokines from innate immune cells is a key response initiating inflammation in response to infection and tissue injury in the body. In response to DAMPs or PAMPs, innate immune cells release high amounts of cytokines to communicate with other cells and thereby to induce an immune response. The main cytokines secreted by innate immune cells includes IFN-γ, TNF-α, IL-6, IL-12, G-CSF, GM-CSF, IL-10, TGF-β, IL-4, IL-12, CCL-4, and the interlukin-1 family of cytokines (extensively explained in chapter 1.5.). The most important cytokines for this Thesis will be next described.

TNF-α

TNF-α is a pleiotropic pro-inflammatory cytokine produced by immune cells during inflammation that belongs to the TNF superfamily of cytokines, being the most studied and the main representative member of this family. TNF-α can be found in two different forms, as a 26 kDa transmembrane protein or as a 17 kDa soluble factor released from the membrane by the action of a metallo-protease called TNF-alpha converting enzyme (TACE) (Blobel, 1997; Idriss & Naismith, 2000). TNF-α is secreted by macrophages, monocytes, NK-cells and neutrophils after their stimulation with bacterial LPS and other TLR ligands that induces a strong *Tnfa* gene expression (Diya et al., 2008; Hirono et al., 2000). TNF-α is known to affect the physiological function, growth, differentiation and survival of different cells, including non-immune cells by signaling towards different TNF receptors (Beutler & Cerami, 1989), therefore TNF-α is important for non-immune-related processes such as metabolism and reproduction (Chen et al., 2009; Romanowska-Prochnicka et al., 2021). TNF-α signaling is also important in diseases such as cancer, autoinflammation and obesity-related insulin resistance (Balkwill, 2006; Borst, 2004; Fragoso et al., 2014). So, several strategies to block TNF-α are used to treat different chronic inflammatory diseases such as rheumatoid arthritis, Chron's disease, ulcerative colitis, or psoriasis (Monaco et al., 2015). A recombinant monoclonal antibody against TNF-α, called Infliximab, has been developed to block TNF-α signaling and is actually approved therapy to treat different autoimmune diseases (Lipsky et al., 2000; Rutgeerts et al., 2005; Taylor et al., 2000). Infliximab has been also recently tested in a clinical trial to treat COVID-19 patients (Fisher et al., 2022).

IL-6

IL-6 is a pleiotropic pro-inflammatory cytokine produced mainly by macrophages involved in inflammation, immune responses and hematopoiesis. IL-6 is a of 21-26 kDa cytokine which biological function is initiated by its direct binding to the IL-6 receptor (IL-6R) that is expressed in different cells. IL-6 is produced linked with a signal peptide, and once the signal peptide is removed, the remaining protein translocate to the lumen of the endoplasmic reticulum. IL-6 is able to bind to the both forms of IL-6R, transmembrane or soluble. Transmembrane IL-6R is expressed mainly in leukocytes and hepatocytes, and soluble IL-6R is present in the serum. After IL-6 binding to the membrane IL-6R, this complex then recruits gp130 forming a hexamer with two molecules of each protein (Boulanger et al., 2003; Murakami et al., 1993). Similar to TNF-α, IL-6 gene expression and release is also induced by different PAMPs and DAMPs through their recognition by TLRs, triggering the activation of NF-κB (DeForge & Remick, 1991; Hirano et al., 2017). In addition to immune

cells, also non-immune cells like mesenchymal cells, endothelial cells, or fibroblasts are involved in the production of IL-6 in response to different stimuli (Akira et al., 1993). IL-6 could be synthesized in response to PAMPs and DAMPs via activation of NF-κB, in the initial stage of inflammation being constitutively released after this activation (Conti et al., 2020). IL-6 signals in the liver to induce the production of acute phase proteins (APP) synthesis such as C-reactive protein (CRP), serum amyloid A (SAA), or fibrinogen (Heinrich et al., 1990). When IL-6 reaches the bone-marrow promotes the release of platelets by inducing megakaryocyte maturation (Ishibashi et al., 1989). IL-6 concentration has been found increased in plasma of patients with different diseases and has been proposed as a biomarker for sepsis and also for some chronic inflammatory diseases such as rheumatoid arthritis (Jekarl et al., 2013; Rincon, 2012). Blocking IL-6 has been shown beneficial to treat several inflammatory diseases such as rheumatoid arthritis, juvenile idiopathic arthritis, systemic sclerosis or myocardial infarction (Tanaka et al., 2018). A recombinant monoclonal antibody that binds IL-6, called Tocilizumab, and impairs signaling via IL-6R has been developed as a therapy for different inflammatory diseases (Emery et al., 2019; Sheppard et al., 2017). Tocilizumab has been recently tested in clinical trials to treat COVID-19 patients (Group, 2021; Salama et al., 2021).

TGF-β

TGF-β is a family of cytokines that include three members: TGF-β1, TGF-β2 and TGF-β3. All of them are synthetized as a precursor that includes a signal peptide to direct TGF-β to the endoplasmic reticulum, a N-terminal region called latency-associated peptide (LAP), and a C-terminal region which is the active mature form of the cytokine (Gleizes et al., 1997). Once the signal peptide is removed, the remaining protein translocate to the lumen of the endoplasmic reticulum, where is packaged as a dimer and cleaved by the endoprotease furin. Furin can also cleave TGF-β in the extracellular space once the unprocessed form of the cytokine is secreted to produce the active form of the cytokine (Munger et al., 1997). In addition, TLR4 activation can enhance the TGF-β signaling through MyD88-dependent pathway, providing a link between pro-inflammatory and pro-fibrogenic signals (Seki et al., 2007). Once secreted, TGF-β triggers signaling in cells by direct binding to the TGF-β receptor complex composed by two type I TGF-β receptors (TGF-βRI) and two type II TGF-β receptors (TGF-βRII) (Kang et al., 2009). The main cell type activated by TGF-β are T cells, being an important regulator of T cell proliferation (Kehrl et al., 1986). Reduced TGF-β signaling in T cells results in an enhanced clonal expansion of $CD8^+$ T cells (Sanjabi et al., 2009), and also enhanced $CD8^+$ T cell apoptosis is related to TGF-β signaling (Cerwenka et

al., 1996). In addition, TGF-β is able to promote the survival of naïve $CD4^+$ T cells and the lack of TGF-β signaling results in dramatically decrease of $CD4^+$ T cells associated with more T cell death (Li et al., 2006). Finally, TGF-β is able to promote the homing of Tregs in the large intestine (Kim et al., 2013). So, depending on the context, TGF-β can enhance or inhibit T cell proliferation, survival and accumulation in different tissues. TGF-β is also a factor strongly inducing tissue regeneration, which will be explained in detail in section 3.2.3.

1.5. The interleukin-1 family of cytokines

The IL-1 family is composed of 11 members of the IL-1 family of cytokines that can be divided into 3 subfamilies according to the IL-1 consensus sequence and the primary ligand binding receptor. These subfamilies include pro-inflammatory cytokines (IL-1α, IL-1β, IL-18, IL-33, IL-36α, IL-36β, and IL-36γ), receptor antagonists (IL-1Ra, IL-36Ra, and IL-38), and anti-inflammatory cytokines (IL-37). Also, IL-18BP, that do not belong to this family, has anti-inflammatory effects blocking IL-18. Some IL-1 family members (such as IL-1α, IL-1β, IL-18 or IL-36) are not released constitutively after translation and they are initially formed as inactive precursors that need to be cleavage in the cytosol to form their active forms that are then released from the cell by unconventional protein release mechanisms. However, another members can be released as a precursor and processed extracellularly (such as IL-33) (Dinarello, 2018). The cleavage site to be processed is normally localized 9 amino acids before the conserved consensus sequence A-X-D (A: any aliphatic amino acid; X: any amino acid; D: aspartic acid), which is present in almost all IL-1 family members (excepting IL-1Ra) (Towne et al., 2011). In some IL-1 members (such as IL-1β or IL-18), the aspartic acid is located in a consensus sequence for caspase cleavage, being caspase-1 the most active caspase cleavage the inactive precursors of these cytokines. The 10 members of the IL-1 receptors (ILRs) family are composed of a TIR cytosolic domain, as TLRs, a central transmembrane domain and an extracellular immunoglobulin (Ig)-like domains (Garlanda, Dinarello, et al., 2013), responsible of different ligand binding. After binding of the IL-1 cytokine to their receptors, ILRs forms dimers through their TIR domains, inducing the recruitment of MyD88, and the activation of the MyD88 dependent pathway. The signal leads to the activation of several transcription factors, such as NF-κB, activator protein-1 (AP-1), JNK, p38 and other MAPKs, ERKs, and members of the IRF, triggering inflammatory and immune responses (Dinarello, 2009).

There are 10 members of the IL-1 family of receptors. The most important receptors studied in this Thesis will be explained in more detail. IL-1R1 binds to IL-1α, IL-1β and IL-

1Ra. In addition, the IL-1 receptor accessory protein (IL-1RAcP) serves as a co-receptor that is required for signal transduction of IL-1/IL-1R1 complexes, and this co-receptor is also necessary for activation of IL-1R1 by other IL-1 family members, such as IL-18 and IL-33 (Wesche et al., 1997). After forming the trimeric complex (IL-1R – IL-1RAcP – IL-1α/β), TIR domains of each receptor chain are close enough to facilitate MyD88 binding, leading to activation of NF-κB (Dinarello, 2018). In some situations, IL-R3 can be found as a soluble receptor form. Soluble IL-1R3 can bind to extracellular IL-1R2. IL-1R2 is a decoy receptor for IL-1β and the formation of a complex with IL-1R3 induce the sequestration of IL-1β and neutralization of its function (Colotta et al., 1993). In addition, intracellular IL-1R2 binds to IL-1α precursor and prevents its release and subsequent processing by calpain. Finally, IL-18 is recognized by IL-18Rα and the co-receptor IL-18Rβ to form a ternary complex. Similarly to IL-1/IL-1R signaling, IL-18 induce activation of NF-κB, but inducing mainly the production of IFN-γ (Rex et al., 2020). There are some other receptors like IL-1R4 that is the ligand binding receptor for IL-33, or IL-1R6 that binds IL-36α, IL-36β, or IL-36γ, but also IL-38 (Gow et al., 2011). However, the IL-1 family of receptors also contains anti-inflammatory receptors, which are IL-1R8, IL-1R9, and IL-1R10 (Garlanda, Riva, et al., 2013).

IL-1α

IL-1α is considered a cytokine with a “dual-function”. The first function of IL-1α is to bind to DNA due to a nuclear localization sequence in the precursor region of the cytokine which allows it to localize in the nucleus, acting as a transcription factor and to increasing gene expression of chemokines like IL-8 (Werman et al., 2004). The second function is to be released from the cell and bind to the IL-1R1 and initiate pro-inflammatory signal transduction. So, when the cell is exposed to pro-apoptotic signal, IL-1α migrates from the cytosol to the nucleus, binding harder to chromatin and failing to induce inflammation. Whereas, when the cell is exposed to necrotic signal, IL-1α leaves the nucleus and migrates to the cytosol to be released as a DAMP, and induces a potent inflammatory response after binding to the IL-1R1 (Cohen et al., 2010; Di Paolo & Shayakhmetov, 2016). As IL-1α is constitutively expressed in epithelial and mesenchymal cell types, after necrosis cell death, it stimulates the production of chemokines resulting in the infiltration of neutrophils first and monocytes after in ischemic tissues exposed to hypoxic conditions (Rider et al., 2011).

In innate immune cells, IL-1α expression is highly induced by NF-kB as a precursor, and although it can be processed by calpain, the precursor is biologically active as it binds and activates IL-1R1 (Kaplanski et al., 1994). Therefore, IL-1α is very important in inflammation and a reduced inflammatory response has been found in models in which IL-

1α is not released (Kamari et al., 2007). IL-1α is also critical for several IFN-γ-induced activities, as these activities depend largely on the basal level of NF-κB, which is maintained by constitutively expressed IL-1α (Hurgin et al., 2007). The precursor of IL-1α can be processed at amino acid serine 113 (Lomedico et al., 1984) by two different enzymes that are the calcium neutral protease (Kobayashi et al., 1990), calpain calcium-dependent protease (Kavita & Mizel, 1995), being copper also required (Mandinova et al., 2003). The precursor or processed IL-1α could be released by necrotic cell death, including the gasdermins-dependent regulated necrosis called pyroptosis, later described in the introduction of this Thesis (Aizawa et al., 2020).

IL-1β

Transcription of IL-1β mRNA has been described for nearly all microbial products via TLR signaling, but also IL-1 itself (IL-1α/β) is able to induce IL-1β mRNA both in rabbits *in vivo* and in human mononuclear cells *in vitro* (Dinarello et al., 1987). Interestingly, a longer half-time life of IL-1β mRNA and a higher induction of its mRNA levels has been shown with IL-1 itself (IL-1α/β) as a stimuli, compared with microbial stimulants (Schindler et al., 1990).

IL-1β is translated into an inactive precursor form (pro-IL-1β) and is accumulated into the cytosol of immune cells until being processed by the activation of caspase-1. However, IL-1β can be also processed by other proteases such as cathepsin D (Mizushina et al., 2019). After pro-IL-1β cleavage, mature IL-1β is formed and secreted outside the cell. Three main mechanisms are described for IL-1β secretion. (1) LPS treatment of macrophages induces the recruitment of IL-1β to autophagosomes. In this way, when autophagy is activated, the sequestered IL-1β is degraded, but, when autophagy is inhibited, this sequestered IL-1β is secreted. Therefore, a portion of cellular IL-1β targeted for degradation can be released to the extracellular milieu (Harris et al., 2011). (2) Cellular IL-1β can get out of the cell by the shedding of microvesicles from the plasma membrane. P2X7 activation by extracellular ATP induces rapid microvesicles shedding and, subsequently, the release of their contents, providing a mechanism for IL-1β release (MacKenzie et al., 2001; Pizzirani et al., 2007). (3) The main pathway inducing the release of processed IL-1β outside the cell is mediated by the activation of caspase-1, the action of gasdermins and the necrotic cell death induced (later explained in the Thesis in section 2.2) (He et al., 2015; Liu et al., 2016; Zhou & Abbott, 2021). Once released, processed form of IL-1β can bind to IL-1R1 as described above, inducing the MyD-88 dependent pathway to activate NF-κB and induce a strong pro-inflammatory response by inducing expression of pro-inflammatory genes (Weber et al., 2010).

IL-18

IL-18 is a cytokine synthesized as an inactive precursor (pro-IL-18) and remains in the cytoplasm of the cells until its activation. IL-18 is cleaved by caspase-1 to produce its active mature form, and caspase-1 deficiency prevents processing of IL-18 in disease (Siegmund et al., 2001). Also, the precursor of IL-18 can be released outside the cell and processed extracellularly by neutrophil proteases like proteinase-3 (Sugawara et al., 2001). Once outside the cell, mature IL-18 can bind to IL-1R5 with low affinity or to IL-1R7 with high affinity forming a heterodimer and inducing the MyD88-dependent pathway to activate NF-κB and induce expression of pro-inflammatory genes (Weber et al., 2010). Despite that, there are several unique and specific differences between IL-18 and IL-1β, for example IL-18 has a constitutive expression and IL-1β expression has to be induced by for example NF-κB activation (Kolinska et al., 2008). Also, IL-18 activation requires high nanogram/ml or higher levels whilst for IL-1β activation low nanogram/ml or picogram/ml range is required (Lee et al., 2004). In presence of IL-12 or IL-15, IL-18 is able to induce IFN-γ (Kannan et al., 2011), but without them, IL-18 presents pro-inflammatory effects. IL-18 is elevated in the blood of patients with pathogen infections (Nanda et al., 2021; Otterdal et al., 2021), septic patients (García-Villalba et al., 2022; Martinez-Garcia et al., 2019; Wu et al., 2019) and COVID-19 patients , and also is related with autoinflammatory diseases such as MAS (Lieben, 2018). Blocking IL-18 with anti-IL-18 recombinant antibodies or with IL-18 binding protein has become an effective treatment for some diseases (Gabay et al., 2018; Robertson et al., 2006).

IL-33

IL-33 was first described as an IL-1R4 ligand (Schmitz et al., 2005), inducing the binding of IL-1R4 and IL-1R3 to form a heterotrimer and activation of immune cells (Ali et al., 2007). IL-33 is an active precursor that can be cleaved by caspase-1 at aspartic acid 111 to inactivate it (Cayrol & Girard, 2009). If IL-33 is not cleaved on the cytosol of the cell, full-length IL-33 is released upon cell damage, and so is considered an alarmin. The processing of IL-33 can also take place extracellularly by some enzymes such as neutrophil elastase or cathepsins (Lefrancais et al., 2012). There are at least 3 mature forms of IL-33 resulting from its cleavage by mast cell proteases that are more potent than the precursor form and activates both mast cells and basophil-like cells to induce inflammation (Lefrancais et al., 2014). In addition, IL-33 has a nuclear localization and induce inflammation when is released, so nuclear compartmentalization is vital for immune homeostasis because the recruitment of IL-33 into the nucleus limit its potent pro-inflammatory effects (Bessa et al.,

2014). On the other hand, treatment with recombinant IL-33 has been effective reducing inflammation in a collagen-induced arthritis mice model (Biton et al., 2016).

IL-36

The IL-36 subfamily is composed by IL-36α, IL-36β, IL-36γ, the IL-36 receptor antagonist (IL-36Ra), and IL-38; all of them are able to bind to the IL-36 receptor (IL-1R6). Neutrophil proteases contribute to the N-terminal processing of IL-36 ligands, and also proteinase-3, cathepsin G, and elastase increased their activity by 500-fold (Henry et al., 2016). IL-36 family is expressed mainly in the skin and particularly in psoriatic skin, so there is a close relation of IL-36 and skin diseases due to infection or inflammation (Buhl & Wenzel, 2019).

IL-1 receptor antagonist (IL-1Ra)

IL-1Ra was first described as an specific inhibitor of IL-1 bioactivity in supernatants of human monocytes (Arend et al., 1985), and in the serum and urine of children with systemic juvenile arthritis (Prieur et al., 1987). The anti-inflammatory action of IL-1Ra is mediated by the competition with IL-1α and IL-1β to bind to IL-1R1 to make their function, so when IL-1Ra binds to IL-1R1 the binding site of the receptor is now allowed for the binding of IL-1 proteins, preventing pro-inflammatory signals (Frank et al., 2012). Four isoforms of IL-1Ra have been described, one secreted isoform (sIL-1Ra), and three isoforms that lack a consensus leader peptide and remain intracellular (icIL-1Ra1, icIL-1Ra2 and icIL-1Ra3). The secreted form of IL-1Ra contains a peptide leader that allows this isoform to be released and antagonize IL-1 activity, and its transcription can be induced after NF-κB activation (Smith et al., 1994). Despite the lack of leader peptide, intracellular IL-1Ra isoforms can be released by dying cells or actively secreted by leaderless pathway of proteins release, and bind with IL-1R1 to antagonize the effects of IL-1 (Gabay et al., 2010). Recombinant IL-1Ra (commercially called Anakinra) is active in blocking the activities of IL-1α and IL-1β by direct inhibition of IL-1R1 (Petrasek et al., 2012). Anakinra is used to treat a large number of common diseases to rare diseases and hereditary diseases (Dinarello & van der Meer, 2013). Anakinra is approved and used for the treatment of rheumatoid arthritis (Bedaiwi et al., 2021) and autoinflammatory syndromes such as Cryopyrin-associated periodic syndromes (CAPS) (Wiken et al., 2018). Also, Anakinra is used to treat another autoinflammatory syndromes such as macrophage activation syndrome (MAS) (Mehta et al., 2020). Anakinra is not only used against genetic diseases, it has been shown to be effective against a wide variety of pathogen-associated diseases for example during sepsis

(Sicignano et al., 2021), active infections (van de Veerdonk, Netea, Dinarello, & van der Meer, 2011) or severe COVID-19 (Kyriazopoulou et al., 2021).

IL-38

IL-38 belongs to the IL-36 subfamily and has a similar effect on immune activation as IL-36Ra. So, once processed IL-38 is an anti-inflammatory molecule that block IL-1R8 and is released by apoptotic cells (Mora et al., 2016). Due to its anti-inflammatory effects, recombinant IL-38 has been used *in vivo* to treat some mice diseases models including proteinuria and skin lesions (Chu et al., 2017), and rheumatoid arthritis (Boutet et al., 2017). Also, IL-38 is elevated in patients with asthma (Chu et al., 2016), and acute ST-segment elevation myocardial infarction (Zhong et al., 2015).

IL-37

IL-37 was first reported in 2000 using *in silico* approaches (Kumar et al., 2000) and has a unique function compared with the other IL-1 family members, as it acts as a suppressor of innate and acquired immunity (Nold-Petry et al., 2015; Nold et al., 2010). IL-37 is able to bind to IL-1R8, which is an anti-inflammatory receptor. The TIR domain of IL-1R8 present a sequence change depriving its binding to MyD88, so a weak or no signal is expected for IL-1R8. Also, the IL-37 complex suppresses the phosphorylation of several inflammatory kinases (Dinarello et al., 2016). IL-37 protein is expressed in a large variety of cells but is not constitutively expressed in blood monocytes, and its production can be induced for example in keratinocytes by beta-defensin-3 (Smithrithee et al., 2015). IL-37 can be processed by caspase-1 (Kumar et al., 2002) and both precursor and processed forms are active (Li et al., 2015). After caspase-1 cleavage, IL-37 is able to translocate to the nucleus and reduces IL-1β, IL-1α, TNF-α, IL-6 and chemokines (Sharma et al., 2008). IL-37 is increased in several human diseases such as inflammatory bowel disease (Imaeda et al., 2013), but also is decreased in other diseases such as hyperhomocystinemia (S. Wang et al., 2020). However, the exact role of IL-37 in different diseases is not well established.

IL-18 binding protein (IL-18BP)

IL-18BP is a constitutive secreted protein with a high affinity to bind to IL-18. The expression and synthesis of IL-18BP in non-leukocytic cells like keratinocytes can be induced by IFN-γ (Muhl et al., 2000), and also by IL-27 acting through a negative loop for inflammation in the skin (Wittmann et al., 2012). The main property of IL-18BP in immune

responses is to reduce the induction of IFN-γ, but also has an important role in controlling Th1 and Th2 responses (Nakanishi et al., 2001). In serum of healthy subjects, the amount of IL-18BP is 20 times elevated compared to IL-18, but the binding between IL-18BP and IL-18 is produced in a 1:1 ratio, a single IL-18BP molecule binds to a single IL-18 molecule (Novick et al., 2001). In disease conditions, an imbalance of IL-18/IL-18BP is produced, so IL-18BP is not able to neutralize IL-18 and therefore the levels of IL-18 are higher than in healthy subjects and IL-18 is now able to bind to its receptor (Mazodier et al., 2005). IL-18BP is also able to bind to IL-37 so the anti-inflammatory property of IL-37 can be affected by IL-18BP (Bufler et al., 2002). So, it has been shown that at low dosing of recombinant IL-18BP, there is a reduction in inflammation in a model of rheumatoid arthritis, but when the dosage increases, the anti-inflammatory effects of IL-18BP are lost because in block IL-37 (Banda et al., 2003).

2. The inflammasome

The term inflammasome was coined by Tschopp and collaborators in 2002 to describe a high-molecular-weight (>700 kDa) multiprotein complex that mediates the activation of effector caspases (Martinon et al., 2002). By activation of caspase-1, inflammasomes can control the maturation and the release of the pro-inflammatory cytokines IL-1β and IL-18, becoming a central modulator of the inflammatory response (Tzeng et al., 2016).

2.1. Inflammasome structure and sensors

Inflammasomes typically consist of a sensor protein that is stimuli-triggered, an adaptor protein called the apoptosis-associated speck-like protein containing a caspase-recruitment and activator domain (ASC), and the pro-inflammatory caspase, caspase-1. Inflammasome assembly can be triggered by different stimuli associated with infection or cellular stress, and culminates with the activation of caspase-1 (Man & Kanneganti, 2015). These stimuli can be detected by the sensor protein of the inflammasome, which gives the inflammasome's name.

The inflammasomes induce caspase-1 activation by the assembly of ASC in large oligomers seeded from the sensor protein. ASC consists of two domains, PYD and CARD (Vajjhala et al., 2012). The recruitment of ASC by the inflammasomes is usually produced via PYD-PYD homotypic interactions. When ASC binds to inflammasomes PYD, it forms a helicoidal seed structure that allows the recruitment of new ASC proteins also via PYD-PYD

binding, forming helical filaments in a prion-like oligomerization process (Dick et al., 2016). For NLRC4 and NLRP1 inflammasome, the interaction with the ASC protein is produced via CARD-CARD homotypic interaction, but the structure formed by this interaction is not well known yet. NLRC4 can bind ASC proteins forming a structure that leaves the CARD domain in the outside of the filament, allowing more ASC proteins to bind. ASC filaments formed from sensors oligomers are then compacted into a discrete single particulate structure which is called ASC speck or pyroptosome (Dick et al., 2016). Within the ASC speck, pro-caspase-1 is able to bind to the complex. Pro-caspase-1 is formed by three domains a p10, a p20 and a CARD that allow to be recruited by ASC CARD domain when ASC is in a oligomeric form. When pro-caspase-1 bind to the ASC complex, the different pro-caspase-1 subunits are close enough to interact and to process another pro-caspase-1 to for the active form, caspase-1. Caspase-1 forms heterotetramers that include the p10 and p20 subunits, but are very unstable and dissociate each other very quickly once they are release from the inflammasome (Boucher et al., 2018). Therefore, the main caspase-1 activity is associated to the inflammasome.

Most of the inflammasome sensor proteins are NLRs, except AIM2, CARD8 or Pyrin. In all cases these sensors contain a CARD and/or a PYD domain. The CARD or PYD domains constitute the signaling domains, and enables the recruitment of pro-caspase-1, directly through CARD-CARD homotypic domain interaction, or indirectly through a PYD-PYD homotypic domain interaction with the adaptor protein ASC, that now recruit pro-caspase-1 through CARD-CARD homotypic domain interactions (Ting et al., 2008).

NLR protein (NLRP)3 and NLR CARD-containing (NLRC)4 are two of the most studied inflammasomes, and since they are central for this Thesis, they will be described in more detail in sections 2.3 and 2.4.

NLRP1 was the first inflammasome described forming a complex with ASC and caspase-1 (Martinon et al., 2002). NLRP1 is composed of a N-terminal PYD, a NOD, a LRRs, a functional-to-find domain (FIIND) and a C-terminal CARD. Recent studies have demonstrated a different activation mechanism of NLRP1. The first step for activation of NLRP1 is the autocleavage of its FIIND domain in response to the presence of cytosolic pathogens-associated molecules like *Bacillus anthracis* lethal toxin (Finger et al., 2012; Levinsohn et al., 2012). In resting conditions, the dipeptidyl peptidases (DPP)8 and DPP9 interact with FIIND of NLRP1 and suppresses its activation (Okondo et al., 2018; Zhong et al., 2018), and their inhibition by Val-boroPro (VbP), a non-selective inhibitor of DPP8 and DPP9, induces pyroptosis in monocytes and macrophages (Okondo et al., 2017). Full length

NLRP1 and DPP9 form a 2:1 complex, and the formation of this complex prevents the C-terminal fragment of NLRP1 to oligomerize (Huang et al., 2021). In addition, the binding of the NLRP1 C-terminal fragment to DPP9 requires full-length NLRP1, which suggests that NLRP1 activation is regulated by the ration between NLRP1 C-terminal fragment and full-length NLRP1 (Hollingsworth et al., 2021). When DPP9 is not bound to NLRP1, the proteasomal degradation of the repressive N-terminal region of NLRP1 occurs, freeing its inflammatory C-terminal fragment which is able to oligomerize, form an inflammasome and induce pyroptosis (Chui et al., 2019; Sandstrom et al., 2019) (**Figure 4**).

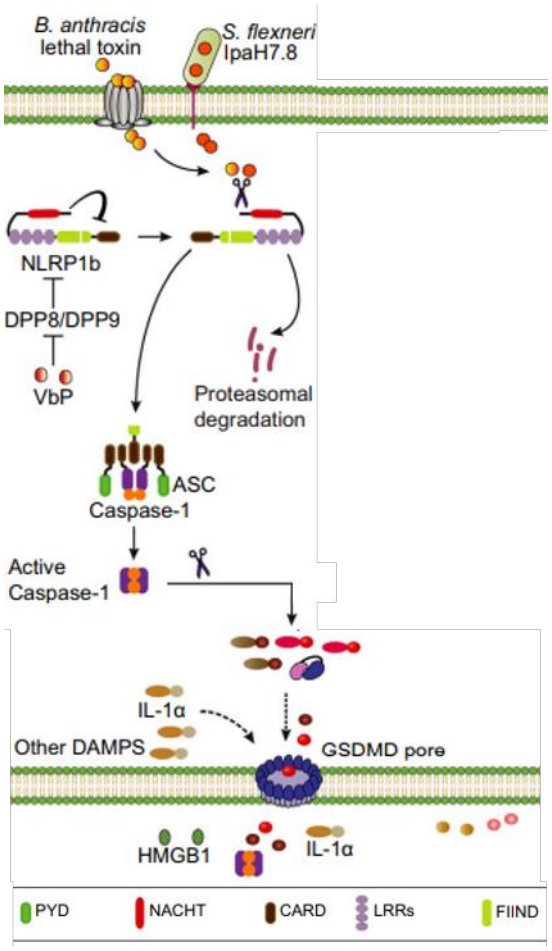

Figure 4. Activation of NLRP1 inflammasome. (A) Autoproteolysis of FIIND domain allows N-terminal fragment degradation by proteasome, freeing C-terminal fragment to assembly an inflammasome complex and induce pyroptosis. **(B)** DPP9 binding to NLRP1 full-length can recruit free C-terminal fragments to avoid pyroptosis. Adapted from: (Chauhan et al., 2020).

NLRP6 inflammasome is a novel NLR family member to form an inflammasome and is composed by a N-terminal PYD, a central NOD, and a C-terminal LRR domain. NLRP6 is mainly expressed in the intestine, playing an important role in intestine homeostasis. NLRP6 can be activated by viral RNA (Wang et al., 2015), bacterial metabolites (Levy et al., 2015), bacterial lipoteichoic acid (LTA) (Hara et al., 2018) and LPS (Leng et al., 2020). Recently, it

has been described that NLRP6 undertakes liquid-liquid phase separation upon interaction with double-stranded RNA. After activation, ASC recruitment via helical assembly, solidifies NLRP6 condensates to recruit caspase-1 and induce pyroptosis. In addition, a disordered poly-lysine sequence K350-354 of NLRP6 is important for multivalent interactions, phase separation, and its activation. Consequently, liquid-liquid phase separation of NLRP6 is a common response to ligand stimulation, which allows to direct NLRP6 to different functional outcomes depending on the cellular milieu (Shen et al., 2021) (**Figure 5**).

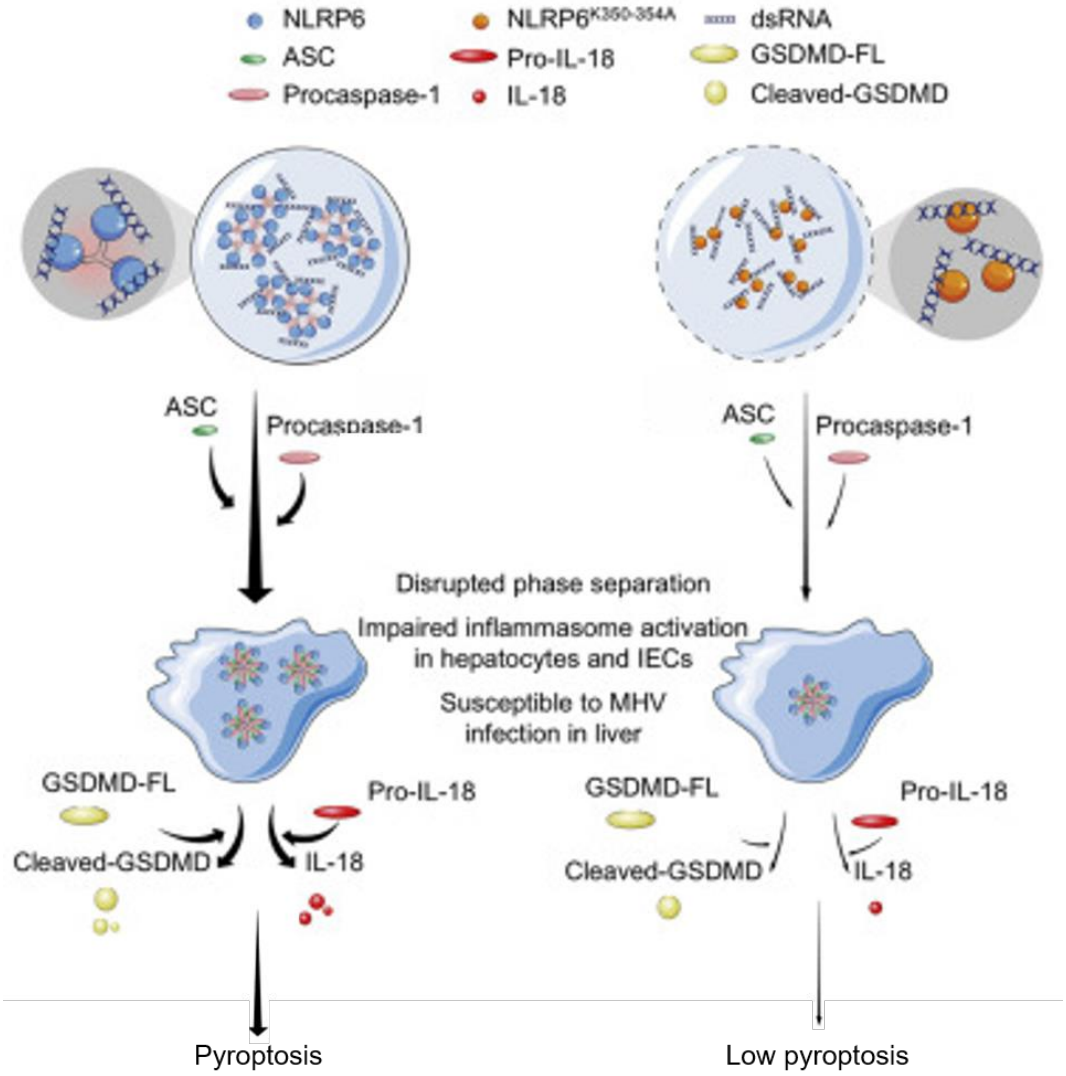

Figure 5. Activation of NLRP6 inflammasome. In intestinal epithelial cells, NLRP6 expression is regulated by microbial and metabolic signals (“signal I”). After, microbial components such as metabolites, RNA, LTA or LPS can bind directly to NLRP6 and serves as a “signal II” to induce NLRP6 inflammasome assembly and activation triggering the release of antimicrobial peptides (AMPs) and pyroptosis and cytokines release. Adapted from: (Li & Zhu, 2020).

In addition to NLRs, also other proteins could be inflammasome sensors and can assemble inflammasomes, these are called non-NLR inflammasomes. The two best studied non-NLR inflammasomes are absent in melanoma 2 (AIM2), CARD8 and Pyrin inflammasomes.

AIM2 inflammasome is the main component of the AIM2-like receptor (ALR) family. The AIM2 inflammasome contains a PYD together with a hematopoietic interferon-inducible nuclear (HIN) domain, which is the responsible to bind dsDNA. AIM2 is able to bind dsDNA from different sources, from microorganisms as virus or bacteria, but also from own host cells, becoming a cytosolic sensor for dsDNA (**Figure 6**). AIM2 was the first non-NLR inflammasome discovered to interact with ASC by PYD-PYD interactions (Wang et al., 2019). After binding to ASC, the AIM2 inflammasome is able to activate caspase-1 and induces the maturation and secretion of IL-1β and IL-18 (Reinholz et al., 2013).

Pyrin inflammasome (not to confuse with the pyrin domain, PYD) is a non-NLR inflammasome composed of a PYD, a B-Box, a coiled-coin domain and a B30.2/SPRY domain (Mariathasan & Monack, 2007). At basal conditions, pyrin present an inactive conformation because is bound to the 14-3-3 protein via phosphorylation in its Ser 242. In presence of bacterial toxins such as *Clostridium difficile* toxin B, there is inactivation of the Rho family of GTPases, as RhoA. This result in dephosphorylation of Pyrin and its dissociation from the 14-3-3 protein allowing pyrin to oligomerize, recruit ASC via PYD-PYD interactions and activate caspase-1 to induce IL-1β and IL-18 processing and release (Masters et al., 2016; Moghaddas et al., 2017) (**Figure 6**).

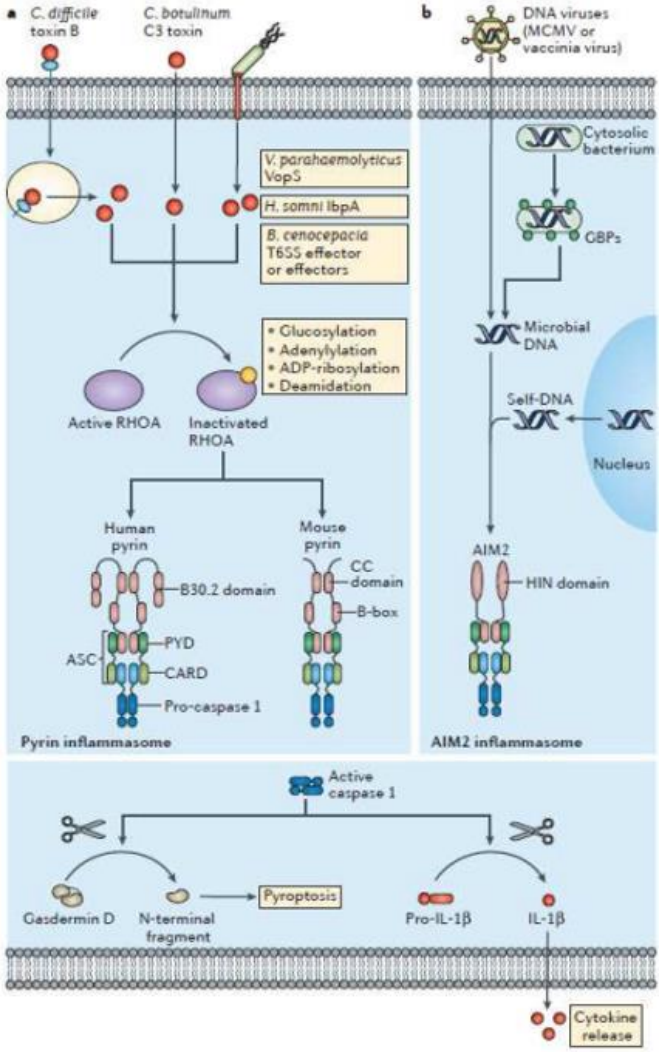

Figure 6. Activation of AIM2 and Pyrin, non-NLR, inflammasomes. (A) Pyrin inflammasome is activated by bacterial toxins such as *Clostridium difficile* toxin B and induce pyroptosis and cytokines release. **(B)** AIM2 inflammasome is activated by the presence of dsDNA in the cytosol of the cell and induce pyroptosis and cytokines release. Adapted from: (Broz & Dixit, 2016).

2.2. Inflammasome effector mechanisms

Caspase-1 is the effector enzyme of the inflammasome, proteolytically processes different proteins in the cells modifying their function, and for example cleaves immature pro-inflammatory cytokines to produce the bioactive forms of IL-1β and IL-18. Additionally, caspase-1 processes GSDMD protein to induce a highly inflammatory form of cell death known as pyroptosis (Bergsbaken et al., 2009; Broz & Dixit, 2016; Broz et al., 2020).

The term pyroptosis is composed of: “pyro” related to fire or fever and “ptosis” that denotes failing, and is an specific type of necrotic cell death frequent during the inflammatory response against pathogens (Yeretssian et al., 2008). However, pyroptosis can also take place in sterile conditions in the absence of infections (Faustin et al., 2009). Pyroptosis was

first described in macrophages infected with *S. typhimurium (Jarvelainen et al., 2003)*, and was considered as a mechanism to stop bacterial infection that proliferate in intracellular macrophages' phagosomes *(Kroemer et al., 2009)*. Pyroptosis is produced after caspase-1 processing of the protein GSDMD. This cleavage separates the pore-forming N-terminal domain ($GSDMD^{NT}$) from the gasdermin-C-terminal repressor domain. The C-terminal domain acts as an inhibitor of the N-terminal domain to avoid its pore-forming conformation. Once processed, $GSDMD^{NT}$ binds to negatively charged phospholipids on the inner leaflet of the plasma membrane to form pores after homo-oligomerization. GSDMD pores present an inner diameter of 10-15 nm and an outer diameter of 32 nm, with a negatively charge conduit pore that favor releasing of mature IL-1β and IL-18 that present a positively charge surface (Andreeva et al., 2021). In many settings the extent of plasma membrane rupture induced by $GSDMD^{NT}$ pores in the dying cells is regulated by the protein ninjurin-1 (Kayagaki et al., 2021), leading to the release of intracellular contents, including inflammasome oligomers (Baroja-Mazo et al., 2014). Finally, pyroptotic cells burst, with the subsequent release of intracellular components, such as oligomeric inflammasomes, the alarmin high mobility group box 1 (HMGB1), mitochondrial DNA or lactate dehydrogenase (LDH), leading to a highly proinflammatory environment (Baroja-Mazo et al., 2014; Broz et al., 2020; de Torre-Minguela et al., 2016; Evavold et al., 2018; Liu et al., 2016). Some cells as neutrophils or monocytes are able to release IL-1β without pyroptotic cell death (Evavold et al., 2018), however, in this scenario caspase-1 is activated in low levels, but the release of IL-1β is also dependent on GSDMD (Boucher et al., 2018). Similarly, low activation of caspase-1 in macrophages leads to an 'hyperactive' state where it could be release of IL-1β without cell death (Evavold et al., 2018). In fact, patches of membrane with GSDMD pores could be released by the endosomal sorting complexes required for transport (ESCRT) machinery, resealing damage plasma membrane (Ruhl et al., 2018).

GSDMD belongs to a protein family, which is composed in humans by five members: GSDMA, GSDMB, GSDMC, GSDMD and GSDME, appearing very conserved upon the different mammalian species (Angosto-Bazarra et al., 2022). All the members of the gasdermin family can be cleaved by different enzymes and their N-terminal domain can induce cell death (De Schutter et al., 2021; Ding et al., 2016). GSDMD is not the only member of gasdermins family that can be cleaved by caspase-1, also an isoform of GSDMB can be cleaved by caspase-1 and induce pyroptosis. However, only granzyme A is able to cleave all the isoforms of GSDMB to induce pyroptosis (Zhou et al., 2020). Also, in some situations, GSDMD can be cleaved by caspase-8 (Schwarzer et al., 2020), as occurs with GSDMC (Zhang et al., 2021). Finally, GSDME can be cleaved by caspase-3 and has been

related also with pyroptosis after apoptosis initiation and with cell death induction in tumor models (Jiang et al., 2020; Wang et al., 2018). Recently, GSDMA has been found to be cleavage by *Streptococcal pyrogenic* endotoxin B (SpeB), after Gln246, triggering keratinocytes pyroptosis (Deng et al., 2022).

2.3. The NLRP3 inflammasome

The NLRP3 inflammasome is the most studied inflammasome, and is related with over 100 preclinical disease models such as cancer (Sharma & Kanneganti, 2021), obesity (Vandanmagsar et al., 2011), sepsis (Alarcon-Vila et al., 2020; Martinez-Garcia et al., 2019), rheumatoid arthritis (Guo et al., 2018), type 2 diabetes (Gora et al., 2021), or Alzheimer (Liu et al., 2020). For this reason, NLRP3 is considered the most promiscuous of the inflammasomes, as it can be activated by a high number of triggers, such as PAMPs, DAMPs or homeostasis-altering molecular processes (HAMPs) (Rathinam et al., 2012).

2.3.1. Mechanisms of activation and regulation

The canonical activation of NLRP3 in macrophages follow a two-step mechanism. The first step is called “priming” and the second step is called “activation” of the NLRP3 inflammasome (**Figure 7**).

The first step is a priming of NLRP3 that is commonly achieved via TLR activation by LPS, to induce the translocation to the nucleus of NF-κB, resulting in the upregulation of *Nlrp3* gene expression and other pro-inflammatory genes such as *Il1b*, *Il6* or *Tnfa*. Nevertheless, NLRP3 is expressed in un-primed macrophages. This priming step could be also triggered by cytokines as TNF-α or IL-1 and strongly enhances NLRP3 inflammasome activation compared with the direct activation of NLRP3 inflammasome with activators without the first priming signal (Bauernfeind et al., 2009; Franchi et al., 2009). This priming step also induce different post-transcriptional modifications of NLRP3, such as de-ubiquitination or phosphorylation/dephosphorylation events among others (Baker et al., 2017). Macrophages primed for a short time, not sufficient to induce an increase in NLRP3 expression, significantly improves inflammasome activation (Juliana et al., 2012; Schroder et al., 2012). Furthermore, NLRP3 is deubiquitinated during priming, so deubiquitinase enzymes (DUBs) such as Lys63-specific deubiquitinase BRCC36 (BRCC3) also plays an important role in NLRP3 activation (Lopez-Castejon et al., 2013; Py et al., 2013).

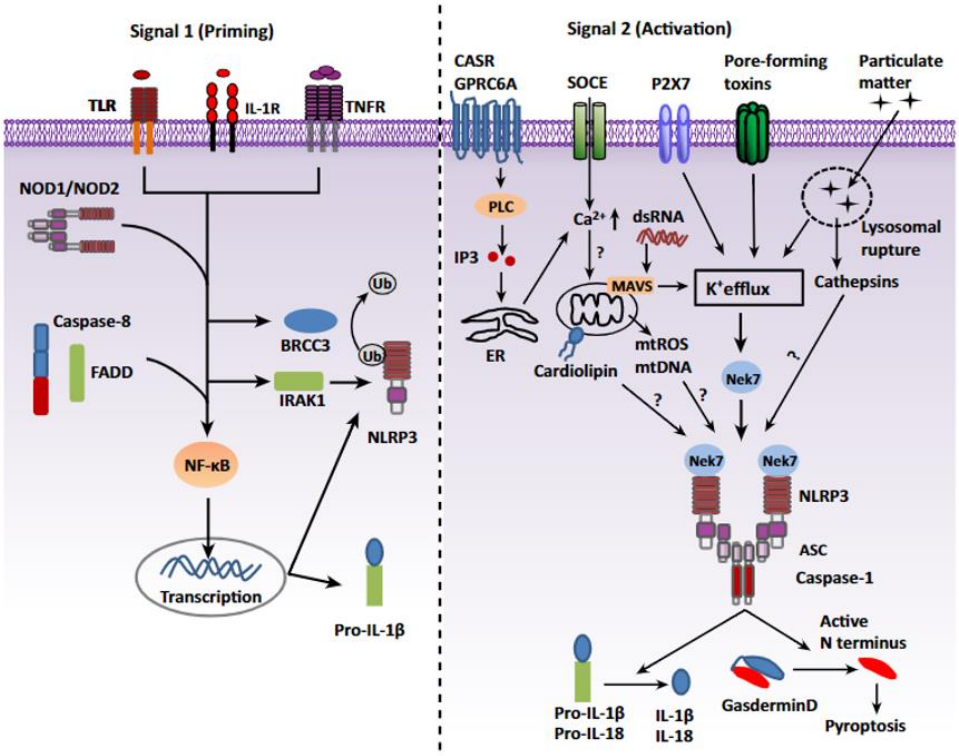

Figure 7. Canonical activation of NLRP3 inflammasome. NLRP3 inflammasome is activated with two signals. Signal one (priming, left) is provided by microbial molecules or endogenous cytokines leading to the upregulation of *Nlrp3* and *Il1b* through the activation of NF-κB. Signal two (activation, right) is provided by a high number of stimuli including PAMPs, DAMPs or HAMPs inducing cytokines release and pyroptosis. Adapted from: (He, Hara, et al., 2016).

The second signal is the activation of the NLRP3 inflammasome by DAMPs, PAMPs or HAMPs. The different triggers of NLRP3 converges in some common cellular signaling. Three main models for NLRP3 activation have been proposed: the ion flux model with the decrease of the concentration of intracellular K^+, the reactive oxygen species (ROS) model, and the lysosome rupture model. The intracellular depletion of K^+ can be triggered either by the activation of selective K^+-conductance channels or by plasma membrane permeabilization (Hafner-Bratkovic & Pelegrin, 2018; Munoz-Planillo et al., 2013). Cellular K^+ efflux induces a stable structural change in the inactive form of NLRP3 inflammasome, encouraging an open conformation as a step previous to activation, and is enabled by the FISNA domain and a unique flexible linker sequence between the PYD and the FISNA domains (Tapia-Abellan et al., 2021). Several NLRP3 activators are shown to induce intracellular K^+ depletion, as an example, extracellular ATP activates the ATP-gated ion channel P2X7 triggering rapid K^+ efflux (W. Wang et al., 2020), and nigericin, a K^+-ionophore, form K^+ conduits in the cell membrane (Mariathasan et al., 2006). Also, the production of ROS and the presence of oxidized mitochondrial DNA in the cytosol can trigger NLRP3 activation. In response to oxidative stress, increased amounts of ROS are sensed

by a thioredoxin and this release thioredoxin-interacting protein (TXNIP) with the latter binding to and activating NLRP3 (Zhou et al., 2010). Additionally, oxidized mitochondrial DNA release from dysfunctional mitochondria can bind to and activate NLRP3 inflammasome (Shimada et al., 2012). In contrast, cardiolipin derived from mitochondria, and independently on ROS production, is able to bind to and activate NLRP3 (Iyer et al., 2013). Finally, the destabilization phagolysosome has been also described to activate NLRP3 inflammasome (Hornung et al., 2008). During frustrated phagocytosis of crystalline or large particulate molecules like uric acid crystals, alum or silica, NLRP3 sense lysosomal rupture and activates (Jin et al., 2011).

The activation of NLRP3 inflammasome induces homo-oligomers of NLRP3 able to recruit and induce oligomerization of the adaptor protein ASC via PYD/PYD homotypic interactions. As explained above, ASC oligomeric filaments recruit caspase-1 to promote its activation within the inflammasome. Several different proteins can bind to NLRP3 and facilitate the activation of this inflammasome. Among them, never in mitosis gene a (NIMA)-related kinase 7 (NEK7), a member of the NIMA related kinases, has an important role in NLRP3 activation (He, Zeng, et al., 2016; Shi et al., 2016). NEK7 binds directly to the NACHT and LRR domains of NLRP3 and acts downstream of the K^+ efflux facilitating the active NLRP3 oligomers (He, Zeng, et al., 2016; Sharif et al., 2019). However, NEK7 implication in NLRP3 activation can be bypassed by TAK1-dependent post-translational priming (Schmacke et al., 2019), suggesting that the activation mechanism of NLRP3 inflammasome can be tangled. Also, post-translational modifications of NLRP3 during the priming step, such as different phosphorylation events in the PYD and NACHT domains (Song et al., 2017; Spalinger et al., 2016; Stutz et al., 2017; Zhang et al., 2017), are important for a correct NLRP3 activation. In addition, interaction of NLRP3 with negatively charged lipids as the phosphatidylinositol-4-phophate on dispersed trans-Golgi network is necessary for its activation (Chen & Chen, 2018). In that sense, a recent inactive NLRP3 oligomeric structure has been resolved as double-ring cages and add novel insight into NLRP3 activation, as double-ring-defective NLRP3 mutants abolish inflammasome punctum formation, caspase-1 processing, and cell death (Andreeva et al., 2021).

NLRP3 inflammasome can also be activated in a non-canonical manner after caspase-4/5 (in humans) or caspase-11 (in mouse) activation triggered by intracellular LPS or other oxidized phospholipids (oxPACP) recognition. oxPACP are abundant endogenous lipids accumulated at sites of tissue damage that are able to induce inflammation after activation of caspase-11. These lipids bind to the catalytic domain of caspase-11 to induce IL-1β

release, but without inducing pyroptosis (Zanoni et al., 2016). Caspase-4/5/11 activation cleaves GSDMD and GSDMD^{NT} pore formation induces K^+ efflux and the activation of the NLRP3 inflammasome (Schmacke et al., 2019) (**Figure 8**).

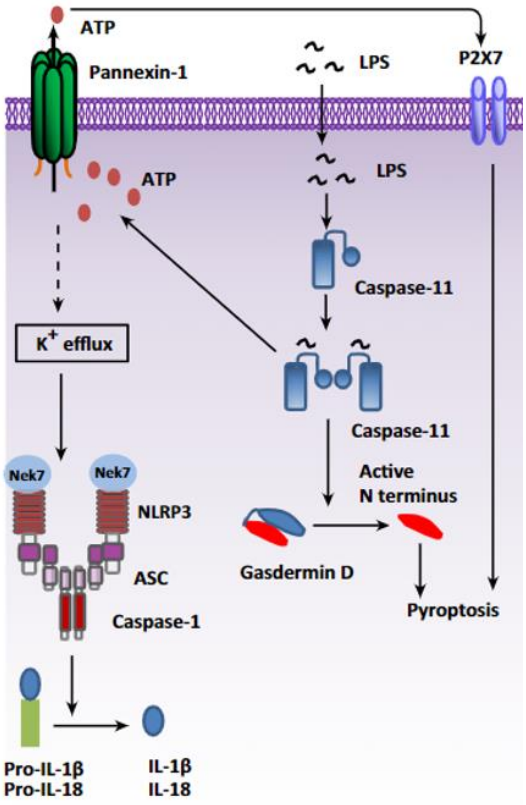

Figure 8. Non-canonical activation of NLRP3 inflammasome. Non-canonical NLRP3 activation is induced by LPS delivered into the cytosol through Gram-negative bacteria infections. Cytosolic LPS can activate caspase-11 to activate the NLRP3 inflammasome and to induce cytokines release and pyroptosis. Adapted from: (He, Hara, et al., 2016).

All the regulation and activation of NLRP3 inflammasome bring to light that the mechanism of NLRP3 activation is a complex pathway not fully understood yet.

2.3.2. Strategies to block the NLRP3 inflammasome

The fact that NLRP3 is involved in the initiation and progression of several human diseases lacking effective therapies has resulted in major advances on the development of several specific small molecules blocking NLRP3. However, since we still do not fully understand the NLRP3 activation process, the mechanism of action of some NLRP3 blocking molecules and their efficacy as novel drugs for humans is still a matter of intense research.

Different small molecules have been produced to control NLRP3 inflammasome activation. The most well-known molecule that block NLRP3 inflammasome is MCC950. MCC950 is a sulfonylurea that was initially developed in the 90s to block IL-1β release, but later it was found as a specific inhibitor of the NLRP3 inflammasome (Coll et al., 2015). Recently, it has been described the mechanism of action of this drug, binding to NLRP3 and impairing the opening of the receptor during activation (Coll et al., 2019; Tapia-Abellan et al., 2019). Recently, it has been shown that MCC950 binding site is on the double-cage inactive structure, and therefore this compound favors the inactive NLRP3 structure (Gayer Nature paper 2021). Another sulfonylurea called Glyburide, a drug used to treat diabetes mellitus type 2, was one of the first NLRP3 inflammasome inhibitors described, and has been demonstrated that can specifically inhibit NLRP3 inflammasome but no other inflammasomes like NLRC4 or AIM2 (Lamkanfi et al., 2009). A synthetic precursor of Glyburide called JC-21 is the most used sulfonamide used to block NLRP3 inflammasome (Marchetti et al., 2014). After the improvement of this molecule, the name changed to JC-171 and it has been described to interact with the allosteric site of NLRP3, which is close to the ATP binding site, and to inhibit the oligomerization of NLRP3 after stimulation (Daniels et al., 2016). There are some other molecules that are able to block NLRP3 inflammasome binding directly to it and reducing its ATPase activity, is the case of the acrylate derivates called INF4E and INF39 which are two irreversible inhibitors of NLRP3 (Cocco et al., 2014; Cocco et al., 2017), the 3,4-methylenedioxy-beta-nitrostyrene (MNS) which does not affect NLRC4 or AIM2 (He et al., 2014), organoboron derivates derived from 2-aminoethyl diphenyl borinate (2-APB) (Baldwin et al., 2017), or the glitazone CY-09 which specifically binds to the Walker A motif of NLRP3 (Jiang et al., 2017) (**Figure 9**).

The effects triggered by the activation of NLRP3 can be also blocked with some molecules. Bay 11-7082 is a vinylsulfone able to block NF-κB activation via IKKβ kinase, and also the NLRP3 inflammasome (Juliana et al., 2010). Another vinylsulfone called parthenolide blocks caspase-1 so prevents the effects triggered by NLRP3, NLRC4 and AIM2 inflammasomes (Juliana et al., 2010). Also, the *Nlrp3* and *Il1b* gene expression has been described to be blocked by the acylhydrazone named EMD638683 in animal models of cardiac fibrosis (Gan et al., 2018). Finally, some non-steroidal anti-inflammatory drugs (NSAIDs) like diclofenac, flufenamic acid, meclofenamic acid, or mefenamic acid has been described to affect NLRP3-dependent IL-1β release in a *in vivo* model of Alzheimer's disease (Boice, 2018). However, these compounds also have other targets such as cyclooxygenase that could synergize with their capacity to block NLRP3 as anti-inflammatory molecules (**Figure 9**).

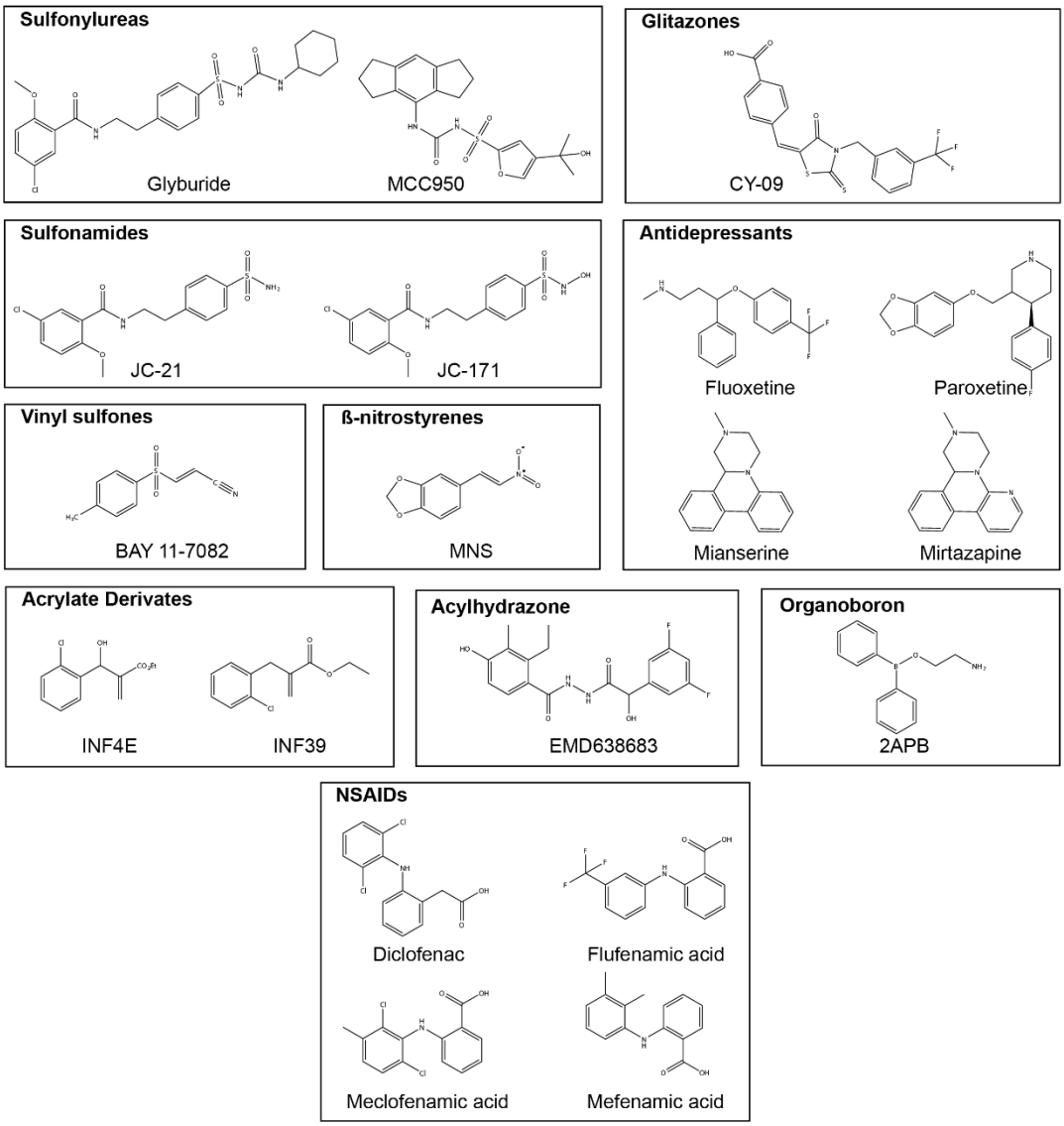

Figure 9. Chemical structure of different NLRP3 inflammasome inhibitors. Chemical structure of different sulfonylureas, sulfonamides, vinylsulfones, β-nitrostyrenes, acrylate derivates, glitazones, antidepressants, acylhydrazones, organoboron and NSAIDs with proved activity as NLRP3 inflammasome inhibitors. Adapted from: (Angosto-Bazarra et al., 2021).

Antidepressants drugs has been also described to block NLRP3 inflammasome but their mechanism of action is not well understood yet (Alcocer-Gomez et al., 2017) (**Figure 9**). To date, a lot of blocking molecules to block not only NLRP3, also another inflammasomes as NLRC4 and AIM2 (reviewed in (Angosto-Bazarra et al., 2021)), or even ASC oligomerization (Soriano-Teruel et al., 2021), have been described, but they are in early stages of development as no clinical trials has been performed yet.

2.4. The NLRC4 inflammasome

NLRC4 consists of a N-terminal CARD domain, followed by NBD, helical domain (HD)-1, winged-helix domain (WHD), HD2 and a C-terminal LRR domains. The NBD, HD1, WHD, and HD2 domains all together conform the central NAIP, CIITA, HET-E, and TP-1 (NACHT) domain, characteristic of the NLR family. The NLRC4 inflammasome regulates caspase-1 activation after recognition of different pathogens that deliver virulence factors into the host cell cytoplasm. The NLRC4 inflammasome could be induced by bacterial flagellin or gram-negative bacteria processing type III secretion system (T3SS) (Sutterwala et al., 2007), but NLRC4 does not directly bind triggering ligands.

2.4.1. Mechanisms of activation and regulation

After the presence of bacterial ligands into the cytosol of the host cell, the NAIPs are the responsible to recognize these ligands and induce NLRC4 oligomerization (Kofoed & Vance, 2011; Zhao et al., 2011). In mice, there are four different NAIPs, NAIP1 and NAIP2 recognize the bacterial needle and inner rod proteins, and NAIP5 and NAIP6 bind to flagellin. Only one NAIP is present in humans, and this NAIP is able to sense the different NLRC4 activators. (Rayamajhi et al., 2013; Yang et al., 2013). NAIPs then bind to NLRC4 and trigger assembly of the NLRC4 inflammasome complex. After the binding of NAIP, NLRC4 change its conformation to a more open state due to a rotation of the LRR domain. In concrete, a rotation occurs between NBD-HD1 and the WHD-HD2 within the NACHT domain, which moves the LRR domain to an open conformation (Hu et al., 2013). This opening results in the surface localization of an area of basic amino acids in the NBD that can then interact with an acidic surface of the next NLRC4 monomer added to the complex, and in the placing of an acidic region of the LRR to interact with the LRR of the previous NLRC4 monomer, stabilizing this opened structure (Hu et al., 2015; L. Zhang et al., 2015). In the case of NAIP, the open structure is predicted to be similar but it lacks the reciprocal acidic surface, that is the reason why NAIP is able to engage one NLRC4 monomer to initiate the inflammasome assembly but cannot be incorporated into an assembling complex inflammasome, resulting in one NAIP protein and ten NLRC4 monomers per active oligomer (Diebolder et al., 2015).

The involvement of ASC in this inflammasome is unclear because NLRC4 could directly promote caspase-1 activation via CARD-CARD homotypic interaction. However, after NLRC4 triggering ASC seems necessary for IL-1β release (Van Opdenbosch et al., 2014), but not for pyroptosis (Broz et al., 2010). Also maximal caspase-1 activation in response to NLRC4 triggering by some bacteria, like *S. typhimurium* or *P. aeruginosa*,

requires the ASC adaptor (Franchi et al., 2007; Mariathasan et al., 2004), but ASC seems dispensable for NLRC4-dependent caspase-1 activation in response to other bacteria like *L. pneumophila* (Case et al., 2009). After activation and similar to all the inflammasomes, caspase-1 is responsible for the cleavage of pro-IL-1β and pro-IL-18 to its mature form and also to generate $GSDMD^{NT}$, inducing pyroptosis and cytokines release (van de Veerdonk, Netea, Dinarello, & Joosten, 2011) (**Figure 10**). However, NLRC4 inflammasome is also able to recruit pro-caspase-8 to the inflammasome complex. Caspase-8 can be recruited and activated in response to *Salmonella* infection and is dependent on both NLRC4 and ASC (Man et al., 2013). As caspase-8 is a pro-apoptotic caspase and in cells lacking caspase-1 and GSDMD, preventing pyroptosis. Therefore, *Salmonella*-induced NLRC4 in cells lacking caspase-1 and GSDMD, results in caspase-8-dependent apoptosis (Mascarenhas et al., 2017).

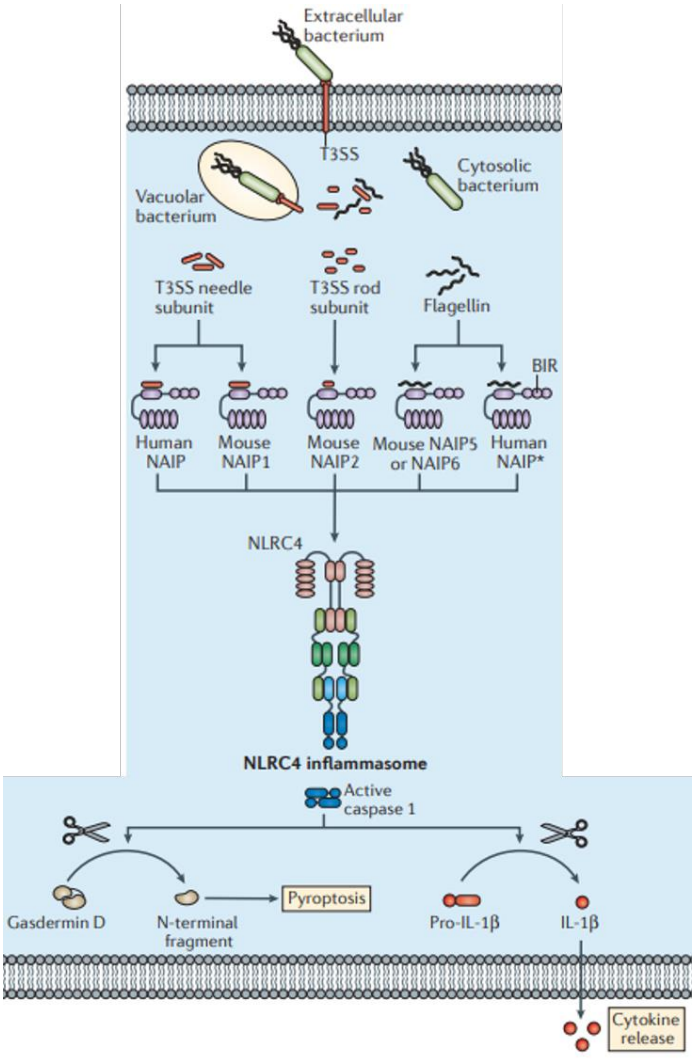

Figure 10. Activation of NLRC4 inflammasome. NLRC4 inflammasome is activated by the presence of T3SS components or flagellin into the cytosol of the host cell. Bacterial components are

recognized by NAIPs which bind to NLRC4 to induce NLRC4 oligomerization, finally inducing pyroptosis and cytokines release. Adapted from: (Broz & Dixit, 2016).

Additional regulatory mechanisms have been described in NLRC4 inflammasome. NLRC4 can be phosphorylated in Ser533 and this phosphorylation is important for NLRC4 activation after *Salmonella* infection, because it probably drives a conformational change in NLRC4 important for its activation (Qu et al., 2012). Another kinase, LRR kinase-2 (LRRK2) is also associated with NLRC4 phosphorylation at Ser533, and also the reduction of this kinase is related to diminished NLRC4 inflammasome activation (W. Liu et al., 2017). This phosphorylation on the Ser533 can be induced by a domain of flagellin called flagellin D0 domain. As this phosphorylation occurs independently of NAIPs, and the activation of NLRC4 is dependent on NAIPs, a sequential priming and activation steps for activation of NLRC4 inflammasome has been proposed (Matusiak et al., 2015). In addition, the δ isoform of protein kinase C (PKCδ) is also able to phosphorylate NLRC4, and the absence of this kinase is described to impair NLRC4 inflammasome-dependent downstream signaling *in vitro* (Qu et al., 2012). Altogether, it has been shown that, similarly to NLRP3, post-translational modifications in NLRC4 are needed for its activation.

3. Inflammation as a trigger of tissue healing and disease

3.1. Autoinflammatory syndromes

Autoinflammatory diseases (AIDs) involve a group of inherited immune disorders which are characterized by regular episodes of systemic sterile inflammation. The genetic basis of around 40 different monogenic AIDs has been identified, with inflammasomopathies representing the principal and best characterized subgroup (described below) (Nigrovic et al., 2020).

Inflammasomopathies are mainly produced by gain-of-function mutations in inflammasome sensor genes, but also by the deficiency of IL-1Ra (DIRA) that results in an excess of IL-1 signaling (Aksentijevich et al., 2009; Reddy et al., 2009), and the deficiency of IL-36Ra (DITRA) that is related with elevated inflammatory markers (Marrakchi et al., 2011; Tauber et al., 2016). Furthermore, autoinflammatory diseases related to interferon, known as interferonophaties, are mainly related to type I interferon family (Uggenti et al., 2019). Interferonpathies can be triggered by different disorders among which it can be found disorders of degradation or processing of endogenous nucleic acids (Kolivras et al., 2008), disorders of enhanced nuclei acid sensing (Adang et al., 2018; Liu et al., 2014), disorders

of proteasome function (Brehm et al., 2015), and disorders of amplified IFN receptor signaling, that can be produced by deficiency of different ubiquitinases (Duncan et al., 2019; Meuwissen et al., 2016; X. Zhang et al., 2015). Also disorders of NF-κB and/or aberrant TNF activity can lead to AIDs like haploinsufficiency of A20 (Zhou et al., 2016), Blau syndrome (Wouters et al., 2014), TNF receptor-associated periodic syndrome (TRAPS) (McDermott et al., 1999), and deficiency of adenosine deaminase 2 (DADA2) (Zhou et al., 2014). Finally, other mechanisms can also lead to autoinflammation and AIDs, like disorders in the retrograde transport from Golgi to the endoplasmic reticulum (Watkin et al., 2015), deficiency of some antibodies (Neves et al., 2018), and defects in complement or its surface inhibitory proteins (Reis et al., 2019) (**Table 1**).

Table 1.- Summary of autoinflammatory syndromes.

Disorder	Cause	Symptoms	Inheritance
Deficiency of IL-1Ra (DIRA)	Mutation in *Il1rn*	Neonatal-onset AIDs-related symptoms	AR
Deficiency of IL-36Ra (DITRA)	Mutation in *Il36rn*	Pustular psoriasis	AR
Aicardi-Goutières syndrome (AGS)	Mutation in *Trex1*	Neurological and liver abnormalities	AD, AR
Proteasome-associated autoinflammatory syndrome (PRAAS)	Mutation in *Psmb8*	Fever and skin lesions	AR
Deficiency of ubiquitin specific protease (USP)-18	Mutation in *Usp18*	Neurological and liver abnormalities	AR
Immunodeficiency 44	Mutation in *Stat2*	Viral infections	AR
Haploinsufficiency of A20 (HA20)	Mutation in *Tnfaip3*	Mucosal ulceration	AD
Blau syndrome	Mutation in *Nod2*	Arthritis, uveitis and dermatitis	AD
TNF receptor-associated periodic syndrome (TRAPS)	Mutation in *Tnfrsf1a*	Fever, myalgia and painful erythema	AD
Deficiency of adenosine deaminase 2 (DADA2)	Mutation in *Ada2*	Systemic vascular inflammation and skin ulceration	AR
COPA syndrome	Mutation in *Copa*	Interstitial lung, joint and kidney abnormalities	AD
Autoinflammation, antibody deficiency and immune dysregulation (APLAID)	Mutation in *Plcg2*	Eye inflammation, enterocolitis and immunodeficiency	AD
Complement factor I deficiency	Mutation in *Cf1*	Bacterial infections	AR

AR: autosomal recessive. / AD: autosomal dominant.

3.1.1. Inflammasomopathies: autoinflammatory syndromes associated to inflammasome

The inflammasomopathies are a consequence of gene defects affecting the sensing proteins of the inflammasome, and the two best characterized inflammasopathies are the CAPS and the NLRC4-associated AID, a consequence of gain-of-function (GoF) mutations in the *Nlrp3* and *Nlrc4* genes respectively. Both diseases are clinically diverse, but share some features such as onset during childhood, cutaneous lesions, recurrent fever and systemic inflammation (Canna et al., 2014; Nigrovic et al., 2020; Romberg et al., 2014). Also, inflammasomopathies related to NLRP1 have been described and its manifestations include skin inflammatory syndrome (Zhong et al., 2016). NLRP12-related disease a due to loss-of-function mutations in *Nlrp12* and are called FCAS2 (Jeru et al., 2008). The unique inflammasome outside the NLR family members that is related to AIDs is pyrin inflammasome because to date, no AIM2-driven inflammasomopathies has been reported. Pyrin inflammasomophaties include pyrin-associated autoinflammation with neutrophilic dermatitis (PAAND), a dominant-inherited disease due to mutations in *Mefv* gene (Masters et al., 2016), mevalonate kinase deficiency (MKD), a inflammasomopathy mediated by dysregulation of the pyrin regulator factor RhoA due to autosomal recessive loss-of-function mutations in *Mkd* (Park et al., 2016), and pyogenic arthritis with pyoderma gangrenosum and acne (PAPA), an autosomal dominant disorder due to mutations in *Pstpip1* gene which encodes a protein able to bind and activate pyrin inflammasome (Marzano et al., 2016). Also, mutations in *Mefv* gene are related to familial Mediterranean fever (FMF), a recessive-inherited disease characterized by recurrent episodes of fever (Park et al., 2016).

3.1.2. Cryopyrin associated periodic syndromes

CAPS individuals develop a wide variety of clinical manifestations in which the periodic skin rashes and fever are the most common characteristics (Hoffman et al., 2001). Depending on the severity of the symptoms, CAPS can be classified into: Neonatal-onset multisystem inflammatory disease (NOMID) as the most severe syndrome, Muckle-Wells syndrome (MWS) with intermediate symptoms, and the familial cold autoinflammatory syndrome (FCAS) as the milder form of CAPS. Some symptoms are characteristic for each sub-phenotype of CAPS, including cold sensitivity in FCAS, AA amyloidosis in MWS, and central nervous system and bone disease in NOMID. The major part of CAPS patients possesses heterozygous germline or somatic gain-of-function mutations in *Nlrp3* gene, also mutations present in mosaicism of this gene has been described to be linked to CAPS

(Aganna et al., 2002; Dode et al., 2002; McGeough et al., 2017). To date, more than 200 gain-of-function mutations are described in *Nlrp3* and associated with CAPS (Touitou et al., 2004). Also, some low penetrance variants have been identified in unaffected people with no significant symptomatology and tested *in vitro* has been found to be risk alleles to develop more common inflammatory diseases (Kuemmerle-Deschner et al., 2017; Verma et al., 2008).

The gold-standard treatment used to treat these diseases is IL-1 blockade, being the main drug used Anakinra, a recombinant form of IL-1Ra, that is efficient in patients with FCAS and MWS, but remarkably in patients with NOMID (Goldbach-Mansky et al., 2006; Hawkins et al., 2003; Hoffman et al., 2004).

3.1.3. Autoinflammatory syndromes associated to *Nlrc4*

The first description of NLRC4-associated disease was in 2014, when two gain-of-function mutations of *Nlrc4*, p.Thr337Ser and p.Val341Ala, were described and associated to MAS (Canna et al., 2014; Romberg et al., 2014). Another gain-of-function mutation present in mosaicism, the p.Ser171Phe, has been described in patients with perinatal autoinflammation and MAS (Liang et al., 2017). MAS is a disease characterized by hectic fever, low peripheral cell counts, hepatobiliary dysfunctions, coagulopathy, dramatically elevated serum ferritin, and hemophagocytosis (Weaver & Behrens, 2014). The patients with MAS are characterized by an extremely and chronic elevation of peripheral IL-18 (Girard et al., 2016; Shimizu et al., 2015). So, IL-18 has become a therapeutic target in patients developing MAS, and for example the use of recombinant IL-18BP to block IL-18 in a patient with MAS achieved a good response and improvement of the symptoms (Canna et al., 2017). The design of specific inhibitors blocking NLRC4 is an important area of development, however, no small molecules blocking NLRC4 have been described so far.

Therefore, not all patients with *Nlrc4* mutations develop MAS or enterocolitis, but these other symptoms are still consistent with those observed in many other autoinflammatory diseases. Also, *Nlrc4* mutations has been identified in patients with another autoinflammatory diseases. The gain-of-function p.His443Pro *Nlrc4* mutation has been identified in a family with FCAS, and has been described to increase the NLRC4 oligomerization and caspase-1 activity leading to a higher IL-1β release (Kitamura et al., 2014). Furthermore, a somatic mosaicism of the *Nlrc4* gene has been described in a patient with a NOMID autoinflammatory syndrome due to the gain-of-function p.Thr177Ala mutation (Kawasaki et al., 2017). Another AIDs-associated symptoms, such as cutaneous

erythematous nodes and urticarial rash, arthralgias, and late-onset enterocolitis have been observed in 13 affected family members, all of them with the *Nlrc4* gain-of-function mutation p.Ser445Pro (Volker-Touw et al., 2017). Recently, the gain-of-function mutation p.Arg207Leu has been reported in two patients with a wide spectrum of symptoms from gastrointestinal to vasoplegic shocks (Bardet et al., 2021). Not only sever autoinflammation is related to *Nlrc4* mutations, recently, the gain-of-function mutation p.Gly172Ser has been identified in two patients with a mild autoinflammatory phenotype including recurrent urticaria and arthralgia (Wang et al., 2021). Redundant mutations present in the same amino acid has also been identified, is the case of the gain-of-function mutations p.Thr337N (Bardet et al., 2021) or p.Val341Leu (Siahanidou et al., 2019).

All the previous described mutations are within close proximity to ADP/ATP binding site, but mutations in LRR domain had been also described. The gain-of-function mutations p.Trp655Cys and p.Gln657Leu has been described in patients with autoinflammatory disease. The first mutation has been identified in two patients with MAS showing that the position of the residue is important in the mechanism of inflammasome assembly with higher levels of IL-18 (Moghaddas et al., 2018), and the second in a patient with higher levels of IgE and IgG that could be induced by elevated free IL-18 in the patient (Chear et al., 2020). Furthermore, not only point mutations has been identified for *Nlrc4*, deletions in the *Nlrc4* gene has been also associated to autoinflammatory diseases-related symptoms in patients with the gain-of-function mutation p.His392del (Barsalou et al., 2018).

3.1.4. Genetics of autoinflammatory syndromes: genetic mosaicism

From a genetic point of view, both germline and post-zygotic variants in the respective genes, *Nlrp3* and *Nlrc4*, have been identified to cause disease. The identification of post-zygotic variants causing genetic mosaicisms was first reported in the *Nlrp3* gene in children affected by severe CAPS (Tanaka et al., 2011), and subsequently in patients with late-onset but otherwise typical CAPS (Mensa-Vilaro et al., 2016; Rowczenio et al., 2017; Zhou et al., 2015). By contrast, only two young patients carrying post-zygotic NLRC4 variants have been reported, with only one patient, described in this Thesis, starting during adulthood (Ionescu et al., 2022; Kawasaki et al., 2017; Liang et al., 2017).

Regarding to *Nlrp3* genetic mosaicisms, in two patients with a non-malignant disorder it has been demonstrated that somatic mosaicism is restricted to the myeloid lineage (de Koning et al., 2015). Also, vertical transmission of the somatic *Nlrp3* mutation p.Thr348Met in CAPS patients with mutational event occurring during embryogenesis has been identified

(Jimenez-Trevino et al., 2013). Mainly *Nlrp3* but also another genetic mosaicism related to autoinflammatory diseases has been widely reviewed by Labrousse et al. in 2018 (Labrousse et al., 2018).

3.2. Inflammation in tissue healing

The effectiveness of tissue repair machinery is critical for all living organisms (Eming et al., 2014), and tissue healing has been described to be dependent on inflammation (de Preux Charles et al., 2016; Kyritsis et al., 2014). After tissue healing, necrosis, clotting reactions and some invading microorganisms can induce an inflammatory response. Immune cells are recruited in the injured site to clear damaged cells and microbes, helping to orchestrate the tissue repair response. Depending on the time and the level in which this inflammation process occurs, the outcome can be different. So, a controlled inflammatory process is needed to achieve a good tissue repairment without leading to fibrosis. Inflammation after tissue healing can be divided into three phases, an early inflammatory step, where the inflammasomes are triggered in innate immune cells that start the repair response, a switch from pro-inflammatory response to pro-regenerative response with a change in macrophage phenotype, and a final tissue homeostasis recovery when immune cells are cleared from the injured site (Eming et al., 2017; Thankam et al., 2018).

Immune cells have to be recruited on the injured site to perform their function. Some damage attractants have been described including small molecules like H_2O_2 and ATP (Niethammer et al., 2009; Weavers, Liepe, et al., 2016), but also other signals that can be able to travel through wound fluids and tissues like cytokines or chemokines are required, being IL-1α and IL-1β strongly upregulated during the inflammatory phase of healing, indicating that the inflammasomes could play an important role (Ridiandries et al., 2018; Werner & Grose, 2003). Naïve immune cells are not able to respond to wound attractants, first they need to be primed by other signals like cellular or tissue debris (Weavers, Evans, et al., 2016).

After immune cells perform an initial protective inflammatory response, resolution of inflammation starts with the death and clearance of inflammatory immune cells such as neutrophils by macrophages that are now repolarized to anti-inflammatory M2 macrophages (Ellett et al., 2015). M2 macrophages present mechanisms to turn off inflammasome activation (Pelegrin & Surprenant, 2009). Also, the released cytokines and chemokines are cleared in the regenerated tissue by the action of neutrophils, and the production of anti-inflammatory cytokines as IL-10 or IL-1Ra (Pase et al., 2012). All these events together with

the release of pro-regenerative molecules like resolvins or TGF-β by the macrophages and other cells are responsible of the recovery of the homeostasis in the tissue (Serhan et al., 2015).

3.2.1. Tendon healing

Two cellular mechanisms of tendon healing, known as extrinsic and intrinsic healing, have been described. However, now is more established that these two mechanisms normally act cooperatively, with a biphasic pattern of tendon healing involving extrinsic circulating cells and intrinsic local cells (Kajikawa et al., 2007). Tendon healing is a three-stage process that progresses consecutively from a short inflammatory phase, that can last one week, followed by a proliferative phase, that can last few weeks, until a remodeling phase, that can last several months (Voleti et al., 2012) (**Figure 11**). However, the duration of each phase is dependent on the location and the severity of the injury (Lin et al., 2004).

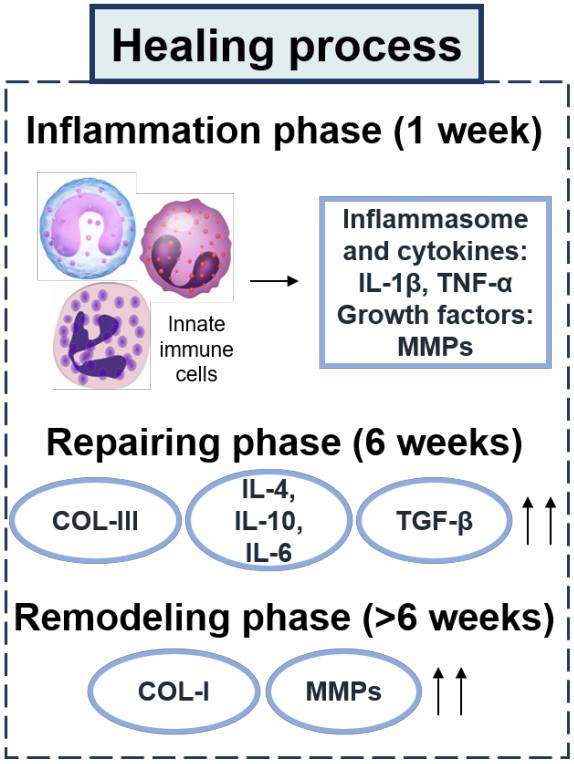

Figure 11. Illustrated scheme representation of healing process of tendons. Adapted from: (D'Addona et al., 2017).

The initial inflammatory phase starts with the formation of a hematoma shortly after injury (Lin et al., 2004). During the inflammatory phase, there is an increase in vascular permeability allowing the influx of inflammatory cells into the healing site. This initial vascular response is essential for tendon healing because diminution of blood supply impairs healing

(Fenwick et al., 2002). The immune cells present into the injured site release different cytokines and growth factors that induce the recruitment and proliferation of macrophages and resident tendon fibroblasts (from now referred as tenocytes). Also, in this first phase, components of the extracellular matrix (ECM), predominantly type III collagen, are synthesized by these recruited tenocytes (James et al., 2008). This inflammatory phase is characterized by the activation of inflammasomes and the release of pro-inflammatory cytokines such as IL-1β and IL-6 (Evans, 1999), however it is not really known which type or the role of the inflammasome involved, and for example MCC950 failed to alter wound healing in an obese animal model (Lee et al., 2018). During the proliferative and remodeling phases, tenocytes proliferate and produce, deposit, orient, and crosslink different types of collagen (Thomopoulos et al., 2015). In the proliferative phase, abundant ECM components such as proteoglycans collagens are synthesized and arranged in a random manner (Sharma & Maffulli, 2005). Finally, in the remodeling phase, firstly, a decrease in cellularity and matrix production is produced, and the tissue becomes more fibrous through the replacement of collagen type III by collagen type I. After, collagen fibers start to organize with a correct disposition along the longitudinal axis of the tendon, restoring tendon stiffness and tensile strength. The process finish with an increase in collagen fibril crosslinking and the formation of more mature tendinous tissue (Docheva et al., 2015).

There are different cell types involved in tendon healing, including infiltrating inflammatory cells, resident tenocytes from the tendon surface or midsubstance, and tendon or marrow-derived mesenchymal stem cells (Manning et al., 2014). Also, cells from the intrasynovial sheath infiltrate into the repair site, impairing tendon gliding and decreasing digital range of motion by promoting adhesions between the sheath and the tendon surface (Gelberman et al., 1985). In some cases, and depending on the tendon, some tendon injuries require repair tendon to bone attachment site. In these situations, fibroblasts from the tendon and surrounding tissues produce disorganized scar tissue at the attachment site of the two tissues (Gimbel et al., 2004), and also osteoclasts are recruited into the repair site and the resorption of bone can impair healing (Ditsios et al., 2003).

Modulation of inflammation in early stages of the tendon healing led to improved healing (Hays et al., 2008). In concrete, regulated inflammation is beneficial to tissue repair, but excessive or persistent inflammation is damaging and can impair tissue repair. On one hand, the controlled release of inflammatory cytokines attracts fibroblasts to the repair site, but on the other hand, excessive cytokine-related signaling can lead to poor clinical outcomes (Lichtnekert et al., 2013; Sugg et al., 2014). Macrophages has a main role not

only in promoting and resolving inflammation, also in facilitate and moderate tissue repair, and the balance between M1 and M2 macrophages and the timing and levels of inflammasome activation and cytokines release is critical to avoid chronic inflammation leading to tendinopathy.

3.2.2. Role of macrophages in tendon healing

Macrophages perform a wide variety of functions in tendon healing some of them are host defense, phagocytosis, and the production of growth factors and both pro-inflammatory and anti-inflammatory molecules (Koh & DiPietro, 2011). The number of macrophages in normal tendon tissue and throughout epitenon is very low (Matthews et al., 2006). After an injury, the number of macrophages recruited in the damaged tendon increase considerably, being attracted by chemoattractants released by the tendon tissues (Marsolais et al., 2001; Wojciak & Crossan, 1993). In addition, the number of macrophages present in damaged tendon remain elevated compared with other immune cells, and the increased amount are observed 14 to 28 after the injury (Marsolais et al., 2001; Sugg et al., 2014). Also, the number of macrophages increase in tendon that are changing with increased fibroblast cellularity and vascularity (Matthews et al., 2006).

In tendon healing, depending on their functional form, macrophages have different phenotypes, including the M1 and M2 macrophages that can perform differential roles (Mosser & Edwards, 2008) (**Figure 12**). Some of the functions performed by the macrophages after tendon damage are phagocytosis (Wojciak & Crossan, 1993), control the activity of the surrounding cells by the release of pro-inflammatory (Sica & Mantovani, 2012) and anti-inflammatory factors (Mosser & Edwards, 2008), stimulate fibroblast proliferation and mediate the deposition of newly formed collagen fibers (de la Durantaye et al., 2014), and the recognition of damaged collagen fibers inducing their collagenolysis (Veres et al., 2015). Recently, it has been proposed that there is a tissue specific differentiation of macrophages, depending on the tissue of residence, the surrounding cells and the different molecular signals recognized by them, in the case of the tendon called “tenophages” (Lehner et al., 2019; Williams et al., 2018).

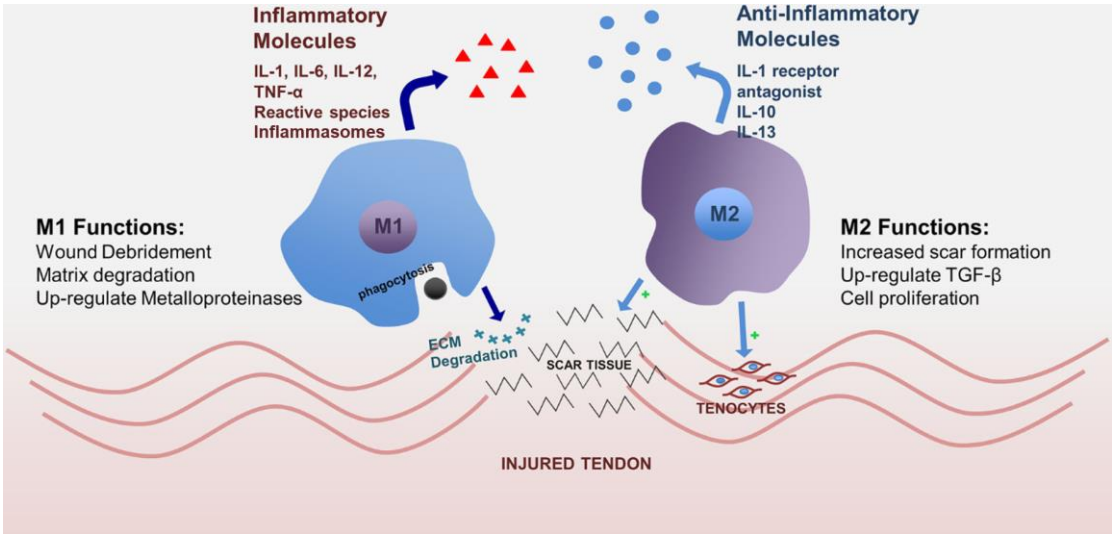

Figure 12. Schematic representation of the function of M1 and M2 macrophages in the healing tendon. M1 macrophages are present in the first stage of tendon healing and release pro-inflammatory molecules, whereas M2 macrophages are present in the final stage of tendon healing and release anti-inflammatory molecules. Adapted from: (Sunwoo et al., 2020).

M1 macrophages in tendon healing

The M1 macrophage phenotype seems to be a main driver of the early inflammatory process in the healing tendon. The initial macrophage infiltrate has been found to be predominantly of the M1 phenotype. The amount of M1 macrophages is really elevated in the first two weeks of tendon healing and restricted to zones of newly formed tendon tissue and tissue resorption (Marsolais et al., 2001; Sugg et al., 2014) (**Figure 13**). So, the M1 macrophage phenotype is responsible for the dissemination of the acute inflammatory response in the healing tendon (Lundborg et al., 1980). These macrophages are able to activate the inflammasome and induce the release a number of pro-inflammatory cytokines and mediators such as IL-1β, IL-6, IL-12, TNF-α, and reactive nitrogen and oxygen species (Barrientos et al., 2008). However, uncontrolled and sustained responses of this M1 macrophages can lead to collateral damage to surrounding healthy tissue (Chamberlain et al., 2011). Furthermore, the M1 macrophages also have a role in ECM degradation (Mosser & Edwards, 2008) and wound debridement by the phagocytosis of debris and apoptotic cells (Veres et al., 2015). Finally, M1 macrophages can influence tendon fibroblasts by inducing an upregulation of pro-inflammatory cytokines such as TNF-α, IL-1β, and COX-2, an upregulation of matrix-metalloproteinases, and a downregulation of factors associated with matrix production (Manning et al., 2015).

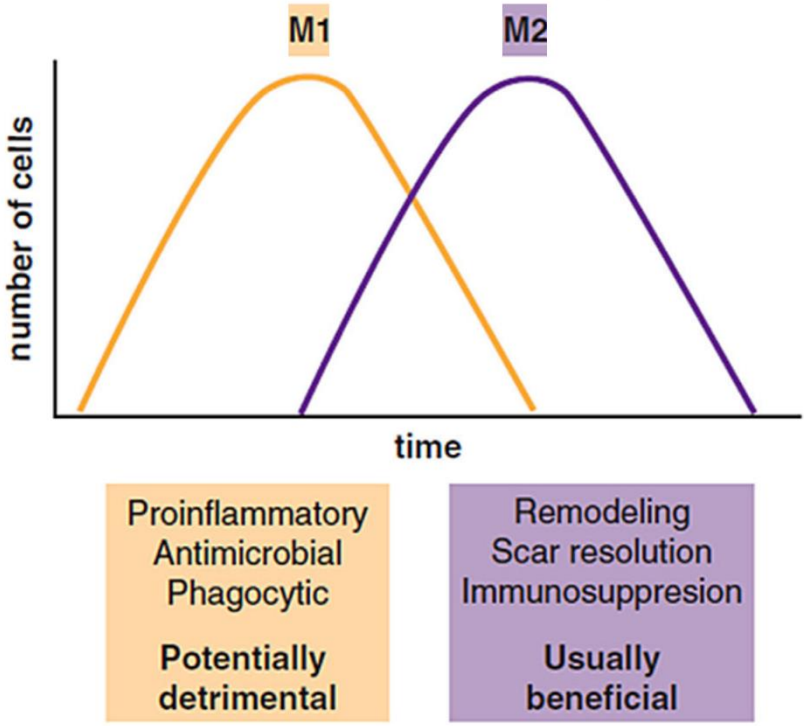

Figure 13. Schematic representation of M1 and M2 macrophages predominancy after tendon injury. Number of M1 macrophages is increased at first times after tendon injury, and the amount of M2 macrophages increase at later times. Adapted from: (Thomopoulos et al., 2015).

M2 macrophages in tendon healing

Contrary to M1 phenotype, M2 macrophage phenotype play an important role in fibroblast proliferation and the stimulation of tissue deposition (Mantovani et al., 2002). The appearance of high numbers of M2 macrophages occurs later in the healing process, and are located in areas of organizing tendon ECM. So, M2 macrophages are present in the healing tendon as early as 3 to 7 days after injury, but only 28 after the initial tendon injury M2 macrophages are the predominant macrophage phenotype (Sugg et al., 2014) (**Figure 13**).

During this time, these macrophages have been linked to an increase in the release of anti-inflammatory cytokines such as IL-1Ra, IL-10, IL-13, and growing factors like ββ (Sugg et al., 2014), NLRP3 inflammasome inhibition (Pelegrin & Surprenant, 2009), cell proliferation, and ECM formation (de la Durantaye et al., 2014). Therefore, these cells have less capacity to kill intracellular and produce minimal levels of pro-inflammatory molecules (Koh & DiPietro, 2011; Mosser & Edwards, 2008). The phagocytic property of macrophages can be the responsible for convert macrophages to an M2 phenotype by phagocytosis of apoptotic cells (Fadok et al., 1998), and also adipose-derived mesenchymal stromal cells are able to induce the conversion to M2 phenotype (Manning et al., 2015). So, the M2

macrophage are involved at the end of the inflammatory response and in the transition into cell proliferation and tissue deposition within the injured tendon. M2 macrophages may also be linked to increased scar formation as an accumulation of macrophages in the areas of adhesion formation within the healing tendons has been shown (Wojciak & Crossan, 1993). Thus, while M2 macrophages can have a pro-regenerative effect with new matrix synthesis, the resulting newly-formed tissue still does not regenerate the structure, composition, and material properties of normal tendon. How the tendon achieves a complete recovery is not well established yet.

3.2.3. Role of cytokines in tendon healing

Several pro-inflammatory and anti-inflammatory cytokines are produced during the tendon healing process by immune cells recruited in the injured site such as neutrophils and macrophages. However, not only immune cells are responsible for cytokines release, also resident tenocytes have been described to produce several endogenic cytokines and growth factors that act in an autocrine and paracrine manner on tenocytes (Pufe et al., 2001; Tsuzaki et al., 2003).

Pro-inflammatory cytokines in tendon healing

Tenocytes express the IL-1R1, so they are sensible to IL-1β signaling (Tsuzaki et al., 2003). In human tenocyte cultures, IL-1β accelerate the degradation of tendon ECM and the loss of the biomechanical resistance and durability of tendon, by the induction of inflammatory and catabolic factors such as cyclooxygenase (COX)-2, prostaglandin (PG)E2, and several matrix metalloproteinases (MMPs) (Archambault et al., 2002; Corps et al., 2002; Yang et al., 2005). Also, IL-1β is up-regulated in ruptured tendon (Berglund et al., 2007). Furthermore, type I collagen expression is downregulated by IL-1β, leading to a reduced stiffness, and also elastin expression is increased in these conditions, with an increase in tendon elasticity and subsequently decrease in tendon elastic modulus (Qi, Chi, et al., 2006). Interestingly, extrinsic fibroblasts that migrate from outside into the healing tendon are less sensitive to IL-1β than tenocytes (John et al., 2010).

Tenocytes also express TNF receptor (TNFR)1 and TNFR2, and both are up-regulated by TNF-α, and also TRAF2 is expressed in tendon (Hosaka et al., 2004). When tenocytes are stimulated with TNF-α, they produce pro-inflammatory cytokines such as IL-1β, TNF-α, and IL-6, but also anti-inflammatory cytokines such as IL-10, and matrix degradative enzymes like MMP1. However, it is not known the type of inflammasome that could be

activated in tenocytes to produce IL-1β. Also, expression of some other ECM components such as elastin are up-regulated by TNF-α (John et al., 2010). TNF-α is up-regulated in inflamed tendons and expressed in scar-formed tendon (Hosaka, Kirisawa, et al., 2005). In addition, TNF-α has been shown to have a pro-apoptotic effect in inflamed tendons, being involved in tendinitis and tendon degeneration (Hosaka, Teraoka, et al., 2005). However, TNF-α is shown to inhibit pro-apoptotic Fas ligand expression in tenocytes derived from close sites of osteoarthritic joints, but not derived from healthy patients (Machner et al., 2003). Altogether, these opposite results indicates that TNF-α pro- or anti-apoptotic affects depend on the environment and particular co-stimuli. In contrast, TNF-α can be considered as a key regulator in degeneration of tendons.

Mechanical factors can also influence cytokine production in tendon, for example heat stress, which can occur during prolonged tendon exercise or overuse, induce TNF-α but not IL-1β expression (Hosaka et al., 2006), and stress deprivation leads to an overexpression of pro-inflammatory cytokines including IL-1β and TNF-α with the subsequent mechanical tendon deterioration (Uchida et al., 2005). Also, TNF-α expression is lower in loaded compared with unloaded tendon repair callus during healing, meaning that mechanobiology is important on healing (Eliasson et al., 2009). In addition, IL-1β impairs the Young's modulus in human tenocytes, which allow the cells to endure higher mechanical loading in damaged tendon (Qi, Chi, et al., 2006). Moreover, IL-1β regulate tenocytes cytoskeletal polymerization and their stiffness which is an important precondition for the cell to adapt to mechanical loading in tendon (Qi, Fox, et al., 2006). Altogether, IL-1β and TNF-α can be considered to have a main role in constructive remodeling of the tendon.

The role of IL-6 in tendon healing is more related to immunoregulatory processes, playing an essential role in this development (Lin et al., 2006; Lin et al., 2005). IL-6 is highly up-regulated in tenocytes after IL-1β and TNF-α treatment (John et al., 2010; Tsuzaki et al., 2003), or after cyclic mechanical stretching (Skutek et al., 2001). In addition, IL-6 production is increased in ruptured tendons (Nakama et al., 2006), and is also up-regulated in tendon and peritendon tissue during exercise (Skutek et al., 2001). After its production, IL-6 is able to induce slightly increase in IL-10 expression, but not its own or IL-1β and TNF-α expression (John et al., 2010). The absence of IL-6 reduces the mechanical properties of healing tendons compared with normal tendons, with a subsequent tendon healing impairment (Lin et al., 2006; Lin et al., 2005). Also, other pro-inflammatory cytokines such as IL-1α, IL-13, and IFN-γ are increased in inflamed native tendon (Hosaka et al., 2002).

Anti-inflammatory cytokines in tendon healing

IL-10 has a main role in tissue healing as is produced by and affect connective tissue cells such as fibroblasts and chondrocytes (Iannone et al., 2001; Yamamoto et al., 2001). Tenocytes also express the type I receptor of IL-10 (IL-10R1) and its expression, as well as IL-10, is induced by pro-inflammatory cytokines like TNF-α (John et al., 2010). Superior healing properties in the absence of IL-4 are related with an up-regulation of IL-10 (Lin et al., 2006). Also, time-dependent effects of IL-10 on biomechanics of healing tendons has been described (Ricchetti et al., 2008). However, the role of IL-10 in tendons and its partnership with another anti-inflammatory cytokines as IL-4 or IL-13, also reported to stimulate tenocytes proliferation (Courneya et al., 2010), is still unclear.

Growth factors in tendon healing

The role of ββ in tendon healing is not only restricted to the last stages of tendon healing since it has been shown to be active in almost all stages of this process (Chang et al., 2000). So, TGF-β has a critical role in tendon healing promoting matrix development (Glass et al., 2014). TGF-β has been linked to the inhibition of pro-inflammatory cytokines including IL-1β, IL-8, GM-CSF, and TNF-α (Fadok et al., 1998). However, its function is not only limited acting as an anti-inflammatory cytokine. TGF-β has also other functions including the stimulation of extrinsic cell migration, the regulation of proteinases (Bennett & Schultz, 1993), the promotion of fibronectin binding interactions (Wojciak & Crossan, 1994), the inhibition of cell proliferation (Zhu et al., 2001), and the stimulation of collagen production (Marui et al., 1997). During tendon healing, neutrophils are phagocyted by macrophages and production of TGF-β by them is also increased. Also, TGF-β increases ECM and collagen production, and inhibits collagen failure, subsequently promoting healing mainly through scar formation (Barrientos et al., 2008). In concrete, TGF-β regulates ECM assembly and remodeling through two different pathways, one that reduces matrix degradation and the other that stimulates matrix accumulation. To do it, TGF-β inhibits the synthesis of extracellular proteinases, and upregulates both the production of proteinases inhibitors and the structural ECM components. Specifically, TGF-β is a key regulator of α1(I) procollagen gene (*COL1A1*) and α2 procollagen gene (*COL1A2*) (Chung et al., 1996; Jimenez et al., 1994). Three TGF-β isoforms are present in mammals, TGF-β1, β2 and β3, and the lack of each one triggers a different phenotype (Bottinger et al., 1997). After tendon injury, TGF-β1 expression is increased in a short period of time, and its production can be induced by lactate (Klein et al., 2001). The levels of this isoforms can remain high for at least

8 weeks after tendon injury, being initially extracellular TGF-β released by immune cells and later cell-associated reflecting *de novo* synthesis (Natsu-ume et al., 1997). TGF-β1 function is dependent on its concentration and has the ability to synergize with other growth factors (Centrella et al., 1991). So, high levels of TGF-β1 are implicated in tendon adhesion formation, decreasing the range of motion of a tendon (Chan et al., 1997). Interestingly, fetal wound healing is characterized by low expression of TGF-β1 and TGF-β2 and high expression of TGF-β3. The opposite is observed in adult wound healing, that is characterized by high levels of TGF-β1 and TGF-β2 and low levels of TGF-β3 (Kim et al., 2011). Furthermore, all three isoforms have effects on type I and III collagen production and cell viability (Klein et al., 2002). In addition, the three isoforms can bind to three different TGF-β receptors (TGFβR) called TGFβR1, R2 and R3, and all of them are up-regulated during tendon healing, both in the tendon and in the epitenon (Ngo et al., 2001).

Despite of having a role in early cellular migration and proliferation, vascular endothelial growth factor (VEGF) is most active after inflammation, during the proliferative and remodeling stages, stimulating angiogenesis (Jackson et al., 1997). This neovascularization induced by VEGF proceeds along the surface of the epitenon, through a normally avascular area, and provides extrinsic cells, nutrients, and other grow factors to the injured area (Molloy et al., 2003). Levels of VEGF has been measured among time after tendon injury, remaining at baseline at days 0 and 4, having a peak at day 7, and then stable declining back to baseline by day 21 (Boyer et al., 2001). This temporal expression of VEGF is consistent with increased vessel length and density observed in and around the tendon repair site after inflammation with a peak at 17 days (Gelberman et al., 1991). VEGF is expressed in the major part of the cells on the injury site, but less expressed in the epitenon cells distant from the site of repair, and its production can be induced by hypoxia and IL-1β (Jackson et al., 1997). Finally, exogenous VEGF applications has been shown to decrease the stiffness of grafted ligaments (Tohyama et al., 2009; Yoshikawa et al., 2006).

3.3. Tendinopathy and chronic inflammation

3.3.1. Tendinopathy and chronic inflammation

Inflammation is one the first events occurring in tendinopathy lesions, even before fibrotic and other degenerative changes in the tendon (Fedorczyk et al., 2010). So, inflammation plays an important role in the early initiation of tendon pathologies. The main causes of tendinopathy are repetitive mechanical overloading and hypoxic injury (Millar et al., 2013; Neviaser et al., 2012), and repetitive mechanical overloading is characterized by

elevated levels of pro-inflammatory markers such as PGE2, TNF-α and IL-1β (Killian et al., 2012).

During exercise, tenocytes have a big demand of oxygen, and increasing oxygen demand during overload can lead to hypoxic conditions with the production of ROS (Yao et al., 2011). After this process, necrosis of different cell types is initiated and cell debris including several DAMPs are phagocytose by macrophages initiating an inflammatory response as described in previous chapters. In this inflammatory phase, IL-1β production has been linked to tendinopathy development. IL-1β induce the expression of the prostaglandin E2 receptor 4 (EP4) in tenocytes enhancing different inflammatory signaling pathways, and finally leading to tendon matrix degradation and tendinopathy. In addition, IL-1β downregulates the expression of type I collagen in tenocytes producing reduced deposition of ECM during tendinopathies (Thampatty et al., 2007). Finally, IL-1β effects are also linked to tendinopathy by the release of substance P contributing to inflammation (Fedorczyk et al., 2010). This initial inflammatory response is required to latter induce the healing process as described above, but aberrant or prolonged inflammation could lead to chronic tendinopathy.

Matrix changes in tendinopathies are characterized by alterations in fibroblasts composition with deposition of additional matrix protein and fibrosis, and a loss of structural organization of collagen (Kannus & Jozsa, 1991). In the initial phase of tendon damage, type III collagen is predominantly produced as a rapid cover to protect the damaged area (Maffulli, Barrass, et al., 2000). In normal tendons, the next step is characterized by the replacement of type III collagen for type I collagen, recovering the linear structured arrangement of the collagen fibers (Maeda et al., 2007). In tendinopathic tendons, this repair mechanism is impaired leading to type III collagen accumulation that has been linked to inferior biomechanical strength and irregular alignment of collagen fibers (Maffulli, Ewen, et al., 2000). On one hand, TGF-β has been described to regulate the collagen architecture during tendon development (Lorda-Diez et al., 2009). The overproduction of TGF-β by the M2 macrophage may be a factor in excessive fibrosis, and has been linked with the development of pathological fibrotic conditions in other tissues (Colwell et al., 2005). Furthermore, diabetic murine flexor digitorum longus tendon shows fibrotic healing and an increase in M2 macrophage activity. These fibrotic tendons exhibit compromised biomechanical strength compared to the repaired tendons of the non-diabetic control group (Ackerman et al., 2017). On the other hand, IL-6 has been described to be a key regulator of collagen synthesis in tendinopathy. Prolonged running causes an increase in the tissue concentration of IL-6 with

an accompanied increase in total collagen synthesis. In addition, recombinant IL-6 administration locally induces collagen synthesis in the peritendinous tissue achieving similar levels as with exercise (Langberg et al., 2002). Also, recombinant TNF-α treated tenocytes present reduced type I collagen deposition which is detrimental to the tendon ECM (John et al., 2010).

Tendinopathy is also linked to another cytokines, such as IL-4, IL-33 or IL-17. In mice model of tendinopathy, the absence of IL-4 is related to lower cross-sectional tendon and worse mechanical properties (Lin et al., 2005). IL-33 is released after biomechanical overload (Kakkar et al., 2012) and cellular damage (Schmitz et al., 2005), and its expression is increased in human tendinopathy compared with normal tendon. Moreover, addition of recombinant IL-33 to human tenocyte cultures induces expression of type III collagen and also of pro-inflammatory cytokines like IL-6 (Millar et al., 2015). IL-17 increased expression has been shown in early tendinopathy before the presence of abnormalities in the tissue. Also, the addition of recombinant IL-17 to human tenocyte cultures induces pro-inflammatory cytokines release and ECM remodeling through type III collagen production (Millar et al., 2016).

3.3.2. Tendinopathy treatments

A wide range of treatments are recommended to treat tendinopathy. All the treatments have the same goals: to reduce symptoms and pain, promote correct tendon healing, and improve tendon function; but so far, there are not a single treatment reaching all these goals. Tendinopathy treatments can be divided into two groups, including passive modalities and active modalities. Passive treatments include pharmacological treatments, injection therapy, extracorporeal shockwave therapy (ESWT), ultrasonography and low-level laser, and active treatments include tendon loading exercise, patient education, and load management (Aicale et al., 2020; Andres & Murrell, 2008; Millar et al., 2021). Recently, a novel physiotherapeutic treatment which is the ultra-sound guided percutaneous electrolysis has been observed to be very effective in the treatment of tendinopathies and because of the interest for this Thesis is going to be explained in detail in the following section (section 3.3.3).

Exercise-based strategies

Exercise regimens called tendon loading programs are the most effective treatment for tendinopathy, being effective in patients with chronic Achilles tendinopathy and patellar

tendinopathy (Lim & Wong, 2018; Visnes & Bahr, 2007). In addition, eccentric training is an effective treatment used in a wide variety of tendinopathies such as common extensor and rotator cuff tendinopathy (Camargo et al., 2014; Murtaugh & Ihm, 2013). The success or the failure of the prescribed loading programs remains in the adherence of the patient to the selected program (Mallows et al., 2017). After exercise-based therapies, tendons respond favorably to load through the improvement in their mechanical, material and morphological properties, but the major part of studies investigating this effect are performed in healthy individuals (Bohm et al., 2015). Also, isometric exercise has been proposed as a proper treatment for patellar tendinopathy because of the dramatic reduction in pain due to its analgesic effects (Rio et al., 2015). However, these effects have not been confirmed in subsequent studies in patients with patellar tendinopathy (Holden et al., 2020), Achilles tendinopathy (O'Neill et al., 2019), and plantar fascia pain (Riel et al., 2018). Finally, heavy slow resistance (HSR) training is an effective treatment for tendinopathies by changing fibril morphology towards a more near to normal appearance (Kongsgaard et al., 2010). Clinical trials studying the efficacy of the use of exercise for tendinopathy treatment has been developed for different exercise-based protocols such as low load exercise or coactivation strengthening (Boudreau et al., 2019; Dejaco et al., 2017). However, not all patients respond to this type of treatments, so, other treatments are used alternatively or in combination with exercise.

Non-steroidal anti-inflammatory drugs

The use of NSAIDs is mainly restricted to reduce pain related to tendinopathy. Oral and local NSAIDs administration appear effective in the treatment of acute tendonitis (Mazieres et al., 2005), but not for the treatment of lateral epicondylitis or Achilles tendinopathy (Astrom & Westlin, 1992; Hay et al., 1999). In addition, long-term NSAID use increase the risk of gastrointestinal, cardiovascular and renal complications. Altogether, NSAIDs are a reasonable treatment to avoid acute pain associated with tendon overuse, but not for the treatment of chronic tendinopathies.

Corticosteroid injection

The use of corticosteroid injection is under discussion because the effectiveness of this treatment is controversial. Tendinopathy has an important inflammatory component associated with an aberrant healing response (Millar et al., 2017), so it is logical to think that corticosteroid would help diminishing this inflammatory response. However, some studies have demonstrated that the treatment with corticosteroids can impair the physiological

healing process leading to progression of tendinopathy (Dean et al., 2014; Puzzitiello et al., 2020). In concrete, no beneficial effects after corticosteroid injection are observed for rotator cuff tendinopathy (Mohamadi et al., 2017), lateral elbow tendinopathy (Claessen et al., 2016), patellar tendinopathy (Everhart et al., 2017), and Achilles tendinopathy (Gross et al., 2013; Kearney et al., 2015). For all these reasons, corticosteroid injection is very little used for tendinopathy treatment.

Glyceryl trinitrate therapy

The administration of glyceryl trinitrate topically is considered a safe and reliable treatment for the management of tendinopathy with significant improvements in pain in short-term and up to 6 months after injury (Challoumas et al., 2019). However, this therapy has some side effects and can be associated with increased incidence of headaches (Nevins & Kanakala, 2020).

Low-energy laser therapy

Low-energy laser therapy uses light at energy levels low enough not to cause a rise in skin temperature. Several studies show the ability of this therapy to reduce inflammation and edema, to induce analgia, and to promote healing in a wide range of musculoskeletal disorders (Cotler et al., 2015). Regarding tendinopathy, the efficacy of this treatment has been shown in lateral elbow tendinopathy (Bjordal et al., 2008), Achilles tendinopathy (Gomes et al., 2017), and rotator cuff tendinopathy (Haslerud et al., 2015), but only with limited healing effects.

High-volume injections

High-volume injections are defined as the injection of a large volume of saline, usually mixed with corticosteroids and/or local anesthesia. This treatment is mainly used for Achilles tendinopathy, but also some evidences are shown for the treatment of patellar tendinopathy (Barker-Davies et al., 2017). In Achilles tendinopathy, high-volume injections applied in combination with eccentric training are able to reduce pain, return patients to prior levels of physical activity, and reduce tendon thickness and intratendinous vascularity compared with exercise alone (Boesen et al., 2017). However, the use of this therapy has been only tested in studies with low amounts of patients, limiting the potential benefits of this treatment.

Shockwave therapy

Shockwave therapy is based on the use of high-energy pressure waves. The effectiveness of this treatment has been shown in Achilles tendinopathy, patellar tendinopathy and proximal hamstring tendinopathy, showing increased effects compared with anti-inflammatory medication or physical therapy, or similar effects compared with eccentric training (Korakakis et al., 2018). This treatment is able to alleviate pain and improve physical performance, so it has been proposed to be considered the main therapy for the treatment of patellar and Achilles tendinopathy when other non-surgical treatments fail (Mani-Babu et al., 2015). Also, its efficacy in lateral elbow tendinopathy has been shown with the previous mentioned beneficial effects (Yan et al., 2019).

Sclerotherapy

Sclerotherapy involves the injection of a sclerosing agent into a blood vessel, resulting in a selective sclerosis of that vessel. The injection of a sclerosing agent, normally polidocanol, into the areas of neovascularization can also eradicate the pain-generating nerve fibers. Some clinical trials evaluating the treatment of tennis elbow tendinopathy, patellar tendinopathy and Achilles tendinopathy with sclerotherapy has been performed (Hoksrud et al., 2006; Ohberg & Alfredson, 2002; Zeisig et al., 2006). The benefits of this therapy have been studied largely in Achilles tendinopathy, showing a considerable decrease in main pain (Alfredson & Ohberg, 2005; Lind et al., 2006). However, although polidocanol injections appears to provide pain relief, it is unclear what role they might play in tendon healing in tendinopathy, and some complications related with this treatment such as tendon rupture has been also reported (Alfredson & Cook, 2007).

Platelet-rich plasma

Platelet-rich plasma (PRP) is a preparation of autologous blood centrifuged to obtain high concentration of platelets, with or without leukocytes. Although PRP continues to be used as a therapy, studies have not confirmed a significant efficacy for PRP in the treatment of tendinopathy (Franchini et al., 2018; Zhou & Wang, 2016). Some controversial results are observed in PRP treatment when is applied. Regarding lateral elbow tendinopathy there are some studies showing a significant improvement in pain after PRP treatment (Arirachakaran et al., 2016; Mishra et al., 2014), but a meta-analysis published in 2014 do not support the use of PRP for lateral elbow tendinopathy (de Vos et al., 2014). Similar controversy is

reported for patellar tendinopathy (Liddle & Rodriguez-Merchan, 2015; Scott et al., 2019), and for Achilles tendinopathy (Liu et al., 2019; Nauwelaers et al., 2021).

Cell therapy

Cell therapy is based on the use of progenitor or stem cells from bone-marrow or adipose tissue as well as autologous tenocytes. Cell therapy has been shown to be effective to treat a wide range of tendon disorders, including rotator cuff tendinopathy, lateral elbow tendinopathy, patellar tendinopathy and Achilles tendinopathy with level 3 of evidence (van den Boom et al., 2020). In the case of Achilles tendinopathy, injection of adipose-derived stem cells shows reduced pain and improved physical function scores at 15 and 30 days after treatment (Usuelli et al., 2018). This therapy has shown promising results but it is novel and require further studies.

Surgery

Surgery for tendinopathies intends to promote a regenerative healing response by triggering a reparative response in the matrix environment. Surgical procedures for tendinopathy involve excision of the degenerative tendon, removal of adhesion around the tendon, decompression of the tendon and/or multiple longitudinal tenotomies (Andres & Murrell, 2008). In patients with Achilles tendinopathy no studies comparing surgery and non-operative treatments has been performed. For patellar tendinopathy, no differences are observed comparing surgery and eccentric loading alone (Bahr et al., 2006), but seems to be better in pain relief compared with sclerosing agents (Willberg et al., 2011). Also, for rotator cuff tendinopathy, no significant differences are observed comparing surgery with plasma-rich platelets injections (Carr et al., 2015), with supervised physiotherapy regimen (Ketola et al., 2017), or with exercise alone (Beard et al., 2018). Finally, in lateral elbow tendinopathy, surgery has been found to provide better long-term pain relief than plasma-rich platelets injections (Merolla et al., 2017).

3.3.3. Ultrasound-guided percutaneous electrolysis

Percutaneous electrolysis is based on the application of galvanic current using a percutaneous needle, and is an emerging and minimally invasive technique that pursues to regenerate damaged tissues (Valera-Garrido et al., 2014). Ultrasound equipment is used to guide the needle used to apply galvanic current into affected soft tissues by direct visualization. Once in the affected area, galvanic current application is able to stimulate

locally the cells. Application of percutaneous needle electrolysis is able to induce a local controlled microtrauma by combining mechanical and electrical stimulation of the tissue. This microtrauma in turn generates a local inflammatory response that makes possible and encourages the repair of the affected tissue (Valera-Garrido et al., 2019). Galvanic current has been successfully used to repair chronic non-resolving lesions, such as tendinopathies developed after prolonged extreme exercise, which often establish a degenerative condition of the tissue that impairs healing and complicates clinical management (Cook & Purdam, 2009; Regan et al., 1992; Soslowsky et al., 2000). As mentioned before, in randomized trials, anti-inflammatory therapies have shown to be ineffectual at treating these types of lesions (Bisset et al., 2006; Coombes et al., 2013) and application of galvanic currents by percutaneous needle alone has been found sufficient when it comes to regenerating the tissue (Bubnov et al., 2013; Chellini et al., 2019; De-la-Cruz-Torres et al., 2020; Margalef et al., 2020; Valera-Garrido et al., 2020; Valera-Garrido et al., 2014; Valera-Garrido et al., 2013). However, the detailed molecular and cellular mechanism behind ultrasound-guided percutaneous electrolysis inducing an inflammatory response is not well known.

OBJECTIVES

The following specific objectives were proposed for the present Thesis:

1. Determine the effect of autoinflammatory-associated NLRC4 mutations on the structure of NLRC4.
2. Evaluate the activation of the NLRC4 and NLRP3 inflammasome by fluorescence microscopy.
3. Characterize the effect of galvanic current application in the activation of the NLRP3 inflammasome in macrophages.
4. Study the implication of the NLRP3 inflammasome in the inflammation and regeneration responses in the Achilles tendon of mice after percutaneous needle electrolysis application.
5. Elucidate the role of NLRP3 inflammasome in a mouse model of sterile tissue damage.

MATERIALS AND METHODS

1. Mice

Mice aged between 6 and 12 weeks were used. Mice were maintained under specific pathogen free (SPF) conditions, with food and water *ad libitum*, with a constant temperature of 25ºC and a light-dark cycle of 12 h. Animal procedure was refined and approved by the University of Murcia animal experimentation committee and approved by the *Animal Service, Murcia Fishing and Farming Council* (reference A13160702). All the strains used were wild-type C57BL/6 mice, NLRP3-deficient mice (*Nlrp3*$^{-/-}$) (Martinon et al., 2006), Caspase-1/11-deficient mice (*Casp-1/11*$^{-/-}$) (Kuida et al., 1995), and ASC-deficient mice (*Pycard*$^{-/-}$) (Mariathasan et al., 2004), all on C57BL/6 background and its use was approved by the Biosecurity committee of the University of Murcia (reference CBE215).

Mice were euthanized with CO_2 at different days after treatments (section 2). The paws were dissected and prepared for Achilles' tendon dissection (section 3), for histological studies (section 5) or for biomechanical testing (section 6).

2. Mice procedure

2.1. Percutaneous needle electrolysis procedure

Mice were anesthetized with a mixture of isoflurane (IsoFlo, Zoetis) at 0.3 ml/h and 1% of O_2, and one Achilles tendon was treated with dry puncture, as a control for the puncture, and the other with percutaneous needle electrolysis. Dry puncture was performed making three punctures on the tendon zone using 16 G and 13 mm acupuncture needles (Agupunt). Percutaneous needle electrolysis was performed making one puncture on the tendon zone and using the protocol called "3-3-3" (3 impacts of 3 milliamps during 3 seconds each one) using an acupuncture needle and a Physio Invasiva® equipment (Prim) (**Figure 14**). Also, tendons without puncture were used as controls. Percutaneous needle puncture effect was evaluated 3, 7, 14 and 21 days after treatment. In addition, dry puncture or percutaneous needle electrolysis were performed 14 and 21 days after collagenase injection (see section 2.2). Also, three treatments with dry puncture or percutaneous needle electrolysis were performed 7 days after collagenase injection (see section 2.2), and the treatments were applied every 3 days.

Figure 14. Representative image of the puncture of Achilles tendon. Achilles tendon puncture with an acupuncture needle is shown.

2.2. Collagenase-induced sterile damage

Mice were anesthetized with isoflurane at 0.3 ml/h and 1% of O_2. One Achilles tendon was treated with 20 µl of collagenase A or denatured collagenase A at 10 µg/µl, and the other with 20 µl of saline solution, as a control. Also, non-treated tendons were used as controls. Denaturation of collagenase was performed incubating collagenase for 1 h at 100ºC with shaking. Collagenase effect was evaluated 1, 3, 7, 10, 14, 21 and 28 days after collagenase injection.

3. Mice Achilles tendon dissection

Mice were euthanized with CO_2, and Achilles' tendons were surgically dissected. Before tendon dissection, paws were skinned carefully to avoid tendon rupture. Achilles' tendon dissection was performed making two cuts in its ends, one in the calcaneal area and the other in the gastrocnemius area, to separate it from the back of the leg.

Once dissected, Achilles' tendon was either completely submerged in RNAlater (Sigma-Aldrich) to keep RNA integrity during 24 h and after, were stored at -80ºC until RNA isolation, or were preserving tibia and adipose tissue and submerged in homo-buffer (70 mM sucrose, 220 mM mannitol, 2 mM Tris-HCl pH: 7,4, 0,1 mM EDTA, 0,1% bovine serum albumin (BSA), proteases and phosphatases inhibitors) and stored at -80ºC for further homogenization.

4. Mice tendon homogenization

Once dissected, tendons were homogenized with homo-buffer and using a Digital Tissue Homogenizer (OMNI International). After homogenization, sample was incubated during 15 min at 4ºC vortexing them from time to time. Sample was then centrifuged at 10,000 rpms during 15 min at 4ºC. Supernatants were collected avoiding contamination from the pellet, transferred to a new tube and stored at -80ºC.

5. Histological studies

5.1. Sample processing

Mice dissected paws were skinned and placed into a histology cassette. The cassette was submerged into 4% buffered formalin solution (DiaPath) during 48 h. Once fixed, samples were sized delimiting the exam zones (tendon and peritendon). After sizing, samples were decalcified in a 40% formic acid solution (Shandon TBD-2 Decalcifier, Thermo Scientific) during 8-12 h.

After decalcification, samples were included in paraffin and processed into a KOS Microwave Multifunctional Tissue Processor (Milestone). Paraffin blocks were ravaged until reaching the interest zone. Then, blocks were cut with a 3 µm thickness. The ravage and the cut of the samples were done with a HM 355S Automatic Microtome (Thermo Scientific). The samples cuts were placed in slides and introduced in an incubator during 1 h at 60ºC to remove the excess of paraffin. Sample cuts were stained (sections 5.2, 5.3 and 5.4) or used for immunohistochemistry (section 5.5).

5.2. Hematoxylin-eosin staining

Hematoxylin-eosin staining was done following a general protocol with serial steps using different solutions. Slides were subsequently submerged into a xylene substitute (Richard-Allan Scientific Clear-Rite 3, ThermoFisher Scientific) twice, in absolute ethanol twice, in 96% ethanol and in 70% ethanol during 5 min each time. Then, slides were washed with water during 5 min.

After rinse them with distilled water, slides were submerged in a hematoxylin solution (Shandon Harris Hematoxylin, ThermoFisher Scientific) during 2 min. After hematoxylin staining, slides were washed again with water during 5 min, rinsed with distilled water and submerged in 70% ethanol during 3 min. Then, the slides were submerged in an alcoholic

eosin solution (Shandon Eosin Y Cytoplasmic Counterstain, ThermoFisher Scientific) during 1 min. After eosin staining, slides were submerged in 96% ethanol twice during 1 min each time, in absolute ethanol twice during 3 min each time and in a xylene substitute twice during 5 min each time.

At the end, the mounting of the coverslip over the slides was done. One drop of permanent mounting media (ClearVue Mountant, Thermo Scientific) was placed between the coverslip and the slides for a correct fixation. All slices were examined with a Zeiss Axio Scope AX10 microscope and pictures were taken with an AxioCam 506 Color (Carl Zeiss).

5.3. Sirius red staining

Sirius red staining of collagen was performed using the Picro Sirius red staining kit (Abcam) and following the manufacturer's instructions. Slides were subsequently submerged into a xylene substitute twice, in absolute ethanol twice, in 96% ethanol and in 70% ethanol during 5 min each time. Then, slides were washed with water during 5 min.

After rinse them with distilled water, slides were submerged into the Picro Sirius red solution (Abcam) during 60 min. After Sirius red staining, slides were rinsed twice with 0,5% acetic acid. Then, the slices were submerged in 96% ethanol during 1 min, in absolute ethanol twice during 3 min each time and in a xylene substitute twice during 5 min each time.

At the end, the mounting of the coverslip over the slides was done as mentioned before. Images were taken under polarized light which allowed us to differentiate between type I collagen and type III collagen (**Figure 15**).

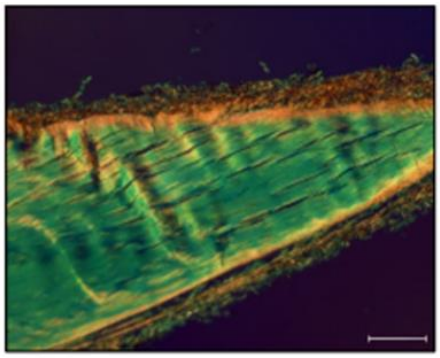

Figure 15. Representative image of calcaneal tendon section stained with picrosirius red and viewed with polarized light. Type I collagen is shown in red/yellow color and type III collagen is shown in green color, scale bar 100 µm.

Collagen type quantification was evaluated using a custom script based on the number of pixels of each color and calculating the percentage of type I or III collagen according to the following equations:

$$\%\ \text{of type I collagen} = \left(\frac{nº\ red/yellow\ pixels}{(total\ nº\ pixels - background\ pixels)}\right) x100$$

$$\%\ \text{of type III collagen} = \left(\frac{nº\ green\ pixels}{(total\ nº\ pixels - background\ pixels)}\right) x100$$

All slices were examined with a Zeiss Axio Scope AX10 microscope and pictures were taken with an AxioCam 506 Color (Carl Zeiss).

In addition, sirius red-stained slices under polarized light were used to quantify different characteristics of collagen by converting pictures to SHG color and then using the CT-Fire algorithm to automatically calculate width and length of collagen fibers in these pictures (Y. Liu et al., 2017).

5.4. Toluidine blue staining

Toluidine blue staining was performed to count mastocytes using a toluidine blue polychrome solution (Bio-Optica) for the metachromatic staining of acid substances. Slides were subsequently submerged into a xylene substitute twice, in absolute ethanol twice, in 96% ethanol and in 70% ethanol during 5 min each time. Then, slides were washed with water during 5 min.

After rinse with distilled water, slides were submerged into the toluidine blue solution (Bio-Optica) during 5 min and washed with water during 5 min. After rinse with distilled water, slides were submerged in 96% ethanol twice during 1 min each time, in absolute ethanol twice during 3 min each time and in a xylene substitute twice during 5 min each time.

At the end, the mounting of the coverslip over the slides was done as mentioned before. All slices were examined with a Zeiss Axio Scope AX10 microscope and pictures were taken with an AxioCam 506 Color (Carl Zeiss).

5.5. Immunohistochemistry

Immunohistochemistry was done for the detection of the mouse macrophage F4/80 antigen using an EnVision+ Sytem-HRP kit (Dako). Slides were subsequently submerged into a xylene substitute twice, in absolute ethanol twice, in 96% ethanol and in 70% ethanol

during 5 min each time. Then, slides were washed with water during 5 min and rinsed with distilled water.

After washing, slides were introduced in an oven with a citrate solution at pH 6.1 (Target Retrieval Solution, Dako) during 30 min at 98ºC and, after, washed with Tris-buffered saline (TBS) during 5 min three times. After washing, the inhibition of the peroxidase was produced incubating the slides with a H_2O_2 solution supplied in the kit during 5 min. Then, slides were washed with T-TBS (TBS 1X, 0.05% Tween) during 4 min. After washing, the primary antibody mouse/rat/rabbit anti-F4/80 antigen (MCA497GA, R&D) diluted 1:50 was added to each slide and incubated O/N at 4ºC. After incubation, slides were tempered in an incubator during 10 min at 37ºC. Slides were washed with T-TBS during 3 min.

After washing, an ImPRESS-HRP goat anti-rat IgG polymer reagent was used as a secondary revealing agent (MP-7404, Vector) and was added to each slide and incubated 30 min at 37ºC. Then, slides were incubated with a 3-3'-diaminobenzidine (DAB) solution composed of DAB+ substrate buffer and DAB+ chromogen (K4007, Dako) supplied with the kit during 5 min. The revealed step produced a positive immunoreaction in dark brown color. A washing step with water was done during 5 min and slides were rinsed with distilled water. After washing, slides were submerged in 96% ethanol during 1 min, in absolute ethanol twice and in a xylene substitute twice during 5 min each time. At the end, the mounting of the coverslip over the slides was done as mentioned before.

5.6. Qualitative evaluation of the samples

Hematoxylin and eosin-stained slices were initially evaluated in a 0 to 3 qualitative scale, being 0 control (healthy tendon) conditions, 1 mild, 2 medium, and 3 severe, for inflammatory infiltrate, tendon cellularity grade and neovascularization. The median value for each of the paws was used as the final value represented in the figures. There were some groups with intermediate values between stages qualified like 0/1, 1/2 and 2/3, expressing a grade intermediate between both.

5.7. Polymorphonuclear cells, macrophages and mastocytes count

Polymorphonuclear cells, macrophages and mastocytes count was made counting three independent fields per sample and in at least 3 independent samples. The count was carried out in the peritendon and adipose tissue surrounding the tendon. The zones with

more cellularity were selected to make the pictures. Pictures were taken with an AxioCam 506 Color (Carl Zeiss) with a 40× objective.

5.8. Tenocyte's nuclei and collagen fibers evaluation

The number and area of tenocytes nuclei was evaluated using a homemade FIJI macro with the help of Dr. Ángel Bernabé García. In brief, hematoxylin and eosin-stained slices were loaded to the program and converted into 8-bit format. After that, a manual triangle threshold to select nuclei was performed and a subtraction of the background was applied. A step of erosion with "Erode" tool was performed for a better separation of proximate nuclei. The selected nuclei were converted to mask and its number, area and circularity were measured with the "Analyze particles" tool.

6. Biomechanical testing

Achilles' tendons were dissected following the protocol described in (Rigozzi et al., 2009). In brief, tendons were dissected maintaining intact the calcaneus and the gastrocnemius/soleus muscles. The tendon sheaths were also maintained in order to preserve the natural anatomical structure and relative orientation of the individual tendon bundles (**Figure 16A**). Gastrocnemius/soleus muscle fibers were then cautiously removed to expose the intramuscular tendon fibers (**Figure 16B**). All mechanical tests were performed with an Autograph AG-X plus 50N-5KN machine (Shimadzu) with a speed of 0.1 mm/s and 1 kN load head. Specimens were clamped for testing with the calcaneus mounted to approximate a neutral anatomical position (**Figure 16C**). Tendon area was calculated measuring tendon width in two segments, frontal and lateral. Tendon area and length were then used to calculate stiffness of tendons. Other parameters as maximum force and maximum tension were also obtained. Elastic module was calculated as the slope of the curve generated representing force vs displacement. The slope was calculated taking into account the curve generated only between 1-2 N of force. All parameters were obtained using Trapezium X software (Shimadzu).

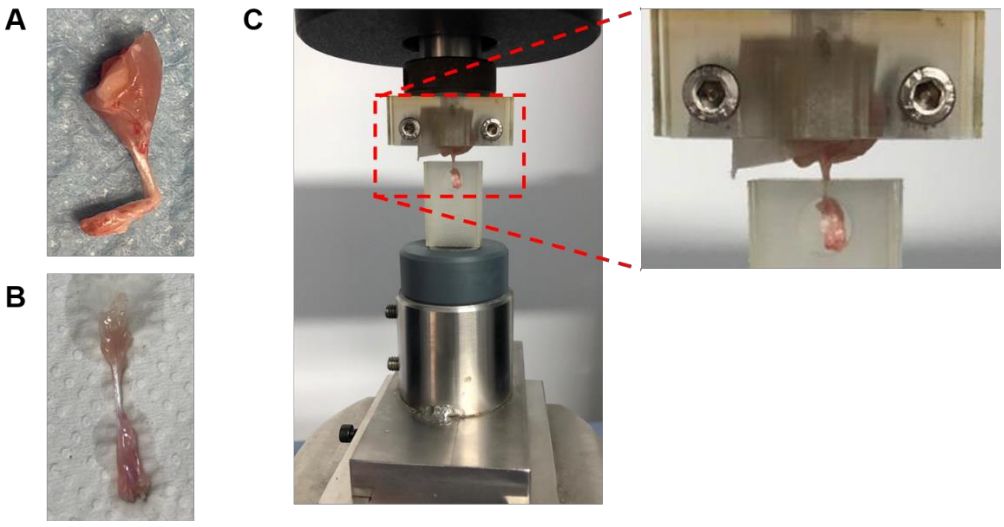

Figure 16. Clamps designed to measure tendon tension. (A) Image illustrating mice paws after dissection, maintaining intact the calcaneus and the gastrocnemius/soleus muscles. **(B)** Image illustrating mice paws after muscle fibers were removed to expose the intramuscular tendon fibers of the calcaneal tendon. **(C)** Image illustrating the orientation and the position of mice paws in the biochemical testing of the calcaneal tendon before starting the load.

7. Bone marrow-derived macrophages culture

7.1. Differentiation of mouse bone marrow-derived macrophages

Mice were euthanized with CO_2, and long bones (tibia and femur) were dissected. Bone marrow extraction was flushed by the irrigation of 20 ml macrophage differentiation medium in the medullar cavity by using a syringe and a needle. Macrophage differentiation medium was composed by high glucose DMEM (Lonza), 15% fetal calf serum (FCS) (Invitrogen), 25% L929-cell culture supernatants (containing macrophage colony-stimulating factor (M-CSF)), 1% penicillin and streptomycin (P/S, Lonza) and 1% L-glutamine (Lonza). The suspension was seeded into three p150 Petri dishes (CellStar) and supplemented with 10 ml of differentiation medium, reaching a total volume of 20 ml per dish. Plates were incubated at 37ºC with a 5 % CO_2 atmosphere in a Healforce incubator (**Figure 17**).

Two days after, 20 ml of differentiation medium was added to each dish, and dishes were incubated at 37ºC and 5 % of CO_2 atmosphere. After 6 days of culture, the supernatant was discarded and cells were washed with phosphate-buffered saline (PBS) sterile solution, composed of NaCl (0.137 M), KCl (0.0027 M), Na_2HPO_4 (0.01 M) and KH_2PO_4 (0.0018 M). Cells were incubated with PBS at 4ºC during 5 min to let detachment of the cells, helping the recovery of the cells with manual scraping. Cell suspension was centrifuged at 400 xg during 5 min, supernatants were discarded and cells were suspended in synchronization

medium: DMEM medium with 20% of FCS and 1% Pencillin/Streptomicin. BMDMs were counted and seeded into well plates at a confluence of 10^6 cells/ml and used the following day for experiments.

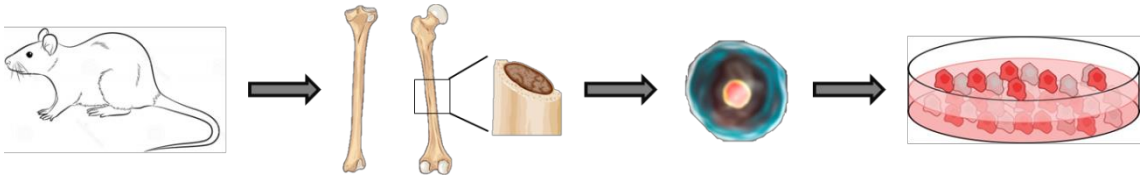

Figure 17. Bone marrow culture scheme. Long bones were dissected, bone marrow was extracted and cells were differentiated. After six days in differentiation culture, cells are completely differentiated in macrophages and ready to be plated.

7.2. Stimulation of mouse bone marrow-derived macrophages

After 24 h from cell seeding, bone marrow-derived macrophages (BMDMs) were primed and stimulated differently depending on the aim of the experiment.

In galvanic current-related experiments, cell density was at 10^6 cells/ml in 2 ml of medium for uncoated tissue culture 6-well plates. BMDMs were primed with either LPS (Sigma-Aldrich) from *E. coli* strain 055:B5 (1 µg/ml) during 2 h or with recombinant mouse IL-4 (BD Pharmigen) (20 ng/ml) for 4 h both at 37ºC and 5 % of CO_2 atmosphere. After priming, supernatants were collected to measure IL-6 and TNF-α, cells were washed and then treated with nigericin (1.5 µM) or with galvanic currents during 6 h in 1 ml of Opti-MEM (Lonza) or Opti-MEM high potassium (Opti-MEM supplemented with 60 mM of KCl) at 37ºC and 5 % of CO_2 atmosphere using a own designed and produced device (**Figure 18**).

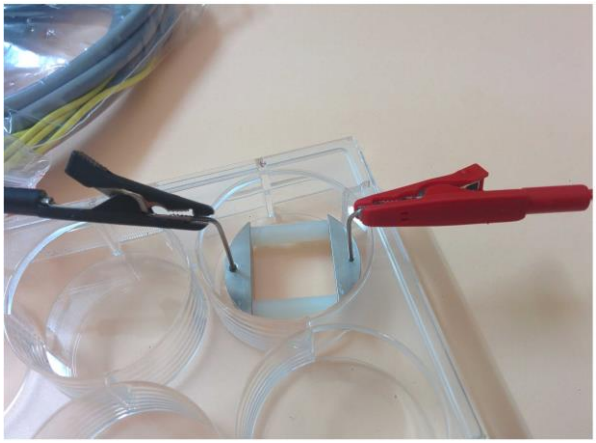

Figure 18. Device designed to apply galvanic current in 6-well plates. The two poles are separated by plastic spacers and generate a homogeneous and constant galvanic current through the well.

Different parameters of galvanic currents were used (**Table 2**), and mostly were applicated at room temperature (RT). Some of them were also applicated at 4ºC as indicated in figure legends.

Table 2.- Galvanic current parameters applied in the different experiments.

Intensity (milliamp, mA)	Time (seconds, s)	Number of pulses
3 / 6 / 12 mA	6 s	2
12 mA	3 / 6 / 12 s	2
12 mA	6 s	2 / 4 / 8

In collagenase-related experiments, cell density was at 10^6 cells/ml in 500 µl of medium for 24-well plates. In some cases, cells were seeded into collagen upholstered well plates. Collagen type I (Thermo Scientific) at 10 µg/ml in E-total buffer (147 mM NaCl, 10 mM HEPES, 13 mM glucose, 2 mM $CaCl_2$, 1 mM $MgCl_2$, and 2 mM KCl, pH 7.4) was added to each well and incubated 16 h at 4 ºC. Collagenase A (Sigma-Aldrich) (10 µg/µl) were used to degrade collagen type I after or before BMDMs were seeded into the plate. Then, cells were primed with LPS (1 µg/ml) during 2 h or with collagenase A (10 µg/µl) during 16 h. After priming, supernatants were collected to measure IL-6 and TNF-α, cells were washed twice with E-total buffer and then, treated in 500 µl of Opti-MEM with ATP (Sigma-Aldrich) (3 mM) during 30 min or with collagenase A (10 µg/µl) during 16 h in Opti-MEM at 37ºC and 5 % of CO_2 atmosphere.

In all experiments, after stimulation, cells of control groups (only treated with LPS) and supernatants of all groups were collected. Supernatants were centrifuged at 1000 xg during 5 min and the pellet of debris was discarded. Cells were lysed with 50 µl of cold lysis buffer: Tris-HCl 50 mM at pH 8.0 (Sigma-Aldrich), NaCl 150 mM, 2% Triton X-100 (Sigma-Aldrich) and supplemented with 100 µl/ml of protease inhibitor mixture (Sigma-Aldrich), and incubated for 30 min on ice. Then cell lysates were centrifuged at 16,000 xg during 15 min at 4ºC. Supernatants from lysed cells were collected and stored together with clarified cell-free supernatants at -80ºC.

8. Human blood samples

In this thesis we used blood from 4 patients with CAPS carrying the p.Ala439Thr NLRP3 variant, 1 patient carrying the p.Ser171Phe NLRC4 mutation present in mosaicism and 4 healthy donors used as control. The clinical research ethics committee of the *Clinical University Hospital Virgen de la Arrixaca* (Murcia, Spain) approved the use of these blood

samples. Informed consent was obtained from all individuals enrolled in the study in accordance with the WMA Declaration of Helsinki. The samples were stored in the *Biobanco en Red de la Región de Murcia* (PT13/0010/0018) integrated in the Spanish National Biobanks Network (B.000859). Whole blood samples were collected in EDTA anticoagulated tubes.

8.1. Peripheral blood mononuclear cells isolation

Peripheral blood mononuclear cells (PBMCs) from whole blood were isolated using a Ficoll-based gradient separation method (Histopaque-1077; Sigma-Aldrich). Special tubes (SepMate-50; StemCell) were used for the gradient separation. 15 ml of Ficoll with a 1.077 g/ml density were added in the bottom of the tube until filling the chamber. Blood was diluted 1:1 with PBS and 6 ml was added carefully after the Ficoll, on the top of the chamber. Once added, blood was centrifuged at 1,200 xg during 15 min. After the centrifugation, four phases were obtained (**Figure 19**), according to their density:

- Erythrocytes and polymorphonuclear cells (bottom of the tube).
- Ficoll phase.
- PBMCs phase, forming a white ring (the layer of interest).
- Plasma phase (top of the tube).

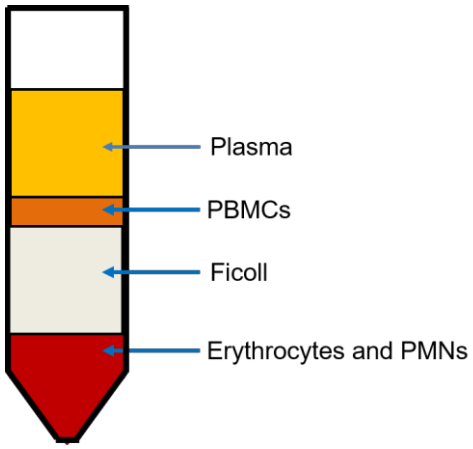

Figure 19. Post-spin Ficoll separation phases scheme. Four phases based on their density were formed, from denser (erythrocytes and PMNs) to less dense (plasma). Between plasma and Ficoll phases the PBMCs phase is located, the layer of interest.

After centrifugation, PBMCs were collected using a Pasteur pipette and washed with 20 ml of PBS twice at 300 xg during 10 min each. Supernatant was discarded, PBMCs were resuspended on 1 ml of Opti-MEM and counted in a Bürker chamber (Marienfield) diluting the cells 1:10 in trypan blue (Sigma-Aldrich) to differentiate live from death (stained) cells. Three quadrants of the chamber were counted diagonally. Final number of cells were obtained dividing total number of cells counted by 3 and then multiplying by the chamber

dimensions and trypan blue dilution, resulting in the number of cells in 1 ml of the sample. Cells were counted using an inverted phase contrast AE2000 microscope (Motic).

Cells were seeded on 24-well plates at a density of 10^6 cells/ml in 500 µl of media and the remaining cells were subsequently frozen at -80ºC and -196ºC. To be frozen cells were centrifuged for 10 min at 300 xg and 10^6 cells were resuspended in 1 ml of freezing buffer (10% dimethyl sulfoxide (DMSO) and 90% FCS), transferred to cryotubes (Greiner Bio-one) and stored at -80ºC using an isopropanol-containing recipient (Nalgen) for 24 h to 48 h. After this period, cells were stored in liquid nitrogen at -196ºC.

Cells were defrosted using a 37ºC bath and viable cells were selected by a negative magnetic selection method using the OctoMacs kit together with separation columns of medium size (Miltenyi Biotec) according to manufacturer's instructions. Briefly, after defrosting, PBMCs suspension was diluted 1:10 in PBS and centrifuged at 300 xg for 10 min. Annexin V conjugated with magnetic beads was equilibrated by 1:5 dilution with binding buffer (Miltenyi Biotec). 500 µl of the Annexin-V magnetic beads mix were added every 10^6 cells and incubated for 15 min at RT. Columns were calibrated with 500 µl of binding buffer, and after that, cells were added. Columns were washed 3 times with 500 µl binding buffer. The final volume obtained was about 2.5 ml, containing live cells. Cells were then counted using a Bürker chamber and trypan blue as mention before and seeded at 10^6 cells/ml in 500 µl of media in 24-well plates for experiments.

8.2. Complete blood and PBMCs stimulation

Cell density of PBMCs was at 10^6 cells/ml in 500 µl of RPMI medium in uncoated tissue culture 24-well plates. Complete blood or PBMCs were left unstimulated or primed with LPS (1 µg/ml) for 2 or 5 h at 37ºC and 5 % of CO_2 atmosphere. After LPS priming, cells were treated with ATP (3 mM) during 30 min or with 4 µg of protective antigen (PA) and 2 µg of flagellin A lethal factor (LFn-FlaA) (here called FlaTox, kindly obtained from Prof. V. Mulero, University of Murcia) during 5 h at 37ºC and 5 % of CO_2 atmosphere.

After stimulation, cells and supernatants of all groups were collected. Supernatants were centrifuged at 1,000 xg during 5 min and the pellet was discarded. Cells were lysed as described in section 19 for isolation of RNA. Cell lysates and clarified cell-free supernatants were stored at -80ºC until use.

9. HEK293T cells

9.1. HEK293T cell culture and transfection

HEK293T cells (CRL-11268; American Type Culture Collection) or HEK293T cells stably expressing the human NLRP3 sensor tagged with YFP (NLRP3-YFP) (Tapia-Abellan et al., 2019) were maintained in DMEM:F12 (1:1) (Lonza) supplemented with 10% FCS, 2 mM Glutamax (Life Technologies), and 1% L-glutamine, in presence of G418 (Acros organics) first at 1 mg/ml and reducing the concentration until 0,3 mg/ml progressively.

To seed HEK293T cells, cell culture medium was removed and cells were washed with PBS. After washing, 1 ml of trypsin with 0,25% of ethylenediaminetetraacetic acid (EDTA) (Sigma-Aldrich) was added to the flask and after 3 min of incubation at 37ºC temperature, 9 ml of fresh medium with FCS were added to inactivate trypsin. Cells were transferred to a 15 ml conical tube and centrifuged at 433 xg during 5 min; supernatant was discarded and new medium was added. Then cells were counted with Bürker chamber and trypan blue, and cultured at different densities depending on the well-plate used and the experiment.

During transfection cell density was at $7x10^5$ cells/ml in 1 ml of medium in 12-well plates. Lipofectamine 2000 (Invitrogen) was used for the transfection of HEK293T cells with different plasmid constructs according to manufacturer's instructions. Briefly, a mix of 1 µg of total DNA in 50 µl Opti-MEM (tube A) and a mix of 3 µl of Lipofectamine 2000 diluted in 50 µl Opti-MEM (tube B) were prepared and tubes were incubated during 5 min at RT. Plasmids used and their concentration are referred in **Table 3**. After incubation, the volume of tube A was added into tube B, mixed gently and the mixture were incubated 20 min at RT. In the meantime, cell culture medium was removed and 900 µl of fresh complete medium were added and the cells were incubated at 37ºC and 5% CO_2 atmosphere during the rest of the time. Then, the Lipofectamine/DNA mixture was added to the cells drop by drop. The plate was swirled gently to mix and incubated at 37ºC and 5% CO_2 atmosphere. 24 h after transfection, formation of NLRC4-YFP puncta was evaluated by fluorescent microscopy.

Table 3.- Information about plasmids used in this Thesis. Ct = C-terminal. Nt = N-terminal.

Plasmid name	Transcript	Promoter	Vector backbone	Concentration	Fused with
pAP2	Human NLRC4 wild-type	CMV	TOPO 3.1	1 µg/µl	YFP-Nt / LUC-Ct
pAP11	Human NLRC4 p.Ser171Phe	CMV	TOPO 3.1	1 µg/µl	YFP-Nt / LUC-Ct
pAP6	Human NLRC4 p.Thr177Ala	CMV	TOPO 3.1	1 µg/µl	YFP-Nt / LUC-Ct

pAP4	Human NLRC4 Thr337Asn	CMV	TOPO 3.1	1 µg/µl	YFP-Nt / LUC-Ct
pAP12	Human NLRC4 Thr337Ser	CMV	TOPO 3.1	1 µg/µl	YFP-Nt / LUC-Ct
pAP7	Human NLRC4 p.Val341Ala	CMV	TOPO 3.1	1 µg/µl	YFP-Nt / LUC-Ct
pAP13	Human NLRC4 p.His443Pro	CMV	TOPO 3.1	1 µg/µl	YFP-Nt / LUC-Ct
pAP5	Human NLRC4 p.Ser445Pro	CMV	TOPO 3.1	1 µg/µl	YFP-Nt / LUC-Ct
pAP8	Human NLRC4 p.Gly633dup	CMV	TOPO 3.1	1 µg/µl	YFP-Nt / LUC-Ct
pAP9	Human NLRC4 p.Trp655Cys	CMV	TOPO 3.1	1 µg/µl	YFP-Nt / LUC-Ct
pAP14	Human NLRC4 p.Gln657Leu	CMV	TOPO 3.1	1 µg/µl	YFP-Nt / LUC-Ct
pAP10	Human NLRC4 p.Cys697Ser	CMV	TOPO 3.1	1 µg/µl	YFP-Nt / LUC-Ct
pAP3	Human NLRC4 p.Asp1009Gly	CMV	TOPO 3.1	1 µg/µl	YFP-Nt / LUC-Ct
hASC-RFP	Human ASC	CMV	pcDNA3	0.1 µg/µl	RFP Ct

9.2. Plasmid construction

Different mutations of human NLRC4 were generated by overlapping PCR to introduce a point mutation. The construct was also double tagged using overlapping PCR in the N-terminus to YFP and in the C-terminus to *Renilla* luciferase (Luc) for following assays. To introduce the point mutation the following PCR protocol was developed 98ºC – 30 s, (98ºC – 10 s, 57ºC – 30 s, 72ºC – 2 min) x 15 cycles, 72ºC – 2 min, 4ºC - ∞, using specific designed primers (**Table 4**) and the Platinum SuperFi high fidelity polymerase (Thermo Scientific) (**Figure 20**).

Table 4.- List of primers used during this Thesis. The specific nucleotide(s) changed to perform the mutation are represented in red.

Use	Sequence (forward - reverse)	Length (nucleotides)	%GC
Introduction of the mutation p.Ser171Phe	GAAGGGGAATTTGGCAAAGGC GCCTTTGCCAAATTCCCCTTC	21	52.3
Introduction of the mutation p.Thr177Ala	AAGGCAAGTCCGCTCTGCT ACGAGAGCGGACTTGCCTT	19	57.8
Introduction of the mutation p.Thr337Asn	TCTCATGAAGAACCCTCTCTTTG CAAAGAGAGGGTTCTTCATGAGA	23	43.4
Introduction of the mutation p.Thr337Ser	TCTCATGAAGAGCCCTCTCTTTG CAAAGAGAGGGCTCTTCATGAGA	23	47.8
Introduction of the mutation p.Val341Ala	CCCTCTCTTTGCGGTCATCACTT AAGTGATGACCGCAAAGAGAGGG	23	52.1
Introduction of the mutation p.His443Pro	AATTCTTTCCCAAGTCATTCCAGG CCTGGAATGACTTGGGAAAGAATT	24	41.6

Introduction of the mutation p.Ser445Pro	CTTTCACAAGCCATTCCAGGAGT ACTCCTGGAATGGCTTGTGAAAG	23	47.8
Introduction of the mutation p.Gly633dup	ACAGGTGGAGGCATCCACATG CATGTGGATGCCTCCACCTGT	21	57.1
Introduction of the mutation p.Trp655Cys	TCTTCAACTGCAAGCAGGAATTC GAATTCCTGCTTGCAGTTGAAGA	23	43.4
Introduction of the mutation p.Gln657Leu	CAACTGGAAGCTGGAATTCAGG CCTGAATTCCAGCTTCCAGTTG	22	50
Introduction of the mutation p.Cys697Ser	CAAATAAAGAGAAGTGCTGGTGTG CACACCAGCACTTCTCTTTATTTG	24	41.6
Introduction of the mutation p.Asp1009Gly	GCAATTTGATGGTGATGATCTCA TGAGATCATCACCATCAAATTGC	23	39,1
Introduce mutations and overlapping PCR	TAATACGACTCACTATAGGG	20	40
Introduce mutations and overlapping PCR	CTGTCCAGCACGTTCATCTGC	21	57.1
Correct alignment of the plasmid in the vector	GCAGATGAACGTGCTGGACAG	21	57.1
Correct alignment of the plasmid in the vector	GATCAGCGGGTTTAAACTC	19	47.3

After this PCR, two PCR amplicons were obtained, and electrophoresis in 0.5% agarose gel and purification of DNA of each fragment with DNeasy gel purification kit (Qiagen) following the manufacturer's instructions were performed. An overlapping PCR was done to join these two fragments to form the final complete fragment with the mutation using the same PCR protocol than before, specific combination of primers (**Table 4**), and the Platinum SuperFi polymerase. Electrophoresis in 0.5% agarose gel was performed and purification of DNA of the final fragment was performed using DNeasy gel purification kit following the manufacturer's instructions (**Figure 20**).

After obtaining the complete fragment, Taq-polymerase were used to add an adenine at each end of the PCR-obtained fragment to be cloned into pcDNA3.1/V5-His TOPO (Life Technologies). After being cloned, construct was transformed into TOP10 *E. coli* strain (Thermo Scientific) by heat-shock protocol incubating the samples at 42ºC during 30 s. After transformation, bacteria were cultured 1 h at 37ºC in 250 µl of SOC medium (provided with the bacteria) to allow its exponential growth and recover from the heat-shock. Then bacteria were seeded into 5 ml of Luria-Bertani (LB) agar (Acros organics) with ampicillin (Sigma-Aldrich) (100 µg/ml) Petri dishes and incubated overnight at 37ºC (**Figure 20**).

After incubation, the following PCR protocol 94ºC – 10 min, 94ºC – 3 min, (98ºC – 10 s, 57ºC – 30 s, 72ºC – 2 min) x 30 cycles, 4ºC - ∞, of 8-10 bacteria colonies were performed to check if the construct was inside the plasmid and in correct orientation (positive bacteria) or not (negative bacteria) using specific primers (**Table 4**). Electrophoresis in 0.7% agarose

gel and visualization under UV light were performed to differentiate positive and negative bacteria (**Figure 20**).

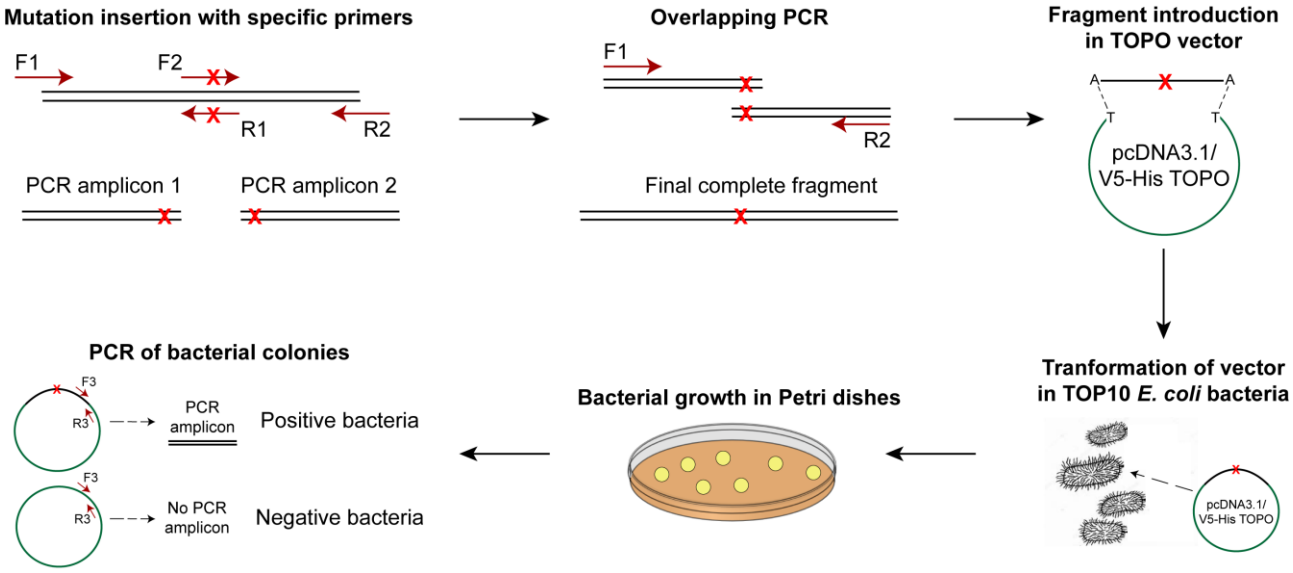

Figure 20. Schematic representation of the procedure performed to obtain plasmid construction. Different steps of the procedure are represented and linked with arrows.

Positive bacteria colonies were then cultured in 5 ml of LB with ampicillin (100 µg/ml) and incubated overnight at 37ºC with vigorous shaking. After that, plasmid DNA was purified using the QIAprep spin miniprep kit (Qiagen) following the manufacturer's instructions and the amount of DNA obtained was measured in a NanoDrop 2000/2000c spectrophotometer (Thermo Scientific).

The purified plasmids were also digested with BamHI and NotI (Thermo Scientific) (10 U/µl) to confirm correct alignment between tags and the NLRC4 sequence, loaded in an agarose gel to develop electrophoresis with RedSafe marker and visualized under UV light. Finally, sequencing of the construct was performed to confirm correct modification and the absence of unwanted mutations.

9.3. HEK293T NLRP3-YFP cell line stimulation

Cells were seeded at $7x10^5$ cells/ml in 1 ml of DMEM:F12 medium. Cells were stimulated in E-total buffer using 2 impacts of 12 mA during 6 s each of galvanic current in presence or absence of 10 µM MCC950 (CP-456773, Sigma-Aldrich, added 30 min before galvanic current application) and incubated for 6 h. After this time, formation of NLRP3-YFP punctawas evaluated by fluorescent microscopy.

10. Microscopy

10.1. Fluorescent microscopy

Fluorescent microscopy was used to analyze NLRP3 or NLRC4 inflammasome puncta formation with or without ASC. Images were acquired with a Nikon Eclipse Ti microscope equipped with a 20× S Plan Fluor objective (numerical aperture, 0.45), and a digital Sight DS-QiMc camera (Nikon) and 472 nm/520 nm filter set (Semrock), and the NIS-Elements AR software (Nikon). Images were analyzed with ImageJ (US National Institutes of Health).

10.2. Second harmonic generation microscopy

This technique was performed with the help of Dr. Juan Manuel Bueno and Rosa María Martínez Ojeda from Optic and Nanophysics University Institute in University of Murcia. A detailed description of the second harmonic generation microscope used can be found in (Skorsetz et al., 2016), a non-lineal optical tool (Campagnola et al., 2001). Unstained collagen molecules are able to generate second harmonic generation signal due to their natural structure with lack of a center of inversion symmetry (Fine & Hansen, 1971). In brief, the imaging instrument combines a Ti:Sapphire femtosecond laser source and an inverted microscope. The laser system emits light pulses of 800 nm of wavelength at a repetition rate of 76 MHz. An XY scanning unit and a Z-motor attached to the microscope objective allow scanning the sample across the plane and depth location of interest. The second harmonic generation signal from the sample propagates back through the same objective used for excitation (dry long-working distance, 20x, 0.8 N.A.), is isolated by a short-wave pass filter (400±5 nm), and finally detected by a photon counting photomultiplier module. A home-made LabView™ software controlled the entire system. The average power at the sample's plane was always below 100 mW. Second harmonic generation images were acquired at 2 Hz. To analyze the structural organization of the collagen fibers in the tendon, an algorithm based on the Hough transform was used (Bueno et al., 2020).

The Hough transform is a mathematical procedure able to detect aligned segments of collagen fibers within an image (**Figure 21**), and provide quantitative information on the degree of organization of the spatially resolved structures. On the basis of a pixel-by-pixel calculation, when a straight line is found, the corresponding polar coordinates are filed in the so-called 2D accumulator matrix. For each new detected straight line, the accumulator increments one unit. The local peaks (i.e., maximum values) in this accumulator space determine the preferential orientations found across the image. The standard deviation of

these orientations is defined as the structural dispersion. A custom Matlab™ script was developed for image processing (Bueno et al., 2020).

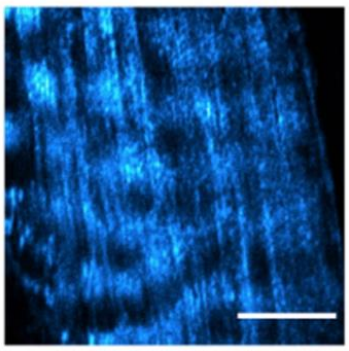

Figure 21. A representative image of accumulation matrix of the algorithm based on the Hough transform from collagen fibers imaged with second harmonic generation microscopy. Calcaneal tendon without staining is showed, scale bar 50 μm.

11. Bioluminescent Resistance Energy Transfer assay

Bioluminescent Resistance Energy Transfer (BRET) assay was used to study the conformational changes produced by the different mutations in NLRC4 constructs. NLRC4 construct without YFP, but with Luciferase was used as negative control (rLuc only).

24 h after HEK293T cell transfection, poly-L-lysine solution (Sigma-Aldrich) were prepared to coat 96-well white plates by diluting 1% poly-L-lysine solution 1:100 in PBS. 100 μl of the mix were added to each well and the plate was incubated 15 min at 37ºC. During incubation time, transfected HEK293T cells were detached in 1 ml of complete medium by gentle pipetting up and down. After poly-L-lysine incubation, wells were washed twice with PBS and 100 μl of cell suspension (1000 cells/μl) were added to each well. Plates were incubated at 37ºC and 5% of CO_2 atmosphere during 24 h.

Then cells were washed twice with PBS and 50 μl of coelenterazine h solution (Invitrogen, 4,5 μM diluted in PBS) was added to each well and the plate was incubated during 7 min at 37ºC to allow luciferase signal to stabilize. After incubation, luminescence was read in a Synergy neo2 multi-mode plate reader (BioTek) at 480 and 530 nm every 150 s for 30 min with a gain of 110 units, and miliBRET units (mBUs) were calculated using the following equation:

$$\text{BRET (mBUs)} = \left(\left(\frac{Lum(535nm)}{Lum(480nm)}\right)^{donor+acceptor} - \left(\frac{Lum(535nm)}{Lum(480nm)}\right)^{rLuc\ only}\right) \times 1000$$

After BRET measurement, YFP fluorescence was measured by exciting at 480 nm and reading emission at 530 nm in the same wells to determine the expression of the BRET sensor in the different transfections.

12. Flow cytometry

Intracellular ASC-speck formation was evaluated by seeding 50 µl of individuals' whole blood samples in polystyrene flow cytometry tubes (Falcon) with RPMI 1640 medium (Lonza) containing 10% FCS and 2 mM Glutamax. Following stimulation as described in section 8.2, tubes were centrifuged 600 xg for 5 min to pellet floating cells, and supernatant was carefully removed. After that, cells were resuspended in 100 µl of staining buffer (PBS with 1% of FCS and 0.1% sodium azide) containing mouse monoclonal FITC-conjugated anti-CD14 (clone M5E2, 557153, BD Biosciences), mouse monoclonal APC-conjugated anti-CD15 (clone HI98, 551376, BD Biosciences), and mouse monoclonal PE-Cy7-conjugated anti-CD16 (clone 3G8, 557744, BD Biosciences), to stain the surface of monocytes. All the antibodies were diluted 1:10 and incubated during 30 min at RT in the dark. After incubation, cells were washed with 2 ml of staining buffer and centrifuged at 600 xg during 5 min at RT. Cells were then resuspended in 500 µl of cell fixation buffer and incubated during 10 min on ice in the dark. Another 2 washes were performed using 2 ml of staining buffer and centrifuging at 400 xg for 5 min at RT. After that, cells were stained for the detection of ASC specks by Time-of-Flight Inflammasome Evaluation (Hurtado-Navarro et al., 2022; Sester et al., 2015). Briefly, 250 µl of permeabilization buffer (PBS with 3% of FCS, 0.1% sodium azide, and 0.1% saponin) were added to each tube. Also, 250 µl of a 1:500 dilution of PE conjugated mouse monoclonal anti-ASC antibody (653903, Biolegend) in staining buffer were added to achieve a final dilution of 1:1000 in the desired tubes. Tubes were incubated 45 min at RT in the dark. After incubation, cells were washed again as mentioned before and resuspended in 500 µl of staining buffer to acquire the cells in a FACS Canto flow cytometer. To calculate the percentage of monocytes in the samples, a gating strategy consisting of $CD14^+$, $CD16^+$, $CD15^-$ cells was applied using the FCS express software (De Novo Software). Flow cytometry was performed with the help of Laura Hurtado Navarro.

13. Enzyme-linked immunosorbent assay

A quantitative sandwich enzyme-linked immunosorbent assay (ELISA) was used in this thesis for quantitative detection of different cytokines (**Figure 22**). ELISA system was

used to detect mouse IL-1β (Thermo Scientific), mouse IL-6 (R&D Systems) and mouse TNF-α (Thermo Scientific) in BMDMs supernatants, and human IL-1β (Invitrogen), human IL-18 (Invitrogen), human IL-6 (R&D Systems) and human TNF-α (R&D Systems) in PBMCs supernatants and complete blood, following manufacturer instructions for each.

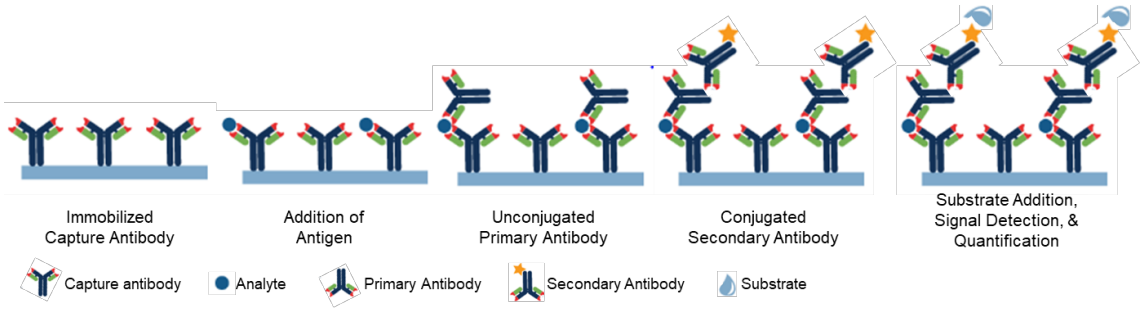

Figure 22. A schematic representation of sandwich ELISA protocol. Image adapted from "Rockland antibodies & assays" web.

ELISA was done in 96-wells plate (Corning Costar) according to the manufacturer's instructions. Briefly, an overnight incubation with 100 ul of capture antibody diluted 1:250 in Coating Buffer (PBS) per well was done at 4ºC. After coating, plates were washed four times with washing buffer (0.05% Tween 20 diluted in PBS). After washing, a blocking step was done with ELISA/ELISPOT Diluent (provided with the kit). Alternatively, blocking step can be done using a solution of BSA. After blocking and washing, a standard with different dilutions of recombinant cytokine and samples were added to the wells and incubated 2 h at RT in order to allow the antigen to bind with the capture antibody. Sample dilutions were done with the corresponding diluent buffer provided in the kit (**Table 5**).

After samples incubation and washing, the primary antibody was added and incubated to allow binding between primary antibody and antigen. After the incubation and washing, the secondary antibody conjugated with horseradish peroxidase (HRP)-avidin was added and incubated.

After secondary antibody incubation and washing, 3,3',5,5'-tetramethybenzidine (TMB, provided with the kit) as substrate reagent was added and incubated according to manufacturer's instructions and protected from light for 15 min. Then 100 µl of stop solution (2 N H_2SO_4) was added. Absorbance at 450 nm was measured in a Synergy Mx plate reader (BioTek), using 570 or 630 nm wavelengths as reference.

Table 5.- Conditions in each ELISA kit used. Differences in coating and sample dilution are described in this table. Coated IL-1β ELISA kit was used to measure *in vivo* IL-1β levels. Uncoated IL-1β ELISA kit was used to measure *in vitro* IL-1β release.

Type of ELISA kit	Coating	Sample dilutions	Brand (Catalog number)
Mouse IL-1β	Uncoated plate	Without dilution (LPS+Nigericin and LPS+(12mA-6s)x8 samples in C57BL/6 mice diluted 1:2)	Invitrogen (88-7013)
Mouse IL-1β	Coated plate	Without dilution	Invitrogen (BMS60002)
Mouse IL-18	Coated plate	1:2	Invitrogen (BMS618-3)
Mouse IL-6	Coated plate	1:25	R&D (M6000B)
Mouse TNF-α	Uncoated plate	1:10	Invitrogen (88-7324)
Human IL-1β	Coated plate	1:2	eBioscience (BMS224INST)
Human IL-18	Coated plate	Without dilution	MBL (7620)
Human IL-6	Coated plate	Without dilution (LPS samples diluted 1:10)	R&D (D6050)
Human TNF-α	Coated plate	Without dilution	R&D (DTA00D)

14. Multiplexing for cytokines detection

Homogenized tendons were used to measure the concentration of different cytokines using the mouse ProcartaPlex Mix&Match 8-plex kit (InvitroGen). Multiplex for the detection of IL-1α, IL-2, IL-6, IL-10, IL-18, CXCL10 and TNF-α was performed using the Luminex color-coded antibody-immobilized beads (InvitroGen) following the manufacturer's instructions. Briefly, 200 µl of washing buffer were added to all wells and incubated at RT during 10 min with shaking. After removing the washing buffer by decantation, samples and standards together with the magnetic beads mix were added and the plate was incubated with shaking at RT for 2 h. After washing the plate three times with a Hand-Held Magnetic Plate Washer (InvitroGen), the mix of detection antibodies was added and the plate was incubated with shaking at RT for 30 min. After washing the plate three times with a Hand-Held Magnetic Plate Washer, Streptavidin-PE antibody was added and the plate was incubated with shaking at RT for 30 min. After washing the plate three times with a Hand-Held Magnetic Plate Washer, reading buffer was added and the plate was incubated with shaking at RT for 5 min. The results were analyzed in a Luminex MAGPIX instrument (Luminex Corporation).

15. Western-blot

Sample processing

Clarified cell supernatants obtained as described in previous section 7 were concentrated by centrifugation at 11,000 xg during 30 min 4ºC through a column with a 10 kDa pore size membrane (Millipore). The aim of the concentration step was to concentrate

the target cytokines and proteins from the cell supernatant. Concentrated supernatants and cell extract obtained from $2x10^6$ cells were diluted with Laemmli buffer (Bio-Rad) at 1:1 ratio. Laemmli buffer contains 2-mercaptoethanol to disrupt proteins' disulphide bonds and to avoid protein aggregation. After addition of Laemmli buffer, samples were heated during 5 min at 95ºC to denature proteins, briefly spun down and loaded in the wells of an acrylamide gel.

Acrylamide gel preparation

Acrylamide/bis-acrylamide gels were prepared before electrophoresis of proteins. 19:1 acrylamide/bis-acrylamide solution (Sigma-Aldrich) was combined with distilled water at different concentrations to prepare the separating gel. A single-phase 15% gel was used to determine caspase-1, IL-1β and GSDMD. To determine NLRC4 tagged with *Renilla* Luciferase, a single-phase 8% gel was used. Separating gel also contained 3 M Tris-HCl at pH 8.8 to allow protein movement through the gel according to their size. On the top of the separating gel, a concentrating gel of 4% of acrylamide/bis-acrylamide containing 0.5 M Tris-HCl at pH 6.8 maintain concentration of proteins in a low conductivity state.

SDS was added to both gels in order to facilitate denaturing conditions and to eliminate the native charge of the proteins, providing negative charge. In this way, proteins will move from cathode to anode independently on their native charge and only dependent on their size. Ammonium persulfate (Sigma-Aldrich) and tetramethylethylenediamine (TEMED) (Sigma-Aldrich) were also added into the gels to initiate polymerization of acrylamide. Polyacrylamide gels were prepared with a 1.5 mm thickness and casted using the Mini-PROTEAN 3 system (Bio-Rad).

After the addition of the separating gel mixture into the cast, a layer of ethanol was added on the top to separate the gel from oxygen and allow a straight gel. After 30-40 min, when solidification occurred, ethanol was retired and the gel was washed with distilled water. Concentrating gel was added upon separating gel and 10-wells Mini-PROTEAN electrophoresis well combs of 1.5 mm thickness (Bio-Rad) were used to cast the concentrating gel with wells. Once solidified, combs were retired and gel was placed into the Mini-PROTEAN electrophoresis cuvette.

Protein electrophoresis and transference

Samples were loaded into the wells together with a pre-stained protein standard (BenchMark, Life Technologies) which contains proteins of 6, 15, 19, 26, 37, 49, 64, 82, 115

and 180 kDa. Protein electrophoresis was performed using a running buffer containing 25 mM Tris, 192 mM glycine, 0,1% SDS and pH 8.3 (Bio-Rad) at 200V for 50 min using a power supply from Bio-Rad.

After protein separation, gels were placed over a 0,45 µm pore-size nitrocellulose membrane (Bio-Rad), wrapped with Whatman® filter papers and casted into gel holders' cassettes (Bio-Rad). The cassette was introduced on the transference cuvette with the gel in the negative pole and the membrane in the positive pole in order to transfer proteins from the gel to the membrane. Protein transference was performed using a transference buffer containing 20% of methanol, 25 mM Tris, 192 mM glycine and pH 8.3 at 350 mA for 1 h using a power supply from Bio-Rad.

Antibody blotting and bioluminescent detection

After transference, membranes were blocked to avoid unspecific antibody binding with skim milk (BD Biosciences) diluted at 5% in TBS with 0,05% Tween (T-TBS) for 1 h at RT with shaking.

After blocking, primary antibody (**Table 6**) was added diluted in T-TBS with 5% of milk and was incubated overnight at 4ºC. After that, membranes were washed three times with T-TBS to eliminate primary antibody that had not been bound, and the secondary antibody conjugated with HRP (GE Healthcare) was added at 1:5000 dilution in T-TBS with 5% of milk and incubated 1 h at RT with shaking. Membranes were then washed again for three times with T-TBS before bioluminescent detection.

Membranes were incubated for 5 min in dark with 1 ml of enhanced chemiluminescence (ECL) plus (Amhershan Biosciences) and light signal was detected using a ChemiDoc HDR (Bio-Rad).

Table 6.- Antibodies used in western blot analysis.

Antibody	Host specie	Clonal expansion	Dilution	Company
Anti-mouse IL-1β	Rabbit	Polyclonal	1:1000	Santa Cruz
Anti-mouse caspase-1 (p20)	Mouse	Monoclonal	1:1000	Adipogen
Anti-mouse gasdermin D	Rabbit	Monoclonal	1:2000	Abcam
Anti-β-actin	Mouse	Monoclonal	1:10000	Santa Cruz
Anti-*Renilla* Luciferase	Rabbit	Polyclonal	1:1000	MBL
Anti-rabbit IgG HRP Linked F(ab')2	-	Polyclonal	1:5000	Sigma-Aldrich
Anti-mouse IgG HRP Linked F(ab')2	-	Polyclonal	1:5000	Sigma-Aldrich

16. Lactate dehydrogenase determination assay

The activity of LDH in cell-free supernatants were determined as indicative of necrotic cell death and pyroptosis with the Cytotoxicity Detection kit (Roche) following the manufacturer's instructions (**Figure 23**). LDH is a stable cytoplasmatic enzyme that goes out the cell when plasma membrane is damage and cell permeabilization is compromised. Cell-free supernatants were diluted 1:4 with Opti-MEM in 96-wells plate. Cell extracts were diluted 1:20 with Opti-MEM and then diluted again 1:4 in 96-wells plate to obtain the total cellular LDH content. Then, 100 µl of LDH detection reagent mix composed of the catalyst (containing diaphorase/NAD^+ mixture) and the dye solution (containing iodotetrazodium chloride (INT) and sodium lactate) was added to each well and absorbance was immediately read at 492 nm every 30 s during 10 min in a Sinergy MX plate reader (BioTek), using 620 nm wavelength as reference. After, the slope of the curve plotting absorbance *versus* time was calculated and used to calculate the final percentage of LDH release.

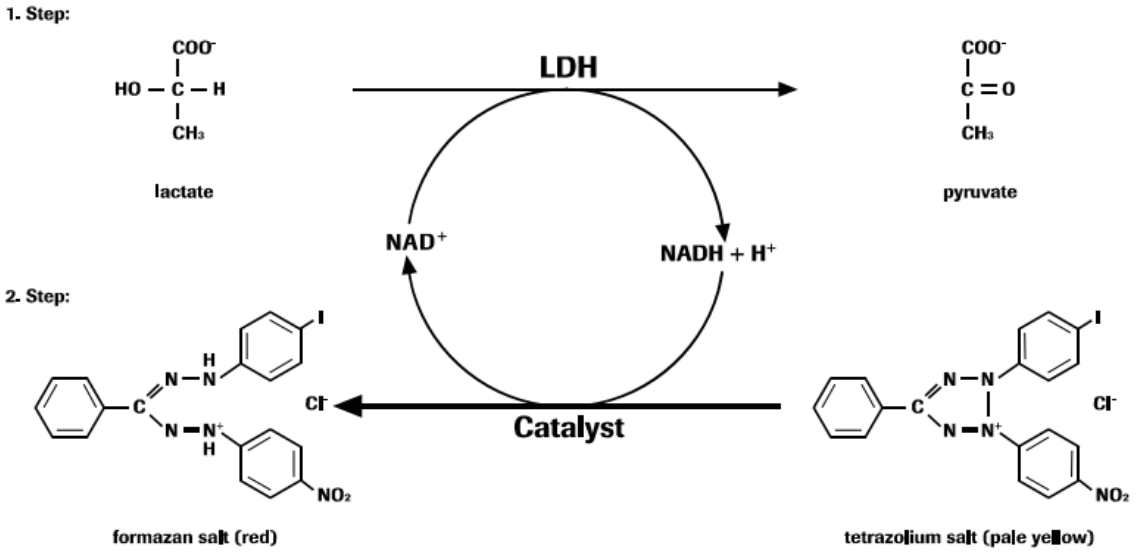

Figure 23. Representation of LDH reaction produced in the kit. First step, LDH transform lactate in pyruvate by the reduction of NAD^+ to $NADH+H^+$. Second step, the catalyst reduces tetrazolium salt (yellow) to formazan (red) by transforming $NADH+H^+$ in NAD^+. Image obtained from Roche Cytotoxicity determination (LDH) protocol.

17. Yo-Pro-1 uptake assay

Yo-Pro-1 staining was used to measure plasma membrane permeabilization at real time during cell stimulation. Yo-Pro-1 is a negative charged molecule, with 629 Da and cell-impermeant properties that strongly binds nucleic acids and emits at 525 nm upon excitation at 480 nm.

For Yo-Pro-1 uptake, macrophages were preincubated for 5 min at 37 ºC with 2.5 µM of Yo-Pro-1 iodide (Life Technologies) after galvanic current application or 1% Triton X100

(Sigma-Aldrich) addition. Yo-Pro-1 fluorescence was measured after the treatments every 5 minutes for the first 30 min and then every 30 min for the following 3 h with an excitation wavelength of 478 nm and emission of 519 nm in a Synergy neo2 (Biotek) multi-mode plate reader.

18. Intracellular K^+ determination

Intracellular K^+ was quantified from macrophages cell lysates as already reported (Compan et al., 2012). In brief, cells were lysed with 200 µl of ultrapure water by three freezing-thaw cycles exchanging the sample from liquid nitrogen to a bath at 37ºC. Cell lysates were centrifuged at 13,200 rpms for 10 min at 4ºC and intracellular K^+ was measured by indirect potentiometry on a Cobas 6000 with ISE module (Roche).

19. mRNA expression determination

RNA extraction and isolation

Total RNA extraction in cell cultures was carried out using RNeasy Mini kit (Qiagen) according to manufacturer's instructions. Briefly, cells were lysed by adding 350 µl of RLT with 1% of 2-mercaptoethanol (Sigma-Aldrich) and scrapping them. After scrapping, one volume of 70% ethanol was added to create conditions that promote selective binding of RNA to RNeasy silica-membrane and the sample was applied into RNeasy Mini spin columns. Total RNA was bound to the membrane and contaminants were washed away with RW1 and RPE washing buffers provided by the kit. Also, an additional step was added between RW1 and RPE washing steps. The sample was treated with DNase I (RNase-Free DNase set, Qiagen) diluted 1:8 in RDD buffer (supplied with the kit) and incubated during 30 min. In all the previous steps the supernatant was discarded each time. All binding and washing steps were performed by centrifugation at 10,300 xg during 1 min. After membrane drying, RNase free water was added, making sure that membranes were completely covered and hydrated, and incubated 5 min. Then, columns were centrifuged at 10,300 xg during 5 min. Final RNA concentration was measured using a NanoDrop 2000/2000c spectrophotometer (Thermo Scientific) and measuring absorbance at 260, 280 and 230 nm. Once quantified, samples were stored at -80ºC.

Total RNA extraction of Achilles tendons was carried out using Qiazol Lysis Reagent (Qiagen) and a Digital Tissue Homogenizer (OMNI International). Frozen Achilles tendons were lysed with 400 µl of Qiazol Lysis Reagent (Qiagen) and tissue homogenization was

carried out at maximum speed using a Digital Tissue Homogenizer (OMNI International) until no piece of tissue were observed. After tissue homogenization, the sample was incubated during 8 min at RT, and then 80 µl of chloroform (Sigma-Aldrich) were added. Tubes were shaken during 15 s, and rested during 3 min at RT. Then, samples were centrifuged at 12,000 xg during 15 min at 4ºC to separate three phases, the Qiazol phase (bottom), the intermediate phase and the chloroform phase (top). The chloroform phase was collected in an Eppendorf tube and one volume of 70% ethanol was added to create conditions that promote selective binding of RNA to RNeasy membrane. The sample was transfer into a RNeasy Mini (Qiagen) spin column and protocol described above was followed to obtain the final mRNA concentration. Once quantified, samples were stored at -80ºC.

Reverse transcription

Total RNA was reverse transcripted using the iScript cDNA Synthesis kit (Bio-Rad) using a mix of oligo(dT) and random hexamer primers. The cDNA transcription was carried out using 10 ng of RNA, 4 µl of iScript reaction mix, 1 µl of iScript reverse transcriptase, and the final volume was adjusted to 20 µl with nuclease-free water. The reaction was performed in Prime Thermal Cycler (Techne) with the following protocol: 25ºC for 5 min, 46ºC for 20 min and 95ºC for 1 min. Reactions were kept at 4ºC until sample storage at -20ºC.

Quantitative PCR analysis

Quantitative PCR was performed using the mix SYBR Premix ExTaq (Takara) in an iCycler MyiQ thermocycler (Bio-Rad). The master mix for the analysis was composed by 5 µl of SYBR Premix ExTaq, 3 µl of nuclease-free water, 1 µl of specific primers and 1 µl of cDNA. Specific primers were predesigned and purchased from Sigma-Aldrich (KiCqStart SYBR Green Primers) to detect the expression of the following mice genes: *Actb*, *Arg1*, *Casp1*, *Cox2*, *Cxcl10*, *Fizz1*, *Gsdmd*, *Il1a*, *Il1b*, *Il1rn*, *Il6*, *Mrc1*, *Nlrp3*, *Pycard*, *Tgfb*, *Tnfa* and *Ym1*, and the ribosomal RNA: *18S*. Also, to detect the expression of the following human genes: *Actb*, *Il1b* and *Il6*.

20. Statistics

Statistical analyses were performed using GraphPad Prism 7 (Graph-Pad Software, Inc). A Shapiro-Wilk normality test was initially performed on all groups to decide the analysis type to be used. For two-group comparisons, nonparametric Mann-Whitney U test (without making the assumption that values are normally distributed) or the parametric unpaired t-

test (for normal distributed data) were used to determine the statistical significance. For more than two group comparisons, one-way ANOVA test (for normal distributed data) or nonparametric Krustal-Wallis test (without making the assumption that values are normally distributed) were used to determine the statistical significance. Data are shown as mean values and error bars represent standard error from the number of independent assays indicated in the figure legend, which are also overlaid in the histograms as dot-plotting. p-value is indicated as *p < 0.05; **p < 0.01; ***p < 0.001; ****p < 0.0001; > 0.05 not significant (ns).

RESULTS

Chapter 1. Evaluation of NLRC4 and NLRP3 activation in recombinant HEK293T system

1.1. Conformational changes in NLRC4 inflammasome due to mutations associated with autoinflammatory diseases

1.1.1. Mutations in NLRC4 induce spontaneous oligomerization and conformational changes in NLRC4 inflammasome complexes

We first generated 12 different plasmids to express in mammalian cells the different pathogenic mutations of NLRC4 most of them described in the previous bibliography: p.Ser171Phe and p.Thr177Ala in the NBD domain; p.Thr337Asn, p.Thr337Ser and p.Val341Ala in the HD1 domain; p.His443Pro and p.Ser445Pro in the WHD domain; and p.Gly633dup, p.Trp655Cys, p.Gln657Leu, p.Cys697Ser and p.Asp1009Gly in the LRR domain. We first confirmed that all constructions were correctly expressed after transient transfections in HEK293T cells (**Figure 25A**). Since NLRC4 was fused to the fluorescent YFP protein, we were able to quantify the number of transfected cells with a puncta distribution of NLRC4 (**Figure 25B**), as a readout of inflammasome activation. We found that the different NLRC4 mutations resulted in a significant higher number of cells with spontaneous puncta distribution when compared with the wild type NLRC4 (**Figure 25C**). We next used BRET assay to study the conformation of NLRC4 carrying different mutations and YFP at N-terminus and rLuc at C-terminus, as increasing BRET signal will result in closer YFP and rLuc and a closed structure of NLRC4 (**Figure 26**). First, we aimed to express at the same level all NLRC4 BRET sensors in transfected HEK293T cells before calculating BRET signal. For that, we measured the fluorescence of YFP by exciting at 480 nm and found that all NLRC4 mutants presented a similar expression (**Figure 27A**). Then, we measured BRET and found that BRET signal was stable during the time for the different NLRC4 mutants (**Figure 27B**). However, BRET signal was different for the different NLRC4 mutants tested (**Figure 27B,C**). A significant decrease in BRET signal compared with NLRC4 wild type was observed in NLRC4 with the following mutations: p.Ser171Phe, p.Thr177Ala, p.His443Pro, p.Ser445Pro, p.Cys697Ser and p.Asp1009Gly (**Figure 27C**). This suggests that the N- and C-terminus of these mutants could be more separated than the wild type NLRC4, so the different mutated NLRC4 could be in an ‘open’ active conformation. On the contrary, NLRC4 mutants p.Thr337Asn, p.Thr337Ser, p.Val341Ala, p.Gly633dup, p.Trp655Cys and p.Gln657Leu did not changed BRET signal when compared with NLRC4 wild type (**Figure 27C**).

1.1.2. p.Ser171Phe NLRC4 variant induce an inflammasome activation without stimulation

We were able to obtain blood samples of a 57-years-old woman with episodes of fever and systemic inflammation carrying the post-zygotic variant c.512C>T in the *Nlrc4* gene. This nucleotide exchange lead to the p.Ser171Phe variant, which had already been classified as pathogenic (Volker-Touw et al., 2017) and we have found that induced a decrease of the NLRC4 BRET signal (**Figure 27C**).

Since the *in vitro* expression of p.Ser171Phe NLRC4 variant in HEK293T cells resulted in a higher number of cells with NLRC4 puncta when compared to wild type NLRC4 (**Figure 25**), we next analyze whether these puncta were leading to a functional NLRC4 inflammasome by expressing the NLRC4 variant p.Ser171Phe together with ASC. We found that the p.Ser171Phe variant induces a higher number of cells with ASC specks when compared to wild type NLRC4 (**Figure 28A,B**). Similarly, in the monocytes of the patient with the p.Ser171Phe NLRC4 variant, we found an increase of the percentage of monocytes with ASC specks when compared to monocytes from healthy controls (HC), and similar to monocytes from CAPS patients with the p.Ala439Thr NLRP3 variant (**Figure 29A**). The HC and the patient with NLRC4 variant presented the same number of circulating monocytes (**Figure 29B**). LPS treatment increased the percentage of monocytes with ASC specks from the patient with the p.Ser171Phe NLRC4 variant compared to HC (**Figure 29A**). These differences disappeared when the canonical NLRP3 inflammasome was activated with LPS and ATP (**Figure 29A**). PBMCs from the patient with the p.Ser171Phe NLRC4 variant released higher amounts of IL-18 when compared to HC (**Figure 29C**), but they failed to release IL-1β, even after the canonical NLRP3 inflammasome activation (**Figure 29D**). This difference between the release of both cytokines could be due to the fact that *Il1b* gene expression was not induced with LPS in the patient with the p.Ser171Phe NLRC4 variant, whereas as a control the expression of *Il6* was induced (**Figure 29E**). A similar release of TNF-α and IL-6 induced by LPS between the PBMCs from the patient with the p.Ser171Phe NLRC4 variant and the PBMCs from the HC ruled out a potential defect on LPS priming (**Figure 30A**). Finally, NLRC4 activation with FlaTox in PBMCs from the patient with the p.Ser171Phe NLRC4 variant resulted in an increased percentage of ASC-specking monocytes and IL-18 release, but not IL-1β (**Figure 30B**). All these data can be found in our recent publication Ionescu*, Peñín-Franch*, et. al., 2021.

1.2. NLRP3 activation by galvanic current

To gain further insights if galvanic current were activating NLRP3, we used HEK293T cells stably expressing NLRP3-YFP protein, a system widely used to assess NLRP3 activation (Chen and Chen, 2018; Compan et al., 2012; Tapia-Abellán et al., 2019, 2021). Fluorescence microscopy experiments showed that the application of 2 impacts of 12 mA of galvanic current for 6 seconds induced the formation of an intracellular NLRP3–YFP punctum (**Figure 31**). This punctum formation was inhibited by the application of the specific NLRP3 inhibitor MCC950 (**Figure 31**), suggesting that galvanic current could induce the activation of the NLRP3 inflammasome. To confirm this observation, we performed additional experiments shown in the following chapters of this Thesis.

Figures of Chapter 1

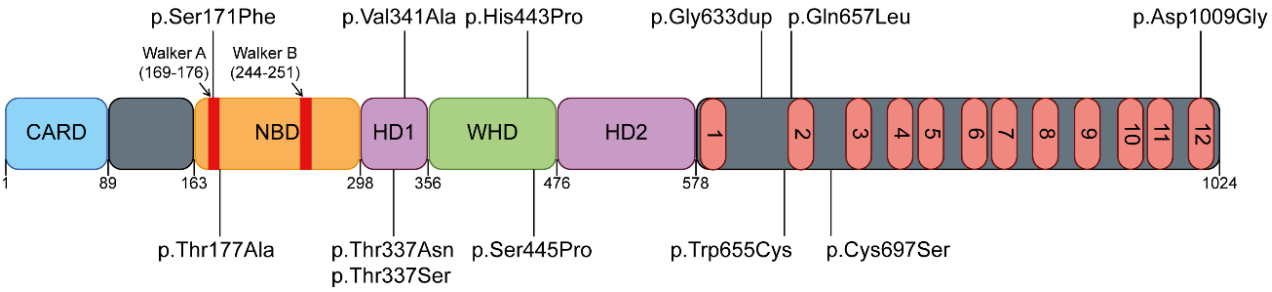
p.Ser171Phe
p.Val341Ala
p.His443Pro
p.Gly633dup
p.Gln657Leu
p.Asp1009Gly
Walker A
(169-176)
Walker B
(244-251)
CARD
NBD
HD1
WHD
HD2
1
2
3
4
5
6
7
8
9
10
11
12
1
89
163
298
356
476
578
1024
p.Thr177Ala
p.Thr337Asn
p.Thr337Ser
p.Ser445Pro
p.Trp655Cys
p.Cys697Ser

Figure 24. Schematic representation of NLRC4 mutants studied in this Thesis. The specific amino acid changes and the position of the mutations along the protein are indicated.

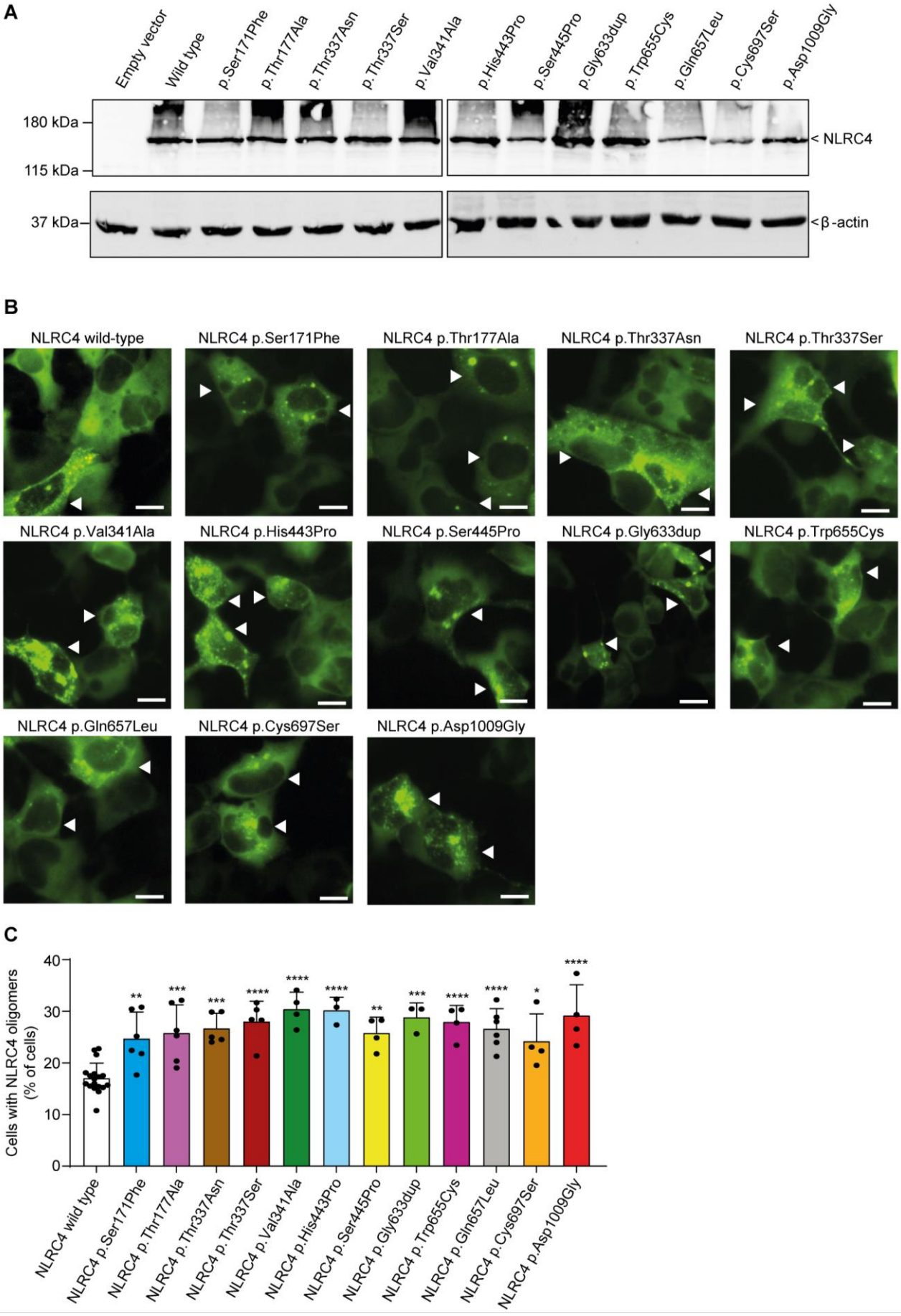
A
Empty vector
Wild type
p.Ser171Phe
p.Thr177Ala
p.Thr337Asn
p.Thr337Ser
p.Val341Ala
p.His443Pro
p.Ser445Pro
p.Gly633dup
p.Trp655Cys
p.Gln657Leu
p.Cys697Ser
p.Asp1009Gly
180 kDa
115 kDa
37 kDa
< NLRC4
<β-actin
B
NLRC4 wild-type
NLRC4 p.Ser171Phe
NLRC4 p.Thr177Ala
NLRC4 p.Thr337Asn
NLRC4 p.Thr337Ser
NLRC4 p.Val341Ala
NLRC4 p.His443Pro
NLRC4 p.Ser445Pro
NLRC4 p.Gly633dup
NLRC4 p.Trp655Cys
NLRC4 p.Gln657Leu
NLRC4 p.Cys697Ser
NLRC4 p.Asp1009Gly
C
Cells with NLRC4 oligomers (% of cells)
40
30
20
10
0
NLRC4 wild type
NLRC4 p.Ser171Phe
NLRC4 p.Thr177Ala
NLRC4 p.Thr337Asn
NLRC4 p.Thr337Ser
NLRC4 p.Val341Ala
NLRC4 p.His443Pro
NLRC4 p.Ser445Pro
NLRC4 p.Gly633dup
NLRC4 p.Trp655Cys
NLRC4 p.Gln657Leu
NLRC4 p.Cys697Ser
NLRC4 p.Asp1009Gly

Figure 25. Expression of human NLRC4 mutants in HEK293T cells. (A) Immunoblot for the expression of wild-type or different NLRC4 mutants in HEK293T cells. **(B)** Representative images of HEK293T expressing wild-type or different NLRC4 mutants tagged with YFP (green); arrowheads denote the cells with NLRC4 puncta; scale bar 10 μm. **(C)** Percentage of HEK293T cells with NLRC4 puncta, expressing either wild-type (white) or the different NLRC4 mutants. Significance between each mutant and wild type NLRC4 is indicated above each column. Center values represent the mean and error bars represent s.e.m.; n= 3-18 independent experiments. ****p<0.0001, ***p<0.0005, **p<0.005, *p<0.05, and ns p>0.05.

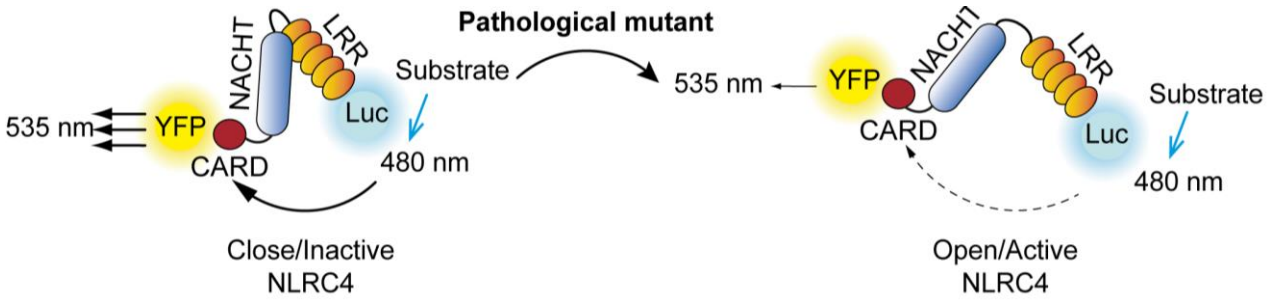
Pathological mutant
535 nm
YFP
CARD
NACHT
LRR
Luc
Substrate
480 nm
Close/Inactive
NLRC4
535 nm
YFP
CARD
NACHT
LRR
Luc
Substrate
480 nm
Open/Active
NLRC4

Figure 26. Schematic representation of BRET assay. The potential close/inactive and open/active states of NLRC4 are represented.

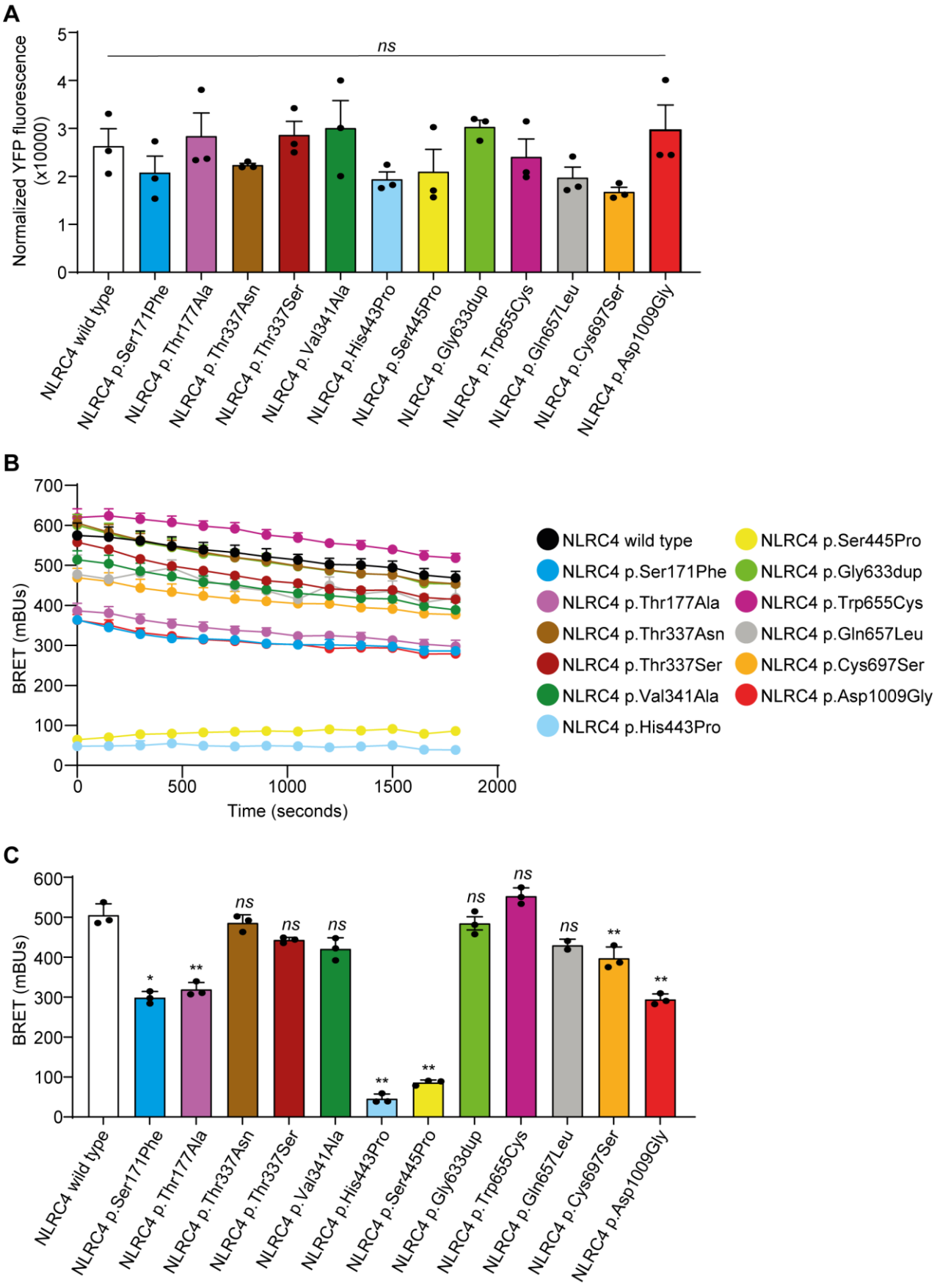
A
Normalized YFP fluorescence (x10000)
ns
NLRC4 wild type
NLRC4 p.Ser171Phe
NLRC4 p.Thr177Ala
NLRC4 p.Thr337Asn
NLRC4 p.Thr337Ser
NLRC4 p.Val341Ala
NLRC4 p.His443Pro
NLRC4 p.Ser445Pro
NLRC4 p.Gly633dup
NLRC4 p.Trp655Cys
NLRC4 p.Gln657Leu
NLRC4 p.Cys697Ser
NLRC4 p.Asp1009Gly
B
BRET (mBUs)
Time (seconds)
C
BRET (mBUs)
ns
*
**

Figure 27. BRET signal of wild type and different NLRC4 mutants. (A) YFP fluorescence of HEK293T cells expressing wild-type (white) and different YFP-NLRC4-Luc mutants. Center values represent mean and error bars the s.e.m.; n= 3 independent experiments. **(B)** BRET signal recorded during 30 min in HEK293T cells expressing wild-type (white) and different YFP-NLRC4-Luc mutants. Center values represent mean and error bars the s.e.m.; n= 3 independent experiments. **(C)** Mean of all time points for BRET signal shown in panel B. Significance between each mutant and wild type NLRC4 is indicated above each column. Center values represent mean and error bars the s.e.m.; n= 3 independent experiments. ****p<0.0001, ***p<0.0005, **p<0.005, *p<0.05, and ns p>0.05.

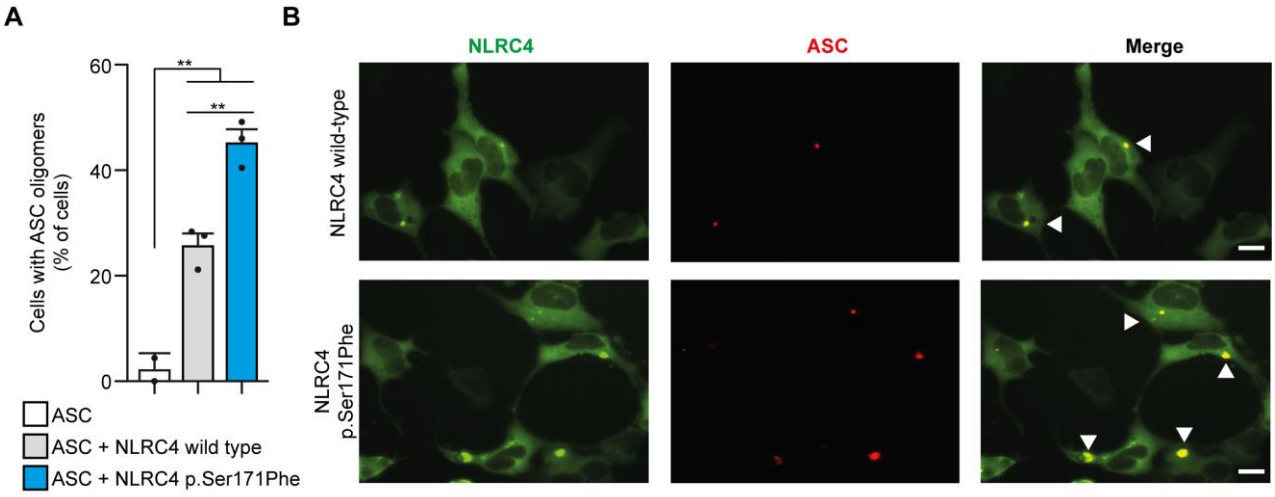
A
B
Cells with ASC oligomers (% of cells)
60
40
20
0
**
**
ASC
ASC + NLRC4 wild type
ASC + NLRC4 p.Ser171Phe
NLRC4
ASC
Merge
NLRC4 wild-type
NLRC4 p.Ser171Phe

Figure 28. Expression of human NLRC4 p.Ser171Phe variant together with ASC in HEK293T cells. **(A)** Percentage of HEK293T cells with oligomers of ASC, expressing ASC alone (white) or with either wild-type NLRC4 (gray) or p.Ser171Phe NLRC4 (blue). **(B)** Representative images of HEK293T expressing wild-type or p.Ser171Phe NLRC4 (green) and ASC (red); arrowheads denotes the cells with oligomerization of ASC; scale bar 10 μm. ****p<0.0001, ***p<0.0005, **p<0.005, *p<0.05, and ns p>0.05.

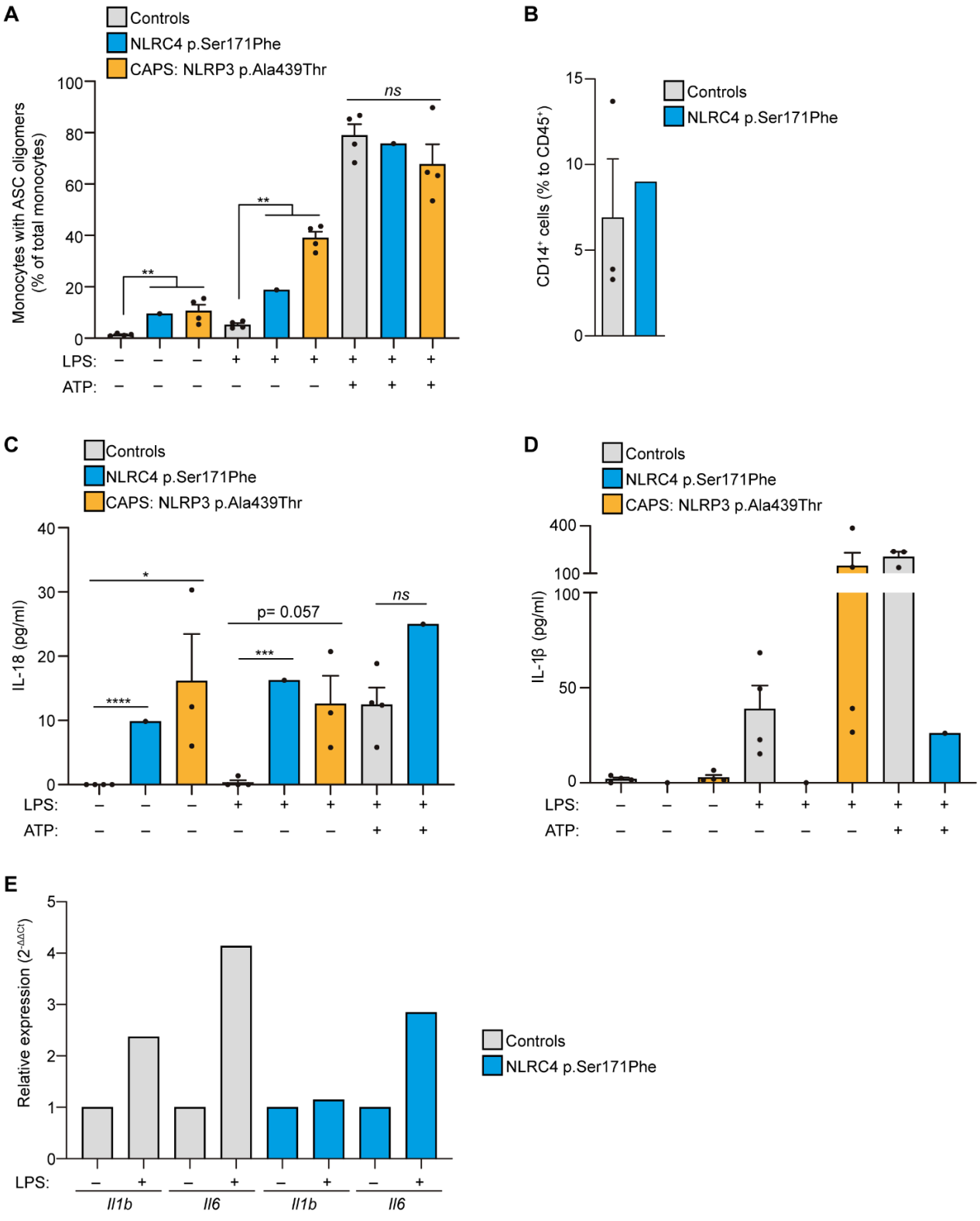
A
Controls
NLRC4 p.Ser171Phe
CAPS: NLRP3 p.Ala439Thr
Monocytes with ASC oligomers (% of total monocytes)
ns
**
**
LPS:
ATP:
B
Controls
NLRC4 p.Ser171Phe
CD14⁺ cells (% to CD45⁺)
C
Controls
NLRC4 p.Ser171Phe
CAPS: NLRP3 p.Ala439Thr
IL-18 (pg/ml)
*
p= 0.057
***
ns
****
LPS:
ATP:
D
Controls
NLRC4 p.Ser171Phe
CAPS: NLRP3 p.Ala439Thr
IL-1β (pg/ml)
LPS:
ATP:
E
Relative expression (2^-ΔΔCt)
LPS:
Il1b
Il6
Il1b
Il6
Controls
NLRC4 p.Ser171Phe

Figure 29. NLRC4 p.Ser171Phe variant induces increased inflammasome activation. (A) Percentage of ASC-specking monocytes identified by the time-of-flight assay from healthy individuals (controls), from the patient with NLRC4 p.Ser171Phe variant and from CAPS patients with the NLRP3 p.Ala439Thr variant primed with LPS and stimulated with ATP. **(B)** Percentage of monocytes (CD14+ cells on CD45+ cells) in the PBMCs from healthy individuals without AID (controls, grey) and from the patient with NLRC4 p.Ser171Phe variant (blue). **(C,D)** IL-18 **(C)** and IL-1β **(D)** release detected in cell-free supernatants from peripheral blood mononuclear cells from healthy individuals without AID (controls) and from the patient with NLRC4 p.Ser171Phe variant and from CAPS patients with the NLRP3 p.Ala439Thr variant primed with LPS and stimulated with ATP. **(E)** *Il1b* and *Il6* gene expression in PBMCs from a healthy individual without AID (control, grey) and from the patient with NLRC4 p.Ser171Phe variant (blue) primed with LPS. ****p<0.0001, ***p<0.0005, **p<0.005, *p<0.05, and ns p>0.05.

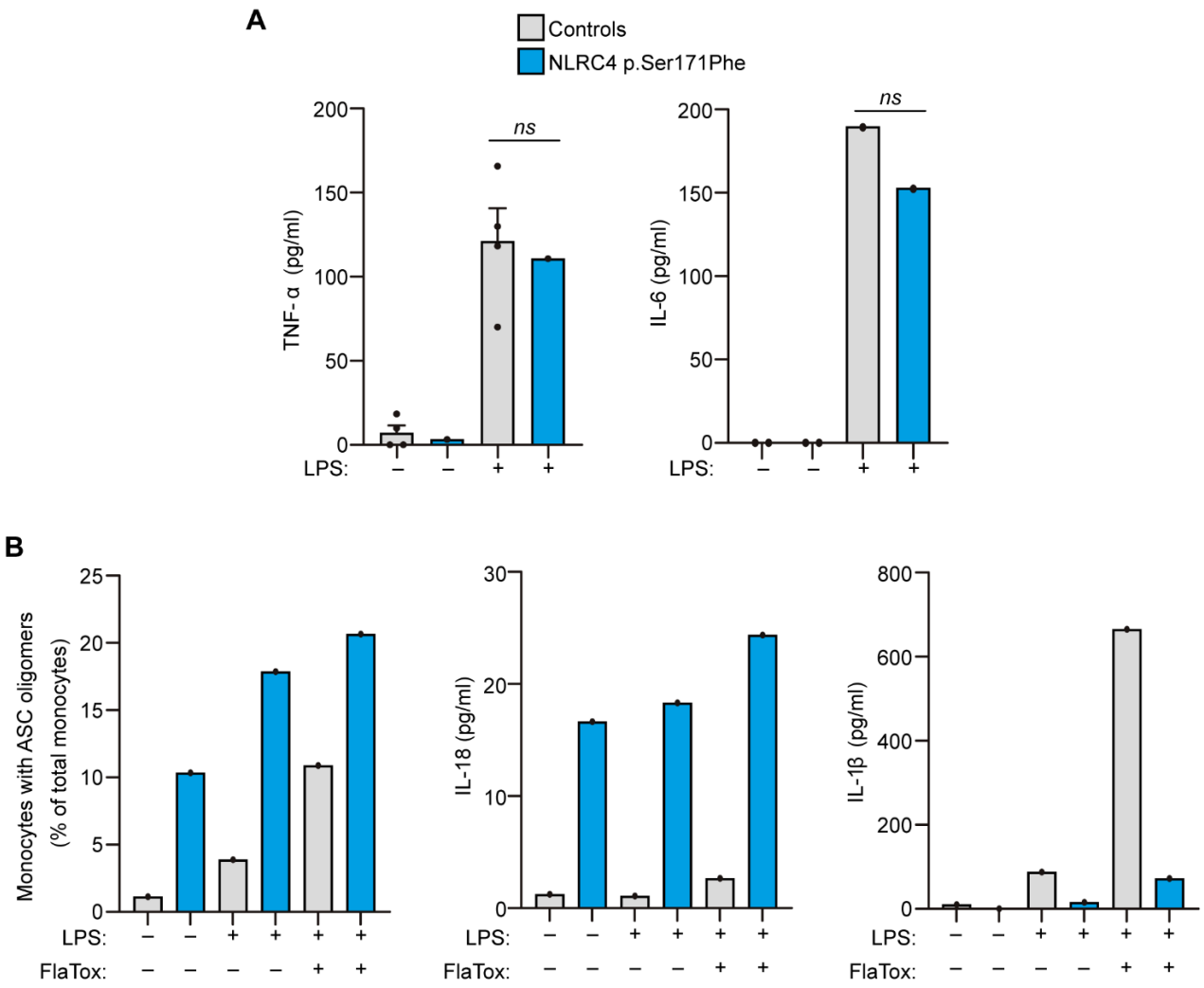
A
Controls
NLRC4 p.Ser171Phe
TNF- α (pg/ml)
IL-6 (pg/ml)
ns
ns
200
150
100
50
0
LPS: – – + +
B
Monocytes with ASC oligomers (% of total monocytes)
IL-18 (pg/ml)
IL-1β (pg/ml)
25
20
15
10
5
0
30
800
600
400
200
LPS: – – + + + +
FlaTox: – – – – + +

Figure 30. NLRC4 p.Ser171Phe variant induces increased IL-18 release. (A) TNF-α (left) and IL-6 (right) release detected in cell-free supernatants from peripheral blood mononuclear cells (PBMCs) from healthy individuals without AID (controls, grey) and from the patient with NLRC4 p.Ser171Phe variant (blue) primed with LPS. **(B)** Percentage of ASC-specking monocytes (left), release of IL-18 (middle) or IL-1β (right) from PBMCs from a healthy individual without AID (control, grey) and from the patient with NLRC4 p.Ser171Phe variant (blue) primed with LPS and stimulated with FlaTox. ****p<0.0001, ***p<0.0005, **p<0.005, *p<0.05, and ns p>0.05.

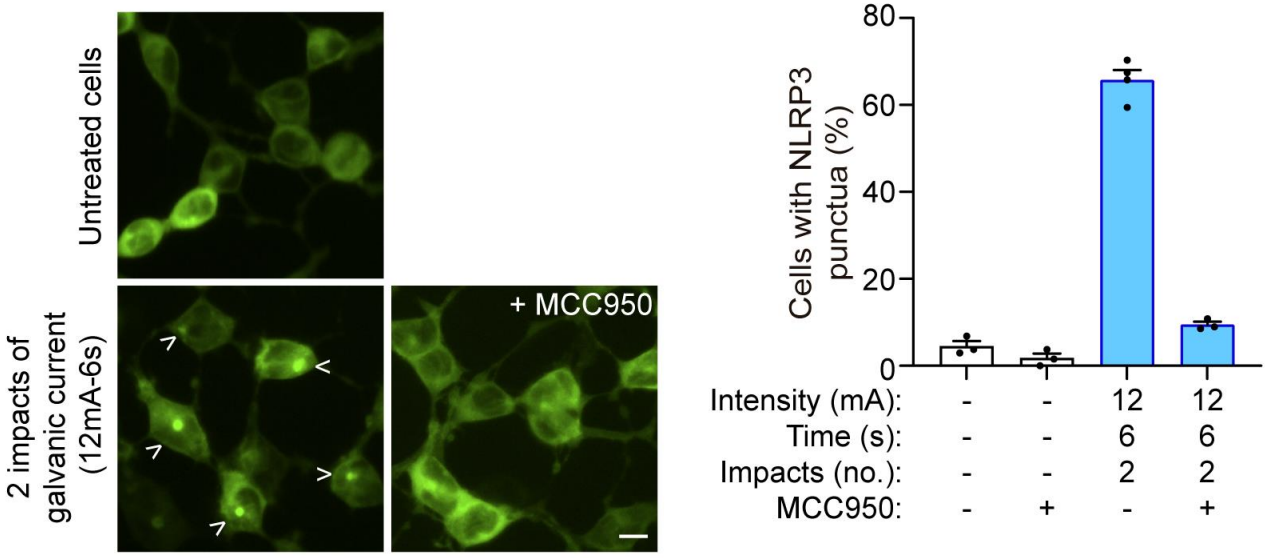
Untreated cells
2 impacts of galvanic current (12mA-6s)
+ MCC950
Cells with NLRP3 punctua (%)
80
60
40
20
0
Intensity (mA): - - 12 12
Time (s): - - 6 6
Impacts (no.): - - 2 2
MCC950: - + - +

Figure 31. NLRP3 activation by galvanic current in HEK293T cells. Fluorescence microscopy of HEK293T cells stably expressing NLRP3–YFP after 6 h of application of 2 impacts of 12 mA of galvanic current for 6 seconds, the specific inhibitor MCC950 (10 μM) was added 30 min before the galvanic current application; scale bar 10 mm; *n*= 3 independent experiments. ****p<0.0001, ***p<0.0005, **p<0.005, *p<0.05, and ns p>0.05.

Chapter 2. Evaluation of the NLRP3 inflammasome activation induced by galvanic current in macrophages.

2.1. Galvanic current enhances macrophage pro-inflammatory M1 phenotype

We initially designed and produced a device to apply galvanic current to adherent cultured cells in 6 well cell culture plates (**Figure 18**, see material and methods section for further details). This device allowed us to explore the effect of galvanic currents in bone marrow derived mouse macrophages. Application of 2 impacts of 12 mA of galvanic current for 6 seconds each, over LPS stimulated macrophages, induced an increase of the expression of *Cox2* and *Il6* genes (**Figure 32A**). However, it did not affect LPS-induced *Il1b* or *Tnfa* pro-inflammatory gene expression (**Figure 32A**).

Interestingly meanwhile *Tnfa* expression was upregulated with galvanic current alone (**Figure 32A**), galvanic currents were not inducing the expression of *Cox2*, *Il6* or *Il1b* genes on non-LPS treated macrophages, or over IL-4 treated macrophages (**Figure 32A**). When macrophages were polarized to M2 by IL-4, galvanic currents decreased the expression of the M2 markers *Arg1*, *Fizz1* and *Mrc1* (**Figure 32B**), however this decrease was small and non-significant for the M2 marker *Ym1* (**Figure 32B**). These data suggest that galvanic current could enhance the pro-inflammatory signature of M1 macrophages whilst decrease M2 polarization.

We next studied the concentration of released pro-inflammatory cytokines from macrophages, and found that galvanic current was not able to increase the concentration of IL-6 or TNF-α released after LPS stimulation (**Figure 32C**), but as expected from the results of Chapter 1, it significantly augmented the release of IL-1β in an intensity dependent manner (**Figure 32C**). This data indicates that the increase of *Il6* and *Tnfa* gene expression detected at mRNA level would not be transcribing to higher amounts of released IL-6 and TNF-α over LPS treatment, but galvanic current could be potentially activating an inflammasome to induce the release of IL-1β. All these data can be found in our recent publication Peñin-Franch, et. al., 2022.

2.2. IL-1β release is dependent on the total load of the galvanic current

As IL-1β release induced by galvanic current was dependent on the intensity of current applicated (**Figure 32C**), we next aimed to asses if changes in the different parameters of galvanic current could induce variations in IL-1β release. We found that 2 pulses of 12 mA during 3, 6 or 12 seconds of galvanic current induced increasing amounts of released IL-1β (**Figure 33A**), and this also happened with increasing number of pulses: 2, 4 or 8 pulses of

12 mA during 6 seconds (**Figure 33A**). However, increasing the time or the number of pulses of galvanic current, cell death was also increased, positively correlating with the increase in the number of pulses applicated (**Figure 33B**).

We next studied different protocols to apply galvanic current to induce IL-1β release with low cell toxicity, and at the same time, that could be clinically relevant and similar to the one used in patients (3 pulses of 3 mA during 3 seconds each). For that, we compared the application of 2 pulses of 12 mA during 6 seconds with 2 pulses of 3 mA during 12 seconds, in order to decrease the intensity of the galvanic current. We found that both protocols induced a similar amount of IL-1β release (**Figure 34A**), without inducing cell death (**Figure 34A**). We then tested low intensity (3 mA) during 6 seconds, but increasing the number of pulses, and found that IL-1β release increased with the number of pulses keeping cell death below 20% (**Figure 34B**). Then, we aimed to study the effect of the temperature meanwhile galvanic current is applicated, since current application induces an increase in temperature in the area under the needle. Applicating galvanic current at 4ºC resulted in no differences in IL-1β and LDH release when compared to 37ºC conditions (**Figure 34C**).

As the release of IL-1β was depended on the different parameters of galvanic current application, we decided to study if the total current load (calculated by multiplying all the values of each parameter: intensity x time x number of impacts) was related with the release of IL-1β. We compared the different parameters of the galvanic current application maintaining the same total current load. We started with protocols with a total load of 72 units and we found that the protocol of 2 impacts of 3 mA during 12 seconds released more IL-1β than the other protocols tested (**Figure 35A**). When the total load was of 144 units, we found that the protocol with 8 impacts of 3 mA during 6 seconds of galvanic current released more IL-1β than the one with 2 impacts of 12 mA during 6 seconds (**Figure 35A**). Finally, we compared two protocols with a total load of 288 units, without differences between them (**Figure 35A**). As the differences in IL-1β release were in the similar scale units (∼100 pg/ml for 72 total load, ∼200 pg/ml for 144 and ∼800 pg/ml for 288 total load), we compared the data for the different total load and obtained that increasing the total load of galvanic current correlated with an increase in IL-1β release and in LDH release (**Figure 35B**). Furthermore, we also observed a positive and significant correlation between the release of IL-1β and the release of LDH with increasing the total load of galvanic current (**Figure 35C**). All these data indicate that, *in vitro*, parameters of galvanic current can be changed to control different concentration of IL-1β release, obtaining optimized conditions with IL-1β release and low cell death to decrease the toxic of the treatment. However, a

higher total load of galvanic current induces high IL-1β release and a high cell death, not to be recommended for treatment.

2.3. Galvanic current activates the NLRP3 inflammasome

Since IL-1β release is induced by the activation of caspase-1 after the canonical or non-canonical inflammasome formation (Broz and Dixit, 2016), we next studied the release of IL-1β induced by galvanic current in macrophages deficient on caspase-1 and -11 to avoid both the canonical and non-canonical inflammasome signaling. We found that *Casp1/11*$^{-/-}$ macrophages fail to release IL-1β induced by galvanic current (**Figure 36A**). We then found that galvanic current application on *Pycard*$^{-/-}$ macrophages also failed to induce the release of IL-1β, denoting that the inflammasome adaptor protein ASC would be also required for the inflammasome activation (**Figure 36A**). Since current application could be considered a sterile danger signal and was inducing oligomerization of NLRP3 (see previous Chapter), we next assessed the implication of NLRP3, an inflammasome sensor important to elicit an immune response in sterile dangerous situations (Broz and Dixit, 2016; Liston and Masters, 2017). *Nlrp3*$^{-/-}$ and the use of the specific NLRP3 inhibitor MCC950 (Coll et al., 2015; Tapia-Abellán et al., 2019) impaired the release of IL-1β induced by galvanic current (**Figure 36A,B**), demonstrating that the NLRP3 inflammasome is activated during galvanic current application. Similarly, galvanic current was also able to induce the release of IL-18 (**Figure 36C**), another cytokine dependent on the activation of the inflammasome. The use of MCC950 or macrophages deficient on NLRP3 failed to release IL-18 after galvanic current application (**Figure 36C**), confirming that galvanic current stimulate NLRP3 to induce the release of both IL-1β and IL-18. As controls, similar results were obtained in parallel with the specific NLRP3 activator nigericin (**Figure 36B and Figure 37A**). Mechanistically, the use of an extracellular buffer with 40 mM of KCl decreased IL-1β release induced by nigericin and galvanic current application, but not the release of IL-1β induced by *Clostridium difficile* toxin B, that activate the Pyrin inflammasome which is a K^+-efflux independent inflammasome (**Figure 36D**). However, application of two pulses of 12 mA of galvanic current for 6 seconds failed to decrease intracellular K^+ (**Figure 36E and Figure 37B**), but increasing the number of pulses of galvanic current to eight resulted in a significant decrease of intracellular K^+ (**Figure 36E**). This data suggests that galvanic current slightly decrease intracellular K^+ when compared to the application of the K^+ ionophore nigericin (**Figure 36E**) and this explains the smaller concentration of IL-1β release induced by galvanic current compared to nigericin application (**Figure 36B**). After galvanic current application we were

able to detect the generation of the active p20 caspase-1 fragment, and processed IL-1β and $GSDMD^{NT}$ (**Figure 36F**). MCC950 was able to abrogate caspase-1 activation and the processed forms of IL-1β and $GSDMD^{NT}$ (**Figure 36F**), suggesting a functional caspase-1 activation and downstream signaling due to canonical NLRP3 activation and discarding the non-canonical NLRP3 activation that would result in GSDMD processing in the presence of MCC950. All these data confirm that galvanic current application induces an activation of the NLRP3 inflammasome and, since NLRP3 deficient macrophages failed to release IL-1β or IL-18, that no other inflammasome expressed in the macrophages was being activated. All these data can be found in our recent publication Peñin-Franch, et. al., 2022.

2.4. Galvanic current toxicity is not mediated by pyroptosis

Since GSDMD was processed and the N-terminus detected upon galvanic current application, we next assessed pyroptosis by means of Yo-Pro-1 uptake to cells, to measure plasma membrane pore formation and cell viability, and LDH leakage from the cell, to determine plasma membrane damage. Two impacts of galvanic currents of different intensities (3, 6, 12 mA) for a period of 6 seconds (conditions that induce IL-1β release as we show in **Figure 32C**) were only inducing a slightly increase of cell death (**Figure 38A**). This increase in cell death was not associated with the activation of the inflammasome, since it was also present in macrophages deficient on NLRP3, ASC or caspase-1/11 (**Figure 38B**), suggesting that was independently of inflammasome-mediated pyroptosis. Increasing the number or the time of 12 mA impacts of galvanic current applicated to the macrophages, resulted in a time-dependent increase of cell death (**Figure 38A**), correlating with higher concentrations of IL-1β and IL-18 release (**Figure 38C**). However, meanwhile IL-1β and IL-18 release was blocked by MCC950 (**Figure 38C**), LDH release was not dependent on NLRP3 activation (**Figure 38D**). This further corroborate that the NLRP3 activation is dependent on the intensity and time of galvanic current application. Similarly, two impacts of 12 mA for a period of 6 seconds were unable to induce plasma membrane permeabilization measured by Yo-Pro-1 uptake during a period of 3 h (**Figure 38E**). Yo-Pro uptake increased over 3 h in an intensity dependent manner (3, 6, 12 mA) when 8 impacts were applicated during 6 seconds (**Figure 38E**). This increase of plasma membrane permeabilization was not reverted after NLRP3 blocking with MCC950 or when ASC-deficient macrophages were used (**Figure 38F**). All these results demonstrate that doses of galvanic current of 3 or 6 mA for impacts of 6 seconds do not compromise cell viability but are able to induce an inflammatory response dependent on NLRP3 activation, in contrast

with current intensities of 12 mA that if prolonged in time could cause significant cell death independently of the inflammasome. All these data can be found in our recent publication Peñin-Franch, et. al., 2022.

Figures of Chapter 2

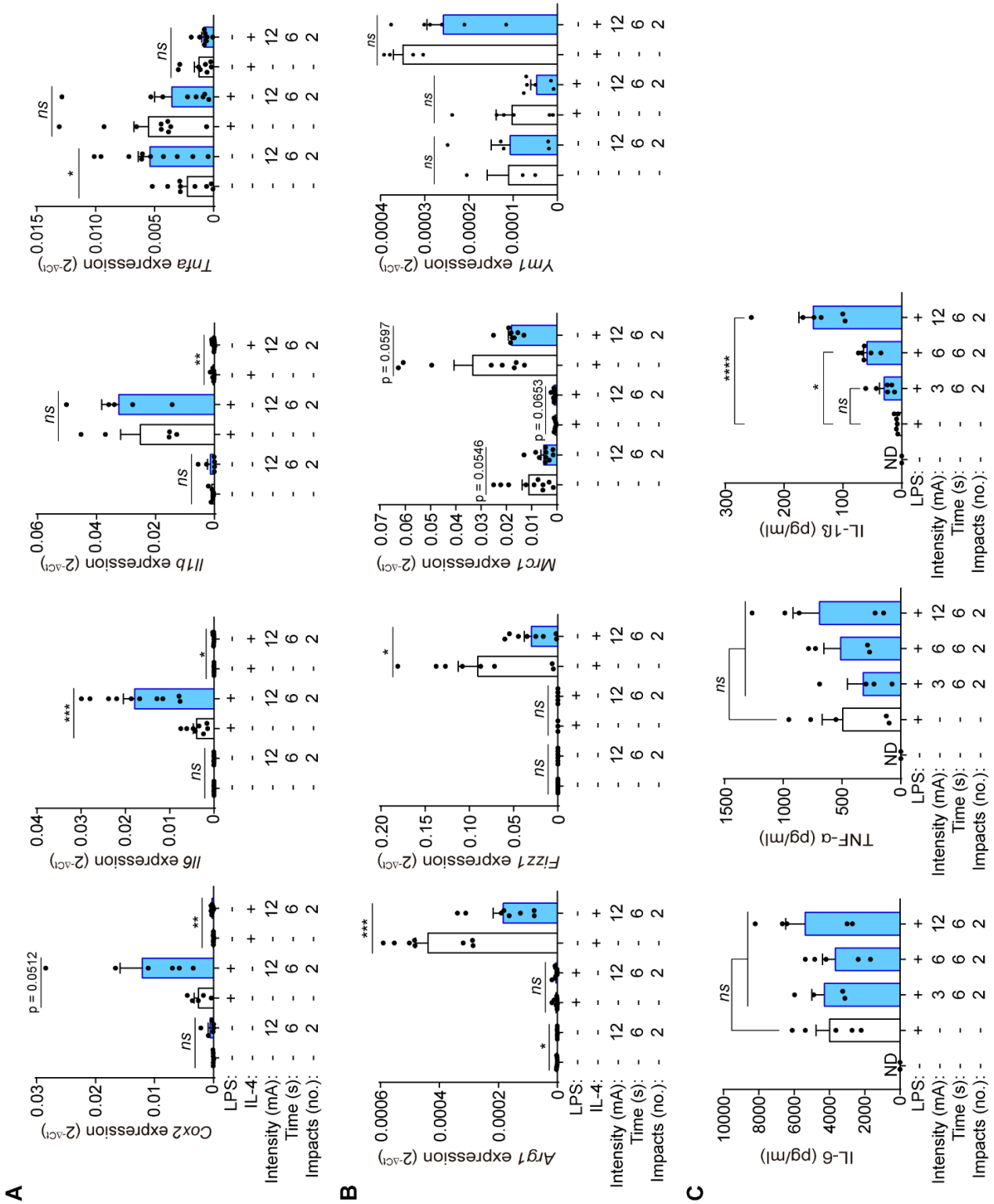
A
B
C
Cox2 expression (2-ΔCt)
Il6 expression (2-ΔCt)
Il1b expression (2-ΔCt)
Tnfa expression (2-ΔCt)
Arg1 expression (2-ΔCt)
Fizz1 expression (2-ΔCt)
Mrc1 expression (2-ΔCt)
Ym1 expression (2-ΔCt)
IL-6 (pg/ml)
TNF-α (pg/ml)
IL-1ß (pg/ml)
p = 0.0512
p = 0.0546
p = 0.0653
p = 0.0597
ns
LPS:
IL-4:
Intensity (mA):
Time (s):
Impacts (no.):
ND

Figure 32. Galvanic current increases the M1 phenotype of macrophages. (A) Quantitative PCR for M1 genes *Cox2*, *Il6*, *Il1b* and *Tnfa* expression from mouse bone-marrow derived macrophages (BMDMs) treated for 2 h with LPS (1 μg/ml) or 4 h with IL-4 (20 ng/μl) as indicated and then 2 impacts of 12 mA of galvanic current for 6 seconds were applicated. Cells were then further cultured for 6 h before analysis. Center values represent the mean and error bars represent s.e.m.; n= 5-10 samples of 5 independent experiments. **(B)** Quantitative PCR for M2 genes Arg1, Fizz1, Mrc1 and Ym1 expression from BMDMs treated as in (A). Center values represent the mean and error bars represent s.e.m.; n= 3-10 samples of 5 independent experiments. **(C)** IL-6, TNF-α and IL-1β release from BMDMs treated as in (A) but different intensities of galvanic current (3, 6, 12 mA) were applicated. Center values represent the mean and error bars represent s.e.m.; n= 2 for untreated cells and n= 4-6 for treatment groups from 4 independent experiments. ****p<0.0001, ***p<0.0005, **p<0.005, *p<0.05, and ns p>0.05.

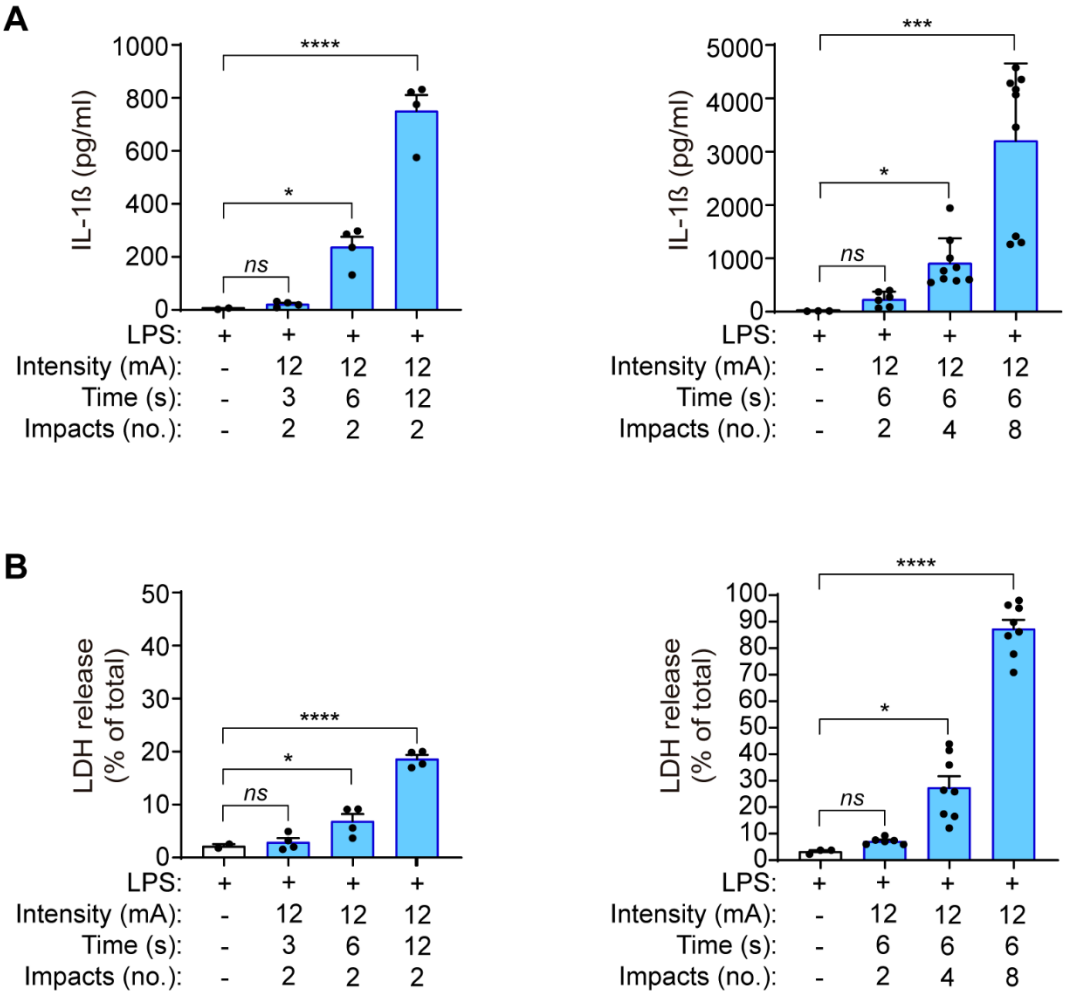
A
IL-1ß (pg/ml)
1000
800
600
400
200
0
****
*
ns
LPS: + + + +
Intensity (mA): - 12 12 12
Time (s): - 3 6 12
Impacts (no.): - 2 2 2
IL-1ß (pg/ml)
5000
4000
3000
2000
1000
0
***
*
ns
LPS: + + + +
Intensity (mA): - 12 12 12
Time (s): - 6 6 6
Impacts (no.): - 2 4 8
B
LDH release (% of total)
50
40
30
20
10
0
****
*
ns
LPS: + + + +
Intensity (mA): - 12 12 12
Time (s): - 3 6 12
Impacts (no.): - 2 2 2
LDH release (% of total)
100
90
80
70
60
50
40
30
20
10
0
****
*
ns
LPS: + + + +
Intensity (mA): - 12 12 12
Time (s): - 6 6 6
Impacts (no.): - 2 4 8

Figure 33. Higher time and number of impacts of galvanic current induce more IL-1β release. (A) IL-1β release from mouse bone marrow derived macrophages (BMDMs) treated for 2 h with LPS (1 μg/ml), then different protocols with increasing time or number of impacts of galvanic current were applicated and incubated for 6 h. **(B)** LDH release from BMDMs treated as in panel A. Center values represent the mean and error bars represent s.e.m.; n= 2-9 samples of at least 2 independent experiments. ****p<0.0001, ***p<0.0005, **p<0.005, *p<0.05, and ns p>0.05.

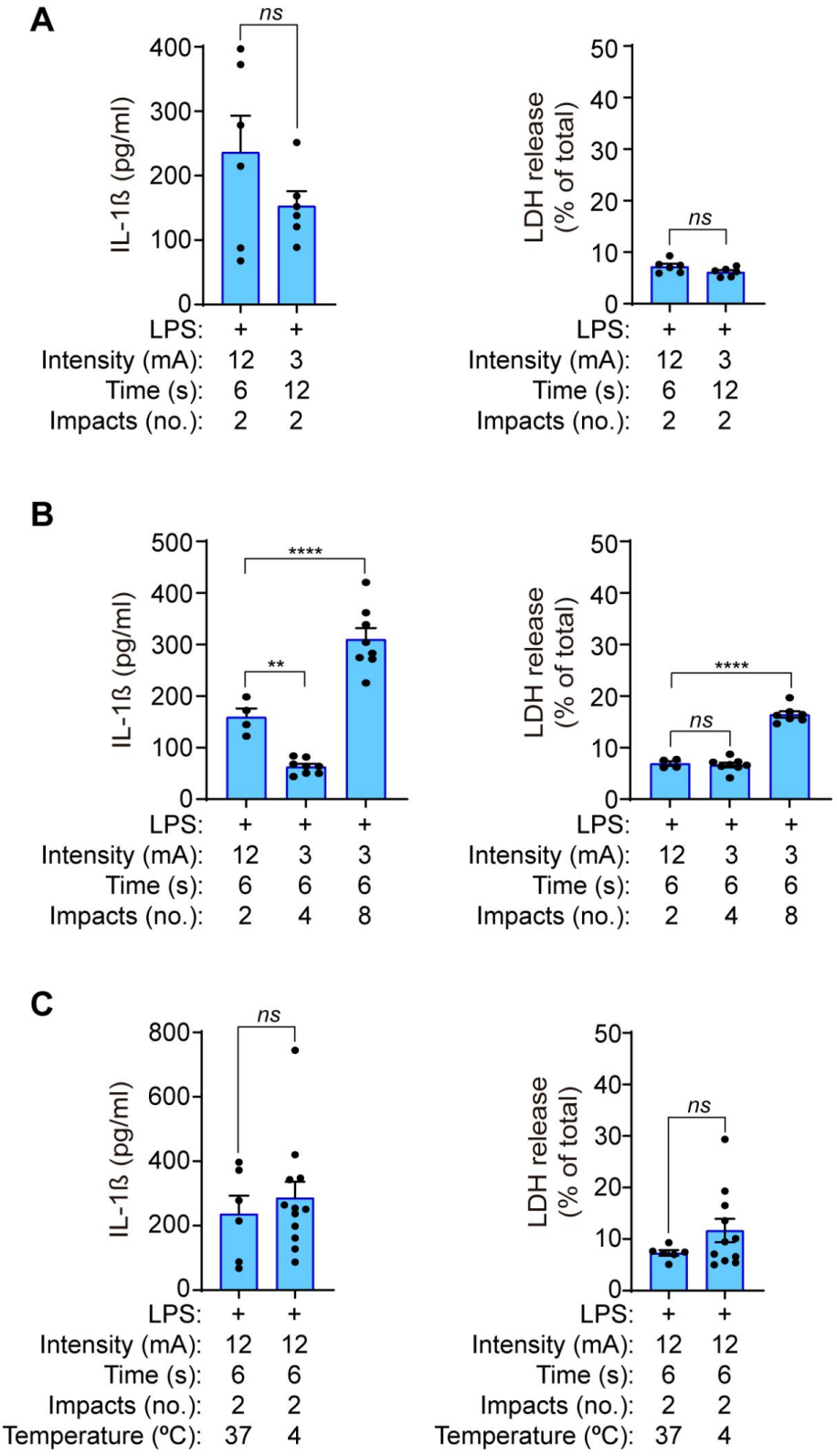
A
IL-1ß (pg/ml)
400
300
200
100
0
ns
LPS: + +
Intensity (mA): 12 3
Time (s): 6 12
Impacts (no.): 2 2
LDH release (% of total)
50
40
30
20
10
0
ns
LPS: + +
Intensity (mA): 12 3
Time (s): 6 12
Impacts (no.): 2 2
B
IL-1ß (pg/ml)
500
400
300
200
100
0
****
**
LPS: + + +
Intensity (mA): 12 3 3
Time (s): 6 6 6
Impacts (no.): 2 4 8
LDH release (% of total)
50
40
30
20
10
0
****
ns
LPS: + + +
Intensity (mA): 12 3 3
Time (s): 6 6 6
Impacts (no.): 2 4 8
C
IL-1ß (pg/ml)
800
600
400
200
0
ns
LPS: + +
Intensity (mA): 12 12
Time (s): 6 6
Impacts (no.): 2 2
Temperature (ºC): 37 4
LDH release (% of total)
50
40
30
20
10
0
ns
LPS: + +
Intensity (mA): 12 12
Time (s): 6 6
Impacts (no.): 2 2
Temperature (ºC): 37 4

Figure 34. Less intensity of galvanic current applicated with increasing time or impacts lead to IL-1β release. (A) IL-1β and LDH release from mouse bone marrow derived macrophages (BMDMs) primed for 2 h with LPS (1 μg/ml), then treated with 2 impacts of 12 mA during 6 seconds or with 2 impacts of 3 mA during 12 seconds and then incubated for 6 h. Center values represent the mean and error bars represent s.e.m.; n= 6 samples of 3 independent experiments. **(B)** IL-1β and LDH release from BMDMs primed as in A, treated with 2 impacts of 12 mA during 6 seconds or with 4 or 8 impacts of 3 mA during 6 seconds and then incubated for 6 h. Center values represent the mean and error bars represent s.e.m.; n= 4-8 samples of 3 independent experiments. **(C)** IL-1β and LDH release from BMDMs primed as in A, treated with 2 impacts of 12 mA during 6 seconds at 37ºC or 4ºC and then incubated for 6 h. Center values represent the mean and error bars represent s.e.m.; n= 6-12 samples of 3 independent experiments. ****p<0.0001, ***p<0.0005, **p<0.005, *p<0.05, and ns p>0.05.

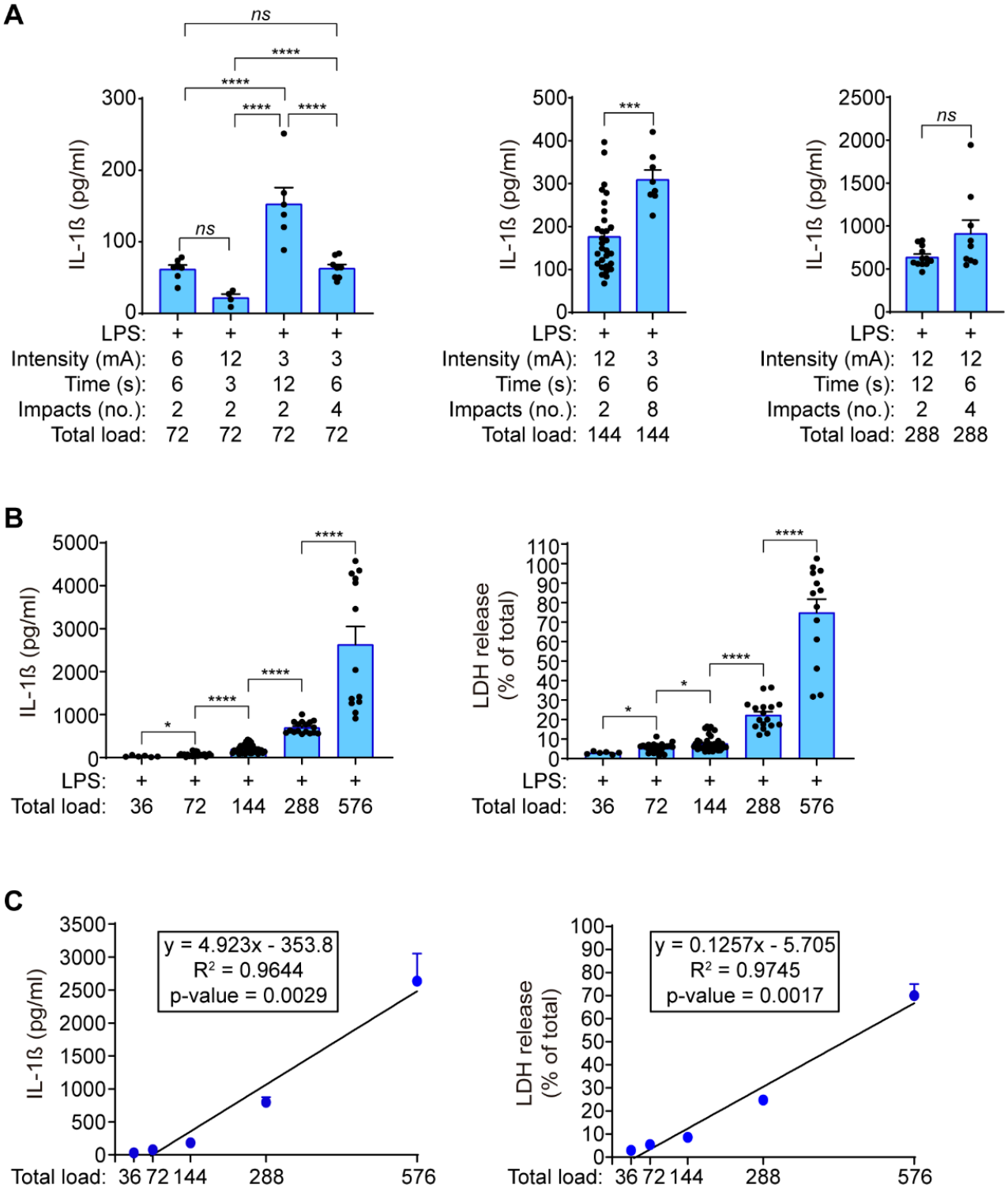
A
IL-1ß (pg/ml)
ns
****
****
****
****
****
300
200
100
0
LPS: + + + +
Intensity (mA): 6 12 3 3
Time (s): 6 3 12 6
Impacts (no.): 2 2 2 4
Total load: 72 72 72 72
***
500
400
300
200
100
0
LPS: + +
Intensity (mA): 12 3
Time (s): 6 6
Impacts (no.): 2 8
Total load: 144 144
ns
2500
2000
1500
1000
500
0
LPS: + +
Intensity (mA): 12 12
Time (s): 12 6
Impacts (no.): 2 4
Total load: 288 288
B
IL-1ß (pg/ml)
*
****
****
****
5000
4000
3000
2000
1000
0
LPS: + + + + +
Total load: 36 72 144 288 576
LDH release (% of total)
*
*
****
****
110
100
90
80
70
60
50
40
30
20
10
0
LPS: + + + + +
Total load: 36 72 144 288 576
C
IL-1ß (pg/ml)
y = 4.923x - 353.8
R² = 0.9644
p-value = 0.0029
3500
3000
2500
2000
1500
1000
500
0
Total load: 36 72 144 288 576
LDH release (% of total)
y = 0.1257x - 5.705
R² = 0.9745
p-value = 0.0017
100
90
80
70
60
50
40
30
20
10
0
Total load: 36 72 144 288 576

Figure 35. Increasing total load of galvanic current correlated with increasing IL-1β and LDH release. (A) IL-1β release from mouse bone marrow derived macrophages (BMDMs) primed for 2 h with LPS (1 μg/ml), then treated with different protocols of galvanic current with 72, 144 or 288 units of total load and incubated for 6 h. Center values represent the mean and error bars represent s.e.m.; n= 4-33 samples of at least 3 independent experiments. **(B,C)** IL-1β and LDH release **(B)** and correlation of IL-1β and LDH release with total load **(C)** from BMDMs primed as in A, then treated with different protocols of galvanic current with 36, 72, 144, 288, 576 units of total load and incubated for 6 h. For 36 units the galvanic current protocol was 2 impacts of 3 mA during 6 seconds, and for 576 units the galvanic current protocol was 8 impacts of 12 mA during 6 seconds. Center values represent the mean and error bars represent s.e.m.; n= 4-33 samples of at least 3 independent experiments. ****$p<0.0001$, ***$p<0.0005$, **$p<0.005$, *$p<0.05$, and ns $p>0.05$.

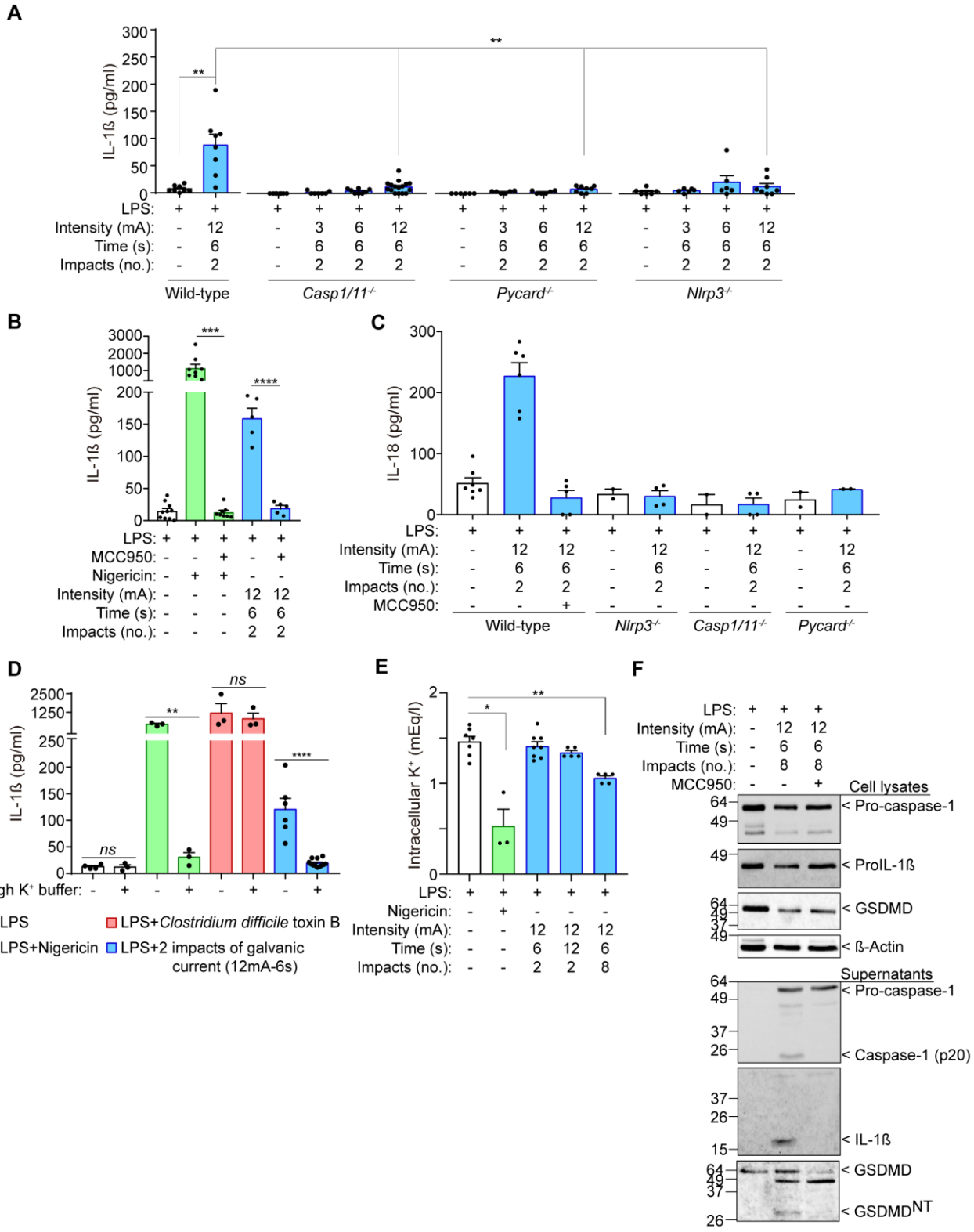
A
IL-1ß (pg/ml)
LPS:
Intensity (mA):
Time (s):
Impacts (no.):
Wild-type
Casp1/11-/-
Pycard-/-
Nlrp3-/-
B
IL-1ß (pg/ml)
LPS:
MCC950:
Nigericin:
Intensity (mA):
Time (s):
Impacts (no.):
C
IL-18 (pg/ml)
LPS:
Intensity (mA):
Time (s):
Impacts (no.):
MCC950:
Wild-type
Nlrp3-/-
Casp1/11-/-
Pycard-/-
D
IL-1ß (pg/ml)
High K+ buffer:
LPS
LPS+Clostridium difficile toxin B
LPS+Nigericin
LPS+2 impacts of galvanic current (12mA-6s)
E
Intracellular K+ (mEq/l)
LPS:
Nigericin:
Intensity (mA):
Time (s):
Impacts (no.):
F
LPS:
Intensity (mA):
Time (s):
Impacts (no.):
MCC950:
Cell lysates
< Pro-caspase-1
< ProIL-1ß
< GSDMD
< ß-Actin
Supernatants
< Pro-caspase-1
< Caspase-1 (p20)
< IL-1ß
< GSDMD
< GSDMDNT

Figure 36. IL-1β release induced by galvanic current is dependent on the NLRP3 inflammasome. (A) IL-1β release from wild type, *Casp1/11*$^{-/-}$, *Pycard*$^{-/-}$ and *Nlrp3*$^{-/-}$ mouse bone marrow derived macrophages (BMDMs) treated for 2 h with LPS (1 µg/ml) and then 2 impacts of different intensities of galvanic current (3, 6, 12 mA) for 6 seconds was applicated. Cells were then further cultured for 6 h before cytokine measurement in supernatant. Center values represent the mean and error bars represent s.e.m.; *n*= 6-16 samples of 10 independent experiments. **(B)** IL-1β release from wild type BMDMs treated as in A but applicating the NLRP3 specific inhibitor MCC950 (10 µM) 30 min before the galvanic current application and during the last 6 h of culture. As a control, cells were treated with nigericin (1,5 µM) instead galvanic current application. Center values represent the mean and error bars represent s.e.m.; *n*= 5-10 samples of 5 independent experiments. **(C)** IL-18 release from BMDMs treated as in A. Center values represent the mean and error bars represent s.e.m.; *n*= 2-7 samples of at least 2 independent experiments. **(D)** IL-1β release from wild type BMDMs treated as in A but applicating a buffer with 40 mM of KCl (high K^+ buffer) during the last 6 h of culture. As controls, cells were treated with nigericin (1,5 µM) or *Clostridium difficile* toxin B (1 µg/ml) instead galvanic current application. Center values represent the mean and error bars represent s.e.m.; *n*= 3-12 samples of 4 independent experiments. **(E)** Intracellular K^+ concentration from wild type BMDMs primed with LPS as in A, but then treated for 6 h with nigericin (1.5 µM) or 2 or 8 impacts of 12 mA for 6 or 12 seconds as indicated. Center values represent the mean and error bars represent s.e.m.; *n*= 3-8 samples of 3 independent experiments. **(F)** Immunoblot of cell extract and supernatants for caspase-1, IL-1β, GSDMD and β-actin from wild type BMDMs treated as in B, but with 8 impacts. Representative of *n*= 2 independent experiments. ****p<0.0001, ***p<0.0005, **p<0.005, *p<0.05, and ns p>0.05.

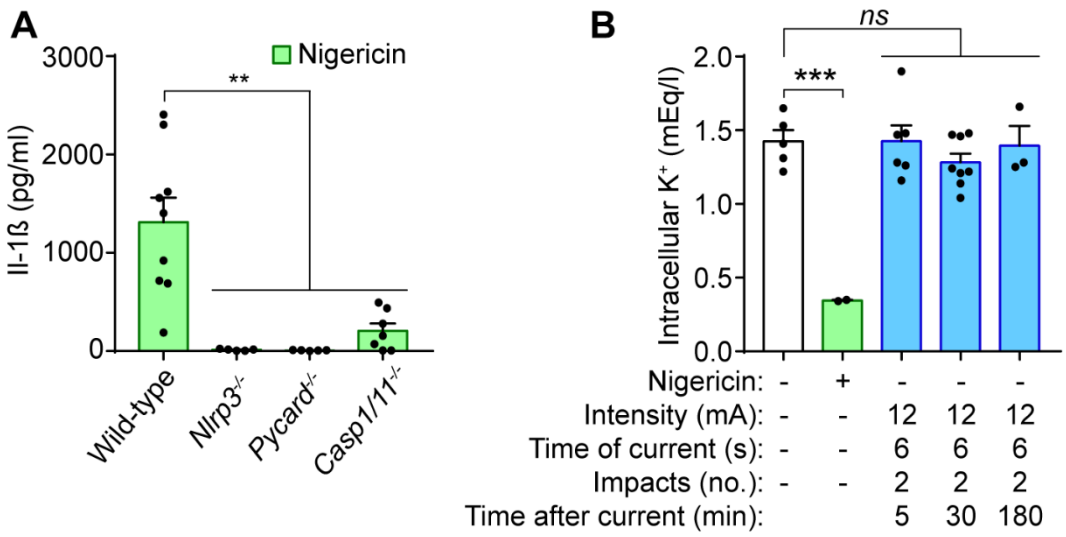
A
Nigericin
Il-1ß (pg/ml)
3000
2000
1000
0
**
Wild-type
Nlrp3-/-
Pycard-/-
Casp1/11-/-
B
ns
***
Intracellular K+ (mEq/l)
2.0
1.5
1.0
0.5
0.0
Nigericin: - + - - -
Intensity (mA): - - 12 12 12
Time of current (s): - - 6 6 6
Impacts (no.): - - 2 2 2
Time after current (min): 5 30 180

Figure 37. Galvanic current does not induce a detectable intracellular K+ decrease. (A) IL-1β release from wild type, *Casp1/11*$^{-/-}$, *Pycard*$^{-/-}$ and *Nlrp3*$^{-/-}$ mouse bone marrow derived macrophages (BMDMs) treated for 2 h with LPS (1 μg/ml) and then with 6 h with nigericin (1 μM). Center values represent the mean and error bars represent s.e.m.; n= 2-8 samples of 3 independent experiments. **(B)** Intracellular K^+ concentration from wild type BMDMs primed with LPS as in A, but then treated for 30 min with nigericin (1.5 μM) or for the indicated time after 2 impacts of 12 mA for 6 seconds. Center values represent the mean and error bars represent s.e.m.; n= 5-9 samples of 9 independent experiments. ****p<0.0001, ***p<0.0005, **p<0.005, *p<0.05, and ns p>0.05.

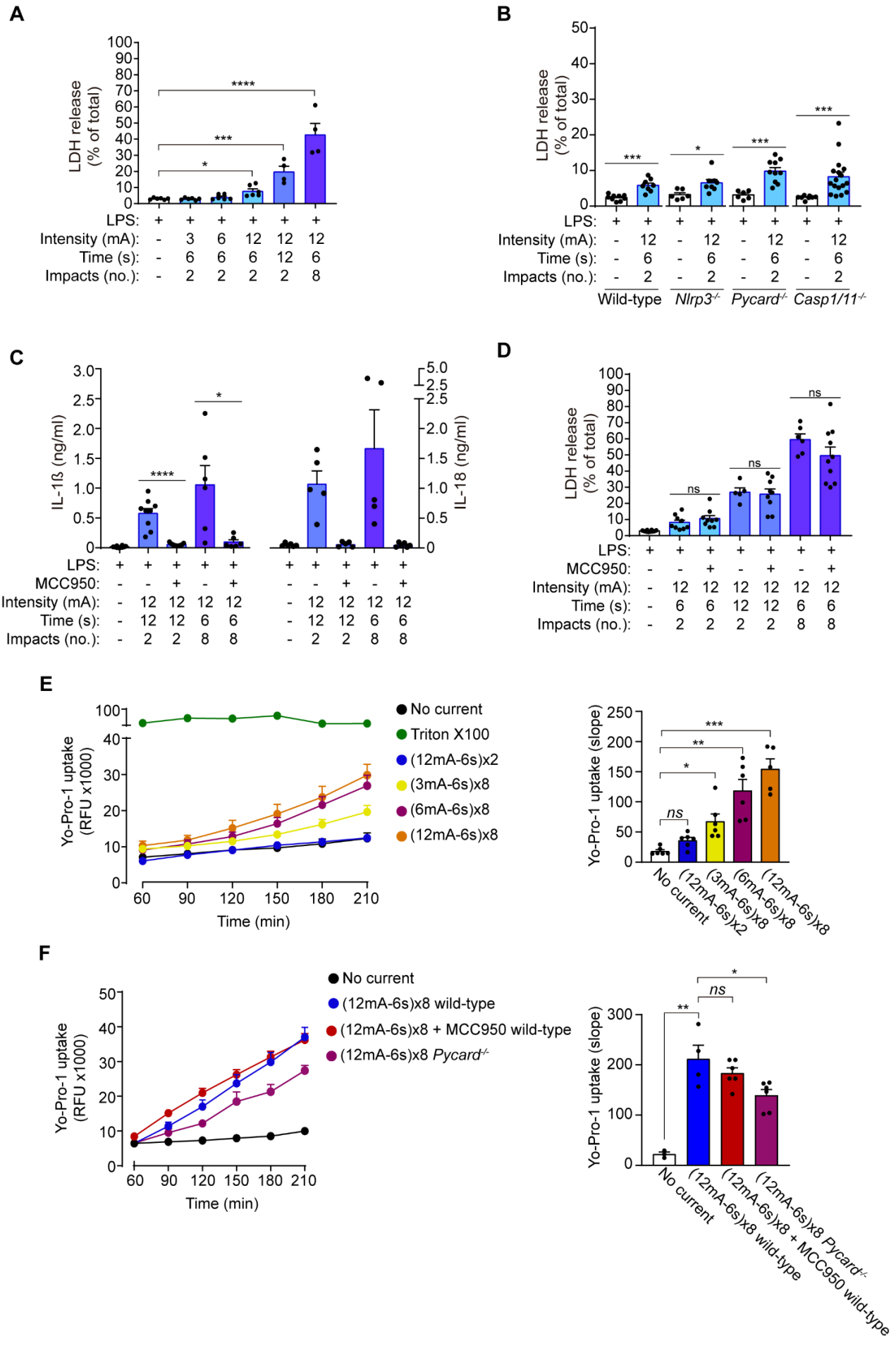
A
LDH release (% of total)
LPS:
Intensity (mA):
Time (s):
Impacts (no.):
B
LDH release (% of total)
Wild-type
Nlrp3-/-
Pycard-/-
Casp1/11-/-
C
IL-1ß (ng/ml)
IL-18 (ng/ml)
MCC950:
D
LDH release (% of total)
ns
E
Yo-Pro-1 uptake (RFU x1000)
Time (min)
No current
Triton X100
(12mA-6s)x2
(3mA-6s)x8
(6mA-6s)x8
(12mA-6s)x8
Yo-Pro-1 uptake (slope)
F
(12mA-6s)x8 wild-type
(12mA-6s)x8 + MCC950 wild-type
(12mA-6s)x8 Pycard-/-

Figure 38. Galvanic current does not induce inflammasome-mediated pyroptosis. (A) Extracellular amount of LDH determining cell membrane damage from mouse bone marrow derived macrophages (BMDMs) treated for 2 h with LPS (1 µg/ml) and then 2 or 8 impacts of different intensities of galvanic current (3, 6, 12 mA) for 6 or 12 seconds were applicated as indicated. Cells were then further cultured for 6 h before LDH determination in supernatant. Center values represent the mean and error bars represent s.e.m.; n= 3-4 samples of 6 independent experiments. **(B)** Extracellular amount of LDH from wild type, *Nlrp3*$^{-/-}$, *Pycard*$^{-/-}$ and *Casp1/11*$^{-/-}$ mouse BMDMs treated as in A. Center values represent the mean and error bars represent s.e.m.; n= 6-17 samples of 12 independent experiments. **(C)** IL-1β (left) and IL-18 (right) release from wild type BMDMs treated as in A, but applicating the NLRP3 specific inhibitor MCC950 (10 µM) during the last 6 h of culture. Center values represent the mean and error bars represent s.e.m.; n= 6-10 samples of 5 independent experiments. **(D)** Extracellular amount of LDH from wild type BMDMs treated as in C. Center values represent the mean and error bars represent s.e.m.; n= 5-10 samples of 5 independent experiments. **(E)** Kinetic of Yo-Pro-1 uptake (upper panel) or slope of the uptake (lower panel) in wild type BMDMs treated for 2 h with LPS (1 µg/ml) and then with different intensities of galvanic current (as indicated) or with the detergent triton X-100 (1 %) during 3.5 h. Center values represent the mean and error bars represent s.e.m.; n= 3-6 of 3 independent experiments. **(F)** Yo-Pro-1 uptake indicating plasma membrane pore formation and cell viability. Kinetic of Yo-Pro-1 uptake (upper panel) or slope of the uptake (lower panel) in wild type or *Pycard*$^{-/-}$ BMDMs treated as in E, but when indicated the NLRP3 specific inhibitor MCC950 (10 µM) was added after galvanic current application. Center values represent the mean and error bars represent s.e.m.; n= 3-6 samples of 3 independent experiments. ****p<0.0001, ***p<0.0005, **p<0.005, *p<0.05, and ns p>0.05.

Chapter 3. Involvement of NLRP3 on the regenerative response of galvanic current in pre-clinical models.

3.1. Galvanic current applicated in Achilles' mice tendon induces inflammation and tissue regeneration dependent on NLRP3 inflammasome

3.1.1. Galvanic current applicated in tendon increases inflammation *in vivo*

In order to study the effect of galvanic current *in vivo*, we applied 3 impacts of 3 mA of galvanic current during 3 seconds in the calcaneal tendon of mice. We found that it resulted in an increase of the number of polymorphonuclear cells 3 days after treatment when compared with tendons treated with needling alone (a puncture without current application, **Figure 39A,B**). This increase returned to basal after 7 days and stayed low up to 21 days after galvanic current application (**Figure 39B**). Similarly, the number of $F4/80^+$ macrophages increased after 3 days of galvanic current application when compared to needling alone and returned to basal levels after 7 days (**Figure 39C,D**). Other immune cell types detected in the tendon, as mastocytes, were not significantly increased by galvanic current application when compared to needling alone (**Figure 40A**). Since polymorphonuclear cells increased similarly than macrophages, we then aimed to investigate if galvanic current could be also inducing the release of IL-1β from neutrophils. However, galvanic current application on LPS-primed neutrophils failed to release IL-1β or LDH (**Figure 40B**). Other histological features of the tendon (general structure of the tendon, number of tenocytes, shape and area of tenocyte nuclei or neo-vascularization) were also not affected by the application of galvanic currents compared to needling alone (**Figure 40C-G**).

We next assessed the expression of different pro-inflammatory cytokines in the calcaneal tendon after 3 days of 3 impacts of 3 mA of galvanic current application during 3 seconds to characterize the molecular inflammatory response in the tendon. Expression of *Il6*, *Il1a* and *Il1b*, as well as the IL-1 receptor antagonist (*Il1rn*) and the chemokine *Cxcl10* were all increasing after percutaneous electrolysis when compared to needling alone (**Figure 41A**). However, as shown in figure 1 the increase in *Il6* cytokine gene expression induced by galvanic current in macrophages did not correlate with an increase in IL-6 cytokine secretion. Different NLRP3 inflammasome genes also exhibit an increase in expression (*Nlrp3*, *Pycard*, *Casp1*) when galvanic current was applicated, but this increase was not significantly when compared to needling (**Figure 41B**). *Gsdmd* expression was not upregulated in the tendons after galvanic current application (**Figure 41B**). These data suggest that galvanic current induces an inflammatory response driven by the infiltration of polymorphonuclear cells and macrophages, together an increase of the expression of

several cytokines and chemokines. All these data can be found in our recent publication Peñin-Franch, et. al., 2022.

3.1.2. The NLRP3 inflammasome controls the *in vivo* inflammatory response induced by galvanic current

In order to evaluate if the NLRP3 inflammasome mediates the inflammatory response in tendons after percutaneous electrolysis, we applied galvanic currents in the calcaneal tendon of *Nlrp3*$^{-/-}$ mice. Application of 3 impacts of 3 mA of galvanic current for 3 seconds in the calcaneal tendon of *Nlrp3*$^{-/-}$ mice resulted in a significant reduction of *Il1b*, *Il1rn* and *Cxcl10* expression after 3 days when compared to wild-type mice (**Figure 42A**). Specific inflammasome associated genes, as *Pycard*, *Casp1* or *Gsdmd* (except for *Nlrp3*) where not affecting their expression in the calcaneal tendon of *Nlrp3*$^{-/-}$ mice after 3 days of galvanic current application when compared to wild type mice (**Figure 42B**). Surprisingly, galvanic current produced a tendency to increase the expression of *Il6* in the tendons of *Nlrp3*$^{-/-}$ after 3 days (**Figure 42C**) and in parallel, the number of polymorphonuclear cells was also increased (**Figure 42D**). However, the number of macrophages was not affected in the *Nlrp3*$^{-/-}$ calcaneal tendon when galvanic current was applicated (**Figure 42D**). We also confirmed a decrease of *Il1b* and *Cxcl10* expression in the tendons of *Pycard*$^{-/-}$ mice after 3 days of galvanic current application (**Figure 43A,B**), suggesting that the NLRP3 inflammasome is important to modulate part of the inflammatory response after galvanic current application. All these data can be found in our recent publication Peñin-Franch, et. al., 2022.

3.1.3. The NLRP3 inflammasome induces a tissue regenerative response to galvanic current application that increase tendon stiffness

Galvanic current application has been widely used to resolve chronic tendinopathies in different tendons (Abat et al., 2016; Rodríguez-Huguet et al., 2020; Valera-Garrido et al., 2014). First, we measured collagen fiber properties of mouse Aquilles tendons 14 days after treatment with 3 mA, 3 s, 3 pulses of galvanic current, but percutaneous electrolysis did not affect collagen fiber properties measured (width and length) when compared to needling alone (**Figure 44A,B**). During tissue regeneration, the production of new extracellular matrix by collagen deposition is a key process (Shook et al., 2018; Wynn, 2008). In order to investigate if the inflammatory response mediated by the NLRP3 inflammasome after galvanic current application is important for tissue regeneration, we measured *Tgfb1*

expression as a key factor inducing collagen production. We found that in vivo the expression of *Tgfb1* after 3 days of galvanic current application in the calcaneal tendon of mice was dependent on NLRP3 (**Figure 45A**). In line, after 7 days of percutaneous electrolysis the levels of type III collagen were decreased, with a parallel increase of type I collagen when compared to needling alone (**Figure 45B**). The increase of type I collagen after 7 days of galvanic current application was reduced in *Nlrp3*$^{-/-}$ mice (**Figure 45C**). NLRP3 also controlled the structural dispersion of collagen fibers, which was decreased by galvanic current application in wild type mice, but increased in *Nlrp3*$^{-/-}$ mice (**Figure 45D**). All these results suggest that the NLRP3 inflammasome controls the response of galvanic current inducing type I collagen production and arranging the collagen fibers. This controlled deposition of collagen fibers induced by galvanic current resulted at mechanical level in an increase of tendon stiffness and a decrease of the maximum tension supported by the tendon (**Figure 45E**). NLRP3 inflammasome was responsible for the increase of tendon stiffness after galvanic current application (**Figure 45E**). Overall, we found that galvanic current application is able to activate the NLRP3 inflammasome and induce the release of IL-1β, initiating an inflammatory response that led to the regeneration of the tendon by increasing type I collagen, the arrangement of the collagen fibers and increasing the resistance of the tendon to change in length (**Figure 51**). All these data can be found in our recent publication Peñin-Franch, et. al., 2022.

3.2. Sterile damage induced by collagenase in Achilles' mice tendon is partially dependent on NLRP3 inflammasome

3.2.1. Tissue damage induced by collagenase in mice Achilles' tendon induces a sterile inflammatory response

Collagenase injection was used to induce sterile damage in Achilles' mice tendons as a model of tendinopathy. We studied the inflammatory response related with this damage and we observed an increase in polymorphonuclear cells infiltration in the periphery of the tendon at 1 day after the injection. The number of polymorphonuclear cells decreased progressively after 3, 7 and 10 days reaching the same levels than control treated tendons with the injection of sterile saline solution at 14 and 21 days (**Figure 46A**). In parallel, an increase in *Il6* gene expression 3 days after treatment was observed in collagenase treated tendons compared with control tendons (**Figure 46B**). This increase was also maintained after 7 and 14 days, but the increase was lower compared with 3 days (**Figure 46B**). However, *Il1b* gene expression increased in tendons compared with control tendons at all

the times measured (**Figure 46B**), although similarly to *Il6*, the induction was decreasing with the time. This induction in *Il1b* and *Il6* expression at 3 days, was not observed when denatured collagenase was injected (**Figure 46C**), suggesting that it is a response to the activity of collagenase and probably to tissue damage. All these results suggest that collagenase injection induce a sterile tissue damage and an inflammatory response characterized at least with an infiltrate of granulocytes and an increase in pro-inflammatory cytokines.

3.2.2. Inflammation induced by collagenase is partially dependent on the NLRP3 inflammasome

We next aimed to asses if the inflammatory response induced by collagenase was dependent on the NLRP3 inflammasome. So, we measured the amount of different pro-inflammatory cytokines 3 days after collagenase injection in wild type, *Nlrp3*$^{-/-}$ and *Pycard*$^{-/-}$ mice. First we found that collagenase induced an increase of IL-1β, IL-18, IL-6 and TNF-α when compared with saline injected tendons in wild type mice (**Figure 47A**). We observed that the increase in IL-1β was not observed in *Nlrp3*$^{-/-}$ or *Pycard*$^{-/-}$ mice injected with collagenase (**Figure 47A**). In contrast, IL-6 increased in wild type, *Nlrp3*$^{-/-}$ and *Pycard*$^{-/-}$ mice treated with collagenase compared with saline injected controls (**Figure 46A**). However, *Nlrp3*$^{-/-}$ and *Pycard*$^{-/-}$ mice presented less IL-6 than wild type mice, however in *Pycard*$^{-/-}$ mice the decrease was not significant (**Figure 47A**). Surprisingly, an induction of IL-18 was observed in wild type and *Nlrp3*$^{-/-}$ mice treated with collagenase compared to controls, but this increase was not present in *Pycard*$^{-/-}$ mice (**Figure 47A**). TNF-α was also induced in all the genotypes treated with collagenase compared with controls, but no differences between genotypes were observed (**Figure 47A**). To evaluate if the changes of cytokine measured in the tendons was due to gene expression, we measured the expression of *Il1b* and *Il6* genes at 3 days after collagenase injection. *Il1b* expression was induced with collagenase in wild type, *Nlrp3*$^{-/-}$ and *Pycard*$^{-/-}$ mice, but no differences were observed between genotypes (**Figure 47B**), suggesting that the defect on the inflammasome was affecting the generation of mature IL-1β protein that is better detected by the ELISA used than the pro-IL-1β. In contrast, *Il6* gene expression was only induced in wild type and *Pycard*$^{-/-}$ tendons, but not in the tendons of the *Nlrp3*$^{-/-}$ mice (**Figure 47B**). Also, a slightly but not significant decrease of both *Il1b* and *Il6* expression between wild type and *Nlrp3*$^{-/-}$ mice treated with collagenase was observed, but no differences were observed between wild type mice and *Pycard*$^{-/-}$ mice (**Figure 47B**).

The amount of the chemokine CXCL10 and the number of polymorphonuclear cells in wild type, *Nlrp3*$^{-/-}$ and *Pycard*$^{-/-}$ mice 3 after collagenase injection was also measured in order to study if the recruitment of inflammatory cells was also dependent on the NLRP3 inflammasome. CXCL10 was increased by collagenase injection in the three genotypes, but no differences between both knock-outs and the wild type mice were observed (**Figure 48A**). Similarly, the a slightly decrease in CXCL10 could be related with the decrease observed in the number of polymorphonuclear cells in *Nlrp3*$^{-/-}$ mice at 1, 3 and 7 days after collagenase injection compared with wild type (**Figure 48B**). *Pycard*$^{-/-}$ treated with collagenase did not present differences in number of polymorphonuclear cells compared with wild type (**Figure 48B**). All this data suggest that the inflammation induced by collagenase is partially dependent on NLRP3 as some pro-inflammatory cytokines decreased in *Nlrp3*$^{-/-}$ mice, but not the number of polymorphonuclear cells. This is in line with the fact that the increase of polymorphonuclear cells induced by galvanic current was also independent on the NLRP3 inflammasome (**Figure 42**).

3.2.3. Galvanic current does not affect the inflammatory response induced by collagenase

In order to assess if galvanic current could improve the lesion of a chronic Achilles tendon injury, collagenase was injected to induce tendon damage and after 14- and 21-days percutaneous needle electrolysis was applicated. We observed that, at 14 days after collagenase injection, dry puncture was able to induce an increase in polymorphonuclear cells that was not present in percutaneous needle electrolysis compared with collagenase-treated tendons (**Figure 49A**). In addition, at 21 days after collagenase injection, no differences were observed both with dry puncture and percutaneous needle electrolysis compared with collagenase-treated tendons (**Figure 49B**). Attending to these results, we treated the tendons with additional applications of percutaneous needle electrolysis, following the protocol that is commonly applicated in clinics, to mimic the treatment of patients with tendinopathies. We applicated either dry puncture or percutaneous needle electrolysis starting 7 days after collagenase injection during three applications every three days. We observed that dry puncture and percutaneous needle electrolysis were not able to induce changes in the number of polymorphonuclear cells (**Figure 50A**) or the circularity of tenocytes' nuclei (**Figure 50B**). We only observed a slightly but not significant increase in the number of tenocytes and the area of tenocytes' nuclei when percutaneous needle electrolysis was applied (**Figure 50C,D**), possibly corresponding to a slightly induction of tenocyte activation.

Figures of Chapter 3

A
Polymorphonuclear cells
Non-treated
Needling
Percutaneous electrolysis
B
Number of polymorphonuclear cells per field of view
Non-treated
Needling
Percutaneous electrolysis
Time (days)
C
F4/80+ cells
Non-treated
Needling
Percutaneous electrolysis
D
Number of F4/80+ cells per field of view
Non-treated
Needling
Percutaneous electrolysis
Time (days)

Figure 39. Galvanic current induces polymorphonuclear and macrophage infiltrate in the calcaneal tendon of mice. (A) Representative hematoxylin and eosin images of wild type mice calcaneal tendon after 3 days application of 3 punctures with needle (needling, green) or 3 impacts of 3 mA for 3 seconds (blue). Scale bar: 50 μm. Magnification shows the presence of polymorphonuclear cells (arrowheads). **(B)** Quantification of polymorphonuclear cells per field of view of calcaneal tendon sections treated and stained as described in A. Center values represent the mean and error bars represent s.e.m.; n= 7-8 independent animals. **(C)** Representative immunostaining images for the macrophage marker F4/80 from the calcaneal tendon of wild type mice treated as described in A. Scale bar: 50 μm. Magnification show the presence of F4/80 positive cells (arrowheads). **(D)** Quantification of F4/80 positive cells per field of view of calcaneal tendon sections treated and stained as described in C. Center values represent the mean and error bars represent s.e.m.; n= 8 independent animals. ****$p<0.0001$, ***$p<0.0005$, **$p<0.005$, *$p<0.05$, and ns $p>0.05$.

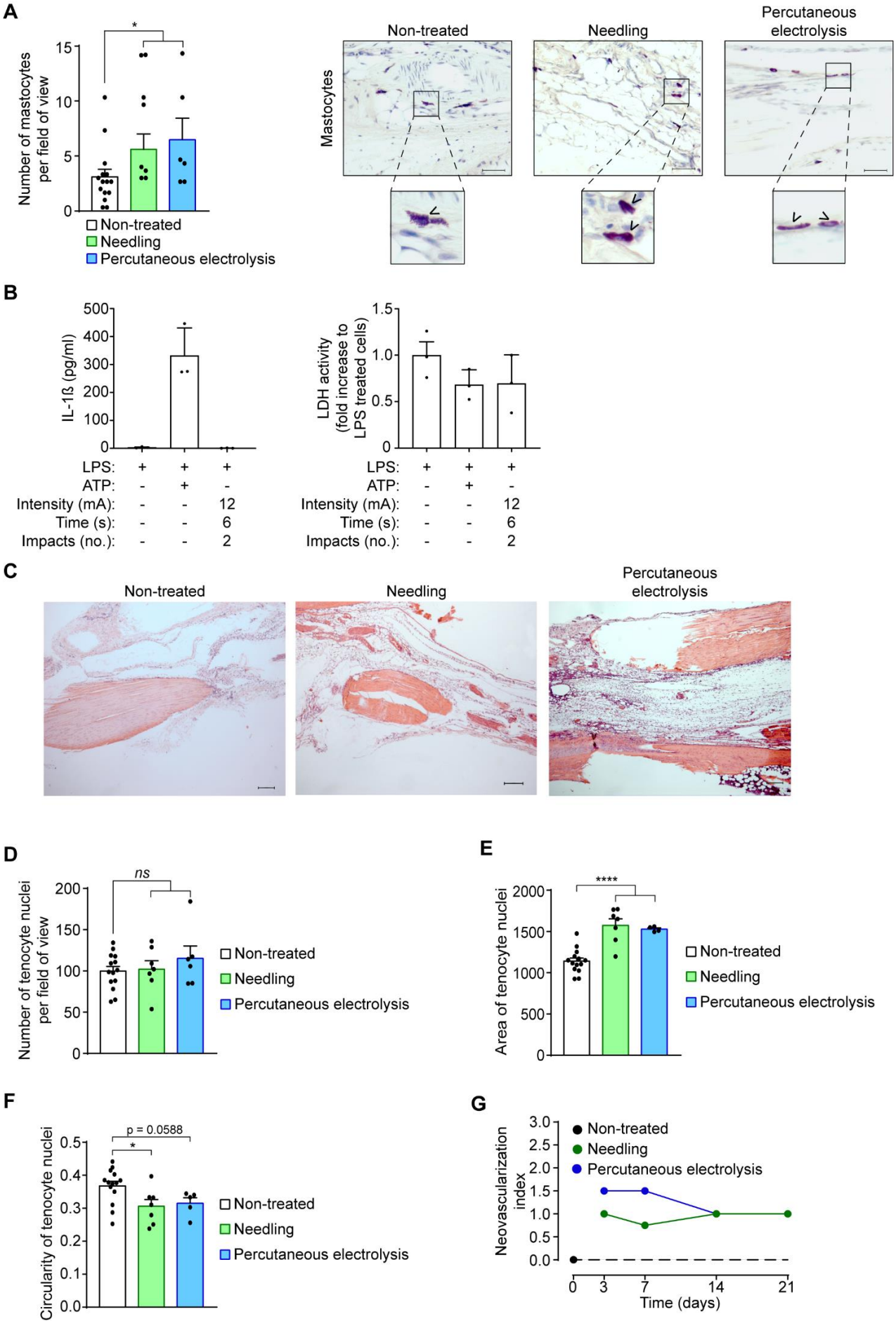
A
Number of mastocytes per field of view
Non-treated
Needling
Percutaneous electrolysis
Mastocytes
B
IL-1ß (pg/ml)
LDH activity (fold increase to LPS treated cells)
LPS:
ATP:
Intensity (mA):
Time (s):
Impacts (no.):
C
D
Number of tenocyte nuclei per field of view
ns
E
Area of tenocyte nuclei
****
F
Circularity of tenocyte nuclei
p = 0.0588
G
Neovascularization index
Time (days)

Figure 40. Galvanic current does not affect tendon mastocytes, tenocytes or vascularity. **(A)** Quantification of mastocytes per field of view of calcaneal tendon sections stained with toluidine blue from wild type mice after 3 days application of 3 punctures with needle (needling, green) or 3 impacts of 3 mA for 3 seconds (blue). Center values represent the mean and error bars represent s.e.m.; n= 6-15 independent animals. Images on the right show representative sections where mastocytes were counted, scale bar 50 μm. **(B)** IL-1β (left) and LDH (right) release from mice bone-marrow isolated neutrophils primed for 2 h with LPS (1 μg/ml) and then treated for 30 min with ATP (3 mM) or 6 h after application of 2 impacts of 12 mA of galvanic current for 6 seconds. Center values represent the mean and error bars represent s.e.m.; n= 3 independent animals. **(C)** Representative hematoxylin and eosin images of wild type mice calcaneal tendon non treated or after 3 days application of 3 punctures with needle (needling) or 3 impacts of 3 mA for 3 seconds (percutaneous electrolysis), scale bar 200 μm. **(D,E,F)** Number **(D)**, area **(E)** and circularity **(F)** of nuclei of tenocytes of calcaneal tendon sections of wild type mice stained with hematoxylin and eosin after 3 days application of 3 punctures with needle (needling, green) or 3 impacts of 3 mA for 3 seconds (blue). Center values represent the mean and error bars represent s.e.m.; n= 4-14 independent animals. **(G)** Relative neovascularization assessed in calcaneal tendon sections stained with hematoxylin and eosin after different time (as indicated) of the application of 3 punctures with needle (needling, green) or 3 impacts of 3 mA for 3 seconds (blue). Center values represent the mean and error bars represent s.e.m.; n= 8-15 independent animals. ****p<0.0001, ***p<0.0005, **p<0.005, *p<0.05, and ns p>0.05.

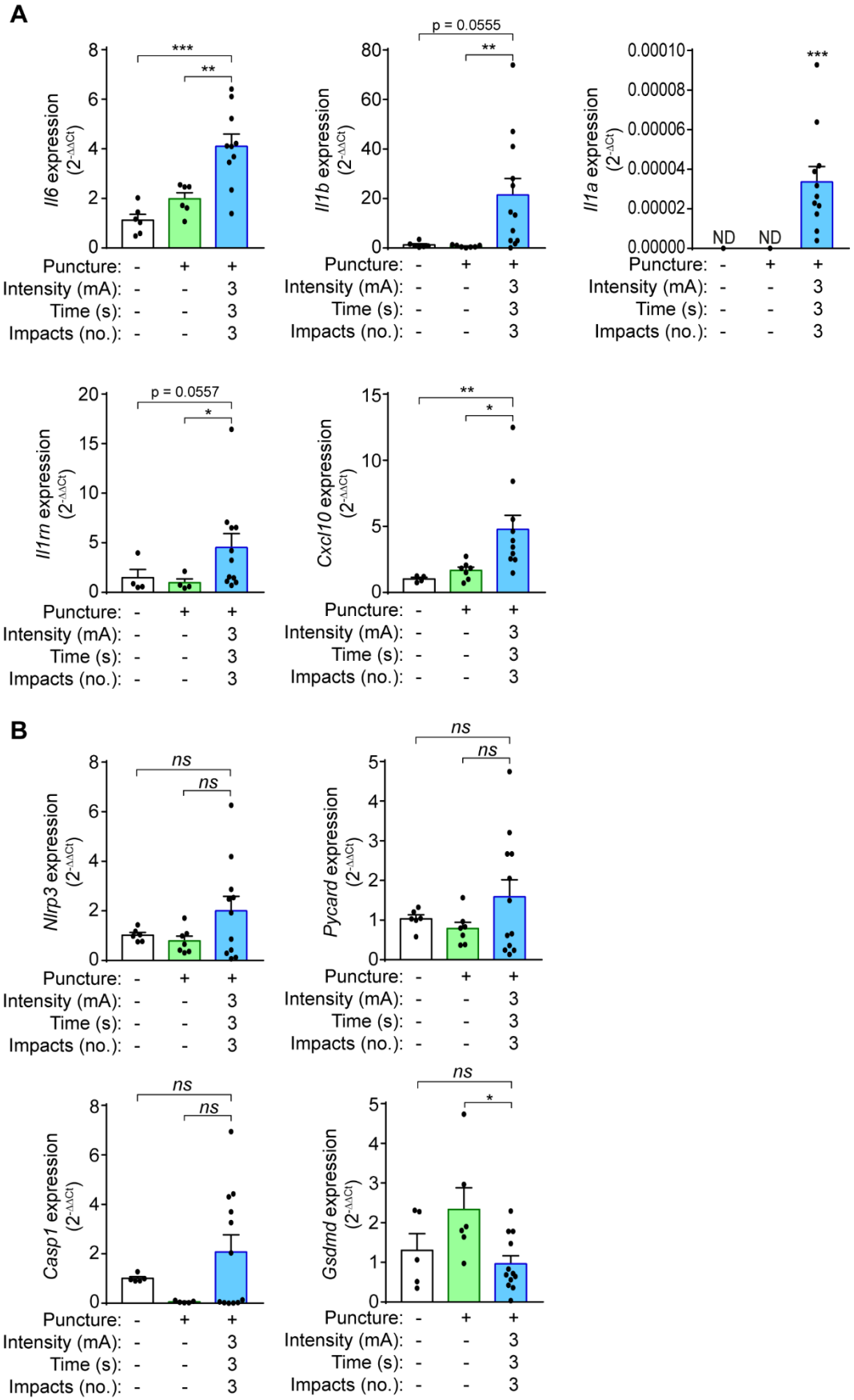
A
Il6 expression (2-ΔΔCt)
***
**
Puncture: - + +
Intensity (mA): - - 3
Time (s): - - 3
Impacts (no.): - - 3
Il1b expression (2-ΔΔCt)
p = 0.0555
**
Puncture: - + +
Intensity (mA): - - 3
Time (s): - - 3
Impacts (no.): - - 3
Il1a expression (2-ΔΔCt)
***
ND
ND
Puncture: - + +
Intensity (mA): - - 3
Time (s): - - 3
Impacts (no.): - - 3
Il1rn expression (2-ΔΔCt)
p = 0.0557
*
Puncture: - + +
Intensity (mA): - - 3
Time (s): - - 3
Impacts (no.): - - 3
Cxcl10 expression (2-ΔΔCt)
**
*
Puncture: - + +
Intensity (mA): - - 3
Time (s): - - 3
Impacts (no.): - - 3
B
Nlrp3 expression (2-ΔΔCt)
ns
ns
Puncture: - + +
Intensity (mA): - - 3
Time (s): - - 3
Impacts (no.): - - 3
Pycard expression (2-ΔΔCt)
ns
ns
Puncture: - + +
Intensity (mA): - - 3
Time (s): - - 3
Impacts (no.): - - 3
Casp1 expression (2-ΔΔCt)
ns
ns
Puncture: - + +
Intensity (mA): - - 3
Time (s): - - 3
Impacts (no.): - - 3
Gsdmd expression (2-ΔΔCt)
ns
*
Puncture: - + +
Intensity (mA): - - 3
Time (s): - - 3
Impacts (no.): - - 3

Figure 41. Galvanic current induces proinflammatory cytokine expression in the calcaneal tendon of mice. (A,B) Quantitative PCR for the indicated genes normalized to *Actb* in the calcaneal tendon of wild type mice after 3 days application of 3 punctures with needle (needling, green) or 3 impacts of 3 mA for 3 seconds (blue), and compared to the expression of genes in non-treated tendons; ND: non detected. Center values represent the mean and error bars represent s.e.m.; n= 4-12 independent animals. ****p<0.0001, ***p<0.0005, **p<0.005, *p<0.05, and ns p>0.05.

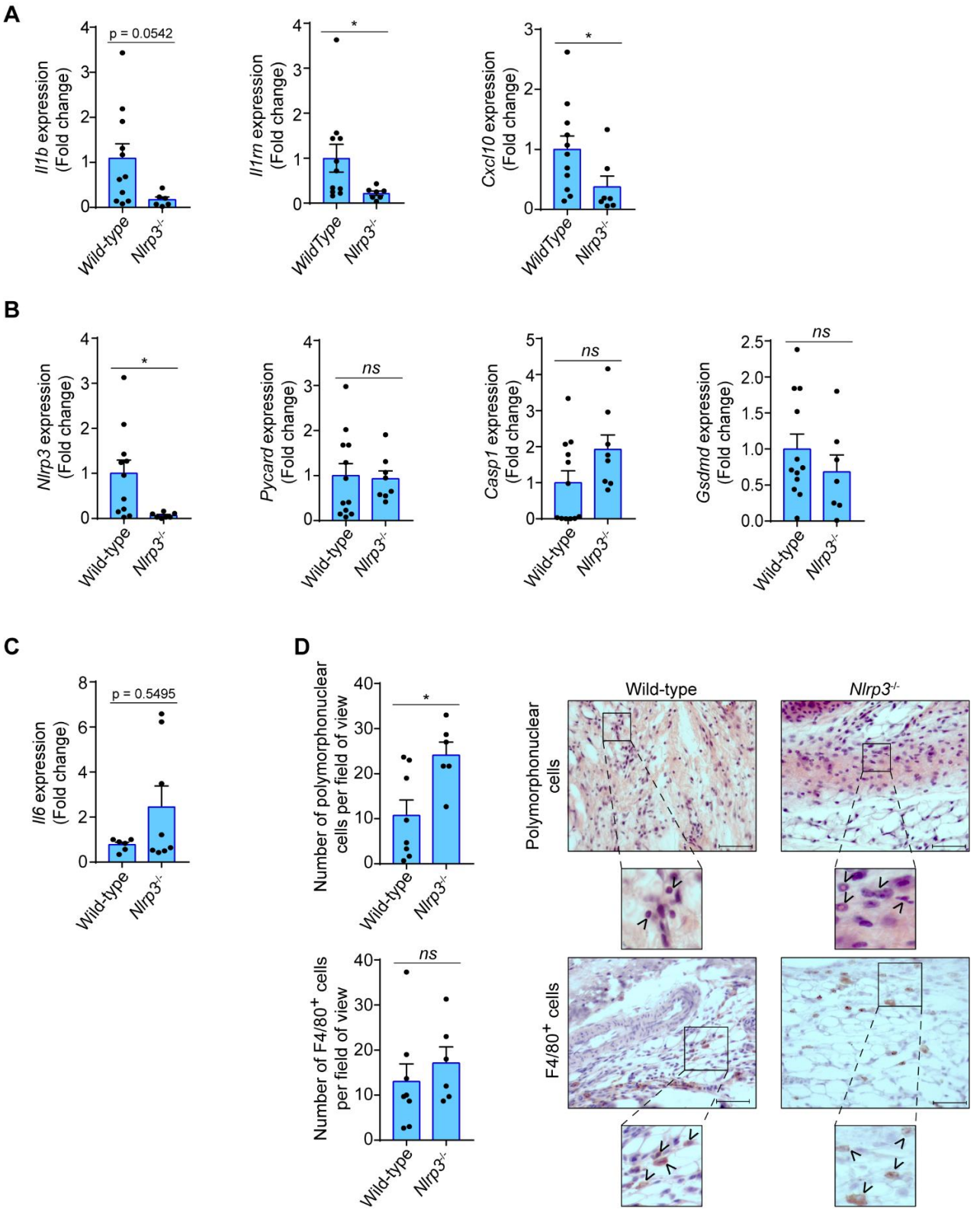
A
Il1b expression (Fold change)
p = 0.0542
Wild-type
Nlrp3-/-
Il1rn expression (Fold change)
*
WildType
Nlrp3-/-
Cxcl10 expression (Fold change)
*
WildType
Nlrp3-/-
B
Nlrp3 expression (Fold change)
*
Wild-type
Nlrp3-/-
Pycard expression (Fold change)
ns
Wild-type
Nlrp3-/-
Casp1 expression (Fold change)
ns
Wild-type
Nlrp3-/-
Gsdmd expression (Fold change)
ns
Wild-type
Nlrp3-/-
C
Il6 expression (Fold change)
p = 0.5495
Wild-type
Nlrp3-/-
D
Number of polymorphonuclear cells per field of view
*
Wild-type
Nlrp3-/-
Number of F4/80+ cells per field of view
ns
Wild-type
Nlrp3-/-
Wild-type
Nlrp3-/-
Polymorphonuclear cells
F4/80+ cells

Figure 42. Inflammatory response in the calcaneal tendon of Nlrp3-/- mice after galvanic current application. (A,B,C) Quantitative PCR for the indicated genes in the calcaneal tendons of *Nlrp3*$^{-/-}$ mice (calculated as $2^{-\Delta\Delta Ct}$) normalized to the expression in wild type (calculated as $2^{-\Delta\Delta Ct}$) after 3 days application of 3 impacts of 3 mA for 3 seconds. Center values represent the mean and error bars represent s.e.m.; n= 3-12 independent animals. **(D)** Quantification of polymorphonuclear (top) and F4/80 positive cells (bottom) per field of view from wild type and *Nlrp3*$^{-/-}$ mice calcaneal tendon treated as in A. Center values represent the mean and error bars represent s.e.m.; n= 6-8 independent animals; representative hematoxylin and eosin images (top) and F4/80 immunostaining (bottom) of calcaneal tendon quantified. Scale bar: 50 μm. Magnification show the presence of polymorphonuclear (top) or F4/80 cells (bottom) denoted by arrowheads. ****p<0.0001, ***p<0.0005, **p<0.005, *p<0.05, and ns p>0.05.

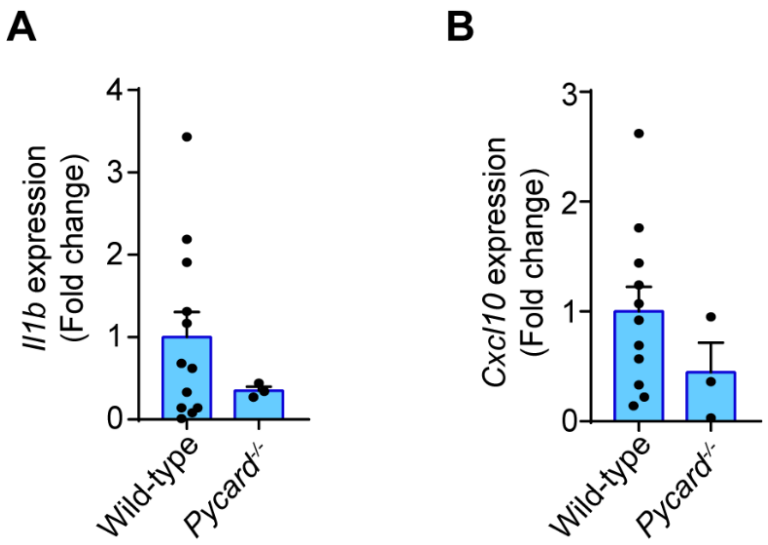
A
Il1b expression
(Fold change)
4
3
2
1
0
Wild-type
Pycard-/-
B
Cxcl10 expression
(Fold change)
3
2
1
0
Wild-type
Pycard-/-

Figure 43. Cytokine expression in the calcaneal tendon of Pycard-/- mice after galvanic current application. (A,B) Quantitative PCR for *Il1b* **(A)** and *Cxcl10* **(B)** in the calcaneal tendons of *Pycard*$^{-/-}$ mice (calculated as $2^{-\Delta\Delta Ct}$) normalized to the expression in wild type (calculated as $2^{-\Delta\Delta Ct}$) after 3 days application of 3 impacts of 3 mA for 3 seconds. Center values represent the mean and error bars represent s.e.m.; n= 3-12 independent animals. ****p<0.0001, ***p<0.0005, **p<0.005, *p<0.05, and ns p>0.05.

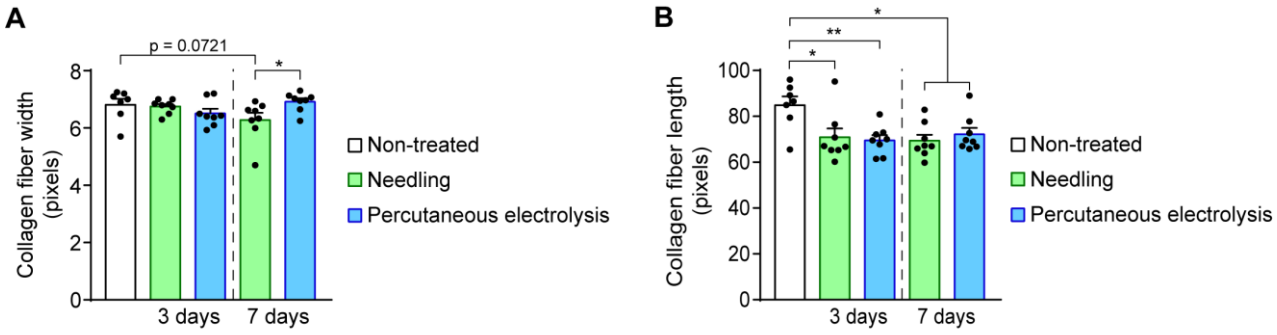
A
p = 0.0721
*
Collagen fiber width (pixels)
0
2
4
6
8
3 days
7 days
Non-treated
Needling
Percutaneous electrolysis
B
*
**
*
Collagen fiber length (pixels)
0
20
40
60
80
100
3 days
7 days
Non-treated
Needling
Percutaneous electrolysis

Figure 44. Galvanic current does not change properties of the collagen. (A,B) Quantification of the collagen fiber properties**:** width **(A)** and length **(B)** in calcaneal tendon sections stained with picrosirius red from wild type mice after 3 and 7 days after application of punctures with needle (needling, green) or 3 impacts of 3 mA for 3 seconds (blue), or in untreated tendons (white). Center values represent the mean and error bars represent s.e.m.; n= 6-8 independent animals. ****p<0.0001, ***p<0.0005, **p<0.005, *p<0.05, and ns p>0.05.

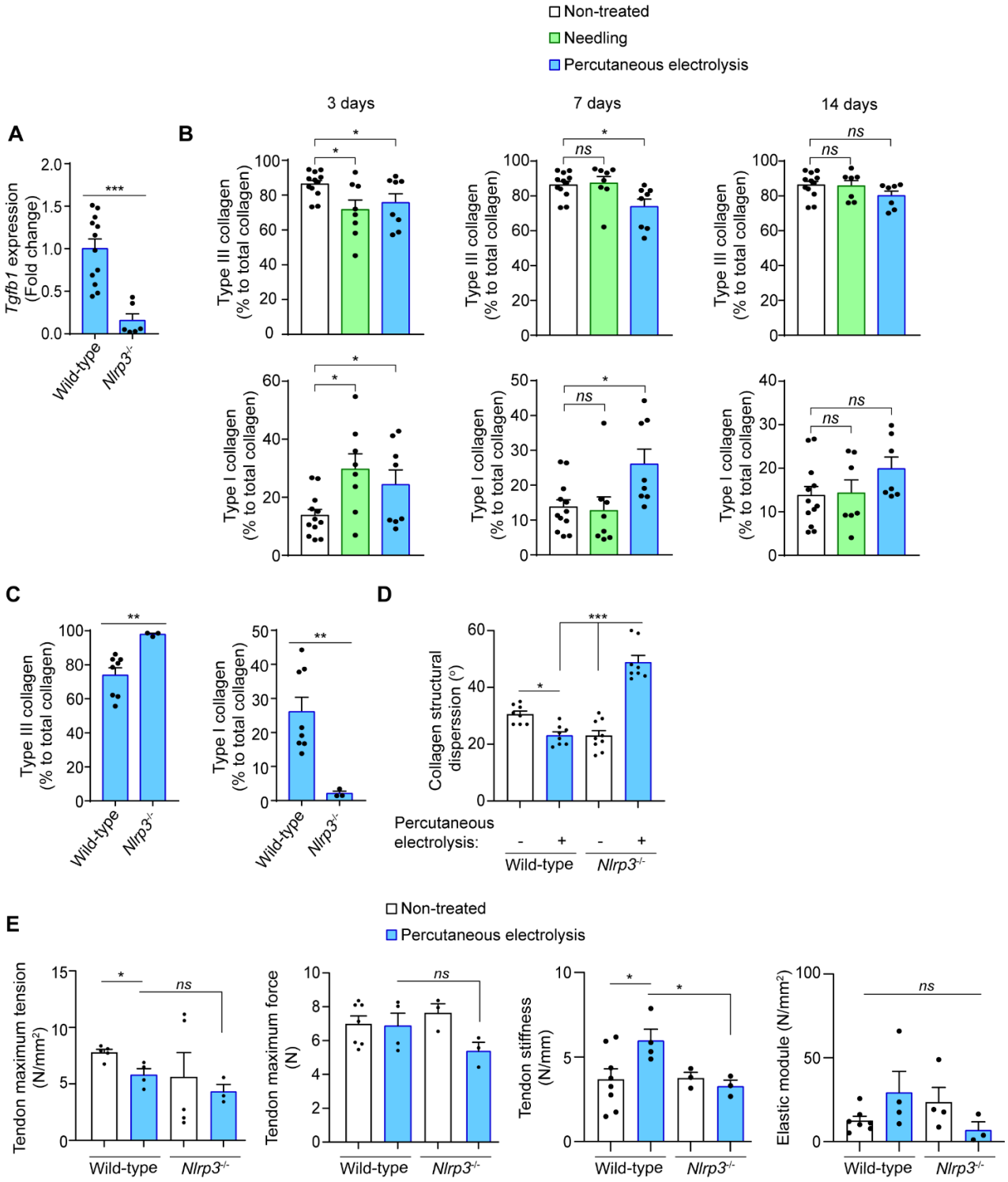
Non-treated
Needling
Percutaneous electrolysis
A
B
C
D
E
3 days
7 days
14 days
Tgfb1 expression (Fold change)
Type III collagen (% to total collagen)
Type I collagen (% to total collagen)
Collagen structural disperssion (°)
Percutaneous electrolysis:
Wild-type
Nlrp3-/-
Tendon maximum tension (N/mm²)
Tendon maximum force (N)
Tendon stiffness (N/mm)
Elastic module (N/mm²)
ns

Figure 45. Galvanic current increase of type I collagen via NLRP3 inflammasome. (A) Quantitative PCR for *Tgfb1* in the calcaneal tendons of *Nlrp3*$^{-/-}$ mice (calculated as $2^{-\Delta\Delta Ct}$) normalized to the expression in wild type (calculated as $2^{-\Delta\Delta Ct}$) after 3 days application of 3 impacts of 3 mA for 3 seconds. Center values represent the mean and error bars represent s.e.m.; n= 6-12 independent animals. **(B,C)** Quantification of the collagen type I and III in calcaneal tendon sections stained with picrosirius red from wild type **(B,C)** and *Nlrp3*$^{-/-}$ **(C)** mice after 3, 7 or 14 days **(B)** or 3 days **(C)** application of punctures with needle (needling, green) or 3 impacts of 3 mA for 3 seconds (blue), or in non-treated tendons (white). Center values represent the mean and error bars represent s.e.m.; n= 3-12 independent animals. **(D)** Quantification of collagen structural dispersion in calcaneal tendon sections imaged with second harmonic generation microscopy and calculated with an algorithm based on the Hough transform from wild type and *Nlrp3*$^{-/-}$ mice after 7 days application of 3 impacts of 3 mA for 3 seconds (blue), or in non-treated tendons (white). Center values represent the mean and error bars represent s.e.m.; n= 3 independent animals imaged at 2 or 3 different tendon areas. **(E)** Biomechanical testing of calcaneal tendon from wild-type and *Nlrp3*$^{-/-}$ mice after 14 days application of 3 impacts of 3 mA for 3 seconds (blue) or from non-treated tendons (white). Center values represent the mean and error bars represent s.e.m.; n= 3-8 independent animals. ****p<0.0001, ***p<0.0005, **p<0.005, *p<0.05, and ns p>0.05.

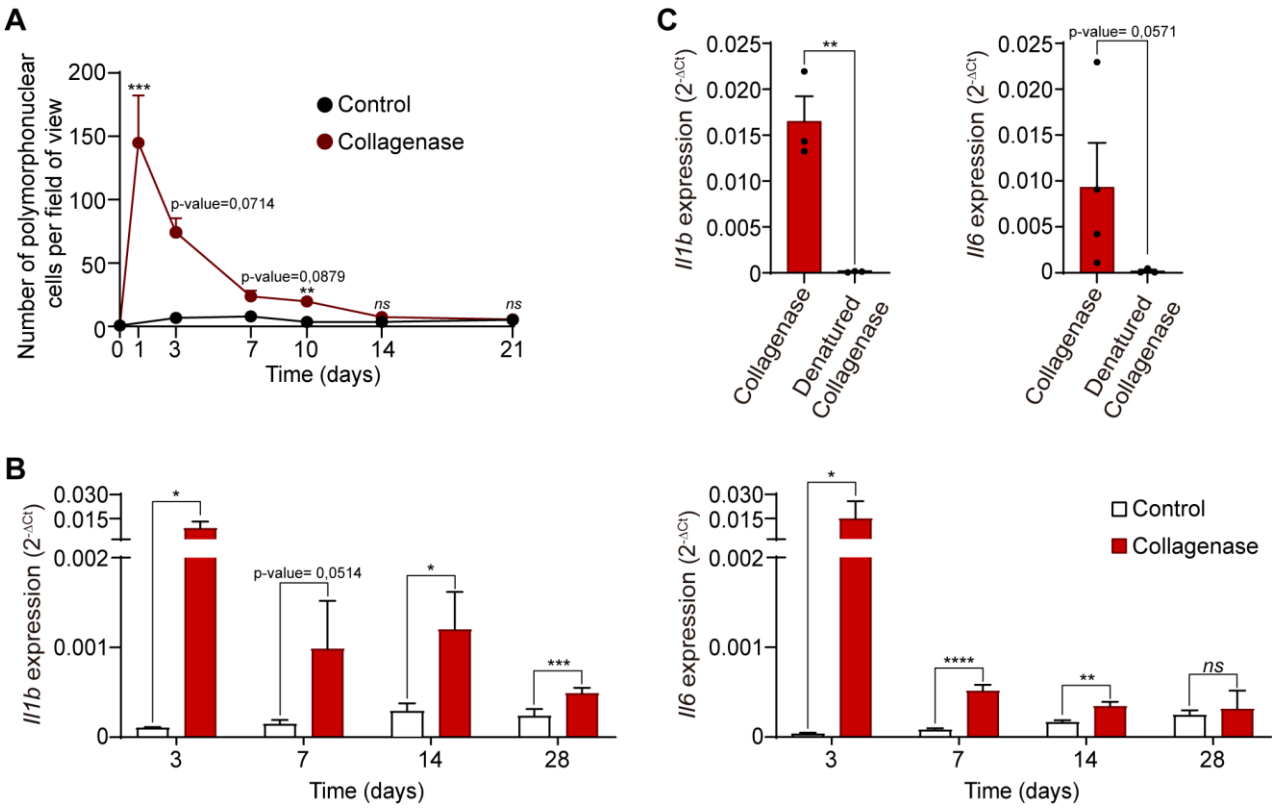
A
Number of polymorphonuclear cells per field of view
200
150
100
50
0
***
Control
Collagenase
p-value=0,0714
p-value=0,0879
**
ns
ns
0 1 3 7 10 14 21
Time (days)
C
Il1b expression (2-ΔCt)
0.025
0.020
0.015
0.010
0.005
0
**
Collagenase
Denatured Collagenase
Il6 expression (2-ΔCt)
p-value= 0,0571
Collagenase
Denatured Collagenase
B
Il1b expression (2-ΔCt)
0.030
0.015
0.002
0.001
0
*
p-value= 0,0514
*
***
3 7 14 28
Time (days)
Il6 expression (2-ΔCt)
*
Control
Collagenase
****
**
ns
3 7 14 28
Time (days)

Figure 46. Collagenase induce an inflammatory response in the mouse calcaneal tendon. **(A)** Quantification of polymorphonuclear cells per field of view of calcaneal tendon sections of mice after different days of injection of 20 µl of collagenase A (10 µg/µl) or 20 µl of saline solution. Center values represent the mean and error bars represent s.e.m.; n= 3-15 independent animals/time point. **(B,C)** Quantitative PCR for *Il1b* (left) and *Il6* (right) in the calcaneal tendons of mice treated as in A or after denatured collagenase injection **(C)**. Center values represent the mean and error bars represent s.e.m.; n= 3-6 independent animals. ****p<0.0001, ***p<0.0005, **p<0.005, *p<0.05, and ns p>0.05.

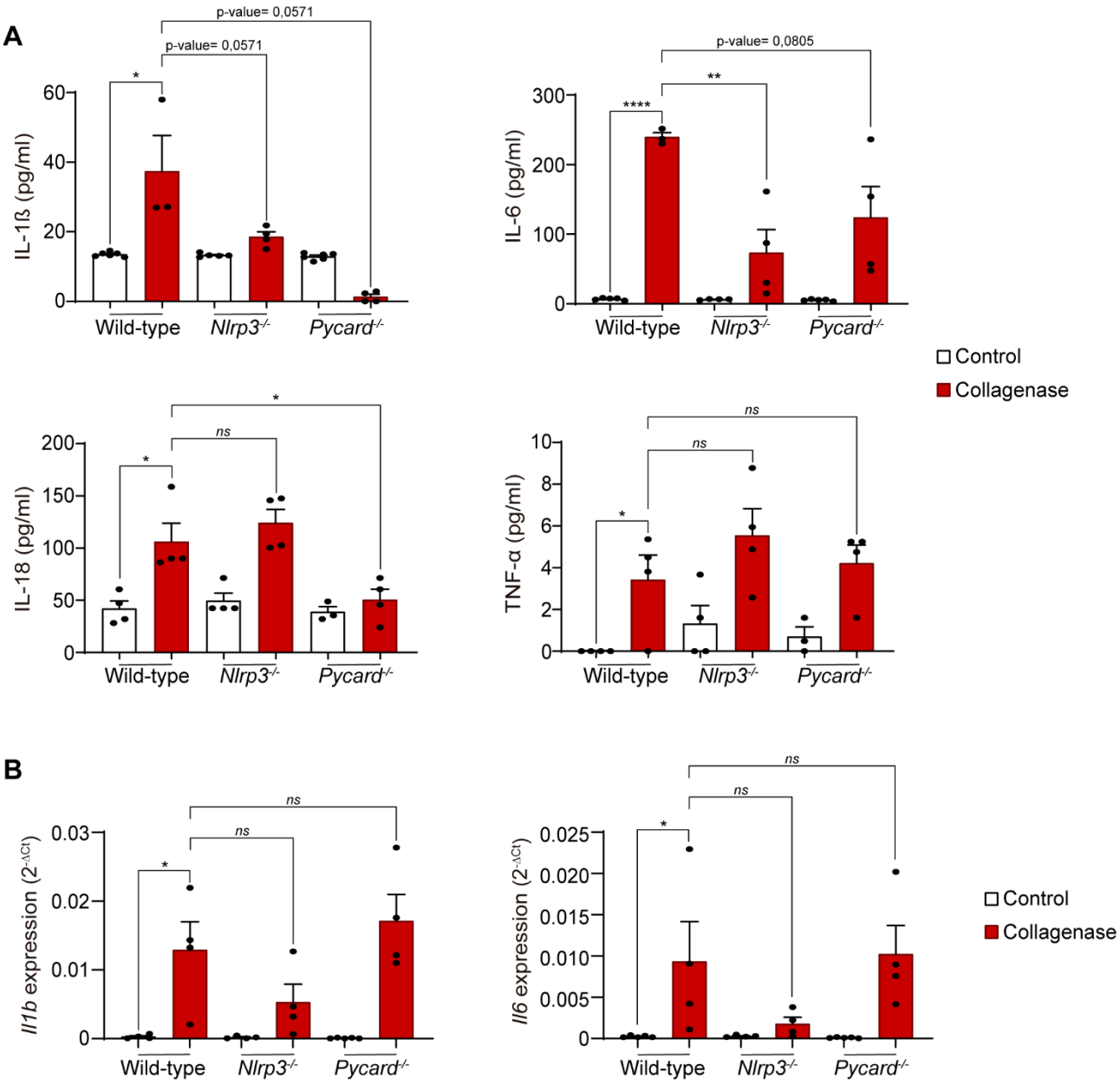
A
p-value= 0,0571
p-value= 0,0571
IL-1ß (pg/ml)
Wild-type
Nlrp3-/-
Pycard-/-
p-value= 0,0805
IL-6 (pg/ml)
IL-18 (pg/ml)
TNF-α (pg/ml)
Control
Collagenase
B
Il1b expression (2-ΔCt)
Il6 expression (2-ΔCt)
ns

Figure 47. NLRP3 inflammasome controls pro-inflammatory cytokines production in the mouse calcaneal tendon after collagenase treatment. (A) ELISA for IL-1β (upper left), IL-6 (upper right), IL-18 (lower left) and TNF-α (lower right) from calcaneal tendons of wild type, *Nlrp3*$^{-/-}$ and *Pycard*$^{-/-}$ mice injected with 20 µl collagenase A (10 µg/µl) or 20 µl of sterile saline solution or non-treated (control). Center values represent the mean and error bars represent s.e.m.; n= 3-6 independent animals. **(B)** Quantitative PCR for *Il1b* (left) and *Il6* (right) in the calcaneal tendons of wild type mice, *Nlrp3*$^{-/-}$ and *Pycard*$^{-/-}$ mice treated as in A. Center values represent the mean and error bars represent s.e.m.; n= 4-5 independent animals. ****p<0.0001, ***p<0.0005, **p<0.005, *p<0.05, and ns p>0.05.

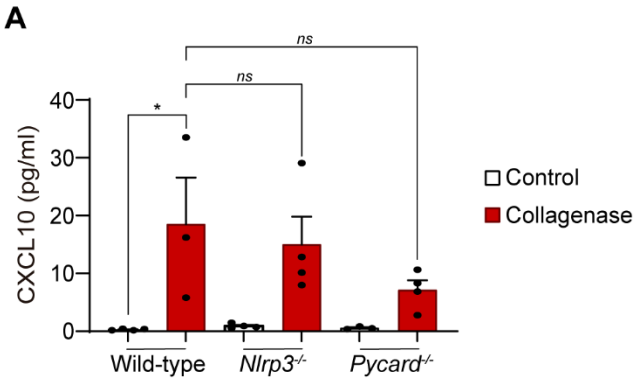
A
ns
ns
*
40
30
20
10
0
CXCL10 (pg/ml)
Wild-type
Nlrp3-/-
Pycard-/-
Control
Collagenase

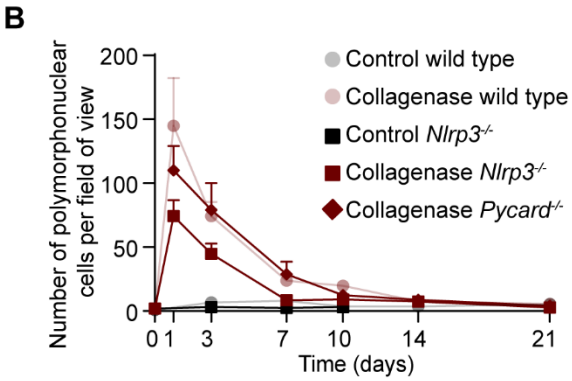
B
200
150
100
50
0
Number of polymorphonuclear cells per field of view
0 1 3 7 10 14 21
Time (days)
Control wild type
Collagenase wild type
Control Nlrp3-/-
Collagenase Nlrp3-/-
Collagenase Pycard-/-

Figure 48 Production of chemokine CXCL10 and polymorphonuclear cells recruitment in the calcaneal tendon of mice treated with collagenase. (A) ELISA for CXCL10 from calcaneal tendons of wild type, *Nlrp3*$^{-/-}$ and *Pycard*$^{-/-}$ mice injected with 20 µl collagenase A (10 µg/µl) or 20 µl of sterile saline solution or non-treated (control). Center values represent the mean and error bars represent s.e.m.; n= 3-4 independent animals. **(B)** Quantification of polymorphonuclear cells per field of view of calcaneal tendons sections of wild type, *Nlrp3*$^{-/-}$ and *Pycard*$^{-/-}$ mice treated as in A. Center values represent the mean and error bars represent s.e.m.; n= 2-15 independent animals.

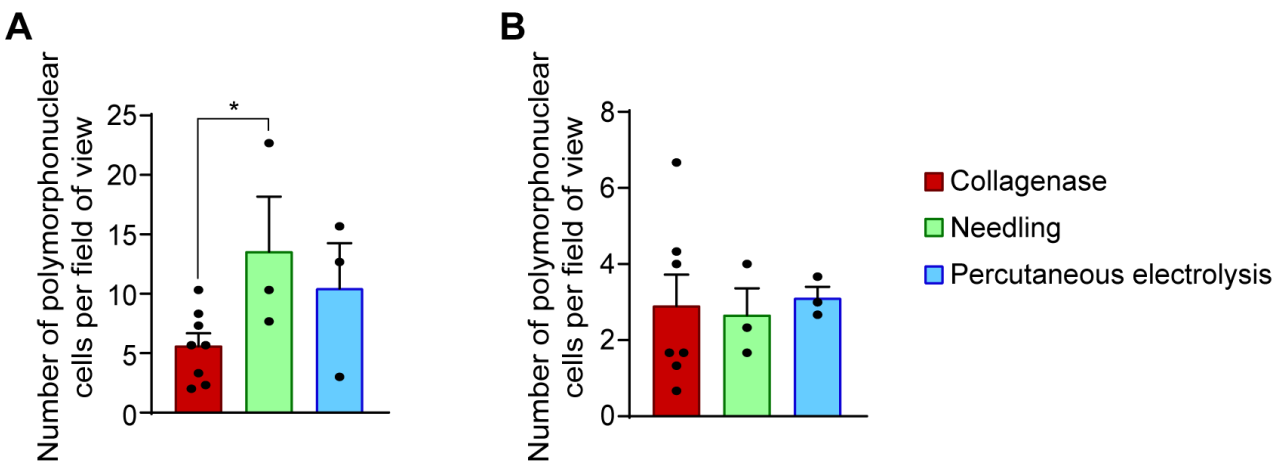
A
Number of polymorphonuclear cells per field of view
25
20
15
10
5
0
*
B
Number of polymorphonuclear cells per field of view
8
6
4
2
0
Collagenase
Needling
Percutaneous electrolysis

Figure 49. Percutaneous needle electrolysis applicated on collagenase-injured Achilles mice tendons. (A,B) Quantification of polymorphonuclear cells per field of view of calcaneal tendon sections of wild-type mice treated 3 times every 3 days with 3 punctures with needle (needling, green) or 3 impacts of 3 mA for 3 seconds (blue) after 14 days **(A)** or 21 days **(B)** of injection of 20 µl of collagenase A (10 µg/µl). Center values represent the mean and error bars represent s.e.m.; n= 3-8 independent animals. ****p<0.0001, ***p<0.0005, **p<0.005, *p<0.05, and ns p>0.05.

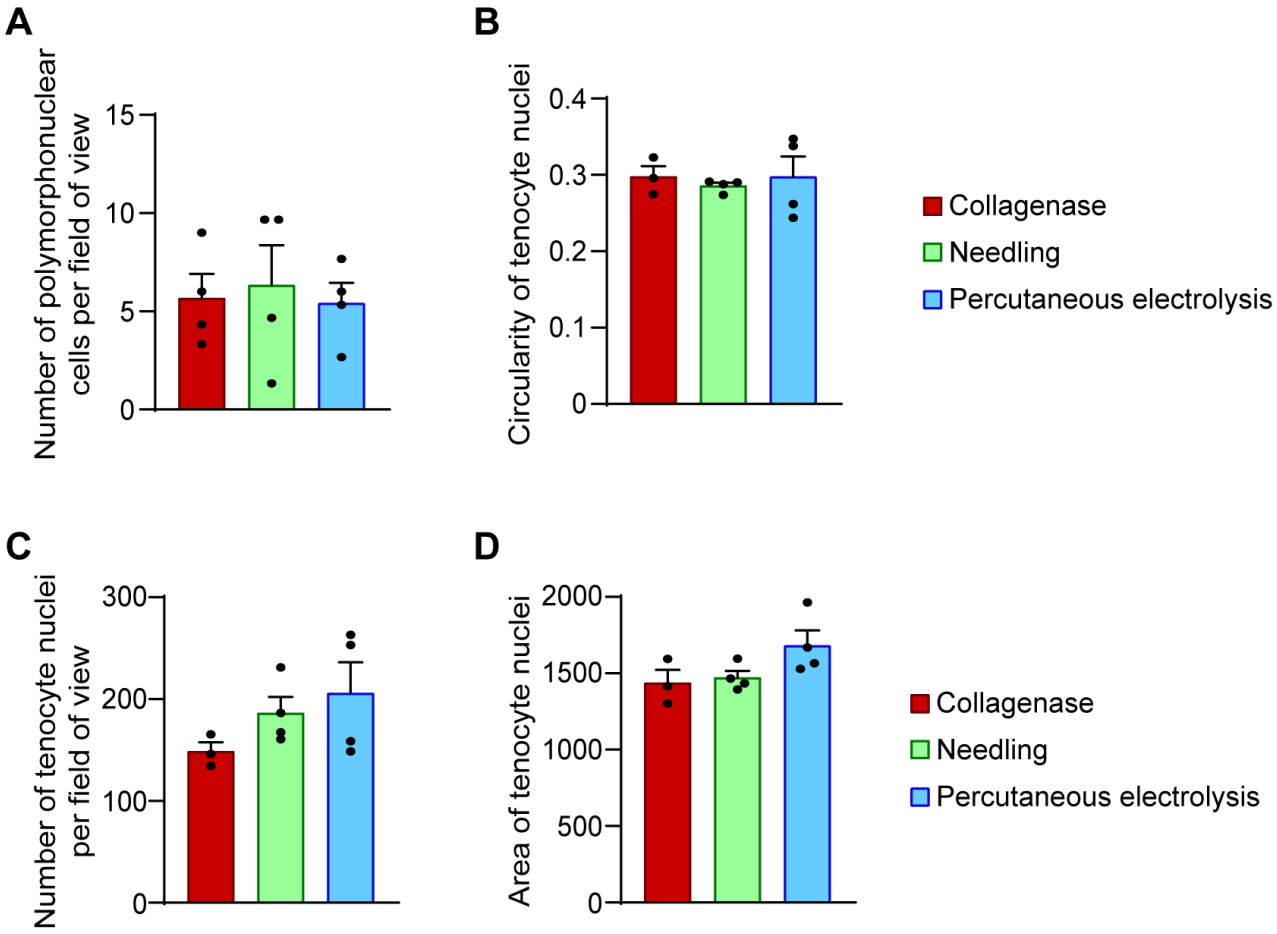
A
Number of polymorphonuclear cells per field of view
15
10
5
0
B
Circularity of tenocyte nuclei
0.4
0.3
0.2
0.1
0
Collagenase
Needling
Percutaneous electrolysis
C
Number of tenocyte nuclei per field of view
300
200
100
0
D
Area of tenocyte nuclei
2000
1500
1000
500
0
Collagenase
Needling
Percutaneous electrolysis

Figure 50. Percutaneous needle electrolysis applicated three times on collagenase-injured Achilles mice tendons. (A) Quantification of polymorphonuclear cells per field of view of calcaneal tendon sections of wild-type mice treated 3 times every 3 days with 3 punctures with needle (needling, green) or 3 impacts of 3 mA for 3 seconds (blue) after 7 days of injection of 20 µl of collagenase A (10 µg/µl). **(B,C,D)** Circularity **(B)**, number **(C)** and area **(D)** of nuclei of tenocytes of calcaneal tendon sections of wild type mice stained with hematoxylin and eosin and treated as in A. Center values represent the mean and error bars represent s.e.m.; n= 4 independent animals. ****p<0.0001, ***p<0.0005, **p<0.005, *p<0.05, and ns p>0.05.

DISCUSSION

Chapter 1. Evaluation of NLRC4 and NLRP3 activation in recombinant HEK293T system

NLRC4 is a cytosolic nucleotide-binding oligomerization domain-like receptor that cooperates with NAIP to detect flagellin and components of the bacterial type 3 secretion system (Duncan & Canna, 2018). Once detected, NLRC4 oligomerizes, forms an inflammasome complex, activates caspase-1, and promotes the production of inflammatory cytokines of the IL-1 family.

Pathogenic gain-of-function variants of NLRC4 have been described as the cause of a dominantly inherited autoinflammatory disorders with variable phenotype presentations. The first phenotype described was characterized by early-onset skin lesions, enterocolitis, arthritis, and recurrent episodes of MAS (Canna et al., 2014; Romberg et al., 2014). Subsequently, new phenotypes were reported, including a familial form of cold-induced autoinflammatory syndrome and painful erythematous nodules (Kitamura et al., 2014; Volker-Touw et al., 2017). Increasing evidence suggests an important role of IL-18, rather than IL-1β, in the pathogenesis of the NLRC4-related diseases, including persistently elevated serum levels of total and free IL-18, and the clinical efficacy of IL-18 blockade (Canna et al., 2017).

In this Thesis, we studied a patient with recurrent fever and systemic inflammation, with the p.Ser171Phe NLRC4 variant present in mosaicism. Interestingly, this NLRC4 variant has previously been reported as mosaicism in a 2-month-old infant with fatal disease and laboratory features of MAS (Liang et al., 2017). The lack of research addressing the functional consequences of the NLRC4 p.Ser171Phe variant in a previous study was the main difficulty in unequivocally establishing its pathogenicity (Liang et al., 2017). To address this issue, different *in vitro* and *ex vivo* analyses were performed. *In vitro* analyses clearly showed a higher degree of NLRC4 oligomerization and ASC speck formation when mutant NLRC4 was expressed in HEK293T cells compared with cells transfected with wild-type NLRC4, an expected behavior for a gain-of-function variant. Data obtained by *ex vivo* assays were also consistent with gain-of-function role for the NLRC4 variant and support hyperactivation of the NLRC4 inflammasome as a disease mechanism, with increased ASC specks and overproduction of IL-18, similar to previous studies on NLRC4-associated MAS (Canna et al., 2014). However, IL-1β release by patient PBMCs was decreased compared with healthy controls and CAPS patients, which is in contrast to previous data on NLRC4-associated MAS indicating exacerbated IL-1β production (Canna et al., 2014). The low IL-1β production by patient's cells could not be attributed to a decrease of monocytes in PBMCs

or to impaired LPS priming and NF-κB activation, as the percentage of monocytes or TNF-α and IL-6 release was similar between patients and healthy controls, indicating normal priming of cells by LPS. However, LPS failed to upregulate *Il1b* gene expression, but not *Il6* gene expression, suggesting that this failure might be responsible for the lack of IL-1β release from the patient's cells.

Therefore, this patient differs from patients with NLRC4-associated MAS reported in other studies in which a higher release of IL-1β and IL-6 was found from LPS-treated monocytes (Canna et al., 2014). These differences could be due to the use of positively isolated monocytes versus whole PBMCs used for *ex vivo* stimulation in this study, the duration of LPS stimulation (4 hours less in our study), or distinct phenotypic responses due to different NLRC4 variants. The results of our *ex vivo* functional experiments, support the treatment of this patient, and potentially other patients with autoinflammatory diseases with NLRC4 gain-of-function mutations, with IL-18 blockage therapies, some of which have already been successfully employed in a patient with severe NLRC4-associated MAS (Canna et al., 2017). The results of these *ex vivo* assays were in concordance with the pattern of cytokines quantified in different serum samples of the patient. Despite these samples being obtained at different times during anti-IL-1 treatments, an increased serum level of IL-18 was persistently detected. These IL-18 levels were similar to those detected in patients carrying the germline p.Ser445Pro NLRC4 pathogenic variant, and statistically higher than those detected in healthy controls and CAPS patients carrying both germline and post-zygotic NLRP3 variants.

Also, the results regarding BRET signal were in line with the gain-of-function behavior of the p.Ser171Phe variant, showing a more open-like conformation of the protein in basal conditions without application of any stimuli. These results are in concordance with the *in silico* structural modeling performed with this variant showing that the mutation destabilizes the contacts of the side chain in closed conformation and stabilizes the local contacts of the open conformation (Ionescu et al., 2022).

In conclusion, the evidence summarized in this Thesis clearly supports a gain-of-function behavior of the p.Ser171Phe variant in a manner similar to other NLRC4 variants previously reported as disease-causing mutations. Furthermore, this patient represents the first case of late-onset autoinflammatory disease associated with NLRC4 as a consequence of a somatic mosaicism of NLRC4, raising the question of whether inflammatory manifestations that begin during adulthood in other patients may be a consequence of a similar genetic defect.

In addition, gain-of-function behavior have been described for other mutations studied in this Thesis. In the mutation p.Thr177Ala a gain-of-function behavior has been suggested by pluripotent cell-based phenotype dissection (Kawasaki et al., 2017). Also 3D structural models were performed, showing a disruption of an hydrogen bond that appears to be important for ADP-mediated winged-helix domain-nucleotide-binding domain interaction in NLRC4 autoinhibition (Kawasaki et al., 2017), probably inducing an open structure of the NLRC4 protein as we have shown with the decrease in BRET signal, and is also consistent with the higher amount of cells presenting spontaneous puncta distribution of NLRC4. Gain-of-function behavior has been described also in p.His443Pro mutation by several functional studies and with the generation of a mouse model containing this mutation with a severe phenotype of auto-inflammation (Kitamura et al., 2014; Raghawan et al., 2019; Raghawan et al., 2017), which is consistent with the pronounced decrease in BRET signal obtained compared with wild-type NLRC4 and the previous mutations p.Ser171Phe and p.Thr177Ala, and also with the higher amount of cells presenting spontaneous oligomerization. Also, the mutation p.Ser445Pro presented a similar pronounced decrease in BRET signal, which could be related with the severe phenotype and early appearance of the symptoms in patients with this mutation (Volker-Touw et al., 2017). However, functional studies have to be performed to confirm the gain-of-function behavior of this mutation, because we observed an increase in cells presenting a puncta distribution of NLRC4 containing this variant compared with wild-type NLRC4.

An increase in the number of cells with spontaneous puncta distribution of NLRC4 was also observed in the mutations p.Thr337Asn and p.Thr337Ser, both with a described gain-of-function behavior that can also be assumed for the p.Thr337Asn mutation because the same amino acid is affected (Bardet et al., 2021; Canna et al., 2014). Surprisingly, no significant BRET signal decrease was observed in both mutations in contrast with the previous results obtained for the p.Thr337Ser mutation showing that this mutation could destabilize the WHD and NBD interactions or directly affect ADP binding, both essential to maintain NLRC4 in an auto-inhibited state (Canna et al., 2014), therefore the results of the BRET signal was difficult to interpret for these modifications. The same results were obtained for the mutation p.Val341Ala with a described gain-of-function behavior, but in this case with a weakly change in the BRET signal suggesting a potential destabilization of the protein structure (Barsalou et al., 2018; Canna et al., 2017; Romberg et al., 2014).

In the case of the mutation p.Trp655Cys the increase in spontaneous oligomerization is in consonance with the previously described increase in percentage of ASC specks and

functional studies (Moghaddas et al., 2018). Furthermore, the conformational changes induced by this mutation has been described after activation of NLRC4, stabilizing the final NLRC4 oligomer (Moghaddas et al., 2018) which has a robust association with the absence of decrease in BRET signal that we observed compared with wild-type NLRC4 without cell stimulation. The same behavior has been described for the mutation p.Gln657Leu which is also in agreement with our oligomerization and BRET results (Chear et al., 2020).

Regarding the mutations p.Gly633dup, p.Cys697Ser and p.Asp1009Gly described in this Thesis, all of them are novel mutations that have not been previously described and presented a significant increase in the percentage of cells with a puncta distribution of NLRC4 compared with wild-type NLRC4, but only a significant decrease in BRET signal was observed in the mutations p.Cys697Ser and p.Asp1009Gly, being more pronounced when the mutation affects the final amino acids of the LRR domain. Functional studies need to be performed in order to confirm the gain-of-function behavior of this mutations and to described the conformational changes that can induce in auto-inhibited NLRC4.

Depending on the domain affected by the mutations studied in this Thesis, different results on the BRET signal of NLRC4 were observed. Mutations affecting the NBD and WHD domains, and final amino acids of the LRR domain presented a decrease in BRET signal, and so probably an “open” conformation than wild-type NLRC4. Therefore, these mutations can induce a conformational change in the NLRC4 structure destabilizing the auto-inhibited basal conformation of NLRC4. Mutations in WHD induced the lower NLRC4 BRET signal, so mutations in this domain can be linked with a higher open structure of the protein. However, the mutations affecting the linker domains HD1 and HD2 did not produce a significant change in the NLRC4 BRET signal and therefore any major conformational change in NLRC4 structure. In addition, the polarity of the mutated amino acids is important for the overall protein conformation. Mutations resulting in a change in the polarity or charge of the amino acids probably induce an “open” conformation of NLRC4 according to the decrease in the recorded BRET signal, and mutations in which amino acids with the same properties are involved did not affect BRET signal and in consequence NLRC4 conformation. This is in agreement with the fact that changes in polarity of the amino acids can disrupt previous interactions to form new bonds with the surrounding amino acids (as for example in (Kawasaki et al., 2017) and (Canna et al., 2014)). Interestingly, NLRC4 mutations in the WHD domain of the protein present the higher decrease in the BRET signal compared with the other NLRC4 mutants, suggesting that changes in this domain induce a conformational change on the structure of NLRC4 probably resulting in an open receptor

conformation. Our data suggests that all NLRC4 mutants induces a spontaneous punctum distribution of NLRC4 in the cell, but only the mutants that produce a change in the polarity of the amino acid significantly decrease the BRET signal compared with NLRC4 wild type. The NLRC4 WHD domain seems to be an important domain compared with other domains of NLRC4 affecting the BRET signal (as for example in (Moghaddas et al., 2018) and (Romberg et al., 2014)).

Altogether, these results indicates that the NBD and WHD domains, and the last amino acids of the LRR domain are critical for the correct inactive basal conformation of NLRC4, and mutations that affect amino acids contained in these domains can induce a change in the NLRC4 conformation, leading to an auto-active NLRC4 structure. Particularly, mutations affecting the NBD domain can destabilize the interaction of the protein with the nucleotide ADP or ATP, mutations affecting the WHD domain can destabilize the WHD-NBD interactions, and mutations affecting the last amino acids of the LRR domain can function allowing the opening of the auto-inhibited NLRC4 by destabilization of LRR-NBD interactions and inducing the formation of the NLRC4 oligomer by facilitating the recognition and binding of different NLRC4 monomers through LRR-LRR interactions.

On the other hand, puncta distribution of NLRP3 has been previously suggested as an activation step of the inflammasome (Chen & Chen, 2018; Compan et al., 2012; Tapia-Abellan et al., 2021; Tapia-Abellan et al., 2019), and here we found that NLRC4 puncta distribution could be also correlate with inflammasome activation in the HEK293T recombinant system. This system was also useful to determine the activation of wild type NLRP3 when galvanic current was applicated.

Chapter 2. Evaluation of the NLRP3 inflammasome activation induced by galvanic current in macrophages.

In this Thesis, we demonstrate how galvanic current application induces in macrophages a pro-inflammatory signature increasing the gene expression of pro-inflammatory markers in M1 macrophages, and also mainly characterized by activation of the NLRP3 inflammasome and release of mature IL-1β and IL-18. This is consistent with the fact that the NLRP3 inflammasome is a key pathway for controlling inflammation in the absence of pathogenic microorganisms (under sterile conditions) by executing a type of pro-inflammatory cell death termed pyroptosis (Broz & Dixit, 2016; Broz et al., 2020; Liston & Masters, 2017). We found that the application of galvanic current, a technique that has been broadly used to treat chronic lesions in humans (Valera-Garrido et al., 2014), was able to activate the NLRP3 inflammasome and induce the release of IL-1β and IL-18.

Galvanic current-induced NLRP3 inflammasome activation was found to be dependent on K^+ efflux, as high extracellular K^+ concentrations were able to block IL-1β release, and high galvanic current intensities decreased intracellular K^+. This is similar to the effect of the well-studied K^+ ionophore nigericin, which dramatically decreases intracellular K^+ and induces the release of IL-1β (Munoz-Planillo et al., 2013; Petrilli et al., 2007; Prochnicki et al., 2016). In fact, the amount of IL-1β released by galvanic current-activated macrophages was lower than when macrophages were activated with nigericin, suggesting that NLRP3 activation is correlated with decreased intracellular K^+ (Tapia-Abellan et al., 2021).

Surprisingly, only a weakly associated pyroptotic cell death dependent on the inflammasome activation was found after application of galvanic current, which could be due to two potentially different mechanisms. The first is that upon galvanic current application an alternative means of GSDMD processing occurs, that is independent of NLRP3, and could inactivate its N-terminal lytic domain, as previously found for GSDMD processing by caspase-3 (Taabazuing et al., 2017). The second is that the small amounts of GSDMD N-terminal found could create a small number of pores in the plasma membrane, thus facilitating their repair by the endosomal sorting complexes required for the transport machinery, which in turn leads to a hyperactive state of the macrophage (Evavold et al., 2018; Ruhl et al., 2018). During this state of the macrophage, IL-1β is released in the absence of cell death (Evavold et al., 2018).

However, an increase in the intensity, time or number of impacts of galvanic current application leads to an increase in cell death that was independent of the inflammasome

and could be related to the current itself. Therefore, clinical application of current intensities higher than 6 mA would probably lead to tissue necrosis and not to an effective reparative process. Galvanic currents of 3 and 6 mA for 2 impacts of 6 s are able to induce NLRP3 inflammasome activation *in vitro*. This is in agreement with the fact that 3 mA galvanic currents are able to induce clinically significant regeneration of lesions (Garcia-Vidal et al., 2019; Margalef et al., 2019; Medina-Mirapeix et al., 2019; Valera-Garrido et al., 2014).

Total load of galvanic current was calculated as the multiplication of the value of every parameter used in the protocol to applicate the current. We found that the release of IL-1β was also dependent on the total load of galvanic current applicated, and in consequence was the case also for the cell death. Interestingly, although some galvanic current protocols had the same total current load, the release of IL-1β varied between them depending on the parameters applicated. Protocols with the same total load in which the time and the number of impacts were high, induced a higher IL-1β release, even with low current intensity, compared with protocols with lower time or number of impacts. These results suggest that protocols of galvanic current with increase time or number of impacts are not recommended for therapeutically galvanic current application, even when low intensities of current are delivered. In addition, previous results showed that the pain processing effect was independent of the dosage of galvanic current administered, and is present even using with 0.3 mA of intensity (Varela-Rodriguez et al., 2022). These results reinforce the use of low-dosage galvanic current protocols. Finally, changes in the temperature while galvanic current was applicated did not vary the release of IL-1β or cell death, so lowering the temperature will not affect the pro-inflammatory effects of galvanic current application in clinics. This effect is in agreement with previous studies using different therapeutic protocols of galvanic current, including the protocol 3:3:3 used in this Thesis, that showed no changes in temperature before and after galvanic current application (Margalef et al., 2021).

With all these results we can conclude that application of galvanic current actives the NLRP3 inflammasome and induces a controlled inflammatory response *in vitro*. However, high-intensity doses of galvanic current over long periods of time or repeated impacts, which means a high total load, could induce high tissue necrosis and are therefore not recommended for clinical practice.

Chapter 3. Involvement of NLRP3 on the regenerative response of galvanic current in pre-clinical models.

3.1. Galvanic current applicated in Achilles' mice tendon induces inflammation and tissue regeneration dependent on NLRP3 inflammasome

The low activation of NLRP3 induced by galvanic current application seen in macrophages could lead to a moderate inflammatory response *in vivo* that is beneficial for tissue regeneration. Indeed, NLRP3 was important in inducing an *in vivo* inflammatory response with increased amounts of different cytokines, including *Il1b* or *Cxcl10*, which conditioned the structure and functions of treated tendons. However, NLRP3 deficiency does not affect *Il6* production or polymorphonuclear cell infiltration when galvanic currents are applied *in vivo*. This demonstrates that galvanic current-induced NLRP3 is able to control a specific inflammatory program *in vivo*, but probably does not affect IL-6-mediated polymorphonuclear cell infiltration in tendons.

Exacerbated NLRP3 activation could led to fibrosis (Alegre et al., 2017; Gaul et al., 2021), suggesting that NLRP3 may control collagen deposition. The mild NLRP3 activation found after galvanic current application was associated with increased *Tgfb1* production, increased type I versus type III collagen in tendons, and decreased structural dispersion of collagen fibers. This is associated with an increase in tendon stiffness, which is related to tendon resistance to length changes, reducing tendon stiffness during aging and resulting in weaker tendons (Krupenevich et al., 2022). This could explain previous clinical findings related to galvanic current therapy, such as the fact that almost all patients treated with galvanic current on tendon injuries had no long-term relapses (Valera-Garrido et al., 2014) and the fact that the application of galvanic current on human tendon lesions in combination with exercise therapy achieved greater functional recovery compared to exercise alone (Moreno et al., 2017), and also compared to combining exercise with other rehabilitation interventions such as electrotherapy or mechanical intervention (Abat et al., 2016; Rodriguez-Huguet et al., 2020).

Thus, our findings could help physicians to choose and combine rehabilitation and orthopedic treatments. However, a limitation of these results is that the use of animals limits us to employing ultrasound-guided puncture when applying galvanic current to the calcaneal tendon in mice, because it is the largest accessible tendon, whereas in humans galvanic current has been applied to the supraspinatus (Rodriguez-Huguet et al., 2020), patellar

(Abat et al., 2016) and lateral epicondyle (Valera-Garrido et al., 2014) tendons. In all tendons, the application of galvanic current had a similar clinical benefit, but we cannot rule out that the mouse calcaneal tendon presents a different response to galvanic current. Indeed, different species have been reported to exhibit different tenocyte inflammatory responses (Oreff et al., 2021), and although mice and humans exhibit broad general similarities in their tenocyte responses (Oreff et al., 2021), galvanic current in the presence of specific NLRP3 blockers, such as MCC950, needs to be applied in additional animal models with species other than mice.

Therefore, this Thesis results report how galvanic current is a feasible technique applied *in vivo* to activate the NLRP3 inflammasome and induce a local inflammatory response to enhance a collagen-mediated regeneration process in the tendon, establishing the molecular mechanism of percutaneous electrolysis for the treatment of chronic lesions and establishing the first treatment aimed to activate NLRP3 (**Figure 51**).

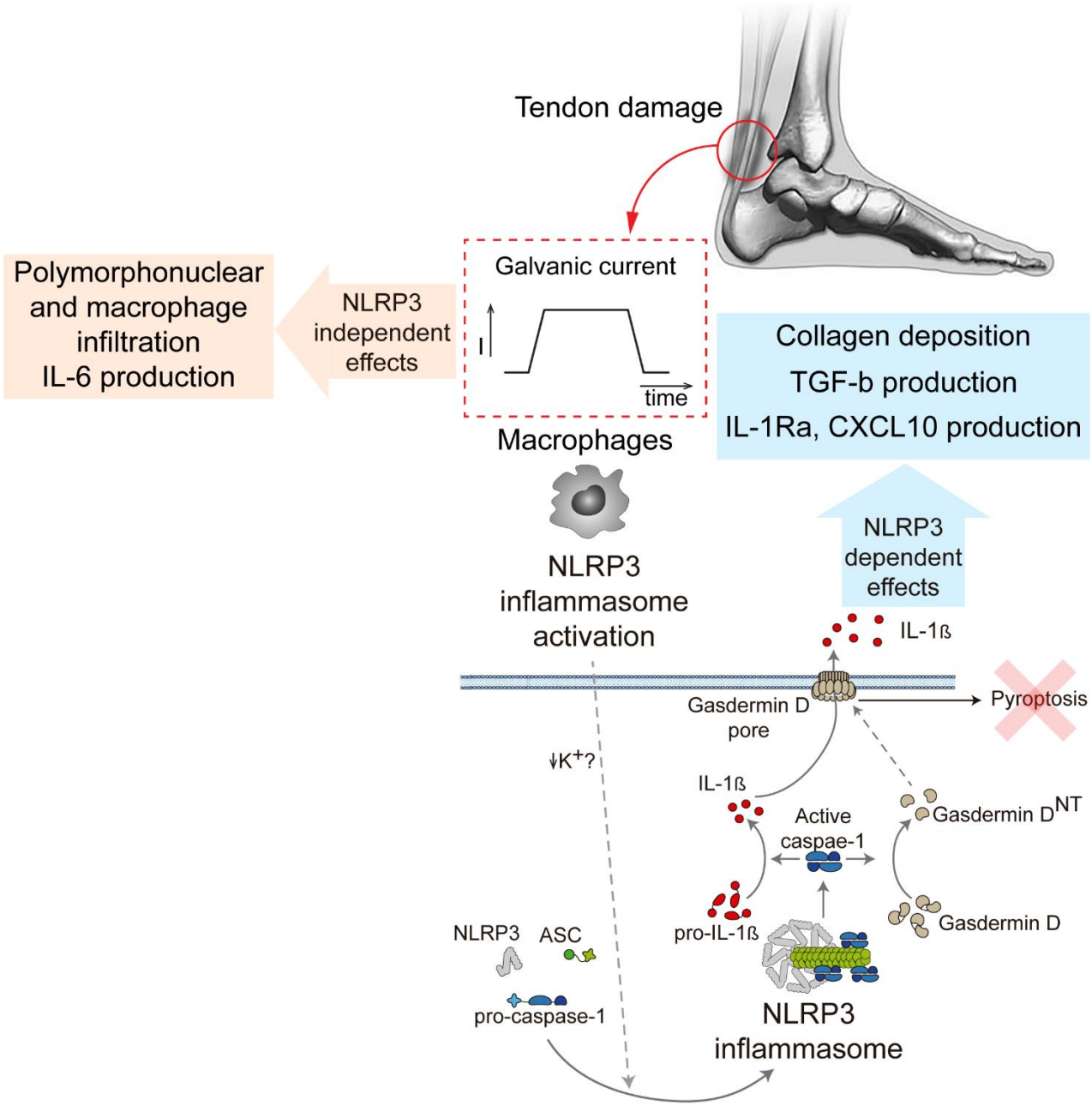

Figure 51. Model summarizing the action of galvanic current in tendon regeneration.

3.2. Sterile damage induced by collagenase in Achilles' mice tendon is partially dependent on NLRP3 inflammasome

Collagenase is a metalloproteinase described to degrade different types of collagen (Krane, 1982) and therefore is a potent enzyme degrading the structure of tissues. After collagenase injection in mice Achilles tendon, an increase in number of polymorphonuclear cells, *Il1b* and *Il6* gene expression is observed. This is in agreement with previous results using collagenase to induce tendinopathy in a rat model in which the expression of other pro-inflammatory molecules such as *Cox2* were also increased after collagenase treatment (Sanchez-Sanchez et al., 2020). These effects were not present when denatured collagenase was injected, meaning that the effect was directly related with collagenase activity itself and not to contaminating endotoxins that it could contain the collagenase. Therefore, this could be considered a model of inflammation due to sterile-tissue injury. In addition, an increase in the production of pro-inflammatory cytokines, like IL-1β, IL-18, TNF-α and IL-6, was observed in collagenase-treated mice compared with controls in wild-type mice, being the production of IL-1β and IL-6, but not IL-18, dependent on NLRP3. This is in opposite to previous studies where there is a decrease of both IL-1β and IL-18 in NLRP3 deficient mice, for example in an acrylamide-induced neurotoxicity model (Sui et al., 2020), or in a bacterial infection model (Yamaguchi et al., 2017). However, also more similar models to collagenase-induced damage, like a model of osteoarthritis induced after transection of anterior cruciate ligament, in which a decrease on IL-1β and IL-18 is observed after treatment with sinomenine, but after that treatment also decrease NLRP3 expression levels which was responsible for the decrease of cytokines (Dong et al., 2019). Therefore, the inflammation observed *in vivo* after collagenase injection could be triggered by two mechanisms, (*i*) the recognition of the collagen fragments by another cell types like neutrophils, as in macrophages degraded collagen inhibit the NLRP3 inflammasome response and this inflammasome has been described to promote neutrophils NETosis under sterile conditions (Munzer et al., 2021), or (*ii*) the degradation of collagen produces a tissue damage that induce the release of different DAMPs, which induce inflammasome activation.

In contrast and as expected, *Pycard*$^{-/-}$ mice present a significant decrease in the production of both IL-1β and IL-18, suggesting that the inflammasome adaptor protein ASC was critical to control production of these two inflammasome-dependent cytokines. This was also found in models of skin allograft rejection, mucositis and myocardial ischemia-reperfusion injury where the ASC knockout mice presented impaired production of both, IL-1β and IL-18 (Amores-Iniesta et al., 2017; Arifa et al., 2014; Sandanger et al., 2013). This

suggests that additional inflammasomes different than NLRP3, but dependent on ASC, could be controlling IL-18 production in the collagenase-damaged model. The AIM2 inflammasome could have a role in this model because after collagen and ECM degradation, necrosis is induced and the presence of cytosolic DNA in macrophages after engulfing necrosed cells can be assumed, as this mechanism has been described in other models of sterile damage (Sun et al., 2017). The AIM2 inflammasome is also present in fibroblasts (Bostanci et al., 2011), and functions in the inflammatory response in the dental pulp (Wang et al., 2013). In these non-immunogenic tissues, IL-18 could be playing a physiological role, as for example, IL-18 is important to maintain intestinal epithelial homeostasis (Rauch et al., 2017; Van Der Kraak et al., 2021). In addition, the role of other cell types different of the macrophages in the inflammation induced after collagenase injection cannot be discarded because *in vitro* macrophages treated with collagenase showed an impaired capacity to release IL-1β and IL-6 and also because other immune cells like neutrophils have a main role in the initial inflammatory stages of tendinopathy (D'Addona et al., 2017).

The fact that in the *Nlrp3*$^{-/-}$ mice a decrease in IL-6 production is observed, without impairment of TNF-α production, could be explained by the presence of NLRP3 inflammasome in different cell types, as fibroblast that can induce specifically the release of IL-6 as a response to cell damage (Solini et al., 1999). This is in concordance with the fact that, as mentioned before, the NLRP3 inflammasome is a key pathway for controlling inflammation under sterile conditions (Broz et al., 2020; Broz and Dixit, 2016; Liston and Masters, 2017). In addition, the decrease in IL-6 production in *Nlrp3*$^{-/-}$ mice correlates with the slightly decrease in the amount of polymorphonuclear cells infiltrated after collagenase injection in this genotype. This decrease could be attributed to IL-6, as the potent chemoattractant chemokine CXCL10 was increased after collagenase injection, but without differences between genotypes. However, CXCL10 and other chemokines production are dependent on NLRP3 in different *in vivo* models, including sterile models of uric acid induced peritonitis (Tapia-Abellan et al., 2021), or acute cholangitis (Gonzalez et al., 2020). All this suggests that multiple inflammasomes, including NLRP3, could be involved in sterile extracellular matrix damage using collagenase and that the inflammasome elicit an inflammatory response dependent on IL-1β, IL-18 and IL-6.

After collagenase injection, application of percutaneous needle electrolysis both as a unique treatment or with several dosage protocol, did not induce changes in the studied parameters. These results could be explained with three possible theories: (i) percutaneous needle electrolysis is not able to interfere with the inflammation of chronic injured Achilles mice tendons, (ii) collagenase-induced damage model is not a good model to induce chronic

tendon damage, or (iii) the time points selected or the number of treatments applicated were not the optimal ones to observe differences in the studied parameters. Further studies are required to validate the therapeutical value of percutaneous needle electrolysis in injury tendons, which could include the development of physiological tendinopathies in mice, as by inducing excessive exercise of the joints.

CONCLUSIONS

1. Mutations affecting the WHD domain of NLRC4 induce significant changes in the conformation of NLRC4.
2. Different NLRC4 mutants described in patients with autoinflammatory syndromes induce a puncta distribution of NLRC4 in the cells.
3. The p.Ser171Phe NLRC4 variant present a gain-of-function behavior in assembly an inflammasome.
4. The postzygotic p.Ser171Phe NLRC4 variant is a plausible cause of the autoinflammatory disease in the enrolled patient.
5. Galvanic current applicated in HEK293T cells expressing NLRP3 results in a puncta distribution of NLRP3 in the cells.
6. Galvanic current applicated in LPS-primed macrophages is able to activate the NLRP3 inflammasome.
7. Galvanic current applicated in LPS-primed macrophages induce the release of IL-1β and IL-18 cytokines.
8. Galvanic current applicated in LPS-primed macrophages do not induce pyroptotic cell death.
9. Increasing the time and the number of pulses in galvanic current applicated to in LPS-primed macrophages is related with an increase in IL-1β release and also in current-dependent cell death.
10. Percutaneous needle electrolysis applicated in the Achilles tendon of mice induces an increase in type I collagen and tendon stiffness, improving tendon resistance.
11. Tendon resistance after percutaneous needle electrolysis is dependent on the NLRP3 inflammasome.
12. Collagenase administration in the Achilles tendon of mice induces a sterile tissue damage and an inflammatory response partially dependent on NLRP3.

13. Collagenase damage of the Achilles tendon of mice is not affected by the application of percutaneous needle electrolysis by delivering 3 times every 3 days with 3 impacts of 3 mA for 3 seconds.

BIBLIOGRAPHY

Abat, F., Sanchez-Sanchez, J. L., Martin-Nogueras, A. M., Calvo-Arenillas, J. I., Yajeya, J., Mendez-Sanchez, R., Monllau, J. C., & Gelber, P. E. (2016, Dec). Randomized controlled trial comparing the effectiveness of the ultrasound-guided galvanic electrolysis technique (USGET) versus conventional electro-physiotherapeutic treatment on patellar tendinopathy. *J Exp Orthop, 3*(1), 34. https://doi.org/10.1186/s40634-016-0070-4

Ackerman, J. E., Geary, M. B., Orner, C. A., Bawany, F., & Loiselle, A. E. (2017). Obesity/Type II diabetes alters macrophage polarization resulting in a fibrotic tendon healing response. *PLoS One, 12*(7), e0181127. https://doi.org/10.1371/journal.pone.0181127

Adang, L. A., Frank, D. B., Gilani, A., Takanohashi, A., Ulrick, N., Collins, A., Cross, Z., Galambos, C., Helman, G., Kanaan, U., Keller, S., Simon, D., Sherbini, O., Hanna, B. D., & Vanderver, A. L. (2018, Dec). Aicardi goutieres syndrome is associated with pulmonary hypertension. *Mol Genet Metab, 125*(4), 351-358. https://doi.org/10.1016/j.ymgme.2018.09.004

Adhikari, A., Xu, M., & Chen, Z. J. (2007, May 14). Ubiquitin-mediated activation of TAK1 and IKK. *Oncogene, 26*(22), 3214-3226. https://doi.org/10.1038/sj.onc.1210413

Aganna, E., Martinon, F., Hawkins, P. N., Ross, J. B., Swan, D. C., Booth, D. R., Lachmann, H. J., Bybee, A., Gaudet, R., Woo, P., Feighery, C., Cotter, F. E., Thome, M., Hitman, G. A., Tschopp, J., & McDermott, M. F. (2002, Sep). Association of mutations in the NALP3/CIAS1/PYPAF1 gene with a broad phenotype including recurrent fever, cold sensitivity, sensorineural deafness, and AA amyloidosis. *Arthritis Rheum, 46*(9), 2445-2452. https://doi.org/10.1002/art.10509

Aicale, R., Bisaccia, R. D., Oliviero, A., Oliva, F., & Maffulli, N. (2020, Aug). Current pharmacological approaches to the treatment of tendinopathy. *Expert Opin Pharmacother, 21*(12), 1467-1477. https://doi.org/10.1080/14656566.2020.1763306

Aizawa, E., Karasawa, T., Watanabe, S., Komada, T., Kimura, H., Kamata, R., Ito, H., Hishida, E., Yamada, N., Kasahara, T., Mori, Y., & Takahashi, M. (2020, May 22). GSDME-Dependent Incomplete Pyroptosis Permits Selective IL-1alpha Release under Caspase-1 Inhibition. *iScience, 23*(5), 101070. https://doi.org/10.1016/j.isci.2020.101070

Akira, S., Taga, T., & Kishimoto, T. (1993). Interleukin-6 in biology and medicine. *Adv Immunol, 54*, 1-78. https://doi.org/10.1016/s0065-2776(08)60532-5

Akira, S., Uematsu, S., & Takeuchi, O. (2006, Feb 24). Pathogen recognition and innate immunity. *Cell, 124*(4), 783-801. https://doi.org/10.1016/j.cell.2006.02.015

Aksentijevich, I., Masters, S. L., Ferguson, P. J., Dancey, P., Frenkel, J., van Royen-Kerkhoff, A., Laxer, R., Tedgard, U., Cowen, E. W., Pham, T. H., Booty, M., Estes, J. D., Sandler, N. G., Plass, N., Stone, D. L., Turner, M. L., Hill, S., Butman, J. A., Schneider, R., Babyn, P., El-Shanti, H. I., Pope, E., Barron, K., Bing, X., Laurence, A., Lee, C. C., Chapelle, D., Clarke, G. I., Ohson, K., Nicholson, M., Gadina, M., Yang, B., Korman, B. D., Gregersen, P. K., van Hagen, P. M., Hak, A. E., Huizing, M., Rahman, P., Douek, D. C., Remmers, E. F., Kastner, D. L., & Goldbach-Mansky, R. (2009, Jun 4). An autoinflammatory disease with deficiency of the interleukin-1-receptor antagonist. *N Engl J Med, 360*(23), 2426-2437. https://doi.org/10.1056/NEJMoa0807865

Alarcon-Vila, C., Baroja-Mazo, A., de Torre-Minguela, C., Martinez, C. M., Martinez-Garcia, J. J., Martinez-Banaclocha, H., Garcia-Palenciano, C., & Pelegrin, P. (2020, Nov 2). CD14 release induced by P2X7 receptor restricts inflammation and increases survival during sepsis. *Elife, 9*. https://doi.org/10.7554/eLife.60849

Alcocer-Gomez, E., Casas-Barquero, N., Williams, M. R., Romero-Guillena, S. L., Canadas-Lozano, D., Bullon, P., Sanchez-Alcazar, J. A., Navarro-Pando, J. M., & Cordero, M. D. (2017, Jul).

Antidepressants induce autophagy dependent-NLRP3-inflammasome inhibition in Major depressive disorder. *Pharmacol Res, 121*, 114-121. https://doi.org/10.1016/j.phrs.2017.04.028

Alegre, F., Pelegrin, P., & Feldstein, A. E. (2017, May). Inflammasomes in Liver Fibrosis. *Semin Liver Dis, 37*(2), 119-127. https://doi.org/10.1055/s-0037-1601350

Alfredson, H., & Cook, J. (2007, Apr). A treatment algorithm for managing Achilles tendinopathy: new treatment options. *Br J Sports Med, 41*(4), 211-216. https://doi.org/10.1136/bjsm.2007.035543

Alfredson, H., & Ohberg, L. (2005, May). Sclerosing injections to areas of neo-vascularisation reduce pain in chronic Achilles tendinopathy: a double-blind randomised controlled trial. *Knee Surg Sports Traumatol Arthrosc, 13*(4), 338-344. https://doi.org/10.1007/s00167-004-0585-6

Ali, S., Huber, M., Kollewe, C., Bischoff, S. C., Falk, W., & Martin, M. U. (2007, Nov 20). IL-1 receptor accessory protein is essential for IL-33-induced activation of T lymphocytes and mast cells. *Proc Natl Acad Sci U S A, 104*(47), 18660-18665. https://doi.org/10.1073/pnas.0705939104

Amores-Iniesta, J., Barbera-Cremades, M., Martinez, C. M., Pons, J. A., Revilla-Nuin, B., Martinez-Alarcon, L., Di Virgilio, F., Parrilla, P., Baroja-Mazo, A., & Pelegrin, P. (2017, Dec 19). Extracellular ATP Activates the NLRP3 Inflammasome and Is an Early Danger Signal of Skin Allograft Rejection. *Cell Rep, 21*(12), 3414-3426. https://doi.org/10.1016/j.celrep.2017.11.079

Andreeva, L., David, L., Rawson, S., Shen, C., Pasricha, T., Pelegrin, P., & Wu, H. (2021, Dec 22). NLRP3 cages revealed by full-length mouse NLRP3 structure control pathway activation. *Cell, 184*(26), 6299-6312 e6222. https://doi.org/10.1016/j.cell.2021.11.011

Andres, B. M., & Murrell, G. A. (2008, Jul). Treatment of tendinopathy: what works, what does not, and what is on the horizon. *Clin Orthop Relat Res, 466*(7), 1539-1554. https://doi.org/10.1007/s11999-008-0260-1

Angosto-Bazarra, D., Alarcon-Vila, C., Hurtado-Navarro, L., Banos, M. C., Rivers-Auty, J., & Pelegrin, P. (2022, Jan 7). Evolutionary analyses of the gasdermin family suggest conserved roles in infection response despite loss of pore-forming functionality. *BMC Biol, 20*(1), 9. https://doi.org/10.1186/s12915-021-01220-z

Angosto-Bazarra, D., Molina-Lopez, C., Penin-Franch, A., Hurtado-Navarro, L., & Pelegrin, P. (2021, Mar 18). Techniques to Study Inflammasome Activation and Inhibition by Small Molecules. *Molecules, 26*(6). https://doi.org/10.3390/molecules26061704

Arango Duque, G., & Descoteaux, A. (2014). Macrophage cytokines: involvement in immunity and infectious diseases. *Front Immunol, 5*, 491. https://doi.org/10.3389/fimmu.2014.00491

Archambault, J., Tsuzaki, M., Herzog, W., & Banes, A. J. (2002, Jan). Stretch and interleukin-1beta induce matrix metalloproteinases in rabbit tendon cells in vitro. *J Orthop Res, 20*(1), 36-39. https://doi.org/10.1016/S0736-0266(01)00075-4

Arend, W. P., Joslin, F. G., & Massoni, R. J. (1985, Jun). Effects of immune complexes on production by human monocytes of interleukin 1 or an interleukin 1 inhibitor. *J Immunol, 134*(6), 3868-3875. https://www.ncbi.nlm.nih.gov/pubmed/2985700

Arifa, R. D., Madeira, M. F., de Paula, T. P., Lima, R. L., Tavares, L. D., Menezes-Garcia, Z., Fagundes, C. T., Rachid, M. A., Ryffel, B., Zamboni, D. S., Teixeira, M. M., & Souza, D. G. (2014, Jul). Inflammasome activation is reactive oxygen species dependent and mediates

irinotecan-induced mucositis through IL-1beta and IL-18 in mice. *Am J Pathol, 184*(7), 2023-2034. https://doi.org/10.1016/j.ajpath.2014.03.012

Arirachakaran, A., Sukthuayat, A., Sisayanarane, T., Laoratanavoraphong, S., Kanchanatawan, W., & Kongtharvonskul, J. (2016, Jun). Platelet-rich plasma versus autologous blood versus steroid injection in lateral epicondylitis: systematic review and network meta-analysis. *J Orthop Traumatol, 17*(2), 101-112. https://doi.org/10.1007/s10195-015-0376-5

Asea, A., Rehli, M., Kabingu, E., Boch, J. A., Bare, O., Auron, P. E., Stevenson, M. A., & Calderwood, S. K. (2002, Apr 26). Novel signal transduction pathway utilized by extracellular HSP70: role of toll-like receptor (TLR) 2 and TLR4. *J Biol Chem, 277*(17), 15028-15034. https://doi.org/10.1074/jbc.M200497200

Astrom, M., & Westlin, N. (1992, Dec). No effect of piroxicam on achilles tendinopathy. A randomized study of 70 patients. *Acta Orthop Scand, 63*(6), 631-634. https://doi.org/10.1080/17453679209169724

Bahr, R., Fossan, B., Loken, S., & Engebretsen, L. (2006, Aug). Surgical treatment compared with eccentric training for patellar tendinopathy (Jumper's Knee). A randomized, controlled trial. *J Bone Joint Surg Am, 88*(8), 1689-1698. https://doi.org/10.2106/JBJS.E.01181

Baker, P. J., De Nardo, D., Moghaddas, F., Tran, L. S., Bachem, A., Nguyen, T., Hayman, T., Tye, H., Vince, J. E., Bedoui, S., Ferrero, R. L., & Masters, S. L. (2017, Jul 1). Posttranslational Modification as a Critical Determinant of Cytoplasmic Innate Immune Recognition. *Physiol Rev, 97*(3), 1165-1209. https://doi.org/10.1152/physrev.00026.2016

Baldwin, A. G., Rivers-Auty, J., Daniels, M. J. D., White, C. S., Schwalbe, C. H., Schilling, T., Hammadi, H., Jaiyong, P., Spencer, N. G., England, H., Luheshi, N. M., Kadirvel, M., Lawrence, C. B., Rothwell, N. J., Harte, M. K., Bryce, R. A., Allan, S. M., Eder, C., Freeman, S., & Brough, D. (2017, Nov 16). Boron-Based Inhibitors of the NLRP3 Inflammasome. *Cell Chem Biol, 24*(11), 1321-1335 e1325. https://doi.org/10.1016/j.chembiol.2017.08.011

Balkwill, F. (2006, Sep). TNF-alpha in promotion and progression of cancer. *Cancer Metastasis Rev, 25*(3), 409-416. https://doi.org/10.1007/s10555-006-9005-3

Banda, N. K., Vondracek, A., Kraus, D., Dinarello, C. A., Kim, S. H., Bendele, A., Senaldi, G., & Arend, W. P. (2003, Feb 15). Mechanisms of inhibition of collagen-induced arthritis by murine IL-18 binding protein. *J Immunol, 170*(4), 2100-2105. https://doi.org/10.4049/jimmunol.170.4.2100

Barbalat, R., Lau, L., Locksley, R. M., & Barton, G. M. (2009, Nov). Toll-like receptor 2 on inflammatory monocytes induces type I interferon in response to viral but not bacterial ligands. *Nat Immunol, 10*(11), 1200-1207. https://doi.org/10.1038/ni.1792

Bardet, J., Laverdure, N., Fusaro, M., Picard, C., Garnier, L., Viel, S., Collardeau-Frachon, S., Guillebon, J. M., Durieu, I., Casari-Thery, C., Mortamet, G., Laurent, A., & Belot, A. (2021, Sep 24). NLRC4 GOF Mutations, a Challenging Diagnosis from Neonatal Age to Adulthood. *J Clin Med, 10*(19). https://doi.org/10.3390/jcm10194369

Barker-Davies, R. M., Nicol, A., McCurdie, I., Watson, J., Baker, P., Wheeler, P., Fong, D., Lewis, M., & Bennett, A. N. (2017, May 22). Study protocol: a double blind randomised control trial of high volume image guided injections in Achilles and patellar tendinopathy in a young active population. *BMC Musculoskelet Disord, 18*(1), 204. https://doi.org/10.1186/s12891-017-1564-7

Baroja-Mazo, A., Martin-Sanchez, F., Gomez, A. I., Martinez, C. M., Amores-Iniesta, J., Compan, V., Barbera-Cremades, M., Yague, J., Ruiz-Ortiz, E., Anton, J., Bujan, S., Couillin, I., Brough,

D., Arostegui, J. I., & Pelegrin, P. (2014, Aug). The NLRP3 inflammasome is released as a particulate danger signal that amplifies the inflammatory response. *Nat Immunol, 15*(8), 738-748. https://doi.org/10.1038/ni.2919

Barrientos, S., Stojadinovic, O., Golinko, M. S., Brem, H., & Tomic-Canic, M. (2008, Sep-Oct). Growth factors and cytokines in wound healing. *Wound Repair Regen, 16*(5), 585-601. https://doi.org/10.1111/j.1524-475X.2008.00410.x

Barsalou, J., Blincoe, A., Fernandez, I., Dal-Soglio, D., Marchitto, L., Selleri, S., Haddad, E., Benyoucef, A., & Touzot, F. (2018). Rapamycin as an Adjunctive Therapy for NLRC4 Associated Macrophage Activation Syndrome. *Front Immunol, 9*, 2162. https://doi.org/10.3389/fimmu.2018.02162

Bauernfeind, F. G., Horvath, G., Stutz, A., Alnemri, E. S., MacDonald, K., Speert, D., Fernandes-Alnemri, T., Wu, J., Monks, B. G., Fitzgerald, K. A., Hornung, V., & Latz, E. (2009, Jul 15). Cutting edge: NF-kappaB activating pattern recognition and cytokine receptors license NLRP3 inflammasome activation by regulating NLRP3 expression. *J Immunol, 183*(2), 787-791. https://doi.org/10.4049/jimmunol.0901363

Beard, D. J., Rees, J. L., Cook, J. A., Rombach, I., Cooper, C., Merritt, N., Shirkey, B. A., Donovan, J. L., Gwilym, S., Savulescu, J., Moser, J., Gray, A., Jepson, M., Tracey, I., Judge, A., Wartolowska, K., Carr, A. J., & Group, C. S. (2018, Jan 27). Arthroscopic subacromial decompression for subacromial shoulder pain (CSAW): a multicentre, pragmatic, parallel group, placebo-controlled, three-group, randomised surgical trial. *Lancet, 391*(10118), 329-338. https://doi.org/10.1016/S0140-6736(17)32457-1

Bedaiwi, M. K., Almaghlouth, I., & Omair, M. A. (2021, Dec). Effectiveness and adverse effects of anakinra in treatment of rheumatoid arthritis: a systematic review. *Eur Rev Med Pharmacol Sci, 25*(24), 7833-7839. https://doi.org/10.26355/eurrev_202112_27630

Bennett, N. T., & Schultz, G. S. (1993, Jun). Growth factors and wound healing: biochemical properties of growth factors and their receptors. *Am J Surg, 165*(6), 728-737. https://doi.org/10.1016/s0002-9610(05)80797-4

Berglund, M., Hart, D. A., & Wiig, M. (2007, Oct). The inflammatory response and hyaluronan synthases in the rabbit flexor tendon and tendon sheath following injury. *J Hand Surg Eur Vol, 32*(5), 581-587. https://doi.org/10.1016/J.JHSE.2007.05.017

Bergsbaken, T., Fink, S. L., & Cookson, B. T. (2009, Feb). Pyroptosis: host cell death and inflammation. *Nat Rev Microbiol, 7*(2), 99-109. https://doi.org/10.1038/nrmicro2070

Bertin, J., & DiStefano, P. S. (2000, Dec). The PYRIN domain: a novel motif found in apoptosis and inflammation proteins. *Cell Death Differ, 7*(12), 1273-1274. https://doi.org/10.1038/sj.cdd.4400774

Bessa, J., Meyer, C. A., de Vera Mudry, M. C., Schlicht, S., Smith, S. H., Iglesias, A., & Cote-Sierra, J. (2014, Dec). Altered subcellular localization of IL-33 leads to non-resolving lethal inflammation. *J Autoimmun, 55*, 33-41. https://doi.org/10.1016/j.jaut.2014.02.012

Beutler, B., & Cerami, A. (1989). The biology of cachectin/TNF--a primary mediator of the host response. *Annu Rev Immunol, 7*, 625-655. https://doi.org/10.1146/annurev.iy.07.040189.003205

Beutler, B., Jiang, Z., Georgel, P., Crozat, K., Croker, B., Rutschmann, S., Du, X., & Hoebe, K. (2006). Genetic analysis of host resistance: Toll-like receptor signaling and immunity at large. *Annu Rev Immunol, 24*, 353-389. https://doi.org/10.1146/annurev.immunol.24.021605.090552

Bisset, L., Beller, E., Jull, G., Brooks, P., Darnell, R., & Vicenzino, B. (2006, Nov 4). Mobilisation with movement and exercise, corticosteroid injection, or wait and see for tennis elbow: randomised trial. *BMJ, 333*(7575), 939. https://doi.org/10.1136/bmj.38961.584653.AE

Biswas, S. K., & Mantovani, A. (2010, Oct). Macrophage plasticity and interaction with lymphocyte subsets: cancer as a paradigm. *Nat Immunol, 11*(10), 889-896. https://doi.org/10.1038/ni.1937

Biton, J., Khaleghparast Athari, S., Thiolat, A., Santinon, F., Lemeiter, D., Herve, R., Delavallee, L., Levescot, A., Roga, S., Decker, P., Girard, J. P., Herbelin, A., Boissier, M. C., & Bessis, N. (2016, Sep 1). In Vivo Expansion of Activated Foxp3+ Regulatory T Cells and Establishment of a Type 2 Immune Response upon IL-33 Treatment Protect against Experimental Arthritis. *J Immunol, 197*(5), 1708-1719. https://doi.org/10.4049/jimmunol.1502124

Bjordal, J. M., Lopes-Martins, R. A., Joensen, J., Couppe, C., Ljunggren, A. E., Stergioulas, A., & Johnson, M. I. (2008, May 29). A systematic review with procedural assessments and meta-analysis of low level laser therapy in lateral elbow tendinopathy (tennis elbow). *BMC Musculoskelet Disord, 9*, 75. https://doi.org/10.1186/1471-2474-9-75

Blobel, C. P. (1997, Aug 22). Metalloprotease-disintegrins: links to cell adhesion and cleavage of TNF alpha and Notch. *Cell, 90*(4), 589-592. https://doi.org/10.1016/s0092-8674(00)80519-x

Boesen, A. P., Hansen, R., Boesen, M. I., Malliaras, P., & Langberg, H. (2017, Jul). Effect of High-Volume Injection, Platelet-Rich Plasma, and Sham Treatment in Chronic Midportion Achilles Tendinopathy: A Randomized Double-Blinded Prospective Study. *Am J Sports Med, 45*(9), 2034-2043. https://doi.org/10.1177/0363546517702862

Bohm, S., Mersmann, F., & Arampatzis, A. (2015, Dec). Human tendon adaptation in response to mechanical loading: a systematic review and meta-analysis of exercise intervention studies on healthy adults. *Sports Med Open, 1*(1), 7. https://doi.org/10.1186/s40798-015-0009-9

Boice, A. (2018). *Development of Small Melucule Neuroprotectants.* Virginia Commonwealth University]. Richmond, VA, USA.

Borst, S. E. (2004, Mar-Apr). The role of TNF-alpha in insulin resistance. *Endocrine, 23*(2-3), 177-182. https://doi.org/10.1385/ENDO:23:2-3:177

Bostanci, N., Meier, A., Guggenheim, B., & Belibasakis, G. N. (2011). Regulation of NLRP3 and AIM2 inflammasome gene expression levels in gingival fibroblasts by oral biofilms. *Cell Immunol, 270*(1), 88-93. https://doi.org/10.1016/j.cellimm.2011.04.002

Bottinger, E. P., Letterio, J. J., & Roberts, A. B. (1997, May). Biology of TGF-beta in knockout and transgenic mouse models. *Kidney Int, 51*(5), 1355-1360. https://doi.org/10.1038/ki.1997.185

Boucher, D., Monteleone, M., Coll, R. C., Chen, K. W., Ross, C. M., Teo, J. L., Gomez, G. A., Holley, C. L., Bierschenk, D., Stacey, K. J., Yap, A. S., Bezbradica, J. S., & Schroder, K. (2018, Mar 5). Caspase-1 self-cleavage is an intrinsic mechanism to terminate inflammasome activity. *J Exp Med, 215*(3), 827-840. https://doi.org/10.1084/jem.20172222

Boudreau, N., Gaudreault, N., Roy, J. S., Bedard, S., & Balg, F. (2019, Mar). The Addition of Glenohumeral Adductor Coactivation to a Rotator Cuff Exercise Program for Rotator Cuff Tendinopathy: A Single-Blind Randomized Controlled Trial. *J Orthop Sports Phys Ther, 49*(3), 126-135. https://doi.org/10.2519/jospt.2019.8240

Boulanger, M. J., Chow, D. C., Brevnova, E. E., & Garcia, K. C. (2003, Jun 27). Hexameric structure and assembly of the interleukin-6/IL-6 alpha-receptor/gp130 complex. *Science, 300*(5628), 2101-2104. https://doi.org/10.1126/science.1083901

Boutet, M. A., Najm, A., Bart, G., Brion, R., Touchais, S., Trichet, V., Layrolle, P., Gabay, C., Palmer, G., Blanchard, F., & Le Goff, B. (2017, Jul). IL-38 overexpression induces anti-inflammatory effects in mice arthritis models and in human macrophages in vitro. *Ann Rheum Dis, 76*(7), 1304-1312. https://doi.org/10.1136/annrheumdis-2016-210630

Boyer, M. I., Watson, J. T., Lou, J., Manske, P. R., Gelberman, R. H., & Cai, S. R. (2001, Sep). Quantitative variation in vascular endothelial growth factor mRNA expression during early flexor tendon healing: an investigation in a canine model. *J Orthop Res, 19*(5), 869-872. https://doi.org/10.1016/S0736-0266(01)00017-1

Brehm, A., Liu, Y., Sheikh, A., Marrero, B., Omoyinmi, E., Zhou, Q., Montealegre, G., Biancotto, A., Reinhardt, A., Almeida de Jesus, A., Pelletier, M., Tsai, W. L., Remmers, E. F., Kardava, L., Hill, S., Kim, H., Lachmann, H. J., Megarbane, A., Chae, J. J., Brady, J., Castillo, R. D., Brown, D., Casano, A. V., Gao, L., Chapelle, D., Huang, Y., Stone, D., Chen, Y., Sotzny, F., Lee, C. C., Kastner, D. L., Torrelo, A., Zlotogorski, A., Moir, S., Gadina, M., McCoy, P., Wesley, R., Rother, K. I., Hildebrand, P. W., Brogan, P., Kruger, E., Aksentijevich, I., & Goldbach-Mansky, R. (2015, Nov 2). Additive loss-of-function proteasome subunit mutations in CANDLE/PRAAS patients promote type I IFN production. *J Clin Invest, 125*(11), 4196-4211. https://doi.org/10.1172/JCI81260

Brennan, T. V., Lin, L., Huang, X., Cardona, D. M., Li, Z., Dredge, K., Chao, N. J., & Yang, Y. (2012, Oct 4). Heparan sulfate, an endogenous TLR4 agonist, promotes acute GVHD after allogeneic stem cell transplantation. *Blood, 120*(14), 2899-2908. https://doi.org/10.1182/blood-2011-07-368720

Broz, P., & Dixit, V. M. (2016, Jul). Inflammasomes: mechanism of assembly, regulation and signalling. *Nat Rev Immunol, 16*(7), 407-420. https://doi.org/10.1038/nri.2016.58

Broz, P., Pelegrin, P., & Shao, F. (2020, Mar). The gasdermins, a protein family executing cell death and inflammation. *Nat Rev Immunol, 20*(3), 143-157. https://doi.org/10.1038/s41577-019-0228-2

Broz, P., von Moltke, J., Jones, J. W., Vance, R. E., & Monack, D. M. (2010, Dec 16). Differential requirement for Caspase-1 autoproteolysis in pathogen-induced cell death and cytokine processing. *Cell Host Microbe, 8*(6), 471-483. https://doi.org/10.1016/j.chom.2010.11.007

Brubaker, S. W., Bonham, K. S., Zanoni, I., & Kagan, J. C. (2015). Innate immune pattern recognition: a cell biological perspective. *Annu Rev Immunol, 33*, 257-290. https://doi.org/10.1146/annurev-immunol-032414-112240

Bubnov, R., Yevseenko, V., & Semeniv, I. (2013, Jun). Ultrasound guided injections of platelets rich plasma for muscle injury in professional athletes. Comparative study. *Med Ultrason, 15*(2), 101-105. https://doi.org/10.11152/mu.2013.2066.152.rb1vy2

Bueno, J. M., Avila, F. J., Hristu, R., Stanciu, S. G., Eftimie, L., & Stanciu, G. A. (2020, Aug 10). Objective analysis of collagen organization in thyroid nodule capsules using second harmonic generation microscopy images and the Hough transform. *Appl Opt, 59*(23), 6925-6931. https://doi.org/10.1364/AO.393721

Bufler, P., Azam, T., Gamboni-Robertson, F., Reznikov, L. L., Kumar, S., Dinarello, C. A., & Kim, S. H. (2002, Oct 15). A complex of the IL-1 homologue IL-1F7b and IL-18-binding protein reduces IL-18 activity. *Proc Natl Acad Sci U S A, 99*(21), 13723-13728. https://doi.org/10.1073/pnas.212519099

Buhl, A. L., & Wenzel, J. (2019). Interleukin-36 in Infectious and Inflammatory Skin Diseases. *Front Immunol, 10*, 1162. https://doi.org/10.3389/fimmu.2019.01162

Cabeza-Cabrerizo, M., Cardoso, A., Minutti, C. M., Pereira da Costa, M., & Reis e Sousa, C. (2021, Apr 26). Dendritic Cells Revisited. *Annu Rev Immunol, 39*, 131-166. https://doi.org/10.1146/annurev-immunol-061020-053707

Camargo, P. R., Alburquerque-Sendin, F., & Salvini, T. F. (2014, Nov 18). Eccentric training as a new approach for rotator cuff tendinopathy: Review and perspectives. *World J Orthop, 5*(5), 634-644. https://doi.org/10.5312/wjo.v5.i5.634

Campagnola, P. J., Clark, H. A., Mohler, W. A., Lewis, A., & Loew, L. M. (2001, Jul). Second-harmonic imaging microscopy of living cells. *J Biomed Opt, 6*(3), 277-286. https://doi.org/10.1117/1.1383294

Canna, S. W., de Jesus, A. A., Gouni, S., Brooks, S. R., Marrero, B., Liu, Y., DiMattia, M. A., Zaal, K. J., Sanchez, G. A., Kim, H., Chapelle, D., Plass, N., Huang, Y., Villarino, A. V., Biancotto, A., Fleisher, T. A., Duncan, J. A., O'Shea, J. J., Benseler, S., Grom, A., Deng, Z., Laxer, R. M., & Goldbach-Mansky, R. (2014, Oct). An activating NLRC4 inflammasome mutation causes autoinflammation with recurrent macrophage activation syndrome. *Nat Genet, 46*(10), 1140-1146. https://doi.org/10.1038/ng.3089

Canna, S. W., Girard, C., Malle, L., de Jesus, A., Romberg, N., Kelsen, J., Surrey, L. F., Russo, P., Sleight, A., Schiffrin, E., Gabay, C., Goldbach-Mansky, R., & Behrens, E. M. (2017, May). Life-threatening NLRC4-associated hyperinflammation successfully treated with IL-18 inhibition. *J Allergy Clin Immunol, 139*(5), 1698-1701. https://doi.org/10.1016/j.jaci.2016.10.022

Carr, A. J., Murphy, R., Dakin, S. G., Rombach, I., Wheway, K., Watkins, B., & Franklin, S. L. (2015, Dec). Platelet-Rich Plasma Injection With Arthroscopic Acromioplasty for Chronic Rotator Cuff Tendinopathy: A Randomized Controlled Trial. *Am J Sports Med, 43*(12), 2891-2897. https://doi.org/10.1177/0363546515608485

Case, C. L., Shin, S., & Roy, C. R. (2009, May). Asc and Ipaf Inflammasomes direct distinct pathways for caspase-1 activation in response to Legionella pneumophila. *Infect Immun, 77*(5), 1981-1991. https://doi.org/10.1128/IAI.01382-08

Cayrol, C., & Girard, J. P. (2009, Jun 2). The IL-1-like cytokine IL-33 is inactivated after maturation by caspase-1. *Proc Natl Acad Sci U S A, 106*(22), 9021-9026. https://doi.org/10.1073/pnas.0812690106

Centrella, M., McCarthy, T. L., & Canalis, E. (1991, Oct). Transforming growth factor-beta and remodeling of bone. *J Bone Joint Surg Am, 73*(9), 1418-1428. https://www.ncbi.nlm.nih.gov/pubmed/1918129

Cerwenka, A., Kovar, H., Majdic, O., & Holter, W. (1996, Jan 15). Fas- and activation-induced apoptosis are reduced in human T cells preactivated in the presence of TGF-beta 1. *J Immunol, 156*(2), 459-464. https://www.ncbi.nlm.nih.gov/pubmed/8543794

Challoumas, D., Kirwan, P. D., Borysov, D., Clifford, C., McLean, M., & Millar, N. L. (2019, Feb). Topical glyceryl trinitrate for the treatment of tendinopathies: a systematic review. *Br J Sports Med, 53*(4), 251-262. https://doi.org/10.1136/bjsports-2018-099552

Chamberlain, C. S., Leiferman, E. M., Frisch, K. E., Wang, S., Yang, X., van Rooijen, N., Baer, G. S., Brickson, S. L., & Vanderby, R. (2011, Jun). The influence of macrophage depletion on

ligament healing. *Connect Tissue Res, 52*(3), 203-211. https://doi.org/10.3109/03008207.2010.511355

Chan, B. P., Chan, K. M., Maffulli, N., Webb, S., & Lee, K. K. (1997, Sep). Effect of basic fibroblast growth factor. An in vitro study of tendon healing. *Clin Orthop Relat Res*(342), 239-247. https://www.ncbi.nlm.nih.gov/pubmed/9308546

Chang, J., Thunder, R., Most, D., Longaker, M. T., & Lineaweaver, W. C. (2000, Jan). Studies in flexor tendon wound healing: neutralizing antibody to TGF-beta1 increases postoperative range of motion. *Plast Reconstr Surg, 105*(1), 148-155. https://doi.org/10.1097/00006534-200001000-00025

Chapman, E. A., Lyon, M., Simpson, D., Mason, D., Beynon, R. J., Moots, R. J., & Wright, H. L. (2019). Caught in a Trap? Proteomic Analysis of Neutrophil Extracellular Traps in Rheumatoid Arthritis and Systemic Lupus Erythematosus. *Front Immunol, 10*, 423. https://doi.org/10.3389/fimmu.2019.00423

Chauhan, D., Vande Walle, L., & Lamkanfi, M. (2020, Sep). Therapeutic modulation of inflammasome pathways. *Immunol Rev, 297*(1), 123-138. https://doi.org/10.1111/imr.12908

Chear, C. T., Nallusamy, R., Canna, S. W., Chan, K. C., Baharin, M. F., Hishamshah, M., Ghani, H., Ripen, A. M., & Mohamad, S. B. (2020, Feb). A novel de novo NLRC4 mutation reinforces the likely pathogenicity of specific LRR domain mutation. *Clin Immunol, 211*, 108328. https://doi.org/10.1016/j.clim.2019.108328

Chellini, F., Tani, A., Zecchi-Orlandini, S., & Sassoli, C. (2019, Feb 5). Influence of Platelet-Rich and Platelet-Poor Plasma on Endogenous Mechanisms of Skeletal Muscle Repair/Regeneration. *Int J Mol Sci, 20*(3). https://doi.org/10.3390/ijms20030683

Chen, J., & Chen, Z. J. (2018, Dec). PtdIns4P on dispersed trans-Golgi network mediates NLRP3 inflammasome activation. *Nature, 564*(7734), 71-76. https://doi.org/10.1038/s41586-018-0761-3

Chen, K. W., Monteleone, M., Boucher, D., Sollberger, G., Ramnath, D., Condon, N. D., von Pein, J. B., Broz, P., Sweet, M. J., & Schroder, K. (2018, Aug 24). Noncanonical inflammasome signaling elicits gasdermin D-dependent neutrophil extracellular traps. *Sci Immunol, 3*(26). https://doi.org/10.1126/sciimmunol.aar6676

Chen, X., Xun, K., Chen, L., & Wang, Y. (2009, Oct). TNF-alpha, a potent lipid metabolism regulator. *Cell Biochem Funct, 27*(7), 407-416. https://doi.org/10.1002/cbf.1596

Cheong, R., Bergmann, A., Werner, S. L., Regal, J., Hoffmann, A., & Levchenko, A. (2006, Feb 3). Transient IkappaB kinase activity mediates temporal NF-kappaB dynamics in response to a wide range of tumor necrosis factor-alpha doses. *J Biol Chem, 281*(5), 2945-2950. https://doi.org/10.1074/jbc.M510085200

Chiu, S., & Bharat, A. (2016, Jun). Role of monocytes and macrophages in regulating immune response following lung transplantation. *Curr Opin Organ Transplant, 21*(3), 239-245. https://doi.org/10.1097/MOT.0000000000000313

Chu, M., Chu, I. M., Yung, E. C., Lam, C. W., Leung, T. F., Wong, G. W., & Wong, C. K. (2016, Jul 18). Aberrant Expression of Novel Cytokine IL-38 and Regulatory T Lymphocytes in Childhood Asthma. *Molecules, 21*(7). https://doi.org/10.3390/molecules21070933

Chu, M., Tam, L. S., Zhu, J., Jiao, D., Liu, H., Cai, Z., Dong, J., Kai Lam, C. W., & Wong, C. K. (2017, Mar). In vivo anti-inflammatory activities of novel cytokine IL-38 in Murphy Roths Large

(MRL)/lpr mice. *Immunobiology, 222*(3), 483-493. https://doi.org/10.1016/j.imbio.2016.10.012

Chui, A. J., Okondo, M. C., Rao, S. D., Gai, K., Griswold, A. R., Johnson, D. C., Ball, D. P., Taabazuing, C. Y., Orth, E. L., Vittimberga, B. A., & Bachovchin, D. A. (2019, Apr 5). N-terminal degradation activates the NLRP1B inflammasome. *Science, 364*(6435), 82-85. https://doi.org/10.1126/science.aau1208

Chung, K. Y., Agarwal, A., Uitto, J., & Mauviel, A. (1996, Feb 9). An AP-1 binding sequence is essential for regulation of the human alpha2(I) collagen (COL1A2) promoter activity by transforming growth factor-beta. *J Biol Chem, 271*(6), 3272-3278. https://doi.org/10.1074/jbc.271.6.3272

Claessen, F., Heesters, B. A., Chan, J. J., Kachooei, A. R., & Ring, D. (2016, Oct). A Meta-Analysis of the Effect of Corticosteroid Injection for Enthesopathy of the Extensor Carpi Radialis Brevis Origin. *J Hand Surg Am, 41*(10), 988-998 e982. https://doi.org/10.1016/j.jhsa.2016.07.097

Clay, G. M., Valadares, D. G., Graff, J. W., Ulland, T. K., Davis, R. E., Scorza, B. M., Zhanbolat, B. S., Chen, Y., Sutterwala, F. S., & Wilson, M. E. (2017, Oct 15). An Anti-Inflammatory Role for NLRP10 in Murine Cutaneous Leishmaniasis. *J Immunol, 199*(8), 2823-2833. https://doi.org/10.4049/jimmunol.1500832

Cocco, M., Garella, D., Di Stilo, A., Borretto, E., Stevanato, L., Giorgis, M., Marini, E., Fantozzi, R., Miglio, G., & Bertinaria, M. (2014, Dec 26). Electrophilic warhead-based design of compounds preventing NLRP3 inflammasome-dependent pyroptosis. *J Med Chem, 57*(24), 10366-10382. https://doi.org/10.1021/jm501072b

Cocco, M., Pellegrini, C., Martinez-Banaclocha, H., Giorgis, M., Marini, E., Costale, A., Miglio, G., Fornai, M., Antonioli, L., Lopez-Castejon, G., Tapia-Abellan, A., Angosto, D., Hafner-Bratkovic, I., Regazzoni, L., Blandizzi, C., Pelegrin, P., & Bertinaria, M. (2017, May 11). Development of an Acrylate Derivative Targeting the NLRP3 Inflammasome for the Treatment of Inflammatory Bowel Disease. *J Med Chem, 60*(9), 3656-3671. https://doi.org/10.1021/acs.jmedchem.6b01624

Cohen, I., Rider, P., Carmi, Y., Braiman, A., Dotan, S., White, M. R., Voronov, E., Martin, M. U., Dinarello, C. A., & Apte, R. N. (2010, Feb 9). Differential release of chromatin-bound IL-1alpha discriminates between necrotic and apoptotic cell death by the ability to induce sterile inflammation. *Proc Natl Acad Sci U S A, 107*(6), 2574-2579. https://doi.org/10.1073/pnas.0915018107

Coll, R. C., Hill, J. R., Day, C. J., Zamoshnikova, A., Boucher, D., Massey, N. L., Chitty, J. L., Fraser, J. A., Jennings, M. P., Robertson, A. A. B., & Schroder, K. (2019, Jun). MCC950 directly targets the NLRP3 ATP-hydrolysis motif for inflammasome inhibition. *Nat Chem Biol, 15*(6), 556-559. https://doi.org/10.1038/s41589-019-0277-7

Coll, R. C., Robertson, A. A., Chae, J. J., Higgins, S. C., Munoz-Planillo, R., Inserra, M. C., Vetter, I., Dungan, L. S., Monks, B. G., Stutz, A., Croker, D. E., Butler, M. S., Haneklaus, M., Sutton, C. E., Nunez, G., Latz, E., Kastner, D. L., Mills, K. H., Masters, S. L., Schroder, K., Cooper, M. A., & O'Neill, L. A. (2015, Mar). A small-molecule inhibitor of the NLRP3 inflammasome for the treatment of inflammatory diseases. *Nat Med, 21*(3), 248-255. https://doi.org/10.1038/nm.3806

Colotta, F., Re, F., Muzio, M., Bertini, R., Polentarutti, N., Sironi, M., Giri, J. G., Dower, S. K., Sims, J. E., & Mantovani, A. (1993, Jul 23). Interleukin-1 type II receptor: a decoy target for IL-1 that is regulated by IL-4. *Science, 261*(5120), 472-475. https://doi.org/10.1126/science.8332913

Colwell, A. S., Phan, T. T., Kong, W., Longaker, M. T., & Lorenz, P. H. (2005, Oct). Hypertrophic scar fibroblasts have increased connective tissue growth factor expression after transforming growth factor-beta stimulation. *Plast Reconstr Surg, 116*(5), 1387-1390; discussion 1391-1382. https://doi.org/10.1097/01.prs.0000182343.99694.28

Compan, V., Baroja-Mazo, A., Lopez-Castejon, G., Gomez, A. I., Martinez, C. M., Angosto, D., Montero, M. T., Herranz, A. S., Bazan, E., Reimers, D., Mulero, V., & Pelegrin, P. (2012, Sep 21). Cell volume regulation modulates NLRP3 inflammasome activation. *Immunity, 37*(3), 487-500. https://doi.org/10.1016/j.immuni.2012.06.013

Conti, P., Ronconi, G., Caraffa, A., Gallenga, C. E., Ross, R., Frydas, I., & Kritas, S. K. (2020, March-April). Induction of pro-inflammatory cytokines (IL-1 and IL-6) and lung inflammation by Coronavirus-19 (COVI-19 or SARS-CoV-2): anti-inflammatory strategies. *J Biol Regul Homeost Agents, 34*(2), 327-331. https://doi.org/10.23812/CONTI-E

Conus, S., Perozzo, R., Reinheckel, T., Peters, C., Scapozza, L., Yousefi, S., & Simon, H. U. (2008, Mar 17). Caspase-8 is activated by cathepsin D initiating neutrophil apoptosis during the resolution of inflammation. *J Exp Med, 205*(3), 685-698. https://doi.org/10.1084/jem.20072152

Cook, J. L., & Purdam, C. R. (2009, Jun). Is tendon pathology a continuum? A pathology model to explain the clinical presentation of load-induced tendinopathy. *Br J Sports Med, 43*(6), 409-416. https://doi.org/10.1136/bjsm.2008.051193

Coombes, B. K., Bisset, L., Brooks, P., Khan, A., & Vicenzino, B. (2013, Feb 6). Effect of corticosteroid injection, physiotherapy, or both on clinical outcomes in patients with unilateral lateral epicondylalgia: a randomized controlled trial. *JAMA, 309*(5), 461-469. https://doi.org/10.1001/jama.2013.129

Corps, A. N., Harrall, R. L., Curry, V. A., Fenwick, S. A., Hazleman, B. L., & Riley, G. P. (2002, Nov). Ciprofloxacin enhances the stimulation of matrix metalloproteinase 3 expression by interleukin-1beta in human tendon-derived cells. A potential mechanism of fluoroquinolone-induced tendinopathy. *Arthritis Rheum, 46*(11), 3034-3040. https://doi.org/10.1002/art.10617

Cotler, H. B., Chow, R. T., Hamblin, M. R., & Carroll, J. (2015). The Use of Low Level Laser Therapy (LLLT) For Musculoskeletal Pain. *MOJ Orthop Rheumatol, 2*(5). https://doi.org/10.15406/mojor.2015.02.00068

Courneya, J. P., Luzina, I. G., Zeller, C. B., Rasmussen, J. F., Bocharov, A., Schon, L. C., & Atamas, S. P. (2010, Jun 10). Interleukins 4 and 13 modulate gene expression and promote proliferation of primary human tenocytes. *Fibrogenesis Tissue Repair, 3*, 9. https://doi.org/10.1186/1755-1536-3-9

D'Addona, A., Maffulli, N., Formisano, S., & Rosa, D. (2017, Oct). Inflammation in tendinopathy. *Surgeon, 15*(5), 297-302. https://doi.org/10.1016/j.surge.2017.04.004

Daniels, M. J., Rivers-Auty, J., Schilling, T., Spencer, N. G., Watremez, W., Fasolino, V., Booth, S. J., White, C. S., Baldwin, A. G., Freeman, S., Wong, R., Latta, C., Yu, S., Jackson, J., Fischer, N., Koziel, V., Pillot, T., Bagnall, J., Allan, S. M., Paszek, P., Galea, J., Harte, M. K., Eder, C., Lawrence, C. B., & Brough, D. (2016, Aug 11). Fenamate NSAIDs inhibit the NLRP3 inflammasome and protect against Alzheimer's disease in rodent models. *Nat Commun, 7*, 12504. https://doi.org/10.1038/ncomms12504

De-la-Cruz-Torres, B., Barrera-Garcia-Martin, I., Valera-Garrido, F., Minaya-Munoz, F., & Romero-Morales, C. (2020). Ultrasound-Guided Percutaneous Needle Electrolysis in Dancers with Chronic Soleus Injury: A Randomized Clinical Trial. *Evid Based Complement Alternat Med, 2020*, 4156258. https://doi.org/10.1155/2020/4156258

de Koning, H. D., van Gijn, M. E., Stoffels, M., Jongekrijg, J., Zeeuwen, P. L., Elferink, M. G., Nijman, I. J., Jansen, P. A., Neveling, K., van der Meer, J. W., Schalkwijk, J., & Simon, A. (2015, Feb). Myeloid lineage-restricted somatic mosaicism of NLRP3 mutations in patients with variant Schnitzler syndrome. *J Allergy Clin Immunol, 135*(2), 561-564. https://doi.org/10.1016/j.jaci.2014.07.050

de la Durantaye, M., Piette, A. B., van Rooijen, N., & Frenette, J. (2014, Feb). Macrophage depletion reduces cell proliferation and extracellular matrix accumulation but increases the ultimate tensile strength of injured Achilles tendons. *J Orthop Res, 32*(2), 279-285. https://doi.org/10.1002/jor.22504

de Preux Charles, A. S., Bise, T., Baier, F., Marro, J., & Jazwinska, A. (2016, Jul). Distinct effects of inflammation on preconditioning and regeneration of the adult zebrafish heart. *Open Biol, 6*(7). https://doi.org/10.1098/rsob.160102

De Schutter, E., Roelandt, R., Riquet, F. B., Van Camp, G., Wullaert, A., & Vandenabeele, P. (2021, Jun). Punching Holes in Cellular Membranes: Biology and Evolution of Gasdermins. *Trends Cell Biol, 31*(6), 500-513. https://doi.org/10.1016/j.tcb.2021.03.004

de Torre-Minguela, C., Barbera-Cremades, M., Gomez, A. I., Martin-Sanchez, F., & Pelegrin, P. (2016, Mar 3). Macrophage activation and polarization modify P2X7 receptor secretome influencing the inflammatory process. *Sci Rep, 6*, 22586. https://doi.org/10.1038/srep22586

de Vos, R. J., Windt, J., & Weir, A. (2014, Jun). Strong evidence against platelet-rich plasma injections for chronic lateral epicondylar tendinopathy: a systematic review. *Br J Sports Med, 48*(12), 952-956. https://doi.org/10.1136/bjsports-2013-093281

Dean, B. J., Lostis, E., Oakley, T., Rombach, I., Morrey, M. E., & Carr, A. J. (2014, Feb). The risks and benefits of glucocorticoid treatment for tendinopathy: a systematic review of the effects of local glucocorticoid on tendon. *Semin Arthritis Rheum, 43*(4), 570-576. https://doi.org/10.1016/j.semarthrit.2013.08.006

DeForge, L. E., & Remick, D. G. (1991, Jan 15). Kinetics of TNF, IL-6, and IL-8 gene expression in LPS-stimulated human whole blood. *Biochem Biophys Res Commun, 174*(1), 18-24. https://doi.org/10.1016/0006-291x(91)90478-p

Dejaco, B., Habets, B., van Loon, C., van Grinsven, S., & van Cingel, R. (2017, Jul). Eccentric versus conventional exercise therapy in patients with rotator cuff tendinopathy: a randomized, single blinded, clinical trial. *Knee Surg Sports Traumatol Arthrosc, 25*(7), 2051-2059. https://doi.org/10.1007/s00167-016-4223-x

Deng, W., Bai, Y., Deng, F., Pan, Y., Mei, S., Zheng, Z., Min, R., Wu, Z., Li, W., Miao, R., Zhang, Z., Kupper, T. S., Lieberman, J., & Liu, X. (2022, Feb). Streptococcal pyrogenic exotoxin B cleaves GSDMA and triggers pyroptosis. *Nature, 602*(7897), 496-502. https://doi.org/10.1038/s41586-021-04384-4

Di Paolo, N. C., & Shayakhmetov, D. M. (2016, Jul 19). Interleukin 1alpha and the inflammatory process. *Nat Immunol, 17*(8), 906-913. https://doi.org/10.1038/ni.3503

Dick, M. S., Sborgi, L., Ruhl, S., Hiller, S., & Broz, P. (2016, Jun 22). ASC filament formation serves as a signal amplification mechanism for inflammasomes. *Nat Commun, 7*, 11929. https://doi.org/10.1038/ncomms11929

Diebolder, C. A., Halff, E. F., Koster, A. J., Huizinga, E. G., & Koning, R. I. (2015, Dec 1). Cryoelectron Tomography of the NAIP5/NLRC4 Inflammasome: Implications for NLR Activation. *Structure, 23*(12), 2349-2357. https://doi.org/10.1016/j.str.2015.10.001

Dinarello, C. A. (2009). Immunological and inflammatory functions of the interleukin-1 family. *Annu Rev Immunol, 27*, 519-550. https://doi.org/10.1146/annurev.immunol.021908.132612

Dinarello, C. A. (2018, Jan). Overview of the IL-1 family in innate inflammation and acquired immunity. *Immunol Rev, 281*(1), 8-27. https://doi.org/10.1111/imr.12621

Dinarello, C. A., Ikejima, T., Warner, S. J., Orencole, S. F., Lonnemann, G., Cannon, J. G., & Libby, P. (1987, Sep 15). Interleukin 1 induces interleukin 1. I. Induction of circulating interleukin 1 in rabbits in vivo and in human mononuclear cells in vitro. *J Immunol, 139*(6), 1902-1910. https://www.ncbi.nlm.nih.gov/pubmed/3497982

Dinarello, C. A., Nold-Petry, C., Nold, M., Fujita, M., Li, S., Kim, S., & Bufler, P. (2016, May). Suppression of innate inflammation and immunity by interleukin-37. *Eur J Immunol, 46*(5), 1067-1081. https://doi.org/10.1002/eji.201545828

Dinarello, C. A., & van der Meer, J. W. (2013, Dec 15). Treating inflammation by blocking interleukin-1 in humans. *Semin Immunol, 25*(6), 469-484. https://doi.org/10.1016/j.smim.2013.10.008

Ding, J., Wang, K., Liu, W., She, Y., Sun, Q., Shi, J., Sun, H., Wang, D. C., & Shao, F. (2016, Jul 7). Pore-forming activity and structural autoinhibition of the gasdermin family. *Nature, 535*(7610), 111-116. https://doi.org/10.1038/nature18590

Ditsios, K., Boyer, M. I., Kusano, N., Gelberman, R. H., & Silva, M. J. (2003, Nov). Bone loss following tendon laceration, repair and passive mobilization. *J Orthop Res, 21*(6), 990-996. https://doi.org/10.1016/S0736-0266(03)00112-8

Diya, Z., Lili, C., Shenglai, L., Zhiyuan, G., & Jie, Y. (2008, Apr). Lipopolysaccharide (LPS) of Porphyromonas gingivalis induces IL-1beta, TNF-alpha and IL-6 production by THP-1 cells in a way different from that of Escherichia coli LPS. *Innate Immun, 14*(2), 99-107. https://doi.org/10.1177/1753425907088244

Docheva, D., Muller, S. A., Majewski, M., & Evans, C. H. (2015, Apr). Biologics for tendon repair. *Adv Drug Deliv Rev, 84*, 222-239. https://doi.org/10.1016/j.addr.2014.11.015

Dode, C., Le Du, N., Cuisset, L., Letourneur, F., Berthelot, J. M., Vaudour, G., Meyrier, A., Watts, R. A., Scott, D. G., Nicholls, A., Granel, B., Frances, C., Garcier, F., Edery, P., Boulinguez, S., Domergues, J. P., Delpech, M., & Grateau, G. (2002, Jun). New mutations of CIAS1 that are responsible for Muckle-Wells syndrome and familial cold urticaria: a novel mutation underlies both syndromes. *Am J Hum Genet, 70*(6), 1498-1506. https://doi.org/10.1086/340786

Dong, H. C., Li, P. N., Chen, C. J., Xu, X., Zhang, H., Liu, G., Zheng, L. J., & Li, P. (2019, Aug). Sinomenine Attenuates Cartilage Degeneration by Regulating miR-223-3p/NLRP3 Inflammasome Signaling. *Inflammation, 42*(4), 1265-1275. https://doi.org/10.1007/s10753-019-00986-3

Duncan, C. J. A., Thompson, B. J., Chen, R., Rice, G. I., Gothe, F., Young, D. F., Lovell, S. C., Shuttleworth, V. G., Brocklebank, V., Corner, B., Skelton, A. J., Bondet, V., Coxhead, J., Duffy, D., Fourrage, C., Livingston, J. H., Pavaine, J., Cheesman, E., Bitetti, S., Grainger, A., Acres, M., Innes, B. A., Mikulasova, A., Sun, R., Hussain, R., Wright, R., Wynn, R., Zarhrate, M., Zeef, L. A. H., Wood, K., Hughes, S. M., Harris, C. L., Engelhardt, K. R., Crow, Y. J., Randall, R. E., Kavanagh, D., Hambleton, S., & Briggs, T. A. (2019, Dec 13). Severe type I interferonopathy and unrestrained interferon signaling due to a homozygous germline mutation in STAT2. *Sci Immunol, 4*(42). https://doi.org/10.1126/sciimmunol.aav7501

Duncan, J. A., & Canna, S. W. (2018, Jan). The NLRC4 Inflammasome. *Immunol Rev, 281*(1), 115-123. https://doi.org/10.1111/imr.12607

Eliasson, P., Andersson, T., & Aspenberg, P. (2009, Aug). Rat Achilles tendon healing: mechanical loading and gene expression. *J Appl Physiol (1985), 107*(2), 399-407. https://doi.org/10.1152/japplphysiol.91563.2008

Ellett, F., Elks, P. M., Robertson, A. L., Ogryzko, N. V., & Renshaw, S. A. (2015, Dec). Defining the phenotype of neutrophils following reverse migration in zebrafish. *J Leukoc Biol, 98*(6), 975-981. https://doi.org/10.1189/jlb.3MA0315-105R

Ellwanger, K., Becker, E., Kienes, I., Sowa, A., Postma, Y., Cardona Gloria, Y., Weber, A. N. R., & Kufer, T. A. (2018, Feb 23). The NLR family pyrin domain-containing 11 protein contributes to the regulation of inflammatory signaling. *J Biol Chem, 293*(8), 2701-2710. https://doi.org/10.1074/jbc.RA117.000152

Emery, P., Rondon, J., Parrino, J., Lin, Y., Pena-Rossi, C., van Hoogstraten, H., Graham, N. M. H., Liu, N., Paccaly, A., Wu, R., & Spindler, A. (2019, May 1). Safety and tolerability of subcutaneous sarilumab and intravenous tocilizumab in patients with rheumatoid arthritis. *Rheumatology (Oxford), 58*(5), 849-858. https://doi.org/10.1093/rheumatology/key361

Eming, S. A., Martin, P., & Tomic-Canic, M. (2014, Dec 3). Wound repair and regeneration: mechanisms, signaling, and translation. *Sci Transl Med, 6*(265), 265sr266. https://doi.org/10.1126/scitranslmed.3009337

Eming, S. A., Wynn, T. A., & Martin, P. (2017, Jun 9). Inflammation and metabolism in tissue repair and regeneration. *Science, 356*(6342), 1026-1030. https://doi.org/10.1126/science.aam7928

Epelman, S., Lavine, K. J., & Randolph, G. J. (2014, Jul 17). Origin and functions of tissue macrophages. *Immunity, 41*(1), 21-35. https://doi.org/10.1016/j.immuni.2014.06.013

Evans, C. H. (1999, Aug). Cytokines and the role they play in the healing of ligaments and tendons. *Sports Med, 28*(2), 71-76. https://doi.org/10.2165/00007256-199928020-00001

Evavold, C. L., Ruan, J., Tan, Y., Xia, S., Wu, H., & Kagan, J. C. (2018, Jan 16). The Pore-Forming Protein Gasdermin D Regulates Interleukin-1 Secretion from Living Macrophages. *Immunity, 48*(1), 35-44 e36. https://doi.org/10.1016/j.immuni.2017.11.013

Everhart, J. S., Cole, D., Sojka, J. H., Higgins, J. D., Magnussen, R. A., Schmitt, L. C., & Flanigan, D. C. (2017, Apr). Treatment Options for Patellar Tendinopathy: A Systematic Review. *Arthroscopy, 33*(4), 861-872. https://doi.org/10.1016/j.arthro.2016.11.007

Fadok, V. A., Bratton, D. L., Konowal, A., Freed, P. W., Westcott, J. Y., & Henson, P. M. (1998, Feb 15). Macrophages that have ingested apoptotic cells in vitro inhibit proinflammatory cytokine production through autocrine/paracrine mechanisms involving TGF-beta, PGE2, and PAF. *J Clin Invest, 101*(4), 890-898. https://doi.org/10.1172/JCI1112

Farahi, N., Singh, N. R., Heard, S., Loutsios, C., Summers, C., Solanki, C. K., Solanki, K., Balan, K. K., Ruparelia, P., Peters, A. M., Condliffe, A. M., & Chilvers, E. R. (2012, Nov 8). Use of 111-Indium-labeled autologous eosinophils to establish the in vivo kinetics of human eosinophils in healthy subjects. *Blood, 120*(19), 4068-4071. https://doi.org/10.1182/blood-2012-07-443424

Faustin, B., Chen, Y., Zhai, D., Le Negrate, G., Lartigue, L., Satterthwait, A., & Reed, J. C. (2009, Mar 10). Mechanism of Bcl-2 and Bcl-X(L) inhibition of NLRP1 inflammasome: loop domain-dependent suppression of ATP binding and oligomerization. *Proc Natl Acad Sci U S A, 106*(10), 3935-3940. https://doi.org/10.1073/pnas.0809414106

Fedorczyk, J. M., Barr, A. E., Rani, S., Gao, H. G., Amin, M., Amin, S., Litvin, J., & Barbe, M. F. (2010, Mar). Exposure-dependent increases in IL-1beta, substance P, CTGF, and tendinosis in flexor digitorum tendons with upper extremity repetitive strain injury. *J Orthop Res, 28*(3), 298-307. https://doi.org/10.1002/jor.20984

Fenwick, S. A., Hazleman, B. L., & Riley, G. P. (2002). The vasculature and its role in the damaged and healing tendon. *Arthritis Res, 4*(4), 252-260. https://doi.org/10.1186/ar416

Fine, S., & Hansen, W. P. (1971, Oct 1). Optical second harmonic generation in biological systems. *Appl Opt, 10*(10), 2350-2353. https://doi.org/10.1364/AO.10.002350

Finger, J. N., Lich, J. D., Dare, L. C., Cook, M. N., Brown, K. K., Duraiswami, C., Bertin, J., & Gough, P. J. (2012, Jul 20). Autolytic proteolysis within the function to find domain (FIIND) is required for NLRP1 inflammasome activity. *J Biol Chem, 287*(30), 25030-25037. https://doi.org/10.1074/jbc.M112.378323

Fisher, B. A., Veenith, T., Slade, D., Gaskell, C., Rowland, M., Whitehouse, T., Scriven, J., Parekh, D., Balasubramaniam, M. S., Cooke, G., Morley, N., Gabriel, Z., Wise, M. P., Porter, J., McShane, H., Ho, L. P., Newsome, P. N., Rowe, A., Sharpe, R., Thickett, D. R., Bion, J., Gates, S., Richards, D., Kearns, P., & investigators, C. (2022, Mar). Namilumab or infliximab compared with standard of care in hospitalised patients with COVID-19 (CATALYST): a randomised, multicentre, multi-arm, multistage, open-label, adaptive, phase 2, proof-of-concept trial. *Lancet Respir Med, 10*(3), 255-266. https://doi.org/10.1016/S2213-2600(21)00460-4

Fragoso, J. M., Vargas Alarcon, G., Jimenez Morales, S., Reyes Hernandez, O. D., & Ramirez Bello, J. (2014, Jul-Aug). [Tumor necrosis factor alpha (TNF-alpha) in autoimmune diseases (AIDs): molecular biology and genetics]. *Gac Med Mex, 150*(4), 334-344. https://www.ncbi.nlm.nih.gov/pubmed/25098219 (El factor de necrosis tumoral alpha (TNF-alpha) en las enfermedades autoinmunes (EA): biologia molecular y genetica.)

Franchi, L., Eigenbrod, T., & Nunez, G. (2009, Jul 15). Cutting edge: TNF-alpha mediates sensitization to ATP and silica via the NLRP3 inflammasome in the absence of microbial stimulation. *J Immunol, 183*(2), 792-796. https://doi.org/10.4049/jimmunol.0900173

Franchi, L., Stoolman, J., Kanneganti, T. D., Verma, A., Ramphal, R., & Nunez, G. (2007, Nov). Critical role for Ipaf in Pseudomonas aeruginosa-induced caspase-1 activation. *Eur J Immunol, 37*(11), 3030-3039. https://doi.org/10.1002/eji.200737532

Franchini, M., Cruciani, M., Mengoli, C., Marano, G., Pupella, S., Veropalumbo, E., Masiello, F., Pati, I., Vaglio, S., & Liumbruno, G. M. (2018, Nov). Efficacy of platelet-rich plasma as conservative treatment in orthopaedics: a systematic review and meta-analysis. *Blood Transfus, 16*(6), 502-513. https://doi.org/10.2450/2018.0111-18

Frank, M. G., Barrientos, R. M., Thompson, B. M., Weber, M. D., Watkins, L. R., & Maier, S. F. (2012, Nov 15). IL-1RA injected intra-cisterna magna confers extended prophylaxis against lipopolysaccharide-induced neuroinflammatory and sickness responses. *J Neuroimmunol, 252*(1-2), 33-39. https://doi.org/10.1016/j.jneuroim.2012.07.010

Gabay, C., Fautrel, B., Rech, J., Spertini, F., Feist, E., Kotter, I., Hachulla, E., Morel, J., Schaeverbeke, T., Hamidou, M. A., Martin, T., Hellmich, B., Lamprecht, P., Schulze-Koops, H., Courvoisier, D. S., Sleight, A., & Schiffrin, E. J. (2018, Jun). Open-label, multicentre, dose-escalating phase II clinical trial on the safety and efficacy of tadekinig alfa (IL-18BP) in adult-onset Still's disease. *Ann Rheum Dis, 77*(6), 840-847. https://doi.org/10.1136/annrheumdis-2017-212608

Gabay, C., Lamacchia, C., & Palmer, G. (2010, Apr). IL-1 pathways in inflammation and human diseases. *Nat Rev Rheumatol, 6*(4), 232-241. https://doi.org/10.1038/nrrheum.2010.4

Gan, W., Ren, J., Li, T., Lv, S., Li, C., Liu, Z., & Yang, M. (2018, Jan). The SGK1 inhibitor EMD638683, prevents Angiotensin II-induced cardiac inflammation and fibrosis by blocking NLRP3 inflammasome activation. *Biochim Biophys Acta Mol Basis Dis, 1864*(1), 1-10. https://doi.org/10.1016/j.bbadis.2017.10.001

Ganesan, S., & Hoglund, P. (2021, Oct). MHC class I molecules co-stimulate NK1.1 signaling and enhance Ca(2+) flux in murine NK cells. *Eur J Immunol, 51*(10), 2531-2534. https://doi.org/10.1002/eji.202048709

Garcia-Vidal, J. A., Pelegrin, P., Escolar-Reina, P., & Medina-Mirapeix, F. (2019). Inflammatory response of two invasive techniques in the mouse with collagenase induced tendinopathy. *Revista Fisioterapia Invasiva / Journal of Invasive Techniques in Physical Therapy, 02*(02), 080.

García-Villalba, J., Hurtado-Navarro, L., Penin-Franch, A., Molina-Lopez, C., Martínez-Alarcón, L., Angosto-Bazarra, D., Baroja-Mazo, A., & Pelegrin, P. (2022). Soluble P2X7 receptor is elevated in the plasma of COVID-19 patients and correlates with disease severity [Research Article]. *Front Immunol*.

Garlanda, C., Dinarello, C. A., & Mantovani, A. (2013, Dec 12). The interleukin-1 family: back to the future. *Immunity, 39*(6), 1003-1018. https://doi.org/10.1016/j.immuni.2013.11.010

Garlanda, C., Riva, F., Bonavita, E., & Mantovani, A. (2013, Dec 15). Negative regulatory receptors of the IL-1 family. *Semin Immunol, 25*(6), 408-415. https://doi.org/10.1016/j.smim.2013.10.019

Gaul, S., Leszczynska, A., Alegre, F., Kaufmann, B., Johnson, C. D., Adams, L. A., Wree, A., Damm, G., Seehofer, D., Calvente, C. J., Povero, D., Kisseleva, T., Eguchi, A., McGeough, M. D., Hoffman, H. M., Pelegrin, P., Laufs, U., & Feldstein, A. E. (2021, Jan). Hepatocyte pyroptosis and release of inflammasome particles induce stellate cell activation and liver fibrosis. *J Hepatol, 74*(1), 156-167. https://doi.org/10.1016/j.jhep.2020.07.041

Geering, B., Stoeckle, C., Conus, S., & Simon, H. U. (2013, Aug). Living and dying for inflammation: neutrophils, eosinophils, basophils. *Trends Immunol, 34*(8), 398-409. https://doi.org/10.1016/j.it.2013.04.002

Geijtenbeek, T. B., & Gringhuis, S. I. (2009, Jul). Signalling through C-type lectin receptors: shaping immune responses. *Nat Rev Immunol, 9*(7), 465-479. https://doi.org/10.1038/nri2569

Gelberman, R. H., Khabie, V., & Cahill, C. J. (1991, Jul). The revascularization of healing flexor tendons in the digital sheath. A vascular injection study in dogs. *J Bone Joint Surg Am, 73*(6), 868-881. https://www.ncbi.nlm.nih.gov/pubmed/1712787

Gelberman, R. H., Vandeberg, J. S., Manske, P. R., & Akeson, W. H. (1985, Nov). The early stages of flexor tendon healing: a morphologic study of the first fourteen days. *J Hand Surg Am, 10*(6 Pt 1), 776-784. https://doi.org/10.1016/s0363-5023(85)80151-9

Gimbel, J. A., Van Kleunen, J. P., Mehta, S., Perry, S. M., Williams, G. R., & Soslowsky, L. J. (2004, May). Supraspinatus tendon organizational and mechanical properties in a chronic rotator cuff tear animal model. *J Biomech, 37*(5), 739-749. https://doi.org/10.1016/j.jbiomech.2003.09.019

Girard, C., Rech, J., Brown, M., Allali, D., Roux-Lombard, P., Spertini, F., Schiffrin, E. J., Schett, G., Manger, B., Bas, S., Del Val, G., & Gabay, C. (2016, Dec). Elevated serum levels of free

interleukin-18 in adult-onset Still's disease. *Rheumatology (Oxford), 55*(12), 2237-2247. https://doi.org/10.1093/rheumatology/kew300

Glass, Z. A., Schiele, N. R., & Kuo, C. K. (2014, Jun 27). Informing tendon tissue engineering with embryonic development. *J Biomech, 47*(9), 1964-1968. https://doi.org/10.1016/j.jbiomech.2013.12.039

Gleizes, P. E., Munger, J. S., Nunes, I., Harpel, J. G., Mazzieri, R., Noguera, I., & Rifkin, D. B. (1997). TGF-beta latency: biological significance and mechanisms of activation. *Stem Cells, 15*(3), 190-197. https://doi.org/10.1002/stem.150190

Goldbach-Mansky, R., Dailey, N. J., Canna, S. W., Gelabert, A., Jones, J., Rubin, B. I., Kim, H. J., Brewer, C., Zalewski, C., Wiggs, E., Hill, S., Turner, M. L., Karp, B. I., Aksentijevich, I., Pucino, F., Penzak, S. R., Haverkamp, M. H., Stein, L., Adams, B. S., Moore, T. L., Fuhlbrigge, R. C., Shaham, B., Jarvis, J. N., O'Neil, K., Vehe, R. K., Beitz, L. O., Gardner, G., Hannan, W. P., Warren, R. W., Horn, W., Cole, J. L., Paul, S. M., Hawkins, P. N., Pham, T. H., Snyder, C., Wesley, R. A., Hoffmann, S. C., Holland, S. M., Butman, J. A., & Kastner, D. L. (2006, Aug 10). Neonatal-onset multisystem inflammatory disease responsive to interleukin-1beta inhibition. *N Engl J Med, 355*(6), 581-592. https://doi.org/10.1056/NEJMoa055137

Gomes, C., Dibai-Filho, A. V., Pallotta, R. C., da Silva, E. A. P., Marques, A. C. F., Marcos, R. L., & de Carvalho, P. T. C. (2017, Nov). Effects of low-level laser therapy on the modulation of tissue temperature and hyperalgesia following a partial Achilles tendon injury in rats. *J Cosmet Laser Ther, 19*(7), 391-396. https://doi.org/10.1080/14764172.2017.1334921

Gomi, K., Kawasaki, K., Kawai, Y., Shiozaki, M., & Nishijima, M. (2002, Mar 15). Toll-like receptor 4-MD-2 complex mediates the signal transduction induced by flavolipin, an amino acid-containing lipid unique to Flavobacterium meningosepticum. *J Immunol, 168*(6), 2939-2943. https://doi.org/10.4049/jimmunol.168.6.2939

Gonzalez, M. I., Vannan, D., Eksteen, B., & Reyes, J. L. (2020, Aug 28). NLRP3 receptor contributes to protection against experimental antigen-mediated cholangitis. *Biosci Rep, 40*(8). https://doi.org/10.1042/BSR20200689

Gora, I. M., Ciechanowska, A., & Ladyzynski, P. (2021, Feb 3). NLRP3 Inflammasome at the Interface of Inflammation, Endothelial Dysfunction, and Type 2 Diabetes. *Cells, 10*(2). https://doi.org/10.3390/cells10020314

Gordon, S. (2002, Dec 27). Pattern recognition receptors: doubling up for the innate immune response. *Cell, 111*(7), 927-930. https://doi.org/10.1016/s0092-8674(02)01201-1

Gow, N. A., van de Veerdonk, F. L., Brown, A. J., & Netea, M. G. (2011, Dec 12). Candida albicans morphogenesis and host defence: discriminating invasion from colonization. *Nat Rev Microbiol, 10*(2), 112-122. https://doi.org/10.1038/nrmicro2711

Gross, C. E., Hsu, A. R., Chahal, J., & Holmes, G. B., Jr. (2013, May). Injectable treatments for noninsertional achilles tendinosis: a systematic review. *Foot Ankle Int, 34*(5), 619-628. https://doi.org/10.1177/1071100713475353

Group, R. C. (2021, May 1). Tocilizumab in patients admitted to hospital with COVID-19 (RECOVERY): a randomised, controlled, open-label, platform trial. *Lancet, 397*(10285), 1637-1645. https://doi.org/10.1016/S0140-6736(21)00676-0

Gundra, U. M., Girgis, N. M., Ruckerl, D., Jenkins, S., Ward, L. N., Kurtz, Z. D., Wiens, K. E., Tang, M. S., Basu-Roy, U., Mansukhani, A., Allen, J. E., & Loke, P. (2014, May 15). Alternatively activated macrophages derived from monocytes and tissue macrophages are phenotypically

and functionally distinct. *Blood, 123*(20), e110-122. https://doi.org/10.1182/blood-2013-08-520619

Guo, C., Fu, R., Wang, S., Huang, Y., Li, X., Zhou, M., Zhao, J., & Yang, N. (2018, Nov). NLRP3 inflammasome activation contributes to the pathogenesis of rheumatoid arthritis. *Clin Exp Immunol, 194*(2), 231-243. https://doi.org/10.1111/cei.13167

Gupta, A. K., Giaglis, S., Hasler, P., & Hahn, S. (2014). Efficient neutrophil extracellular trap induction requires mobilization of both intracellular and extracellular calcium pools and is modulated by cyclosporine A. *PLoS One, 9*(5), e97088. https://doi.org/10.1371/journal.pone.0097088

Hafner-Bratkovic, I., & Pelegrin, P. (2018, Jun). Ion homeostasis and ion channels in NLRP3 inflammasome activation and regulation. *Curr Opin Immunol, 52*, 8-17. https://doi.org/10.1016/j.coi.2018.03.010

Hara, H., Seregin, S. S., Yang, D., Fukase, K., Chamaillard, M., Alnemri, E. S., Inohara, N., Chen, G. Y., & Nunez, G. (2018, Nov 29). The NLRP6 Inflammasome Recognizes Lipoteichoic Acid and Regulates Gram-Positive Pathogen Infection. *Cell, 175*(6), 1651-1664 e1614. https://doi.org/10.1016/j.cell.2018.09.047

Harris, J., Hartman, M., Roche, C., Zeng, S. G., O'Shea, A., Sharp, F. A., Lambe, E. M., Creagh, E. M., Golenbock, D. T., Tschopp, J., Kornfeld, H., Fitzgerald, K. A., & Lavelle, E. C. (2011, Mar 18). Autophagy controls IL-1beta secretion by targeting pro-IL-1beta for degradation. *J Biol Chem, 286*(11), 9587-9597. https://doi.org/10.1074/jbc.M110.202911

Haslerud, S., Magnussen, L. H., Joensen, J., Lopes-Martins, R. A., & Bjordal, J. M. (2015, Jun). The efficacy of low-level laser therapy for shoulder tendinopathy: a systematic review and meta-analysis of randomized controlled trials. *Physiother Res Int, 20*(2), 108-125. https://doi.org/10.1002/pri.1606

Hawkins, P. N., Lachmann, H. J., & McDermott, M. F. (2003, Jun 19). Interleukin-1-receptor antagonist in the Muckle-Wells syndrome. *N Engl J Med, 348*(25), 2583-2584. https://doi.org/10.1056/NEJM200306193482523

Hay, E. M., Paterson, S. M., Lewis, M., Hosie, G., & Croft, P. (1999, Oct 9). Pragmatic randomised controlled trial of local corticosteroid injection and naproxen for treatment of lateral epicondylitis of elbow in primary care. *BMJ, 319*(7215), 964-968. https://doi.org/10.1136/bmj.319.7215.964

Hays, P. L., Kawamura, S., Deng, X. H., Dagher, E., Mithoefer, K., Ying, L., & Rodeo, S. A. (2008, Mar). The role of macrophages in early healing of a tendon graft in a bone tunnel. *J Bone Joint Surg Am, 90*(3), 565-579. https://doi.org/10.2106/JBJS.F.00531

He, W. T., Wan, H., Hu, L., Chen, P., Wang, X., Huang, Z., Yang, Z. H., Zhong, C. Q., & Han, J. (2015, Dec). Gasdermin D is an executor of pyroptosis and required for interleukin-1beta secretion. *Cell Res, 25*(12), 1285-1298. https://doi.org/10.1038/cr.2015.139

He, Y., Hara, H., & Nunez, G. (2016, Dec). Mechanism and Regulation of NLRP3 Inflammasome Activation. *Trends Biochem Sci, 41*(12), 1012-1021. https://doi.org/10.1016/j.tibs.2016.09.002

He, Y., Varadarajan, S., Munoz-Planillo, R., Burberry, A., Nakamura, Y., & Nunez, G. (2014, Jan 10). 3,4-methylenedioxy-beta-nitrostyrene inhibits NLRP3 inflammasome activation by blocking assembly of the inflammasome. *J Biol Chem, 289*(2), 1142-1150. https://doi.org/10.1074/jbc.M113.515080

He, Y., Zeng, M. Y., Yang, D., Motro, B., & Nunez, G. (2016, Feb 18). NEK7 is an essential mediator of NLRP3 activation downstream of potassium efflux. *Nature, 530*(7590), 354-357. https://doi.org/10.1038/nature16959

Heinrich, P. C., Castell, J. V., & Andus, T. (1990, Feb 1). Interleukin-6 and the acute phase response. *Biochem J, 265*(3), 621-636. https://doi.org/10.1042/bj2650621

Henry, C. M., Sullivan, G. P., Clancy, D. M., Afonina, I. S., Kulms, D., & Martin, S. J. (2016, Feb 2). Neutrophil-Derived Proteases Escalate Inflammation through Activation of IL-36 Family Cytokines. *Cell Rep, 14*(4), 708-722. https://doi.org/10.1016/j.celrep.2015.12.072

Hijdra, D., Vorselaars, A. D., Grutters, J. C., Claessen, A. M., & Rijkers, G. T. (2013). Phenotypic characterization of human intermediate monocytes. *Front Immunol, 4*, 339. https://doi.org/10.3389/fimmu.2013.00339

Hirano, S., Zhou, Q., Furuyama, A., & Kanno, S. (2017, Dec). Differential Regulation of IL-1beta and IL-6 Release in Murine Macrophages. *Inflammation, 40*(6), 1933-1943. https://doi.org/10.1007/s10753-017-0634-1

Hirono, I., Nam, B. H., Kurobe, T., & Aoki, T. (2000, Oct 15). Molecular cloning, characterization, and expression of TNF cDNA and gene from Japanese flounder Paralychthys olivaceus. *J Immunol, 165*(8), 4423-4427. https://doi.org/10.4049/jimmunol.165.8.4423

Hiscott, J., Marois, J., Garoufalis, J., D'Addario, M., Roulston, A., Kwan, I., Pepin, N., Lacoste, J., Nguyen, H., Bensi, G., & et al. (1993, Oct). Characterization of a functional NF-kappa B site in the human interleukin 1 beta promoter: evidence for a positive autoregulatory loop. *Mol Cell Biol, 13*(10), 6231-6240. https://doi.org/10.1128/mcb.13.10.6231-6240.1993

Hoffman, H. M., Mueller, J. L., Broide, D. H., Wanderer, A. A., & Kolodner, R. D. (2001, Nov). Mutation of a new gene encoding a putative pyrin-like protein causes familial cold autoinflammatory syndrome and Muckle-Wells syndrome. *Nat Genet, 29*(3), 301-305. https://doi.org/10.1038/ng756

Hoffman, H. M., Rosengren, S., Boyle, D. L., Cho, J. Y., Nayar, J., Mueller, J. L., Anderson, J. P., Wanderer, A. A., & Firestein, G. S. (2004, Nov 13-19). Prevention of cold-associated acute inflammation in familial cold autoinflammatory syndrome by interleukin-1 receptor antagonist. *Lancet, 364*(9447), 1779-1785. https://doi.org/10.1016/S0140-6736(04)17401-1

Hoffmann, A., Levchenko, A., Scott, M. L., & Baltimore, D. (2002, Nov 8). The IkappaB-NF-kappaB signaling module: temporal control and selective gene activation. *Science, 298*(5596), 1241-1245. https://doi.org/10.1126/science.1071914

Hoksrud, A., Ohberg, L., Alfredson, H., & Bahr, R. (2006, Nov). Ultrasound-guided sclerosis of neovessels in painful chronic patellar tendinopathy: a randomized controlled trial. *Am J Sports Med, 34*(11), 1738-1746. https://doi.org/10.1177/0363546506289168

Holden, S., Lyng, K., Graven-Nielsen, T., Riel, H., Olesen, J. L., Larsen, L. H., & Rathleff, M. S. (2020, Mar). Isometric exercise and pain in patellar tendinopathy: A randomized crossover trial. *J Sci Med Sport, 23*(3), 208-214. https://doi.org/10.1016/j.jsams.2019.09.015

Hollingsworth, L. R., Sharif, H., Griswold, A. R., Fontana, P., Mintseris, J., Dagbay, K. B., Paulo, J. A., Gygi, S. P., Bachovchin, D. A., & Wu, H. (2021, Apr). DPP9 sequesters the C terminus of NLRP1 to repress inflammasome activation. *Nature, 592*(7856), 778-783. https://doi.org/10.1038/s41586-021-03350-4

Hornung, V., Bauernfeind, F., Halle, A., Samstad, E. O., Kono, H., Rock, K. L., Fitzgerald, K. A., & Latz, E. (2008, Aug). Silica crystals and aluminum salts activate the NALP3 inflammasome

through phagosomal destabilization. *Nat Immunol, 9*(8), 847-856. https://doi.org/10.1038/ni.1631

Hosaka, Y., Kirisawa, R., Ueda, H., Yamaguchi, M., & Takehana, K. (2005, Oct). Differences in tumor necrosis factor (TNF)alpha and TNF receptor-1-mediated intracellular signaling factors in normal, inflamed and scar-formed horse tendons. *J Vet Med Sci, 67*(10), 985-991. https://doi.org/10.1292/jvms.67.985

Hosaka, Y., Kirisawa, R., Yamamoto, E., Ueda, H., Iwai, H., & Takehana, K. (2002, Oct). Localization of cytokines in tendinocytes of the superficial digital flexor tendon in the horse. *J Vet Med Sci, 64*(10), 945-947. https://doi.org/10.1292/jvms.64.945

Hosaka, Y., Ozoe, S., Kirisawa, R., Ueda, H., Takehana, K., & Yamaguchi, M. (2006, Oct). Effect of heat on synthesis of gelatinases and pro-inflammatory cytokines in equine tendinocytes. *Biomed Res, 27*(5), 233-241. https://doi.org/10.2220/biomedres.27.233

Hosaka, Y., Sakamoto, Y., Kirisawa, R., Watanabe, T., Ueda, H., Takehana, K., & Yamaguchi, M. (2004, Nov). Distribution of TNF receptors and TNF receptor-associated intracellular signaling factors on equine tendinocytes in vitro. *Jpn J Vet Res, 52*(3), 135-144. https://www.ncbi.nlm.nih.gov/pubmed/15631011

Hosaka, Y., Teraoka, H., Yamamoto, E., Ueda, H., & Takehana, K. (2005, Jan). Mechanism of cell death in inflamed superficial digital flexor tendon in the horse. *J Comp Pathol, 132*(1), 51-58. https://doi.org/10.1016/j.jcpa.2004.06.006

Hu, Z., Yan, C., Liu, P., Huang, Z., Ma, R., Zhang, C., Wang, R., Zhang, Y., Martinon, F., Miao, D., Deng, H., Wang, J., Chang, J., & Chai, J. (2013, Jul 12). Crystal structure of NLRC4 reveals its autoinhibition mechanism. *Science, 341*(6142), 172-175. https://doi.org/10.1126/science.1236381

Hu, Z., Zhou, Q., Zhang, C., Fan, S., Cheng, W., Zhao, Y., Shao, F., Wang, H. W., Sui, S. F., & Chai, J. (2015, Oct 23). Structural and biochemical basis for induced self-propagation of NLRC4. *Science, 350*(6259), 399-404. https://doi.org/10.1126/science.aac5489

Huang, M., Zhang, X., Toh, G. A., Gong, Q., Wang, J., Han, Z., Wu, B., Zhong, F., & Chai, J. (2021, Apr). Structural and biochemical mechanisms of NLRP1 inhibition by DPP9. *Nature, 592*(7856), 773-777. https://doi.org/10.1038/s41586-021-03320-w

Hurgin, V., Novick, D., Werman, A., Dinarello, C. A., & Rubinstein, M. (2007, Mar 20). Antiviral and immunoregulatory activities of IFN-gamma depend on constitutively expressed IL-1alpha. *Proc Natl Acad Sci U S A, 104*(12), 5044-5049. https://doi.org/10.1073/pnas.0611608104

Hurtado-Navarro, L., Baroja-Mazo, A., Martinez-Banaclocha, H., & Pelegrin, P. (2022). Assessment of ASC Oligomerization by Flow Cytometry. *Methods Mol Biol, 2459*, 1-9. https://doi.org/10.1007/978-1-0716-2144-8_1

Iannone, F., De Bari, C., Dell'Accio, F., Covelli, M., Cantatore, F. P., Patella, V., Lo Bianco, G., & Lapadula, G. (2001, Mar-Apr). Interleukin-10 and interleukin-10 receptor in human osteoarthritic and healthy chondrocytes. *Clin Exp Rheumatol, 19*(2), 139-145. https://www.ncbi.nlm.nih.gov/pubmed/11332442

Idriss, H. T., & Naismith, J. H. (2000, Aug 1). TNF alpha and the TNF receptor superfamily: structure-function relationship(s). *Microsc Res Tech, 50*(3), 184-195. https://doi.org/10.1002/1097-0029(20000801)50:3<184::AID-JEMT2>3.0.CO;2-H

Imaeda, H., Takahashi, K., Fujimoto, T., Kasumi, E., Ban, H., Bamba, S., Sonoda, H., Shimizu, T., Fujiyama, Y., & Andoh, A. (2013, Jun). Epithelial expression of interleukin-37b in

inflammatory bowel disease. *Clin Exp Immunol, 172*(3), 410-416. https://doi.org/10.1111/cei.12061

Imai, Y., Kuba, K., Neely, G. G., Yaghubian-Malhami, R., Perkmann, T., van Loo, G., Ermolaeva, M., Veldhuizen, R., Leung, Y. H., Wang, H., Liu, H., Sun, Y., Pasparakis, M., Kopf, M., Mech, C., Bavari, S., Peiris, J. S., Slutsky, A. S., Akira, S., Hultqvist, M., Holmdahl, R., Nicholls, J., Jiang, C., Binder, C. J., & Penninger, J. M. (2008, Apr 18). Identification of oxidative stress and Toll-like receptor 4 signaling as a key pathway of acute lung injury. *Cell, 133*(2), 235-249. https://doi.org/10.1016/j.cell.2008.02.043

Inohara, Chamaillard, McDonald, C., & Nunez, G. (2005). NOD-LRR proteins: role in host-microbial interactions and inflammatory disease. *Annu Rev Biochem, 74*, 355-383. https://doi.org/10.1146/annurev.biochem.74.082803.133347

Ionescu, D., Penin-Franch, A., Mensa-Vilaro, A., Castillo, P., Hurtado-Navarro, L., Molina-Lopez, C., Romero-Chala, S., Plaza, S., Fabregat, V., Bujan, S., Marques, J., Casals, F., Yague, J., Oliva, B., Fernandez-Pereira, L. M., Pelegrin, P., & Arostegui, J. I. (2022, Apr). First Description of Late-Onset Autoinflammatory Disease Due to Somatic NLRC4 Mosaicism. *Arthritis Rheumatol, 74*(4), 692-699. https://doi.org/10.1002/art.41999

Ishibashi, T., Kimura, H., Shikama, Y., Uchida, T., Kariyone, S., Hirano, T., Kishimoto, T., Takatsuki, F., & Akiyama, Y. (1989, Sep). Interleukin-6 is a potent thrombopoietic factor in vivo in mice. *Blood, 74*(4), 1241-1244. https://www.ncbi.nlm.nih.gov/pubmed/2788464

Italiani, P., & Boraschi, D. (2014). From Monocytes to M1/M2 Macrophages: Phenotypical vs. Functional Differentiation. *Front Immunol, 5*, 514. https://doi.org/10.3389/fimmu.2014.00514

Iwai, K. (2012, Jul). Diverse ubiquitin signaling in NF-kappaB activation. *Trends Cell Biol, 22*(7), 355-364. https://doi.org/10.1016/j.tcb.2012.04.001

Iyer, S. S., He, Q., Janczy, J. R., Elliott, E. I., Zhong, Z., Olivier, A. K., Sadler, J. J., Knepper-Adrian, V., Han, R., Qiao, L., Eisenbarth, S. C., Nauseef, W. M., Cassel, S. L., & Sutterwala, F. S. (2013, Aug 22). Mitochondrial cardiolipin is required for Nlrp3 inflammasome activation. *Immunity, 39*(2), 311-323. https://doi.org/10.1016/j.immuni.2013.08.001

Jackson, J. R., Minton, J. A., Ho, M. L., Wei, N., & Winkler, J. D. (1997, Jul). Expression of vascular endothelial growth factor in synovial fibroblasts is induced by hypoxia and interleukin 1beta. *J Rheumatol, 24*(7), 1253-1259. https://www.ncbi.nlm.nih.gov/pubmed/9228120

James, R., Kesturu, G., Balian, G., & Chhabra, A. B. (2008, Jan). Tendon: biology, biomechanics, repair, growth factors, and evolving treatment options. *J Hand Surg Am, 33*(1), 102-112. https://doi.org/10.1016/j.jhsa.2007.09.007

Jarvelainen, H. A., Galmiche, A., & Zychlinsky, A. (2003, Apr). Caspase-1 activation by Salmonella. *Trends Cell Biol, 13*(4), 204-209. https://doi.org/10.1016/s0962-8924(03)00032-1

Jekarl, D. W., Lee, S. Y., Lee, J., Park, Y. J., Kim, Y., Park, J. H., Wee, J. H., & Choi, S. P. (2013, Apr). Procalcitonin as a diagnostic marker and IL-6 as a prognostic marker for sepsis. *Diagn Microbiol Infect Dis, 75*(4), 342-347. https://doi.org/10.1016/j.diagmicrobio.2012.12.011

Jeru, I., Duquesnoy, P., Fernandes-Alnemri, T., Cochet, E., Yu, J. W., Lackmy-Port-Lis, M., Grimprel, E., Landman-Parker, J., Hentgen, V., Marlin, S., McElreavey, K., Sarkisian, T., Grateau, G., Alnemri, E. S., & Amselem, S. (2008, Feb 5). Mutations in NALP12 cause hereditary periodic fever syndromes. *Proc Natl Acad Sci U S A, 105*(5), 1614-1619. https://doi.org/10.1073/pnas.0708616105

Jiang, H., He, H., Chen, Y., Huang, W., Cheng, J., Ye, J., Wang, A., Tao, J., Wang, C., Liu, Q., Jin, T., Jiang, W., Deng, X., & Zhou, R. (2017, Nov 6). Identification of a selective and direct NLRP3 inhibitor to treat inflammatory disorders. *J Exp Med, 214*(11), 3219-3238. https://doi.org/10.1084/jem.20171419

Jiang, M., Qi, L., Li, L., & Li, Y. (2020). The caspase-3/GSDME signal pathway as a switch between apoptosis and pyroptosis in cancer. *Cell Death Discov, 6*, 112. https://doi.org/10.1038/s41420-020-00349-0

Jimenez-Trevino, S., Gonzalez-Roca, E., Ruiz-Ortiz, E., Yague, J., Ramos, E., & Arostegui, J. I. (2013, Jun). First report of vertical transmission of a somatic NLRP3 mutation in cryopyrin-associated periodic syndromes. *Ann Rheum Dis, 72*(6), 1109-1110. https://doi.org/10.1136/annrheumdis-2012-202913

Jimenez, S. A., Varga, J., Olsen, A., Li, L., Diaz, A., Herhal, J., & Koch, J. (1994, Apr 29). Functional analysis of human alpha 1(I) procollagen gene promoter. Differential activity in collagen-producing and -nonproducing cells and response to transforming growth factor beta 1. *J Biol Chem, 269*(17), 12684-12691. https://www.ncbi.nlm.nih.gov/pubmed/8175678

Jin, C., Frayssinet, P., Pelker, R., Cwirka, D., Hu, B., Vignery, A., Eisenbarth, S. C., & Flavell, R. A. (2011, Sep 6). NLRP3 inflammasome plays a critical role in the pathogenesis of hydroxyapatite-associated arthropathy. *Proc Natl Acad Sci U S A, 108*(36), 14867-14872. https://doi.org/10.1073/pnas.1111101108

Jin, M. S., Kim, S. E., Heo, J. Y., Lee, M. E., Kim, H. M., Paik, S. G., Lee, H., & Lee, J. O. (2007, Sep 21). Crystal structure of the TLR1-TLR2 heterodimer induced by binding of a tri-acylated lipopeptide. *Cell, 130*(6), 1071-1082. https://doi.org/10.1016/j.cell.2007.09.008

John, T., Lodka, D., Kohl, B., Ertel, W., Jammrath, J., Conrad, C., Stoll, C., Busch, C., & Schulze-Tanzil, G. (2010, Aug). Effect of pro-inflammatory and immunoregulatory cytokines on human tenocytes. *J Orthop Res, 28*(8), 1071-1077. https://doi.org/10.1002/jor.21079

Juliana, C., Fernandes-Alnemri, T., Kang, S., Farias, A., Qin, F., & Alnemri, E. S. (2012, Oct 19). Non-transcriptional priming and deubiquitination regulate NLRP3 inflammasome activation. *J Biol Chem, 287*(43), 36617-36622. https://doi.org/10.1074/jbc.M112.407130

Juliana, C., Fernandes-Alnemri, T., Wu, J., Datta, P., Solorzano, L., Yu, J. W., Meng, R., Quong, A. A., Latz, E., Scott, C. P., & Alnemri, E. S. (2010, Mar 26). Anti-inflammatory compounds parthenolide and Bay 11-7082 are direct inhibitors of the inflammasome. *J Biol Chem, 285*(13), 9792-9802. https://doi.org/10.1074/jbc.M109.082305

Kajikawa, Y., Morihara, T., Watanabe, N., Sakamoto, H., Matsuda, K., Kobayashi, M., Oshima, Y., Yoshida, A., Kawata, M., & Kubo, T. (2007, Mar). GFP chimeric models exhibited a biphasic pattern of mesenchymal cell invasion in tendon healing. *J Cell Physiol, 210*(3), 684-691. https://doi.org/10.1002/jcp.20876

Kakkar, R., Hei, H., Dobner, S., & Lee, R. T. (2012, Feb 24). Interleukin 33 as a mechanically responsive cytokine secreted by living cells. *J Biol Chem, 287*(9), 6941-6948. https://doi.org/10.1074/jbc.M111.298703

Kamari, Y., Werman-Venkert, R., Shaish, A., Werman, A., Harari, A., Gonen, A., Voronov, E., Grosskopf, I., Sharabi, Y., Grossman, E., Iwakura, Y., Dinarello, C. A., Apte, R. N., & Harats, D. (2007, Nov). Differential role and tissue specificity of interleukin-1alpha gene expression in atherogenesis and lipid metabolism. *Atherosclerosis, 195*(1), 31-38. https://doi.org/10.1016/j.atherosclerosis.2006.11.026

Kang, J. S., Liu, C., & Derynck, R. (2009, Aug). New regulatory mechanisms of TGF-beta receptor function. *Trends Cell Biol, 19*(8), 385-394. https://doi.org/10.1016/j.tcb.2009.05.008

Kannan, Y., Yu, J., Raices, R. M., Seshadri, S., Wei, M., Caligiuri, M. A., & Wewers, M. D. (2011, Mar 10). IkappaBzeta augments IL-12- and IL-18-mediated IFN-gamma production in human NK cells. *Blood, 117*(10), 2855-2863. https://doi.org/10.1182/blood-2010-07-294702

Kannus, P., & Jozsa, L. (1991, Dec). Histopathological changes preceding spontaneous rupture of a tendon. A controlled study of 891 patients. *J Bone Joint Surg Am, 73*(10), 1507-1525. https://www.ncbi.nlm.nih.gov/pubmed/1748700

Kaplanski, G., Farnarier, C., Kaplanski, S., Porat, R., Shapiro, L., Bongrand, P., & Dinarello, C. A. (1994, Dec 15). Interleukin-1 induces interleukin-8 secretion from endothelial cells by a juxtacrine mechanism. *Blood, 84*(12), 4242-4248. https://www.ncbi.nlm.nih.gov/pubmed/7994038

Karre, K. (2002, Mar). NK cells, MHC class I molecules and the missing self. *Scand J Immunol, 55*(3), 221-228. https://doi.org/10.1046/j.1365-3083.2002.01053.x

Kato, H., Takeuchi, O., Sato, S., Yoneyama, M., Yamamoto, M., Matsui, K., Uematsu, S., Jung, A., Kawai, T., Ishii, K. J., Yamaguchi, O., Otsu, K., Tsujimura, T., Koh, C. S., Reis e Sousa, C., Matsuura, Y., Fujita, T., & Akira, S. (2006, May 4). Differential roles of MDA5 and RIG-I helicases in the recognition of RNA viruses. *Nature, 441*(7089), 101-105. https://doi.org/10.1038/nature04734

Kavita, U., & Mizel, S. B. (1995, Nov 17). Differential sensitivity of interleukin-1 alpha and -beta precursor proteins to cleavage by calpain, a calcium-dependent protease. *J Biol Chem, 270*(46), 27758-27765. https://doi.org/10.1074/jbc.270.46.27758

Kawagoe, T., Sato, S., Matsushita, K., Kato, H., Matsui, K., Kumagai, Y., Saitoh, T., Kawai, T., Takeuchi, O., & Akira, S. (2008, Jun). Sequential control of Toll-like receptor-dependent responses by IRAK1 and IRAK2. *Nat Immunol, 9*(6), 684-691. https://doi.org/10.1038/ni.1606

Kawasaki, Y., Oda, H., Ito, J., Niwa, A., Tanaka, T., Hijikata, A., Seki, R., Nagahashi, A., Osawa, M., Asaka, I., Watanabe, A., Nishimata, S., Shirai, T., Kawashima, H., Ohara, O., Nakahata, T., Nishikomori, R., Heike, T., & Saito, M. K. (2017, Feb). Identification of a High-Frequency Somatic NLRC4 Mutation as a Cause of Autoinflammation by Pluripotent Cell-Based Phenotype Dissection. *Arthritis Rheumatol, 69*(2), 447-459. https://doi.org/10.1002/art.39960

Kayagaki, N., Kornfeld, O. S., Lee, B. L., Stowe, I. B., O'Rourke, K., Li, Q., Sandoval, W., Yan, D., Kang, J., Xu, M., Zhang, J., Lee, W. P., McKenzie, B. S., Ulas, G., Payandeh, J., Roose-Girma, M., Modrusan, Z., Reja, R., Sagolla, M., Webster, J. D., Cho, V., Andrews, T. D., Morris, L. X., Miosge, L. A., Goodnow, C. C., Bertram, E. M., & Dixit, V. M. (2021, Mar). NINJ1 mediates plasma membrane rupture during lytic cell death. *Nature, 591*(7848), 131-136. https://doi.org/10.1038/s41586-021-03218-7

Kearney, R. S., Parsons, N., Metcalfe, D., & Costa, M. L. (2015, May 26). Injection therapies for Achilles tendinopathy. *Cochrane Database Syst Rev*(5), CD010960. https://doi.org/10.1002/14651858.CD010960.pub2

Kehrl, J. H., Wakefield, L. M., Roberts, A. B., Jakowlew, S., Alvarez-Mon, M., Derynck, R., Sporn, M. B., & Fauci, A. S. (1986, May 1). Production of transforming growth factor beta by human T lymphocytes and its potential role in the regulation of T cell growth. *J Exp Med, 163*(5), 1037-1050. https://doi.org/10.1084/jem.163.5.1037

Keshari, R. S., Jyoti, A., Dubey, M., Kothari, N., Kohli, M., Bogra, J., Barthwal, M. K., & Dikshit, M. (2012). Cytokines induced neutrophil extracellular traps formation: implication for the

inflammatory disease condition. *PLoS One, 7*(10), e48111. https://doi.org/10.1371/journal.pone.0048111

Ketola, S., Lehtinen, J. T., & Arnala, I. (2017, Jun). Arthroscopic decompression not recommended in the treatment of rotator cuff tendinopathy: a final review of a randomised controlled trial at a minimum follow-up of ten years. *Bone Joint J, 99-B*(6), 799-805. https://doi.org/10.1302/0301-620X.99B6.BJJ-2016-0569.R1

Killian, M. L., Cavinatto, L., Galatz, L. M., & Thomopoulos, S. (2012, Feb). The role of mechanobiology in tendon healing. *J Shoulder Elbow Surg, 21*(2), 228-237. https://doi.org/10.1016/j.jse.2011.11.002

Kim, H. M., Galatz, L. M., Das, R., Havlioglu, N., Rothermich, S. Y., & Thomopoulos, S. (2011, Apr). The role of transforming growth factor beta isoforms in tendon-to-bone healing. *Connect Tissue Res, 52*(2), 87-98. https://doi.org/10.3109/03008207.2010.483026

Kim, S. V., Xiang, W. V., Kwak, C., Yang, Y., Lin, X. W., Ota, M., Sarpel, U., Rifkin, D. B., Xu, R., & Littman, D. R. (2013, Jun 21). GPR15-mediated homing controls immune homeostasis in the large intestine mucosa. *Science, 340*(6139), 1456-1459. https://doi.org/10.1126/science.1237013

Kitamura, A., Sasaki, Y., Abe, T., Kano, H., & Yasutomo, K. (2014, Nov 17). An inherited mutation in NLRC4 causes autoinflammation in human and mice. *J Exp Med, 211*(12), 2385-2396. https://doi.org/10.1084/jem.20141091

Klein, M. B., Pham, H., Yalamanchi, N., & Chang, J. (2001, Sep). Flexor tendon wound healing in vitro: the effect of lactate on tendon cell proliferation and collagen production. *J Hand Surg Am, 26*(5), 847-854. https://doi.org/10.1053/jhsu.2001.26185

Klein, M. B., Yalamanchi, N., Pham, H., Longaker, M. T., & Chang, J. (2002, Jul). Flexor tendon healing in vitro: effects of TGF-beta on tendon cell collagen production. *J Hand Surg Am, 27*(4), 615-620. https://doi.org/10.1053/jhsu.2002.34004

Kobayashi, T., Kouzaki, H., & Kita, H. (2010, Jun 1). Human eosinophils recognize endogenous danger signal crystalline uric acid and produce proinflammatory cytokines mediated by autocrine ATP. *J Immunol, 184*(11), 6350-6358. https://doi.org/10.4049/jimmunol.0902673

Kobayashi, Y., Yamamoto, K., Saido, T., Kawasaki, H., Oppenheim, J. J., & Matsushima, K. (1990, Jul). Identification of calcium-activated neutral protease as a processing enzyme of human interleukin 1 alpha. *Proc Natl Acad Sci U S A, 87*(14), 5548-5552. https://doi.org/10.1073/pnas.87.14.5548

Kofoed, E. M., & Vance, R. E. (2011, Aug 28). Innate immune recognition of bacterial ligands by NAIPs determines inflammasome specificity. *Nature, 477*(7366), 592-595. https://doi.org/10.1038/nature10394

Koh, T. J., & DiPietro, L. A. (2011, Jul 11). Inflammation and wound healing: the role of the macrophage. *Expert Rev Mol Med, 13*, e23. https://doi.org/10.1017/S1462399411001943

Kolaczkowska, E., & Kubes, P. (2013, Mar). Neutrophil recruitment and function in health and inflammation. *Nat Rev Immunol, 13*(3), 159-175. https://doi.org/10.1038/nri3399

Kolinska, J., Lisa, V., Clark, J. A., Kozakova, H., Zakostelecka, M., Khailova, L., Sinkora, M., Kitanovicova, A., & Dvorak, B. (2008, May). Constitutive expression of IL-18 and IL-18R in differentiated IEC-6 cells: effect of TNF-alpha and IFN-gamma treatment. *J Interferon Cytokine Res, 28*(5), 287-296. https://doi.org/10.1089/jir.2006.0130

Kolivras, A., Aeby, A., Crow, Y. J., Rice, G. I., Sass, U., & Andre, J. (2008, Aug). Cutaneous histopathological findings of Aicardi-Goutieres syndrome, overlap with chilblain lupus. *J Cutan Pathol, 35*(8), 774-778. https://doi.org/10.1111/j.1600-0560.2007.00900.x

Kongsgaard, M., Qvortrup, K., Larsen, J., Aagaard, P., Doessing, S., Hansen, P., Kjaer, M., & Magnusson, S. P. (2010, Apr). Fibril morphology and tendon mechanical properties in patellar tendinopathy: effects of heavy slow resistance training. *Am J Sports Med, 38*(4), 749-756. https://doi.org/10.1177/0363546509350915

Korakakis, V., Whiteley, R., Tzavara, A., & Malliaropoulos, N. (2018, Mar). The effectiveness of extracorporeal shockwave therapy in common lower limb conditions: a systematic review including quantification of patient-rated pain reduction. *Br J Sports Med, 52*(6), 387-407. https://doi.org/10.1136/bjsports-2016-097347

Koyama, S., Ishii, K. J., Coban, C., & Akira, S. (2008, Sep). Innate immune response to viral infection. *Cytokine, 43*(3), 336-341. https://doi.org/10.1016/j.cyto.2008.07.009

Krane, S. M. (1982, Jul). Collagenases and collagen degradation. *J Invest Dermatol, 79 Suppl 1*, 83s-86s. https://doi.org/10.1111/1523-1747.ep12545849

Kratky, W., Reis e Sousa, C., Oxenius, A., & Sporri, R. (2011, Oct 18). Direct activation of antigen-presenting cells is required for CD8+ T-cell priming and tumor vaccination. *Proc Natl Acad Sci U S A, 108*(42), 17414-17419. https://doi.org/10.1073/pnas.1108945108

Kroemer, G., Galluzzi, L., Vandenabeele, P., Abrams, J., Alnemri, E. S., Baehrecke, E. H., Blagosklonny, M. V., El-Deiry, W. S., Golstein, P., Green, D. R., Hengartner, M., Knight, R. A., Kumar, S., Lipton, S. A., Malorni, W., Nunez, G., Peter, M. E., Tschopp, J., Yuan, J., Piacentini, M., Zhivotovsky, B., Melino, G., & Nomenclature Committee on Cell, D. (2009, Jan). Classification of cell death: recommendations of the Nomenclature Committee on Cell Death 2009. *Cell Death Differ, 16*(1), 3-11. https://doi.org/10.1038/cdd.2008.150

Krupenevich, R. L., Beck, O. N., Sawicki, G. S., & Franz, J. R. (2022). Reduced Achilles Tendon Stiffness Disrupts Calf Muscle Neuromechanics in Elderly Gait. *Gerontology, 68*(3), 241-251. https://doi.org/10.1159/000516910

Kuemmerle-Deschner, J. B., Verma, D., Endres, T., Broderick, L., de Jesus, A. A., Hofer, F., Blank, N., Krause, K., Rietschel, C., Horneff, G., Aksentijevich, I., Lohse, P., Goldbach-Mansky, R., Hoffman, H. M., & Benseler, S. M. (2017, Nov). Clinical and Molecular Phenotypes of Low-Penetrance Variants of NLRP3: Diagnostic and Therapeutic Challenges. *Arthritis Rheumatol, 69*(11), 2233-2240. https://doi.org/10.1002/art.40208

Kuida, K., Lippke, J. A., Ku, G., Harding, M. W., Livingston, D. J., Su, M. S., & Flavell, R. A. (1995, Mar 31). Altered cytokine export and apoptosis in mice deficient in interleukin-1 beta converting enzyme. *Science, 267*(5206), 2000-2003. https://doi.org/10.1126/science.7535475

Kumar, S., Hanning, C. R., Brigham-Burke, M. R., Rieman, D. J., Lehr, R., Khandekar, S., Kirkpatrick, R. B., Scott, G. F., Lee, J. C., Lynch, F. J., Gao, W., Gambotto, A., & Lotze, M. T. (2002, Apr 21). Interleukin-1F7B (IL-1H4/IL-1F7) is processed by caspase-1 and mature IL-1F7B binds to the IL-18 receptor but does not induce IFN-gamma production. *Cytokine, 18*(2), 61-71. https://doi.org/10.1006/cyto.2002.0873

Kumar, S., McDonnell, P. C., Lehr, R., Tierney, L., Tzimas, M. N., Griswold, D. E., Capper, E. A., Tal-Singer, R., Wells, G. I., Doyle, M. L., & Young, P. R. (2000, Apr 7). Identification and initial characterization of four novel members of the interleukin-1 family. *J Biol Chem, 275*(14), 10308-10314. https://doi.org/10.1074/jbc.275.14.10308

Kyriazopoulou, E., Huet, T., Cavalli, G., Gori, A., Kyprianou, M., Pickkers, P., Eugen-Olsen, J., Clerici, M., Veas, F., Chatellier, G., Kaplanski, G., Netea, M. G., Pontali, E., Gattorno, M., Cauchois, R., Kooistra, E., Kox, M., Bandera, A., Beaussier, H., Mangioni, D., Dagna, L., van der Meer, J. W. M., Giamarellos-Bourboulis, E. J., Hayem, G., & International Collaborative Group for Anakinra in, C. (2021, Oct). Effect of anakinra on mortality in patients with COVID-19: a systematic review and patient-level meta-analysis. *Lancet Rheumatol, 3*(10), e690-e697. https://doi.org/10.1016/S2665-9913(21)00216-2

Kyritsis, N., Kizil, C., & Brand, M. (2014, Feb). Neuroinflammation and central nervous system regeneration in vertebrates. *Trends Cell Biol, 24*(2), 128-135. https://doi.org/10.1016/j.tcb.2013.08.004

Labrousse, M., Kevorkian-Verguet, C., Boursier, G., Rowczenio, D., Maurier, F., Lazaro, E., Aggarwal, M., Lemelle, I., Mura, T., Belot, A., Touitou, I., & Sarrabay, G. (2018, Sep). Mosaicism in autoinflammatory diseases: Cryopyrin-associated periodic syndromes (CAPS) and beyond. A systematic review. *Crit Rev Clin Lab Sci, 55*(6), 432-442. https://doi.org/10.1080/10408363.2018.1488805

Lamkanfi, M., Mueller, J. L., Vitari, A. C., Misaghi, S., Fedorova, A., Deshayes, K., Lee, W. P., Hoffman, H. M., & Dixit, V. M. (2009, Oct 5). Glyburide inhibits the Cryopyrin/Nalp3 inflammasome. *J Cell Biol, 187*(1), 61-70. https://doi.org/10.1083/jcb.200903124

Langberg, H., Olesen, J. L., Gemmer, C., & Kjaer, M. (2002, Aug 1). Substantial elevation of interleukin-6 concentration in peritendinous tissue, in contrast to muscle, following prolonged exercise in humans. *J Physiol, 542*(Pt 3), 985-990. https://doi.org/10.1113/jphysiol.2002.019141

Lee, J. K., Kim, S. H., Lewis, E. C., Azam, T., Reznikov, L. L., & Dinarello, C. A. (2004, Jun 8). Differences in signaling pathways by IL-1beta and IL-18. *Proc Natl Acad Sci U S A, 101*(23), 8815-8820. https://doi.org/10.1073/pnas.0402800101

Lee, J. S., Robertson, A. A. B., Cooper, M. A., & Khosrotehrani, K. (2018, Oct 23). The Small Molecule NLRP3 Inflammasome Inhibitor MCC950 Does Not Alter Wound Healing in Obese Mice. *Int J Mol Sci, 19*(11). https://doi.org/10.3390/ijms19113289

Lefrancais, E., Duval, A., Mirey, E., Roga, S., Espinosa, E., Cayrol, C., & Girard, J. P. (2014, Oct 28). Central domain of IL-33 is cleaved by mast cell proteases for potent activation of group-2 innate lymphoid cells. *Proc Natl Acad Sci U S A, 111*(43), 15502-15507. https://doi.org/10.1073/pnas.1410700111

Lefrancais, E., Roga, S., Gautier, V., Gonzalez-de-Peredo, A., Monsarrat, B., Girard, J. P., & Cayrol, C. (2012, Jan 31). IL-33 is processed into mature bioactive forms by neutrophil elastase and cathepsin G. *Proc Natl Acad Sci U S A, 109*(5), 1673-1678. https://doi.org/10.1073/pnas.1115884109

Lehner, C., Spitzer, G., Gehwolf, R., Wagner, A., Weissenbacher, N., Deininger, C., Emmanuel, K., Wichlas, F., Tempfer, H., & Traweger, A. (2019, Dec 16). Tenophages: a novel macrophage-like tendon cell population expressing CX3CL1 and CX3CR1. *Dis Model Mech, 12*(12). https://doi.org/10.1242/dmm.041384

Leng, F., Yin, H., Qin, S., Zhang, K., Guan, Y., Fang, R., Wang, H., Li, G., Jiang, Z., Sun, F., Wang, D. C., & Xie, C. (2020, Jan 13). NLRP6 self-assembles into a linear molecular platform following LPS binding and ATP stimulation. *Sci Rep, 10*(1), 198. https://doi.org/10.1038/s41598-019-57043-0

Levinsohn, J. L., Newman, Z. L., Hellmich, K. A., Fattah, R., Getz, M. A., Liu, S., Sastalla, I., Leppla, S. H., & Moayeri, M. (2012). Anthrax lethal factor cleavage of Nlrp1 is required for activation

of the inflammasome. *PLoS Pathog, 8*(3), e1002638. https://doi.org/10.1371/journal.ppat.1002638

Levy, M., Thaiss, C. A., Zeevi, D., Dohnalova, L., Zilberman-Schapira, G., Mahdi, J. A., David, E., Savidor, A., Korem, T., Herzig, Y., Pevsner-Fischer, M., Shapiro, H., Christ, A., Harmelin, A., Halpern, Z., Latz, E., Flavell, R. A., Amit, I., Segal, E., & Elinav, E. (2015, Dec 3). Microbiota-Modulated Metabolites Shape the Intestinal Microenvironment by Regulating NLRP6 Inflammasome Signaling. *Cell, 163*(6), 1428-1443. https://doi.org/10.1016/j.cell.2015.10.048

Li, M. O., Wan, Y. Y., Sanjabi, S., Robertson, A. K., & Flavell, R. A. (2006). Transforming growth factor-beta regulation of immune responses. *Annu Rev Immunol, 24*, 99-146. https://doi.org/10.1146/annurev.immunol.24.021605.090737

Li, R., & Zhu, S. (2020, Dec). NLRP6 inflammasome. *Mol Aspects Med, 76*, 100859. https://doi.org/10.1016/j.mam.2020.100859

Li, S., Neff, C. P., Barber, K., Hong, J., Luo, Y., Azam, T., Palmer, B. E., Fujita, M., Garlanda, C., Mantovani, A., Kim, S., & Dinarello, C. A. (2015, Feb 24). Extracellular forms of IL-37 inhibit innate inflammation in vitro and in vivo but require the IL-1 family decoy receptor IL-1R8. *Proc Natl Acad Sci U S A, 112*(8), 2497-2502. https://doi.org/10.1073/pnas.1424626112

Liang, J., Alfano, D. N., Squires, J. E., Riley, M. M., Parks, W. T., Kofler, J., El-Gharbawy, A., Madan-Kheterpal, S., Acquaro, R., & Picarsic, J. (2017, Nov-Dec). Novel NLRC4 Mutation Causes a Syndrome of Perinatal Autoinflammation With Hemophagocytic Lymphohistiocytosis, Hepatosplenomegaly, Fetal Thrombotic Vasculopathy, and Congenital Anemia and Ascites. *Pediatr Dev Pathol, 20*(6), 498-505. https://doi.org/10.1177/1093526616686890

Libermann, T. A., & Baltimore, D. (1990, May). Activation of interleukin-6 gene expression through the NF-kappa B transcription factor. *Mol Cell Biol, 10*(5), 2327-2334. https://doi.org/10.1128/mcb.10.5.2327-2334.1990

Lichtnekert, J., Kawakami, T., Parks, W. C., & Duffield, J. S. (2013, Aug). Changes in macrophage phenotype as the immune response evolves. *Curr Opin Pharmacol, 13*(4), 555-564. https://doi.org/10.1016/j.coph.2013.05.013

Liddle, A. D., & Rodriguez-Merchan, E. C. (2015, Oct). Platelet-Rich Plasma in the Treatment of Patellar Tendinopathy: A Systematic Review. *Am J Sports Med, 43*(10), 2583-2590. https://doi.org/10.1177/0363546514560726

Lieben, L. (2018, Feb 1). Autoinflammatory diseases: Free IL-18 causes macrophage activation syndrome. *Nat Rev Rheumatol*. https://doi.org/10.1038/nrrheum.2018.11

Lim, H. Y., & Wong, S. H. (2018, Oct). Effects of isometric, eccentric, or heavy slow resistance exercises on pain and function in individuals with patellar tendinopathy: A systematic review. *Physiother Res Int, 23*(4), e1721. https://doi.org/10.1002/pri.1721

Lin, T. W., Cardenas, L., Glaser, D. L., & Soslowsky, L. J. (2006). Tendon healing in interleukin-4 and interleukin-6 knockout mice. *J Biomech, 39*(1), 61-69. https://doi.org/10.1016/j.jbiomech.2004.11.009

Lin, T. W., Cardenas, L., & Soslowsky, L. J. (2004, Jun). Biomechanics of tendon injury and repair. *J Biomech, 37*(6), 865-877. https://doi.org/10.1016/j.jbiomech.2003.11.005

Lin, T. W., Cardenas, L., & Soslowsky, L. J. (2005, Jan). Tendon properties in interleukin-4 and interleukin-6 knockout mice. *J Biomech, 38*(1), 99-105. https://doi.org/10.1016/j.jbiomech.2004.03.008

Lind, B., Ohberg, L., & Alfredson, H. (2006, Dec). Sclerosing polidocanol injections in mid-portion Achilles tendinosis: remaining good clinical results and decreased tendon thickness at 2-year follow-up. *Knee Surg Sports Traumatol Arthrosc, 14*(12), 1327-1332. https://doi.org/10.1007/s00167-006-0161-3

Ling, L., Cao, Z., & Goeddel, D. V. (1998, Mar 31). NF-kappaB-inducing kinase activates IKK-alpha by phosphorylation of Ser-176. *Proc Natl Acad Sci U S A, 95*(7), 3792-3797. https://doi.org/10.1073/pnas.95.7.3792

Lipsky, P. E., van der Heijde, D. M., St Clair, E. W., Furst, D. E., Breedveld, F. C., Kalden, J. R., Smolen, J. S., Weisman, M., Emery, P., Feldmann, M., Harriman, G. R., Maini, R. N., & Anti-Tumor Necrosis Factor Trial in Rheumatoid Arthritis with Concomitant Therapy Study, G. (2000, Nov 30). Infliximab and methotrexate in the treatment of rheumatoid arthritis. Anti-Tumor Necrosis Factor Trial in Rheumatoid Arthritis with Concomitant Therapy Study Group. *N Engl J Med, 343*(22), 1594-1602. https://doi.org/10.1056/NEJM200011303432202

Liston, A., & Masters, S. L. (2017, Mar). Homeostasis-altering molecular processes as mechanisms of inflammasome activation. *Nat Rev Immunol, 17*(3), 208-214. https://doi.org/10.1038/nri.2016.151

Liu, C. J., Yu, K. L., Bai, J. B., Tian, D. H., & Liu, G. L. (2019, Apr). Platelet-rich plasma injection for the treatment of chronic Achilles tendinopathy: A meta-analysis. *Medicine (Baltimore), 98*(16), e15278. https://doi.org/10.1097/MD.0000000000015278

Liu, W., Liu, X., Li, Y., Zhao, J., Liu, Z., Hu, Z., Wang, Y., Yao, Y., Miller, A. W., Su, B., Cookson, M. R., Li, X., & Kang, Z. (2017, Oct 2). LRRK2 promotes the activation of NLRC4 inflammasome during Salmonella Typhimurium infection. *J Exp Med, 214*(10), 3051-3066. https://doi.org/10.1084/jem.20170014

Liu, X., Zhang, Z., Ruan, J., Pan, Y., Magupalli, V. G., Wu, H., & Lieberman, J. (2016, Jul 7). Inflammasome-activated gasdermin D causes pyroptosis by forming membrane pores. *Nature, 535*(7610), 153-158. https://doi.org/10.1038/nature18629

Liu, Y., Dai, Y., Li, Q., Chen, C., Chen, H., Song, Y., Hua, F., & Zhang, Z. (2020, Sep 25). Beta-amyloid activates NLRP3 inflammasome via TLR4 in mouse microglia. *Neurosci Lett, 736*, 135279. https://doi.org/10.1016/j.neulet.2020.135279

Liu, Y., Jesus, A. A., Marrero, B., Yang, D., Ramsey, S. E., Sanchez, G. A. M., Tenbrock, K., Wittkowski, H., Jones, O. Y., Kuehn, H. S., Lee, C. R., DiMattia, M. A., Cowen, E. W., Gonzalez, B., Palmer, I., DiGiovanna, J. J., Biancotto, A., Kim, H., Tsai, W. L., Trier, A. M., Huang, Y., Stone, D. L., Hill, S., Kim, H. J., St Hilaire, C., Gurprasad, S., Plass, N., Chapelle, D., Horkayne-Szakaly, I., Foell, D., Barysenka, A., Candotti, F., Holland, S. M., Hughes, J. D., Mehmet, H., Issekutz, A. C., Raffeld, M., McElwee, J., Fontana, J. R., Minniti, C. P., Moir, S., Kastner, D. L., Gadina, M., Steven, A. C., Wingfield, P. T., Brooks, S. R., Rosenzweig, S. D., Fleisher, T. A., Deng, Z., Boehm, M., Paller, A. S., & Goldbach-Mansky, R. (2014, Aug 7). Activated STING in a vascular and pulmonary syndrome. *N Engl J Med, 371*(6), 507-518. https://doi.org/10.1056/NEJMoa1312625

Liu, Y., Keikhosravi, A., Mehta, G. S., Drifka, C. R., & Eliceiri, K. W. (2017). Methods for Quantifying Fibrillar Collagen Alignment. *Methods Mol Biol, 1627*, 429-451. https://doi.org/10.1007/978-1-4939-7113-8_28

Lomedico, P. T., Gubler, U., Hellmann, C. P., Dukovich, M., Giri, J. G., Pan, Y. C., Collier, K., Semionow, R., Chua, A. O., & Mizel, S. B. (1984, Nov 29-Dec 5). Cloning and expression of murine interleukin-1 cDNA in Escherichia coli. *Nature, 312*(5993), 458-462. https://doi.org/10.1038/312458a0

Lopez-Castejon, G., Luheshi, N. M., Compan, V., High, S., Whitehead, R. C., Flitsch, S., Kirov, A., Prudovsky, I., Swanton, E., & Brough, D. (2013, Jan 25). Deubiquitinases regulate the activity of caspase-1 and interleukin-1beta secretion via assembly of the inflammasome. *J Biol Chem, 288*(4), 2721-2733. https://doi.org/10.1074/jbc.M112.422238

Lorda-Diez, C. I., Montero, J. A., Martinez-Cue, C., Garcia-Porrero, J. A., & Hurle, J. M. (2009, Oct 23). Transforming growth factors beta coordinate cartilage and tendon differentiation in the developing limb mesenchyme. *J Biol Chem, 284*(43), 29988-29996. https://doi.org/10.1074/jbc.M109.014811

Lundborg, G., Hansson, H. A., Rank, F., & Rydevik, B. (1980, Sep). Superficial repair of severed flexor tendons in synovial environment. An experimental, ultrastructural study on cellular mechanisms. *J Hand Surg Am, 5*(5), 451-461. https://doi.org/10.1016/s0363-5023(80)80075-x

Machner, A., Baier, A., Wille, A., Drynda, S., Pap, G., Drynda, A., Mawrin, C., Buhling, F., Gay, S., Neumann, W., & Pap, T. (2003). Higher susceptibility to Fas ligand induced apoptosis and altered modulation of cell death by tumor necrosis factor-alpha in periarticular tenocytes from patients with knee joint osteoarthritis. *Arthritis Res Ther, 5*(5), R253-261. https://doi.org/10.1186/ar789

MacKenzie, A., Wilson, H. L., Kiss-Toth, E., Dower, S. K., North, R. A., & Surprenant, A. (2001, Nov). Rapid secretion of interleukin-1beta by microvesicle shedding. *Immunity, 15*(5), 825-835. https://doi.org/10.1016/s1074-7613(01)00229-1

Maeda, E., Noguchi, H., Tohyama, H., Yasuda, K., & Hayashi, K. (2007). The tensile properties of collagen fascicles harvested from regenerated and residual tissues in the patellar tendon after removal of the central third. *Biomed Mater Eng, 17*(2), 77-85. https://www.ncbi.nlm.nih.gov/pubmed/17377216

Maffulli, N., Barrass, V., & Ewen, S. W. (2000, Nov-Dec). Light microscopic histology of achilles tendon ruptures. A comparison with unruptured tendons. *Am J Sports Med, 28*(6), 857-863. https://doi.org/10.1177/03635465000280061401

Maffulli, N., Ewen, S. W., Waterston, S. W., Reaper, J., & Barrass, V. (2000, Jul-Aug). Tenocytes from ruptured and tendinopathic achilles tendons produce greater quantities of type III collagen than tenocytes from normal achilles tendons. An in vitro model of human tendon healing. *Am J Sports Med, 28*(4), 499-505. https://doi.org/10.1177/03635465000280040901

Mallows, A., Debenham, J., Walker, T., & Littlewood, C. (2017, May). Association of psychological variables and outcome in tendinopathy: a systematic review. *Br J Sports Med, 51*(9), 743-748. https://doi.org/10.1136/bjsports-2016-096154

Man, S. M., & Kanneganti, T. D. (2015, May). Regulation of inflammasome activation. *Immunol Rev, 265*(1), 6-21. https://doi.org/10.1111/imr.12296

Man, S. M., Tourlomousis, P., Hopkins, L., Monie, T. P., Fitzgerald, K. A., & Bryant, C. E. (2013, Nov 15). Salmonella infection induces recruitment of Caspase-8 to the inflammasome to modulate IL-1beta production. *J Immunol, 191*(10), 5239-5246. https://doi.org/10.4049/jimmunol.1301581

Mandinova, A., Soldi, R., Graziani, I., Bagala, C., Bellum, S., Landriscina, M., Tarantini, F., Prudovsky, I., & Maciag, T. (2003, Jul 1). S100A13 mediates the copper-dependent stress-induced release of IL-1alpha from both human U937 and murine NIH 3T3 cells. *J Cell Sci, 116*(Pt 13), 2687-2696. https://doi.org/10.1242/jcs.00471

Mani-Babu, S., Morrissey, D., Waugh, C., Screen, H., & Barton, C. (2015, Mar). The effectiveness of extracorporeal shock wave therapy in lower limb tendinopathy: a systematic review. *Am J Sports Med, 43*(3), 752-761. https://doi.org/10.1177/0363546514531911

Manning, C. N., Havlioglu, N., Knutsen, E., Sakiyama-Elbert, S. E., Silva, M. J., Thomopoulos, S., & Gelberman, R. H. (2014, May). The early inflammatory response after flexor tendon healing: a gene expression and histological analysis. *J Orthop Res, 32*(5), 645-652. https://doi.org/10.1002/jor.22575

Manning, C. N., Martel, C., Sakiyama-Elbert, S. E., Silva, M. J., Shah, S., Gelberman, R. H., & Thomopoulos, S. (2015, Apr 16). Adipose-derived mesenchymal stromal cells modulate tendon fibroblast responses to macrophage-induced inflammation in vitro. *Stem Cell Res Ther, 6*, 74. https://doi.org/10.1186/s13287-015-0059-4

Mantovani, A., Cassatella, M. A., Costantini, C., & Jaillon, S. (2011, Jul 25). Neutrophils in the activation and regulation of innate and adaptive immunity. *Nat Rev Immunol, 11*(8), 519-531. https://doi.org/10.1038/nri3024

Mantovani, A., Sozzani, S., Locati, M., Allavena, P., & Sica, A. (2002, Nov). Macrophage polarization: tumor-associated macrophages as a paradigm for polarized M2 mononuclear phagocytes. *Trends Immunol, 23*(11), 549-555. https://doi.org/10.1016/s1471-4906(02)02302-5

Marchetti, C., Chojnacki, J., Toldo, S., Mezzaroma, E., Tranchida, N., Rose, S. W., Federici, M., Van Tassell, B. W., Zhang, S., & Abbate, A. (2014, Apr). A novel pharmacologic inhibitor of the NLRP3 inflammasome limits myocardial injury after ischemia-reperfusion in the mouse. *J Cardiovasc Pharmacol, 63*(4), 316-322. https://doi.org/10.1097/FJC.0000000000000053

Margalef, R., Bosque, M., Minaya-Munoz, F., Valera-Garrido, F., & Santafe, M. M. (2021, Oct). Safety analysis of percutaneous needle electrolysis: a study of needle composition, morphology, and electrical resistance. *Acupunct Med, 39*(5), 471-477. https://doi.org/10.1177/0964528420988007

Margalef, R., Bosque, M., Monclus, P., Flores, P., Minaya-Munoz, F., Valera-Garrido, F., & Santafe, M. M. (2020). Percutaneous Application of Galvanic Current in Rodents Reverses Signs of Myofascial Trigger Points. *Evid Based Complement Alternat Med, 2020*, 4173218. https://doi.org/10.1155/2020/4173218

Margalef, R., Minaya-Munoz, F., Valera-Garrido, F., & Santafe, M. M. (2019). Vasodilation secondary to exposure to galvanic currents. *Revista Fisioterapia Invasiva / Journal of Invasive Techniques in Physical Therapy, 02*(02), 107.

Mariathasan, S., & Monack, D. M. (2007, Jan). Inflammasome adaptors and sensors: intracellular regulators of infection and inflammation. *Nat Rev Immunol, 7*(1), 31-40. https://doi.org/10.1038/nri1997

Mariathasan, S., Newton, K., Monack, D. M., Vucic, D., French, D. M., Lee, W. P., Roose-Girma, M., Erickson, S., & Dixit, V. M. (2004, Jul 8). Differential activation of the inflammasome by caspase-1 adaptors ASC and Ipaf. *Nature, 430*(6996), 213-218. https://doi.org/10.1038/nature02664

Mariathasan, S., Weiss, D. S., Newton, K., McBride, J., O'Rourke, K., Roose-Girma, M., Lee, W. P., Weinrauch, Y., Monack, D. M., & Dixit, V. M. (2006, Mar 9). Cryopyrin activates the inflammasome in response to toxins and ATP. *Nature, 440*(7081), 228-232. https://doi.org/10.1038/nature04515

Marrakchi, S., Guigue, P., Renshaw, B. R., Puel, A., Pei, X. Y., Fraitag, S., Zribi, J., Bal, E., Cluzeau, C., Chrabieh, M., Towne, J. E., Douangpanya, J., Pons, C., Mansour, S., Serre, V., Makni,

H., Mahfoudh, N., Fakhfakh, F., Bodemer, C., Feingold, J., Hadj-Rabia, S., Favre, M., Genin, E., Sahbatou, M., Munnich, A., Casanova, J. L., Sims, J. E., Turki, H., Bachelez, H., & Smahi, A. (2011, Aug 18). Interleukin-36-receptor antagonist deficiency and generalized pustular psoriasis. *N Engl J Med, 365*(7), 620-628. https://doi.org/10.1056/NEJMoa1013068

Marsolais, D., Cote, C. H., & Frenette, J. (2001, Nov). Neutrophils and macrophages accumulate sequentially following Achilles tendon injury. *J Orthop Res, 19*(6), 1203-1209. https://doi.org/10.1016/S0736-0266(01)00031-6

Martinez-Garcia, J. J., Martinez-Banaclocha, H., Angosto-Bazarra, D., de Torre-Minguela, C., Baroja-Mazo, A., Alarcon-Vila, C., Martinez-Alarcon, L., Amores-Iniesta, J., Martin-Sanchez, F., Ercole, G. A., Martinez, C. M., Gonzalez-Lisorge, A., Fernandez-Pacheco, J., Martinez-Gil, P., Adriouch, S., Koch-Nolte, F., Lujan, J., Acosta-Villegas, F., Parrilla, P., Garcia-Palenciano, C., & Pelegrin, P. (2019, Jun 20). P2X7 receptor induces mitochondrial failure in monocytes and compromises NLRP3 inflammasome activation during sepsis. *Nat Commun, 10*(1), 2711. https://doi.org/10.1038/s41467-019-10626-x

Martinez, F. O., Helming, L., & Gordon, S. (2009). Alternative activation of macrophages: an immunologic functional perspective. *Annu Rev Immunol, 27*, 451-483. https://doi.org/10.1146/annurev.immunol.021908.132532

Martinon, F., Burns, K., & Tschopp, J. (2002, Aug). The inflammasome: a molecular platform triggering activation of inflammatory caspases and processing of proIL-beta. *Mol Cell, 10*(2), 417-426. https://doi.org/10.1016/s1097-2765(02)00599-3

Martinon, F., Mayor, A., & Tschopp, J. (2009). The inflammasomes: guardians of the body. *Annu Rev Immunol, 27*, 229-265. https://doi.org/10.1146/annurev.immunol.021908.132715

Martinon, F., Petrilli, V., Mayor, A., Tardivel, A., & Tschopp, J. (2006, Mar 9). Gout-associated uric acid crystals activate the NALP3 inflammasome. *Nature, 440*(7081), 237-241. https://doi.org/10.1038/nature04516

Marui, T., Niyibizi, C., Georgescu, H. I., Cao, M., Kavalkovich, K. W., Levine, R. E., & Woo, S. L. (1997, Jan). Effect of growth factors on matrix synthesis by ligament fibroblasts. *J Orthop Res, 15*(1), 18-23. https://doi.org/10.1002/jor.1100150104

Marzano, A. V., Borghi, A., Meroni, P. L., & Cugno, M. (2016, Nov). Pyoderma gangrenosum and its syndromic forms: evidence for a link with autoinflammation. *Br J Dermatol, 175*(5), 882-891. https://doi.org/10.1111/bjd.14691

Mascarenhas, D. P. A., Cerqueira, D. M., Pereira, M. S. F., Castanheira, F. V. S., Fernandes, T. D., Manin, G. Z., Cunha, L. D., & Zamboni, D. S. (2017, Aug). Inhibition of caspase-1 or gasdermin-D enable caspase-8 activation in the Naip5/NLRC4/ASC inflammasome. *PLoS Pathog, 13*(8), e1006502. https://doi.org/10.1371/journal.ppat.1006502

Masters, S. L., Lagou, V., Jeru, I., Baker, P. J., Van Eyck, L., Parry, D. A., Lawless, D., De Nardo, D., Garcia-Perez, J. E., Dagley, L. F., Holley, C. L., Dooley, J., Moghaddas, F., Pasciuto, E., Jeandel, P. Y., Sciot, R., Lyras, D., Webb, A. I., Nicholson, S. E., De Somer, L., van Nieuwenhove, E., Ruuth-Praz, J., Copin, B., Cochet, E., Medlej-Hashim, M., Megarbane, A., Schroder, K., Savic, S., Goris, A., Amselem, S., Wouters, C., & Liston, A. (2016, Mar 30). Familial autoinflammation with neutrophilic dermatosis reveals a regulatory mechanism of pyrin activation. *Sci Transl Med, 8*(332), 332ra345. https://doi.org/10.1126/scitranslmed.aaf1471

Matthews, T. J., Hand, G. C., Rees, J. L., Athanasou, N. A., & Carr, A. J. (2006, Apr). Pathology of the torn rotator cuff tendon. Reduction in potential for repair as tear size increases. *J Bone Joint Surg Br, 88*(4), 489-495. https://doi.org/10.1302/0301-620X.88B4.16845

Matusiak, M., Van Opdenbosch, N., Vande Walle, L., Sirard, J. C., Kanneganti, T. D., & Lamkanfi, M. (2015, Feb 3). Flagellin-induced NLRC4 phosphorylation primes the inflammasome for activation by NAIP5. *Proc Natl Acad Sci U S A, 112*(5), 1541-1546. https://doi.org/10.1073/pnas.1417945112

Mazieres, B., Rouanet, S., Guillon, Y., Scarsi, C., & Reiner, V. (2005, Aug). Topical ketoprofen patch in the treatment of tendinitis: a randomized, double blind, placebo controlled study. *J Rheumatol, 32*(8), 1563-1570. https://www.ncbi.nlm.nih.gov/pubmed/16078335

Mazodier, K., Marin, V., Novick, D., Farnarier, C., Robitail, S., Schleinitz, N., Veit, V., Paul, P., Rubinstein, M., Dinarello, C. A., Harle, J. R., & Kaplanski, G. (2005, Nov 15). Severe imbalance of IL-18/IL-18BP in patients with secondary hemophagocytic syndrome. *Blood, 106*(10), 3483-3489. https://doi.org/10.1182/blood-2005-05-1980

McDermott, M. F., Aksentijevich, I., Galon, J., McDermott, E. M., Ogunkolade, B. W., Centola, M., Mansfield, E., Gadina, M., Karenko, L., Pettersson, T., McCarthy, J., Frucht, D. M., Aringer, M., Torosyan, Y., Teppo, A. M., Wilson, M., Karaarslan, H. M., Wan, Y., Todd, I., Wood, G., Schlimgen, R., Kumarajeewa, T. R., Cooper, S. M., Vella, J. P., Amos, C. I., Mulley, J., Quane, K. A., Molloy, M. G., Ranki, A., Powell, R. J., Hitman, G. A., O'Shea, J. J., & Kastner, D. L. (1999, Apr 2). Germline mutations in the extracellular domains of the 55 kDa TNF receptor, TNFR1, define a family of dominantly inherited autoinflammatory syndromes. *Cell, 97*(1), 133-144. https://doi.org/10.1016/s0092-8674(00)80721-7

McGeough, M. D., Wree, A., Inzaugarat, M. E., Haimovich, A., Johnson, C. D., Pena, C. A., Goldbach-Mansky, R., Broderick, L., Feldstein, A. E., & Hoffman, H. M. (2017, Dec 1). TNF regulates transcription of NLRP3 inflammasome components and inflammatory molecules in cryopyrinopathies. *J Clin Invest, 127*(12), 4488-4497. https://doi.org/10.1172/JCI90699

Medina-Mirapeix, F., Garcia-Vidal, J. A., Escolar-Reina, P., & Martínez-Cáceres, C. M. (2019). Histopathological analysis of the inflammatory response of two invasive techniques in the calcaneal tendon of a mouse. *Revista Fisioterapia Invasiva / Journal of Invasive Techniques in Physical Therapy, 02*(02), 091.

Mehta, P., Cron, R. Q., Hartwell, J., Manson, J. J., & Tattersall, R. S. (2020, Jun). Silencing the cytokine storm: the use of intravenous anakinra in haemophagocytic lymphohistiocytosis or macrophage activation syndrome. *Lancet Rheumatol, 2*(6), e358-e367. https://doi.org/10.1016/S2665-9913(20)30096-5

Mensa-Vilaro, A., Teresa Bosque, M., Magri, G., Honda, Y., Martinez-Banaclocha, H., Casorran-Berges, M., Sintes, J., Gonzalez-Roca, E., Ruiz-Ortiz, E., Heike, T., Martinez-Garcia, J. J., Baroja-Mazo, A., Cerutti, A., Nishikomori, R., Yague, J., Pelegrin, P., Delgado-Beltran, C., & Arostegui, J. I. (2016, Dec). Brief Report: Late-Onset Cryopyrin-Associated Periodic Syndrome Due to Myeloid-Restricted Somatic NLRP3 Mosaicism. *Arthritis Rheumatol, 68*(12), 3035-3041. https://doi.org/10.1002/art.39770

Merolla, G., Dellabiancia, F., Ricci, A., Mussoni, M. P., Nucci, S., Zanoli, G., Paladini, P., & Porcellini, G. (2017, Jul). Arthroscopic Debridement Versus Platelet-Rich Plasma Injection: A Prospective, Randomized, Comparative Study of Chronic Lateral Epicondylitis With a Nearly 2-Year Follow-Up. *Arthroscopy, 33*(7), 1320-1329. https://doi.org/10.1016/j.arthro.2017.02.009

Meuwissen, M. E., Schot, R., Buta, S., Oudesluijs, G., Tinschert, S., Speer, S. D., Li, Z., van Unen, L., Heijsman, D., Goldmann, T., Lequin, M. H., Kros, J. M., Stam, W., Hermann, M., Willemsen, R., Brouwer, R. W., Van, I. W. F., Martin-Fernandez, M., de Coo, I., Dudink, J., de Vries, F. A., Bertoli Avella, A., Prinz, M., Crow, Y. J., Verheijen, F. W., Pellegrini, S., Bogunovic, D., & Mancini, G. M. (2016, Jun 27). Human USP18 deficiency underlies type 1

interferonopathy leading to severe pseudo-TORCH syndrome. *J Exp Med, 213*(7), 1163-1174. https://doi.org/10.1084/jem.20151529

Millar, N. L., Akbar, M., Campbell, A. L., Reilly, J. H., Kerr, S. C., McLean, M., Frleta-Gilchrist, M., Fazzi, U. G., Leach, W. J., Rooney, B. P., Crowe, L. A., Murrell, G. A., & McInnes, I. B. (2016, Jun 6). IL-17A mediates inflammatory and tissue remodelling events in early human tendinopathy. *Sci Rep, 6*, 27149. https://doi.org/10.1038/srep27149

Millar, N. L., Gilchrist, D. S., Akbar, M., Reilly, J. H., Kerr, S. C., Campbell, A. L., Murrell, G. A. C., Liew, F. Y., Kurowska-Stolarska, M., & McInnes, I. B. (2015, Apr 10). MicroRNA29a regulates IL-33-mediated tissue remodelling in tendon disease. *Nat Commun, 6*, 6774. https://doi.org/10.1038/ncomms7774

Millar, N. L., Murrell, G. A., & McInnes, I. B. (2013, May). Alarmins in tendinopathy: unravelling new mechanisms in a common disease. *Rheumatology (Oxford), 52*(5), 769-779. https://doi.org/10.1093/rheumatology/kes409

Millar, N. L., Murrell, G. A., & McInnes, I. B. (2017, Jan 25). Inflammatory mechanisms in tendinopathy - towards translation. *Nat Rev Rheumatol, 13*(2), 110-122. https://doi.org/10.1038/nrrheum.2016.213

Millar, N. L., Silbernagel, K. G., Thorborg, K., Kirwan, P. D., Galatz, L. M., Abrams, G. D., Murrell, G. A. C., McInnes, I. B., & Rodeo, S. A. (2021, Jan 7). Tendinopathy. *Nat Rev Dis Primers, 7*(1), 1. https://doi.org/10.1038/s41572-020-00234-1

Mishra, A. K., Skrepnik, N. V., Edwards, S. G., Jones, G. L., Sampson, S., Vermillion, D. A., Ramsey, M. L., Karli, D. C., & Rettig, A. C. (2014, Feb). Efficacy of platelet-rich plasma for chronic tennis elbow: a double-blind, prospective, multicenter, randomized controlled trial of 230 patients. *Am J Sports Med, 42*(2), 463-471. https://doi.org/10.1177/0363546513494359

Mizushina, Y., Karasawa, T., Aizawa, K., Kimura, H., Watanabe, S., Kamata, R., Komada, T., Mato, N., Kasahara, T., Koyama, S., Bando, M., Hagiwara, K., & Takahashi, M. (2019, Jul 1). Inflammasome-Independent and Atypical Processing of IL-1beta Contributes to Acid Aspiration-Induced Acute Lung Injury. *J Immunol, 203*(1), 236-246. https://doi.org/10.4049/jimmunol.1900168

Moghaddas, F., Llamas, R., De Nardo, D., Martinez-Banaclocha, H., Martinez-Garcia, J. J., Mesa-Del-Castillo, P., Baker, P. J., Gargallo, V., Mensa-Vilaro, A., Canna, S., Wicks, I. P., Pelegrin, P., Arostegui, J. I., & Masters, S. L. (2017, Dec). A novel Pyrin-Associated Autoinflammation with Neutrophilic Dermatosis mutation further defines 14-3-3 binding of pyrin and distinction to Familial Mediterranean Fever. *Ann Rheum Dis, 76*(12), 2085-2094. https://doi.org/10.1136/annrheumdis-2017-211473

Moghaddas, F., Zeng, P., Zhang, Y., Schutzle, H., Brenner, S., Hofmann, S. R., Berner, R., Zhao, Y., Lu, B., Chen, X., Zhang, L., Cheng, S., Winkler, S., Lehmberg, K., Canna, S. W., Czabotar, P. E., Wicks, I. P., De Nardo, D., Hedrich, C. M., Zeng, H., & Masters, S. L. (2018, Dec). Autoinflammatory mutation in NLRC4 reveals a leucine-rich repeat (LRR)-LRR oligomerization interface. *J Allergy Clin Immunol, 142*(6), 1956-1967 e1956. https://doi.org/10.1016/j.jaci.2018.04.033

Mohamadi, A., Chan, J. J., Claessen, F. M., Ring, D., & Chen, N. C. (2017, Jan). Corticosteroid Injections Give Small and Transient Pain Relief in Rotator Cuff Tendinosis: A Meta-analysis. *Clin Orthop Relat Res, 475*(1), 232-243. https://doi.org/10.1007/s11999-016-5002-1

Molloy, T., Wang, Y., & Murrell, G. (2003). The roles of growth factors in tendon and ligament healing. *Sports Med, 33*(5), 381-394. https://doi.org/10.2165/00007256-200333050-00004

Monaco, C., Nanchahal, J., Taylor, P., & Feldmann, M. (2015, Jan). Anti-TNF therapy: past, present and future. *Int Immunol, 27*(1), 55-62. https://doi.org/10.1093/intimm/dxu102

Mora, J., Schlemmer, A., Wittig, I., Richter, F., Putyrski, M., Frank, A. C., Han, Y., Jung, M., Ernst, A., Weigert, A., & Brune, B. (2016, Oct 1). Interleukin-38 is released from apoptotic cells to limit inflammatory macrophage responses. *J Mol Cell Biol, 8*(5), 426-438. https://doi.org/10.1093/jmcb/mjw006

Moreno, C., Mattiussi, G., Nunez, F. J., Messina, G., & Rejc, E. (2017, Oct). Intratissue percutaneous electolysis combined with active physical therapy for the treatment of adductor longus enthesopathy-related groin pain: a randomized trial. *J Sports Med Phys Fitness, 57*(10), 1318-1329. https://doi.org/10.23736/S0022-4707.16.06466-5

Mosser, D. M., & Edwards, J. P. (2008, Dec). Exploring the full spectrum of macrophage activation. *Nat Rev Immunol, 8*(12), 958-969. https://doi.org/10.1038/nri2448

Motojima, M., Matsusaka, T., Kon, V., & Ichikawa, I. (2010). Fibrinogen that appears in Bowman's space of proteinuric kidneys in vivo activates podocyte Toll-like receptors 2 and 4 in vitro. *Nephron Exp Nephrol, 114*(2), e39-47. https://doi.org/10.1159/000254390

Muhl, H., Kampfer, H., Bosmann, M., Frank, S., Radeke, H., & Pfeilschifter, J. (2000, Jan 27). Interferon-gamma mediates gene expression of IL-18 binding protein in nonleukocytic cells. *Biochem Biophys Res Commun, 267*(3), 960-963. https://doi.org/10.1006/bbrc.1999.2064

Munger, J. S., Harpel, J. G., Gleizes, P. E., Mazzieri, R., Nunes, I., & Rifkin, D. B. (1997, May). Latent transforming growth factor-beta: structural features and mechanisms of activation. *Kidney Int, 51*(5), 1376-1382. https://doi.org/10.1038/ki.1997.188

Munoz-Planillo, R., Kuffa, P., Martinez-Colon, G., Smith, B. L., Rajendiran, T. M., & Nunez, G. (2013, Jun 27). K(+) efflux is the common trigger of NLRP3 inflammasome activation by bacterial toxins and particulate matter. *Immunity, 38*(6), 1142-1153. https://doi.org/10.1016/j.immuni.2013.05.016

Munzer, P., Negro, R., Fukui, S., di Meglio, L., Aymonnier, K., Chu, L., Cherpokova, D., Gutch, S., Sorvillo, N., Shi, L., Magupalli, V. G., Weber, A. N. R., Scharf, R. E., Waterman, C. M., Wu, H., & Wagner, D. D. (2021). NLRP3 Inflammasome Assembly in Neutrophils Is Supported by PAD4 and Promotes NETosis Under Sterile Conditions. *Front Immunol, 12*, 683803. https://doi.org/10.3389/fimmu.2021.683803

Murakami, M., Hibi, M., Nakagawa, N., Nakagawa, T., Yasukawa, K., Yamanishi, K., Taga, T., & Kishimoto, T. (1993, Jun 18). IL-6-induced homodimerization of gp130 and associated activation of a tyrosine kinase. *Science, 260*(5115), 1808-1810. https://doi.org/10.1126/science.8511589

Murphy, K., & Weaver, C. (2017). *Janeway's Immunobiology 9th edition*. Garland Science.

Murtaugh, B., & Ihm, J. M. (2013, May-Jun). Eccentric training for the treatment of tendinopathies. *Curr Sports Med Rep, 12*(3), 175-182. https://doi.org/10.1249/JSR.0b013e3182933761

Nadif, R., Zerimech, F., Bouzigon, E., & Matran, R. (2013, Oct). The role of eosinophils and basophils in allergic diseases considering genetic findings. *Curr Opin Allergy Clin Immunol, 13*(5), 507-513. https://doi.org/10.1097/ACI.0b013e328364e9c0

Nakama, K., Gotoh, M., Yamada, T., Mitsui, Y., Yasukawa, H., Imaizumi, T., Higuchi, F., & Nagata, K. (2006, Nov-Dec). Interleukin-6-induced activation of signal transducer and activator of transcription-3 in ruptured rotator cuff tendon. *J Int Med Res, 34*(6), 624-631. https://doi.org/10.1177/147323000603400607

Nakanishi, K., Yoshimoto, T., Tsutsui, H., & Okamura, H. (2001, Mar). Interleukin-18 is a unique cytokine that stimulates both Th1 and Th2 responses depending on its cytokine milieu. *Cytokine Growth Factor Rev, 12*(1), 53-72. https://doi.org/10.1016/s1359-6101(00)00015-0

Nanda, J. D., Jung, C. J., Satria, R. D., Jhan, M. K., Shen, T. J., Tseng, P. C., Wang, Y. T., Ho, T. S., & Lin, C. F. (2021). Serum IL-18 Is a Potential Biomarker for Predicting Severe Dengue Disease Progression. *J Immunol Res, 2021*, 7652569. https://doi.org/10.1155/2021/7652569

Natsu-ume, T., Nakamura, N., Shino, K., Toritsuka, Y., Horibe, S., & Ochi, T. (1997, Nov). Temporal and spatial expression of transforming growth factor-beta in the healing patellar ligament of the rat. *J Orthop Res, 15*(6), 837-843. https://doi.org/10.1002/jor.1100150608

Nauwelaers, A. K., Van Oost, L., & Peers, K. (2021, Jul). Evidence for the use of PRP in chronic midsubstance Achilles tendinopathy: A systematic review with meta-analysis. *Foot Ankle Surg, 27*(5), 486-495. https://doi.org/10.1016/j.fas.2020.07.009

Neves, J. F., Doffinger, R., Barcena-Morales, G., Martins, C., Papapietro, O., Plagnol, V., Curtis, J., Martins, M., Kumararatne, D., Cordeiro, A. I., Neves, C., Borrego, L. M., Katan, M., & Nejentsev, S. (2018). Novel PLCG2 Mutation in a Patient With APLAID and Cutis Laxa. *Front Immunol, 9*, 2863. https://doi.org/10.3389/fimmu.2018.02863

Neviaser, A., Andarawis-Puri, N., & Flatow, E. (2012, Feb). Basic mechanisms of tendon fatigue damage. *J Shoulder Elbow Surg, 21*(2), 158-163. https://doi.org/10.1016/j.jse.2011.11.014

Nevins, E. J., & Kanakala, V. (2020, Dec). Topical diltiazem and glyceryl-trinitrate for chronic anal fissure: A meta-analysis of randomised controlled trials. *Turk J Surg, 36*(4), 347-352. https://doi.org/10.47717/turkjsurg.2020.4895

Newton, K., & Dixit, V. M. (2012, Mar 1). Signaling in innate immunity and inflammation. *Cold Spring Harb Perspect Biol, 4*(3). https://doi.org/10.1101/cshperspect.a006049

Ngo, M., Pham, H., Longaker, M. T., & Chang, J. (2001, Oct). Differential expression of transforming growth factor-beta receptors in a rabbit zone II flexor tendon wound healing model. *Plast Reconstr Surg, 108*(5), 1260-1267. https://doi.org/10.1097/00006534-200110000-00025

Niethammer, P., Grabher, C., Look, A. T., & Mitchison, T. J. (2009, Jun 18). A tissue-scale gradient of hydrogen peroxide mediates rapid wound detection in zebrafish. *Nature, 459*(7249), 996-999. https://doi.org/10.1038/nature08119

Nigrovic, P. A., Lee, P. Y., & Hoffman, H. M. (2020, Nov). Monogenic autoinflammatory disorders: Conceptual overview, phenotype, and clinical approach. *J Allergy Clin Immunol, 146*(5), 925-937. https://doi.org/10.1016/j.jaci.2020.08.017

Nold-Petry, C. A., Lo, C. Y., Rudloff, I., Elgass, K. D., Li, S., Gantier, M. P., Lotz-Havla, A. S., Gersting, S. W., Cho, S. X., Lao, J. C., Ellisdon, A. M., Rotter, B., Azam, T., Mangan, N. E., Rossello, F. J., Whisstock, J. C., Bufler, P., Garlanda, C., Mantovani, A., Dinarello, C. A., & Nold, M. F. (2015, Apr). IL-37 requires the receptors IL-18Ralpha and IL-1R8 (SIGIRR) to carry out its multifaceted anti-inflammatory program upon innate signal transduction. *Nat Immunol, 16*(4), 354-365. https://doi.org/10.1038/ni.3103

Nold, M. F., Nold-Petry, C. A., Zepp, J. A., Palmer, B. E., Bufler, P., & Dinarello, C. A. (2010, Nov). IL-37 is a fundamental inhibitor of innate immunity. *Nat Immunol, 11*(11), 1014-1022. https://doi.org/10.1038/ni.1944

Novick, D., Schwartsburd, B., Pinkus, R., Suissa, D., Belzer, I., Sthoeger, Z., Keane, W. F., Chvatchko, Y., Kim, S. H., Fantuzzi, G., Dinarello, C. A., & Rubinstein, M. (2001, Jun 21). A

novel IL-18BP ELISA shows elevated serum IL-18BP in sepsis and extensive decrease of free IL-18. *Cytokine, 14*(6), 334-342. https://doi.org/10.1006/cyto.2001.0914

O'Neill, S., Radia, J., Bird, K., Rathleff, M. S., Bandholm, T., Jorgensen, M., & Thorborg, K. (2019, Sep). Acute sensory and motor response to 45-s heavy isometric holds for the plantar flexors in patients with Achilles tendinopathy. *Knee Surg Sports Traumatol Arthrosc, 27*(9), 2765-2773. https://doi.org/10.1007/s00167-018-5050-z

Ochoa, M. C., Minute, L., Rodriguez, I., Garasa, S., Perez-Ruiz, E., Inoges, S., Melero, I., & Berraondo, P. (2017, Apr). Antibody-dependent cell cytotoxicity: immunotherapy strategies enhancing effector NK cells. *Immunol Cell Biol, 95*(4), 347-355. https://doi.org/10.1038/icb.2017.6

Ohberg, L., & Alfredson, H. (2002, Jun). Ultrasound guided sclerosis of neovessels in painful chronic Achilles tendinosis: pilot study of a new treatment. *Br J Sports Med, 36*(3), 173-175; discussion 176-177. https://doi.org/10.1136/bjsm.36.3.173

Okondo, M. C., Johnson, D. C., Sridharan, R., Go, E. B., Chui, A. J., Wang, M. S., Poplawski, S. E., Wu, W., Liu, Y., Lai, J. H., Sanford, D. G., Arciprete, M. O., Golub, T. R., Bachovchin, W. W., & Bachovchin, D. A. (2017, Jan). DPP8 and DPP9 inhibition induces pro-caspase-1-dependent monocyte and macrophage pyroptosis. *Nat Chem Biol, 13*(1), 46-53. https://doi.org/10.1038/nchembio.2229

Okondo, M. C., Rao, S. D., Taabazuing, C. Y., Chui, A. J., Poplawski, S. E., Johnson, D. C., & Bachovchin, D. A. (2018, Mar 15). Inhibition of Dpp8/9 Activates the Nlrp1b Inflammasome. *Cell Chem Biol, 25*(3), 262-267 e265. https://doi.org/10.1016/j.chembiol.2017.12.013

Oreff, G. L., Fenu, M., Vogl, C., Ribitsch, I., & Jenner, F. (2021, Jun 14). Species variations in tenocytes' response to inflammation require careful selection of animal models for tendon research. *Sci Rep, 11*(1), 12451. https://doi.org/10.1038/s41598-021-91914-9

Otterdal, K., Berg, A., Michelsen, A. E., Yndestad, A., Patel, S., Gregersen, I., Halvorsen, B., Ueland, T., Langeland, N., & Aukrust, P. (2021, Oct 18). IL-18 and IL-18 binding protein are related to disease severity and parasitemia during falciparum malaria. *BMC Infect Dis, 21*(1), 1073. https://doi.org/10.1186/s12879-021-06751-y

Park, B. S., Song, D. H., Kim, H. M., Choi, B. S., Lee, H., & Lee, J. O. (2009, Apr 30). The structural basis of lipopolysaccharide recognition by the TLR4-MD-2 complex. *Nature, 458*(7242), 1191-1195. https://doi.org/10.1038/nature07830

Park, Y. H., Wood, G., Kastner, D. L., & Chae, J. J. (2016, Aug). Pyrin inflammasome activation and RhoA signaling in the autoinflammatory diseases FMF and HIDS. *Nat Immunol, 17*(8), 914-921. https://doi.org/10.1038/ni.3457

Pase, L., Layton, J. E., Wittmann, C., Ellett, F., Nowell, C. J., Reyes-Aldasoro, C. C., Varma, S., Rogers, K. L., Hall, C. J., Keightley, M. C., Crosier, P. S., Grabher, C., Heath, J. K., Renshaw, S. A., & Lieschke, G. J. (2012, Oct 9). Neutrophil-delivered myeloperoxidase dampens the hydrogen peroxide burst after tissue wounding in zebrafish. *Curr Biol, 22*(19), 1818-1824. https://doi.org/10.1016/j.cub.2012.07.060

Pasqual, G., Chudnovskiy, A., Tas, J. M. J., Agudelo, M., Schweitzer, L. D., Cui, A., Hacohen, N., & Victora, G. D. (2018, Jan 25). Monitoring T cell-dendritic cell interactions in vivo by intercellular enzymatic labelling. *Nature, 553*(7689), 496-500. https://doi.org/10.1038/nature25442

Pelegrin, P., & Surprenant, A. (2009, Jul 22). Dynamics of macrophage polarization reveal new mechanism to inhibit IL-1beta release through pyrophosphates. *EMBO J, 28*(14), 2114-2127. https://doi.org/10.1038/emboj.2009.163

Petrasek, J., Bala, S., Csak, T., Lippai, D., Kodys, K., Menashy, V., Barrieau, M., Min, S. Y., Kurt-Jones, E. A., & Szabo, G. (2012, Oct). IL-1 receptor antagonist ameliorates inflammasome-dependent alcoholic steatohepatitis in mice. *J Clin Invest, 122*(10), 3476-3489. https://doi.org/10.1172/JCI60777

Petretto, A., Bruschi, M., Pratesi, F., Croia, C., Candiano, G., Ghiggeri, G., & Migliorini, P. (2019). Neutrophil extracellular traps (NET) induced by different stimuli: A comparative proteomic analysis. *PLoS One, 14*(7), e0218946. https://doi.org/10.1371/journal.pone.0218946

Petrilli, V., Papin, S., Dostert, C., Mayor, A., Martinon, F., & Tschopp, J. (2007, Sep). Activation of the NALP3 inflammasome is triggered by low intracellular potassium concentration. *Cell Death Differ, 14*(9), 1583-1589. https://doi.org/10.1038/sj.cdd.4402195

Pillay, J., den Braber, I., Vrisekoop, N., Kwast, L. M., de Boer, R. J., Borghans, J. A., Tesselaar, K., & Koenderman, L. (2010, Jul 29). In vivo labeling with 2H2O reveals a human neutrophil lifespan of 5.4 days. *Blood, 116*(4), 625-627. https://doi.org/10.1182/blood-2010-01-259028

Pizzirani, C., Ferrari, D., Chiozzi, P., Adinolfi, E., Sandona, D., Savaglio, E., & Di Virgilio, F. (2007, May 1). Stimulation of P2 receptors causes release of IL-1beta-loaded microvesicles from human dendritic cells. *Blood, 109*(9), 3856-3864. https://doi.org/10.1182/blood-2005-06-031377

Prager, I., Liesche, C., van Ooijen, H., Urlaub, D., Verron, Q., Sandstrom, N., Fasbender, F., Claus, M., Eils, R., Beaudouin, J., Onfelt, B., & Watzl, C. (2019, Sep 2). NK cells switch from granzyme B to death receptor-mediated cytotoxicity during serial killing. *J Exp Med, 216*(9), 2113-2127. https://doi.org/10.1084/jem.20181454

Prieur, A. M., Kaufmann, M. T., Griscelli, C., & Dayer, J. M. (1987, Nov 28). Specific interleukin-1 inhibitor in serum and urine of children with systemic juvenile chronic arthritis. *Lancet, 2*(8570), 1240-1242. https://doi.org/10.1016/s0140-6736(87)91854-x

Prochnicki, T., Mangan, M. S., & Latz, E. (2016). Recent insights into the molecular mechanisms of the NLRP3 inflammasome activation. *F1000Res, 5*. https://doi.org/10.12688/f1000research.8614.1

Pufe, T., Petersen, W., Tillmann, B., & Mentlein, R. (2001, Oct). The angiogenic peptide vascular endothelial growth factor is expressed in foetal and ruptured tendons. *Virchows Arch, 439*(4), 579-585. https://doi.org/10.1007/s004280100422

Puzzitiello, R. N., Patel, B. H., Nwachukwu, B. U., Allen, A. A., Forsythe, B., & Salzler, M. J. (2020, May). Adverse Impact of Corticosteroid Injection on Rotator Cuff Tendon Health and Repair: A Systematic Review. *Arthroscopy, 36*(5), 1468-1475. https://doi.org/10.1016/j.arthro.2019.12.006

Py, B. F., Kim, M. S., Vakifahmetoglu-Norberg, H., & Yuan, J. (2013, Jan 24). Deubiquitination of NLRP3 by BRCC3 critically regulates inflammasome activity. *Mol Cell, 49*(2), 331-338. https://doi.org/10.1016/j.molcel.2012.11.009

Qi, J., Chi, L., Maloney, M., Yang, X., Bynum, D., & Banes, A. J. (2006, Oct). Interleukin-1beta increases elasticity of human bioartificial tendons. *Tissue Eng, 12*(10), 2913-2925. https://doi.org/10.1089/ten.2006.12.2913

Qi, J., Fox, A. M., Alexopoulos, L. G., Chi, L., Bynum, D., Guilak, F., & Banes, A. J. (2006, Jul). IL-1beta decreases the elastic modulus of human tenocytes. *J Appl Physiol (1985), 101*(1), 189-195. https://doi.org/10.1152/japplphysiol.01128.2005

Qu, Y., Misaghi, S., Izrael-Tomasevic, A., Newton, K., Gilmour, L. L., Lamkanfi, M., Louie, S., Kayagaki, N., Liu, J., Komuves, L., Cupp, J. E., Arnott, D., Monack, D., & Dixit, V. M. (2012, Oct 25). Phosphorylation of NLRC4 is critical for inflammasome activation. *Nature, 490*(7421), 539-542. https://doi.org/10.1038/nature11429

Raghawan, A. K., Ramaswamy, R., Radha, V., & Swarup, G. (2019, Oct 22). HSC70 regulates cold-induced caspase-1 hyperactivation by an autoinflammation-causing mutant of cytoplasmic immune receptor NLRC4. *Proc Natl Acad Sci U S A, 116*(43), 21694-21703. https://doi.org/10.1073/pnas.1905261116

Raghawan, A. K., Sripada, A., Gopinath, G., Pushpanjali, P., Kumar, Y., Radha, V., & Swarup, G. (2017, Jan 27). A Disease-associated Mutant of NLRC4 Shows Enhanced Interaction with SUG1 Leading to Constitutive FADD-dependent Caspase-8 Activation and Cell Death. *J Biol Chem, 292*(4), 1218-1230. https://doi.org/10.1074/jbc.M116.763979

Randolph, G. J., Beaulieu, S., Lebecque, S., Steinman, R. M., & Muller, W. A. (1998, Oct 16). Differentiation of monocytes into dendritic cells in a model of transendothelial trafficking. *Science, 282*(5388), 480-483. https://doi.org/10.1126/science.282.5388.480

Rathinam, V. A., Vanaja, S. K., & Fitzgerald, K. A. (2012, Mar 19). Regulation of inflammasome signaling. *Nat Immunol, 13*(4), 333-342. https://doi.org/10.1038/ni.2237

Rauch, I., Deets, K. A., Ji, D. X., von Moltke, J., Tenthorey, J. L., Lee, A. Y., Philip, N. H., Ayres, J. S., Brodsky, I. E., Gronert, K., & Vance, R. E. (2017, Apr 18). NAIP-NLRC4 Inflammasomes Coordinate Intestinal Epithelial Cell Expulsion with Eicosanoid and IL-18 Release via Activation of Caspase-1 and -8. *Immunity, 46*(4), 649-659. https://doi.org/10.1016/j.immuni.2017.03.016

Rayamajhi, M., Zak, D. E., Chavarria-Smith, J., Vance, R. E., & Miao, E. A. (2013, Oct 15). Cutting edge: Mouse NAIP1 detects the type III secretion system needle protein. *J Immunol, 191*(8), 3986-3989. https://doi.org/10.4049/jimmunol.1301549

Reddy, S., Jia, S., Geoffrey, R., Lorier, R., Suchi, M., Broeckel, U., Hessner, M. J., & Verbsky, J. (2009, Jun 4). An autoinflammatory disease due to homozygous deletion of the IL1RN locus. *N Engl J Med, 360*(23), 2438-2444. https://doi.org/10.1056/NEJMoa0809568

Reed, J. C., Doctor, K., Rojas, A., Zapata, J. M., Stehlik, C., Fiorentino, L., Damiano, J., Roth, W., Matsuzawa, S., Newman, R., Takayama, S., Marusawa, H., Xu, F., Salvesen, G., Godzik, A., Group, R. G., & Members, G. S. L. (2003, Jun). Comparative analysis of apoptosis and inflammation genes of mice and humans. *Genome Res, 13*(6B), 1376-1388. https://doi.org/10.1101/gr.1053803

Regan, W., Wold, L. E., Coonrad, R., & Morrey, B. F. (1992, Nov-Dec). Microscopic histopathology of chronic refractory lateral epicondylitis. *Am J Sports Med, 20*(6), 746-749. https://doi.org/10.1177/036354659202000618

Reinholz, M., Kawakami, Y., Salzer, S., Kreuter, A., Dombrowski, Y., Koglin, S., Kresse, S., Ruzicka, T., & Schauber, J. (2013, Oct). HPV16 activates the AIM2 inflammasome in keratinocytes. *Arch Dermatol Res, 305*(8), 723-732. https://doi.org/10.1007/s00403-013-1375-0

Reis, E. S., Mastellos, D. C., Hajishengallis, G., & Lambris, J. D. (2019, Aug). New insights into the immune functions of complement. *Nat Rev Immunol, 19*(8), 503-516. https://doi.org/10.1038/s41577-019-0168-x

Rex, D. A. B., Agarwal, N., Prasad, T. S. K., Kandasamy, R. K., Subbannayya, Y., & Pinto, S. M. (2020, Jun). A comprehensive pathway map of IL-18-mediated signalling. *J Cell Commun Signal, 14*(2), 257-266. https://doi.org/10.1007/s12079-019-00544-4

Ricchetti, E. T., Reddy, S. C., Ansorge, H. L., Zgonis, M. H., Van Kleunen, J. P., Liechty, K. W., Soslowsky, L. J., & Beredjiklian, P. K. (2008, Dec). Effect of interleukin-10 overexpression on the properties of healing tendon in a murine patellar tendon model. *J Hand Surg Am, 33*(10), 1843-1852. https://doi.org/10.1016/j.jhsa.2008.07.020

Rider, P., Carmi, Y., Guttman, O., Braiman, A., Cohen, I., Voronov, E., White, M. R., Dinarello, C. A., & Apte, R. N. (2011, Nov 1). IL-1alpha and IL-1beta recruit different myeloid cells and promote different stages of sterile inflammation. *J Immunol, 187*(9), 4835-4843. https://doi.org/10.4049/jimmunol.1102048

Ridiandries, A., Tan, J. T. M., & Bursill, C. A. (2018, Oct 18). The Role of Chemokines in Wound Healing. *Int J Mol Sci, 19*(10). https://doi.org/10.3390/ijms19103217

Riel, H., Vicenzino, B., Jensen, M. B., Olesen, J. L., Holden, S., & Rathleff, M. S. (2018, Dec). The effect of isometric exercise on pain in individuals with plantar fasciopathy: A randomized crossover trial. *Scand J Med Sci Sports, 28*(12), 2643-2650. https://doi.org/10.1111/sms.13296

Rincon, M. (2012, Nov). Interleukin-6: from an inflammatory marker to a target for inflammatory diseases. *Trends Immunol, 33*(11), 571-577. https://doi.org/10.1016/j.it.2012.07.003

Rio, E., Kidgell, D., Purdam, C., Gaida, J., Moseley, G. L., Pearce, A. J., & Cook, J. (2015, Oct). Isometric exercise induces analgesia and reduces inhibition in patellar tendinopathy. *Br J Sports Med, 49*(19), 1277-1283. https://doi.org/10.1136/bjsports-2014-094386

Robertson, M. J., Mier, J. W., Logan, T., Atkins, M., Koon, H., Koch, K. M., Kathman, S., Pandite, L. N., Oei, C., Kirby, L. C., Jewell, R. C., Bell, W. N., Thurmond, L. M., Weisenbach, J., Roberts, S., & Dar, M. M. (2006, Jul 15). Clinical and biological effects of recombinant human interleukin-18 administered by intravenous infusion to patients with advanced cancer. *Clin Cancer Res, 12*(14 Pt 1), 4265-4273. https://doi.org/10.1158/1078-0432.CCR-06-0121

Rodriguez-Huguet, M., Gongora-Rodriguez, J., Rodriguez-Huguet, P., Ibanez-Vera, A. J., Rodriguez-Almagro, D., Martin-Valero, R., Diaz-Fernandez, A., & Lomas-Vega, R. (2020, Jun 12). Effectiveness of Percutaneous Electrolysis in Supraspinatus Tendinopathy: A Single-Blinded Randomized Controlled Trial. *J Clin Med, 9*(6). https://doi.org/10.3390/jcm9061837

Romanowska-Prochnicka, K., Felis-Giemza, A., Olesinska, M., Wojdasiewicz, P., Paradowska-Gorycka, A., & Szukiewicz, D. (2021, Mar 13). The Role of TNF-alpha and Anti-TNF-alpha Agents during Preconception, Pregnancy, and Breastfeeding. *Int J Mol Sci, 22*(6). https://doi.org/10.3390/ijms22062922

Romberg, N., Al Moussawi, K., Nelson-Williams, C., Stiegler, A. L., Loring, E., Choi, M., Overton, J., Meffre, E., Khokha, M. K., Huttner, A. J., West, B., Podoltsev, N. A., Boggon, T. J., Kazmierczak, B. I., & Lifton, R. P. (2014, Oct). Mutation of NLRC4 causes a syndrome of enterocolitis and autoinflammation. *Nat Genet, 46*(10), 1135-1139. https://doi.org/10.1038/ng.3066

Rossaint, J., Herter, J. M., Van Aken, H., Napirei, M., Doring, Y., Weber, C., Soehnlein, O., & Zarbock, A. (2014, Apr 17). Synchronized integrin engagement and chemokine activation is crucial in neutrophil extracellular trap-mediated sterile inflammation. *Blood, 123*(16), 2573-2584. https://doi.org/10.1182/blood-2013-07-516484

Rowczenio, D. M., Gomes, S. M., Arostegui, J. I., Mensa-Vilaro, A., Omoyinmi, E., Trojer, H., Baginska, A., Baroja-Mazo, A., Pelegrin, P., Savic, S., Lane, T., Williams, R., Brogan, P., Lachmann, H. J., & Hawkins, P. N. (2017). Late-Onset Cryopyrin-Associated Periodic Syndromes Caused by Somatic NLRP3 Mosaicism-UK Single Center Experience. *Front Immunol, 8*, 1410. https://doi.org/10.3389/fimmu.2017.01410

Rowe, S. J., Allen, L., Ridger, V. C., Hellewell, P. G., & Whyte, M. K. (2002, Dec 1). Caspase-1-deficient mice have delayed neutrophil apoptosis and a prolonged inflammatory response to lipopolysaccharide-induced acute lung injury. *J Immunol, 169*(11), 6401-6407. https://doi.org/10.4049/jimmunol.169.11.6401

Ruhl, S., Shkarina, K., Demarco, B., Heilig, R., Santos, J. C., & Broz, P. (2018, Nov 23). ESCRT-dependent membrane repair negatively regulates pyroptosis downstream of GSDMD activation. *Science, 362*(6417), 956-960. https://doi.org/10.1126/science.aar7607

Rutgeerts, P., Sandborn, W. J., Feagan, B. G., Reinisch, W., Olson, A., Johanns, J., Travers, S., Rachmilewitz, D., Hanauer, S. B., Lichtenstein, G. R., de Villiers, W. J., Present, D., Sands, B. E., & Colombel, J. F. (2005, Dec 8). Infliximab for induction and maintenance therapy for ulcerative colitis. *N Engl J Med, 353*(23), 2462-2476. https://doi.org/10.1056/NEJMoa050516

Said-Sadier, N., & Ojcius, D. M. (2012, Nov-Dec). Alarmins, inflammasomes and immunity. *Biomed J, 35*(6), 437-449. https://doi.org/10.4103/2319-4170.104408

Salama, C., Han, J., Yau, L., Reiss, W. G., Kramer, B., Neidhart, J. D., Criner, G. J., Kaplan-Lewis, E., Baden, R., Pandit, L., Cameron, M. L., Garcia-Diaz, J., Chavez, V., Mekebeb-Reuter, M., Lima de Menezes, F., Shah, R., Gonzalez-Lara, M. F., Assman, B., Freedman, J., & Mohan, S. V. (2021, Jan 7). Tocilizumab in Patients Hospitalized with Covid-19 Pneumonia. *N Engl J Med, 384*(1), 20-30. https://doi.org/10.1056/NEJMoa2030340

Sanchez-Sanchez, J. L., Calderon-Diez, L., Herrero-Turrion, J., Mendez-Sanchez, R., Arias-Buria, J. L., & Fernandez-de-Las-Penas, C. (2020, Oct 15). Changes in Gene Expression Associated with Collagen Regeneration and Remodeling of Extracellular Matrix after Percutaneous Electrolysis on Collagenase-Induced Achilles Tendinopathy in an Experimental Animal Model: A Pilot Study. *J Clin Med, 9*(10). https://doi.org/10.3390/jcm9103316

Sandanger, O., Ranheim, T., Vinge, L. E., Bliksoen, M., Alfsnes, K., Finsen, A. V., Dahl, C. P., Askevold, E. T., Florholmen, G., Christensen, G., Fitzgerald, K. A., Lien, E., Valen, G., Espevik, T., Aukrust, P., & Yndestad, A. (2013, Jul 1). The NLRP3 inflammasome is up-regulated in cardiac fibroblasts and mediates myocardial ischaemia-reperfusion injury. *Cardiovasc Res, 99*(1), 164-174. https://doi.org/10.1093/cvr/cvt091

Sandstrom, A., Mitchell, P. S., Goers, L., Mu, E. W., Lesser, C. F., & Vance, R. E. (2019, Apr 5). Functional degradation: A mechanism of NLRP1 inflammasome activation by diverse pathogen enzymes. *Science, 364*(6435). https://doi.org/10.1126/science.aau1330

Sanjabi, S., Mosaheb, M. M., & Flavell, R. A. (2009, Jul 17). Opposing effects of TGF-beta and IL-15 cytokines control the number of short-lived effector CD8+ T cells. *Immunity, 31*(1), 131-144. https://doi.org/10.1016/j.immuni.2009.04.020

Schindler, R., Ghezzi, P., & Dinarello, C. A. (1990, Mar 15). IL-1 induces IL-1. IV. IFN-gamma suppresses IL-1 but not lipopolysaccharide-induced transcription of IL-1. *J Immunol, 144*(6), 2216-2222. https://www.ncbi.nlm.nih.gov/pubmed/2107255

Schmacke, N. A., Gaidt, M. M., Szymanska, I., O'Duill, F., Stafford, C. A., Chauhan, D., Fröhlich, A. L., Nagl, D., Pinci, F., Schmid-Burgk, J. L., & Hornung, V. (2019). Priming enables a NEK7-

independent route of NLRP3 activation. *bioRxiv, 799320*. https://doi.org/https://doi.org/10.1101/799320

Schmitz, J., Owyang, A., Oldham, E., Song, Y., Murphy, E., McClanahan, T. K., Zurawski, G., Moshrefi, M., Qin, J., Li, X., Gorman, D. M., Bazan, J. F., & Kastelein, R. A. (2005, Nov). IL-33, an interleukin-1-like cytokine that signals via the IL-1 receptor-related protein ST2 and induces T helper type 2-associated cytokines. *Immunity, 23*(5), 479-490. https://doi.org/10.1016/j.immuni.2005.09.015

Schroder, K., Sagulenko, V., Zamoshnikova, A., Richards, A. A., Cridland, J. A., Irvine, K. M., Stacey, K. J., & Sweet, M. J. (2012, Dec). Acute lipopolysaccharide priming boosts inflammasome activation independently of inflammasome sensor induction. *Immunobiology, 217*(12), 1325-1329. https://doi.org/10.1016/j.imbio.2012.07.020

Schwarzer, R., Jiao, H., Wachsmuth, L., Tresch, A., & Pasparakis, M. (2020, Jun 16). FADD and Caspase-8 Regulate Gut Homeostasis and Inflammation by Controlling MLKL- and GSDMD-Mediated Death of Intestinal Epithelial Cells. *Immunity, 52*(6), 978-993 e976. https://doi.org/10.1016/j.immuni.2020.04.002

Scott, A., LaPrade, R. F., Harmon, K. G., Filardo, G., Kon, E., Della Villa, S., Bahr, R., Moksnes, H., Torgalsen, T., Lee, J., Dragoo, J. L., & Engebretsen, L. (2019, Jun). Platelet-Rich Plasma for Patellar Tendinopathy: A Randomized Controlled Trial of Leukocyte-Rich PRP or Leukocyte-Poor PRP Versus Saline. *Am J Sports Med, 47*(7), 1654-1661. https://doi.org/10.1177/0363546519837954

Seki, E., De Minicis, S., Osterreicher, C. H., Kluwe, J., Osawa, Y., Brenner, D. A., & Schwabe, R. F. (2007, Nov). TLR4 enhances TGF-beta signaling and hepatic fibrosis. *Nat Med, 13*(11), 1324-1332. https://doi.org/10.1038/nm1663

Serbina, N. V., Jia, T., Hohl, T. M., & Pamer, E. G. (2008). Monocyte-mediated defense against microbial pathogens. *Annu Rev Immunol, 26*, 421-452. https://doi.org/10.1146/annurev.immunol.26.021607.090326

Serhan, C. N., Chiang, N., & Dalli, J. (2015, May). The resolution code of acute inflammation: Novel pro-resolving lipid mediators in resolution. *Semin Immunol, 27*(3), 200-215. https://doi.org/10.1016/j.smim.2015.03.004

Sester, D. P., Thygesen, S. J., Sagulenko, V., Vajjhala, P. R., Cridland, J. A., Vitak, N., Chen, K. W., Osborne, G. W., Schroder, K., & Stacey, K. J. (2015, Jan 1). A novel flow cytometric method to assess inflammasome formation. *J Immunol, 194*(1), 455-462. https://doi.org/10.4049/jimmunol.1401110

Shakhov, A. N., Collart, M. A., Vassalli, P., Nedospasov, S. A., & Jongeneel, C. V. (1990, Jan 1). Kappa B-type enhancers are involved in lipopolysaccharide-mediated transcriptional activation of the tumor necrosis factor alpha gene in primary macrophages. *J Exp Med, 171*(1), 35-47. https://doi.org/10.1084/jem.171.1.35

Shapouri-Moghaddam, A., Mohammadian, S., Vazini, H., Taghadosi, M., Esmaeili, S. A., Mardani, F., Seifi, B., Mohammadi, A., Afshari, J. T., & Sahebkar, A. (2018, Sep). Macrophage plasticity, polarization, and function in health and disease. *J Cell Physiol, 233*(9), 6425-6440. https://doi.org/10.1002/jcp.26429

Sharif, H., Wang, L., Wang, W. L., Magupalli, V. G., Andreeva, L., Qiao, Q., Hauenstein, A. V., Wu, Z., Nunez, G., Mao, Y., & Wu, H. (2019, Jun). Structural mechanism for NEK7-licensed activation of NLRP3 inflammasome. *Nature, 570*(7761), 338-343. https://doi.org/10.1038/s41586-019-1295-z

Sharma, B. R., & Kanneganti, T. D. (2021, May). NLRP3 inflammasome in cancer and metabolic diseases. *Nat Immunol, 22*(5), 550-559. https://doi.org/10.1038/s41590-021-00886-5

Sharma, P., & Maffulli, N. (2005, Jan). Tendon injury and tendinopathy: healing and repair. *J Bone Joint Surg Am, 87*(1), 187-202. https://doi.org/10.2106/JBJS.D.01850

Sharma, S., Kulk, N., Nold, M. F., Graf, R., Kim, S. H., Reinhardt, D., Dinarello, C. A., & Bufler, P. (2008, Apr 15). The IL-1 family member 7b translocates to the nucleus and down-regulates proinflammatory cytokines. *J Immunol, 180*(8), 5477-5482. https://doi.org/10.4049/jimmunol.180.8.5477

Shen, C., Li, R., Negro, R., Cheng, J., Vora, S. M., Fu, T. M., Wang, A., He, K., Andreeva, L., Gao, P., Tian, Z., Flavell, R. A., Zhu, S., & Wu, H. (2021, Nov 11). Phase separation drives RNA virus-induced activation of the NLRP6 inflammasome. *Cell, 184*(23), 5759-5774 e5720. https://doi.org/10.1016/j.cell.2021.09.032

Sheppard, M., Laskou, F., Stapleton, P. P., Hadavi, S., & Dasgupta, B. (2017, Sep 2). Tocilizumab (Actemra). *Hum Vaccin Immunother, 13*(9), 1972-1988. https://doi.org/10.1080/21645515.2017.1316909

Shi, H., Wang, Y., Li, X., Zhan, X., Tang, M., Fina, M., Su, L., Pratt, D., Bu, C. H., Hildebrand, S., Lyon, S., Scott, L., Quan, J., Sun, Q., Russell, J., Arnett, S., Jurek, P., Chen, D., Kravchenko, V. V., Mathison, J. C., Moresco, E. M., Monson, N. L., Ulevitch, R. J., & Beutler, B. (2016, Mar). NLRP3 activation and mitosis are mutually exclusive events coordinated by NEK7, a new inflammasome component. *Nat Immunol, 17*(3), 250-258. https://doi.org/10.1038/ni.3333

Shimada, K., Crother, T. R., Karlin, J., Dagvadorj, J., Chiba, N., Chen, S., Ramanujan, V. K., Wolf, A. J., Vergnes, L., Ojcius, D. M., Rentsendorj, A., Vargas, M., Guerrero, C., Wang, Y., Fitzgerald, K. A., Underhill, D. M., Town, T., & Arditi, M. (2012, Mar 23). Oxidized mitochondrial DNA activates the NLRP3 inflammasome during apoptosis. *Immunity, 36*(3), 401-414. https://doi.org/10.1016/j.immuni.2012.01.009

Shimizu, M., Nakagishi, Y., Inoue, N., Mizuta, M., Ko, G., Saikawa, Y., Kubota, T., Yamasaki, Y., Takei, S., & Yachie, A. (2015, Oct). Interleukin-18 for predicting the development of macrophage activation syndrome in systemic juvenile idiopathic arthritis. *Clin Immunol, 160*(2), 277-281. https://doi.org/10.1016/j.clim.2015.06.005

Siahanidou, T., Nikaina, E., Kontogiorgou, C., Tzanoudaki, M., Stefanaki, K., Skiathitou, A. V., Petropoulou, T., & Kanariou, M. (2019, Apr). Autoinflammation with Infantile Enterocolitis Associated with Recurrent Perianal Abscesses. *J Clin Immunol, 39*(3), 237-240. https://doi.org/10.1007/s10875-019-00611-w

Sica, A., & Mantovani, A. (2012, Mar). Macrophage plasticity and polarization: in vivo veritas. *J Clin Invest, 122*(3), 787-795. https://doi.org/10.1172/JCI59643

Sicignano, L. L., Massaro, M. G., Savino, M., Rigante, D., Gerardino, L., & Manna, R. (2021, Aug). Early introduction of anakinra improves acute pericarditis and prevents tamponade in Staphylococcal sepsis. *Intern Emerg Med, 16*(5), 1391-1394. https://doi.org/10.1007/s11739-020-02627-2

Siegmund, B., Fantuzzi, G., Rieder, F., Gamboni-Robertson, F., Lehr, H. A., Hartmann, G., Dinarello, C. A., Endres, S., & Eigler, A. (2001, Oct). Neutralization of interleukin-18 reduces severity in murine colitis and intestinal IFN-gamma and TNF-alpha production. *Am J Physiol Regul Integr Comp Physiol, 281*(4), R1264-1273. https://doi.org/10.1152/ajpregu.2001.281.4.R1264

Simon, H. U. (2009, Apr). Cell death in allergic diseases. *Apoptosis, 14*(4), 439-446. https://doi.org/10.1007/s10495-008-0299-1

Skorsetz, M., Artal, P., & Bueno, J. M. (2016, Mar). Performance evaluation of a sensorless adaptive optics multiphoton microscope. *J Microsc, 261*(3), 249-258. https://doi.org/10.1111/jmi.12325

Skutek, M., van Griensven, M., Zeichen, J., Brauer, N., & Bosch, U. (2001, Sep). Cyclic mechanical stretching enhances secretion of Interleukin 6 in human tendon fibroblasts. *Knee Surg Sports Traumatol Arthrosc, 9*(5), 322-326. https://doi.org/10.1007/s001670100217

Smith, M. F., Jr., Eidlen, D., Arend, W. P., & Gutierrez-Hartmann, A. (1994, Oct 15). LPS-induced expression of the human IL-1 receptor antagonist gene is controlled by multiple interacting promoter elements. *J Immunol, 153*(8), 3584-3593. https://www.ncbi.nlm.nih.gov/pubmed/7930581

Smithrithee, R., Niyonsaba, F., Kiatsurayanon, C., Ushio, H., Ikeda, S., Okumura, K., & Ogawa, H. (2015, Jan). Human beta-defensin-3 increases the expression of interleukin-37 through CCR6 in human keratinocytes. *J Dermatol Sci, 77*(1), 46-53. https://doi.org/10.1016/j.jdermsci.2014.12.001

Solini, A., Chiozzi, P., Morelli, A., Fellin, R., & Di Virgilio, F. (1999, Feb). Human primary fibroblasts in vitro express a purinergic P2X7 receptor coupled to ion fluxes, microvesicle formation and IL-6 release. *J Cell Sci, 112 (Pt 3)*, 297-305. https://doi.org/10.1242/jcs.112.3.297

Song, N., Liu, Z. S., Xue, W., Bai, Z. F., Wang, Q. Y., Dai, J., Liu, X., Huang, Y. J., Cai, H., Zhan, X. Y., Han, Q. Y., Wang, H., Chen, Y., Li, H. Y., Li, A. L., Zhang, X. M., Zhou, T., & Li, T. (2017, Oct 5). NLRP3 Phosphorylation Is an Essential Priming Event for Inflammasome Activation. *Mol Cell, 68*(1), 185-197 e186. https://doi.org/10.1016/j.molcel.2017.08.017

Soriano-Teruel, P. M., Garcia-Lainez, G., Marco-Salvador, M., Pardo, J., Arias, M., DeFord, C., Merfort, I., Vicent, M. J., Pelegrin, P., Sancho, M., & Orzaez, M. (2021, Dec 13). Identification of an ASC oligomerization inhibitor for the treatment of inflammatory diseases. *Cell Death Dis, 12*(12), 1155. https://doi.org/10.1038/s41419-021-04420-1

Soslowsky, L. J., Thomopoulos, S., Tun, S., Flanagan, C. L., Keefer, C. C., Mastaw, J., & Carpenter, J. E. (2000, Mar-Apr). Neer Award 1999. Overuse activity injures the supraspinatus tendon in an animal model: a histologic and biomechanical study. *J Shoulder Elbow Surg, 9*(2), 79-84. https://www.ncbi.nlm.nih.gov/pubmed/10810684

Spalinger, M. R., Kasper, S., Gottier, C., Lang, S., Atrott, K., Vavricka, S. R., Scharl, S., Raselli, T., Frey-Wagner, I., Gutte, P. M., Grutter, M. G., Beer, H. D., Contassot, E., Chan, A. C., Dai, X., Rawlings, D. J., Mair, F., Becher, B., Falk, W., Fried, M., Rogler, G., & Scharl, M. (2016, May 2). NLRP3 tyrosine phosphorylation is controlled by protein tyrosine phosphatase PTPN22. *J Clin Invest, 126*(5), 1783-1800. https://doi.org/10.1172/JCI83669

Stutz, A., Kolbe, C. C., Stahl, R., Horvath, G. L., Franklin, B. S., van Ray, O., Brinkschulte, R., Geyer, M., Meissner, F., & Latz, E. (2017, Jun 5). NLRP3 inflammasome assembly is regulated by phosphorylation of the pyrin domain. *J Exp Med, 214*(6), 1725-1736. https://doi.org/10.1084/jem.20160933

Sugawara, S., Uehara, A., Nochi, T., Yamaguchi, T., Ueda, H., Sugiyama, A., Hanzawa, K., Kumagai, K., Okamura, H., & Takada, H. (2001, Dec 1). Neutrophil proteinase 3-mediated induction of bioactive IL-18 secretion by human oral epithelial cells. *J Immunol, 167*(11), 6568-6575. https://doi.org/10.4049/jimmunol.167.11.6568

Sugg, K. B., Lubardic, J., Gumucio, J. P., & Mendias, C. L. (2014, Jul). Changes in macrophage phenotype and induction of epithelial-to-mesenchymal transition genes following acute Achilles tenotomy and repair. *J Orthop Res, 32*(7), 944-951. https://doi.org/10.1002/jor.22624

Sui, X., Yang, J., Zhang, G., Yuan, X., Li, W., Long, J., Luo, Y., Li, Y., & Wang, Y. (2020, Feb 28). NLRP3 inflammasome inhibition attenuates subacute neurotoxicity induced by acrylamide in vitro and in vivo. *Toxicology, 432*, 152392. https://doi.org/10.1016/j.tox.2020.152392

Sun, Q., Loughran, P., Shapiro, R., Shrivastava, I. H., Antoine, D. J., Li, T., Yan, Z., Fan, J., Billiar, T. R., & Scott, M. J. (2017, Jan). Redox-dependent regulation of hepatocyte absent in melanoma 2 inflammasome activation in sterile liver injury in mice. *Hepatology, 65*(1), 253-268. https://doi.org/10.1002/hep.28893

Sun, S. C. (2017, Sep). The non-canonical NF-kappaB pathway in immunity and inflammation. *Nat Rev Immunol, 17*(9), 545-558. https://doi.org/10.1038/nri.2017.52

Sunwoo, J. Y., Eliasberg, C. D., Carballo, C. B., & Rodeo, S. A. (2020, Aug). The role of the macrophage in tendinopathy and tendon healing. *J Orthop Res, 38*(8), 1666-1675. https://doi.org/10.1002/jor.24667

Sutterwala, F. S., Mijares, L. A., Li, L., Ogura, Y., Kazmierczak, B. I., & Flavell, R. A. (2007, Dec 24). Immune recognition of Pseudomonas aeruginosa mediated by the IPAF/NLRC4 inflammasome. *J Exp Med, 204*(13), 3235-3245. https://doi.org/10.1084/jem.20071239

Swanson, J. A., & Watts, C. (1995, Nov). Macropinocytosis. *Trends Cell Biol, 5*(11), 424-428. https://doi.org/10.1016/s0962-8924(00)89101-1

Taabazuing, C. Y., Okondo, M. C., & Bachovchin, D. A. (2017, Apr 20). Pyroptosis and Apoptosis Pathways Engage in Bidirectional Crosstalk in Monocytes and Macrophages. *Cell Chem Biol, 24*(4), 507-514 e504. https://doi.org/10.1016/j.chembiol.2017.03.009

Tada, H., Nemoto, E., Shimauchi, H., Watanabe, T., Mikami, T., Matsumoto, T., Ohno, N., Tamura, H., Shibata, K., Akashi, S., Miyake, K., Sugawara, S., & Takada, H. (2002). Saccharomyces cerevisiae- and Candida albicans-derived mannan induced production of tumor necrosis factor alpha by human monocytes in a CD14- and Toll-like receptor 4-dependent manner. *Microbiol Immunol, 46*(7), 503-512. https://doi.org/10.1111/j.1348-0421.2002.tb02727.x

Takeuchi, O., & Akira, S. (2010, Mar 19). Pattern recognition receptors and inflammation. *Cell, 140*(6), 805-820. https://doi.org/10.1016/j.cell.2010.01.022

Tanaka, N., Izawa, K., Saito, M. K., Sakuma, M., Oshima, K., Ohara, O., Nishikomori, R., Morimoto, T., Kambe, N., Goldbach-Mansky, R., Aksentijevich, I., de Saint Basile, G., Neven, B., van Gijn, M., Frenkel, J., Arostegui, J. I., Yague, J., Merino, R., Ibanez, M., Pontillo, A., Takada, H., Imagawa, T., Kawai, T., Yasumi, T., Nakahata, T., & Heike, T. (2011, Nov). High incidence of NLRP3 somatic mosaicism in patients with chronic infantile neurologic, cutaneous, articular syndrome: results of an International Multicenter Collaborative Study. *Arthritis Rheum, 63*(11), 3625-3632. https://doi.org/10.1002/art.30512

Tanaka, T., Narazaki, M., & Kishimoto, T. (2018, Aug 1). Interleukin (IL-6) Immunotherapy. *Cold Spring Harb Perspect Biol, 10*(8). https://doi.org/10.1101/cshperspect.a028456

Tapia-Abellan, A., Angosto-Bazarra, D., Alarcon-Vila, C., Banos, M. C., Hafner-Bratkovic, I., Oliva, B., & Pelegrin, P. (2021, Sep 17). Sensing low intracellular potassium by NLRP3 results in a stable open structure that promotes inflammasome activation. *Sci Adv, 7*(38), eabf4468. https://doi.org/10.1126/sciadv.abf4468

Tapia-Abellan, A., Angosto-Bazarra, D., Martinez-Banaclocha, H., de Torre-Minguela, C., Ceron-Carrasco, J. P., Perez-Sanchez, H., Arostegui, J. I., & Pelegrin, P. (2019, Jun). MCC950 closes the active conformation of NLRP3 to an inactive state. *Nat Chem Biol, 15*(6), 560-564. https://doi.org/10.1038/s41589-019-0278-6

Tauber, M., Bal, E., Pei, X. Y., Madrange, M., Khelil, A., Sahel, H., Zenati, A., Makrelouf, M., Boubridaa, K., Chiali, A., Smahi, N., Otsmane, F., Bouajar, B., Marrakchi, S., Turki, H., Bourrat, E., Viguier, M., Hamel, Y., Bachelez, H., & Smahi, A. (2016, Sep). IL36RN Mutations Affect Protein Expression and Function: A Basis for Genotype-Phenotype Correlation in Pustular Diseases. *J Invest Dermatol, 136*(9), 1811-1819. https://doi.org/10.1016/j.jid.2016.04.038

Taylor, P. C., Peters, A. M., Paleolog, E., Chapman, P. T., Elliott, M. J., McCloskey, R., Feldmann, M., & Maini, R. N. (2000, Jan). Reduction of chemokine levels and leukocyte traffic to joints by tumor necrosis factor alpha blockade in patients with rheumatoid arthritis. *Arthritis Rheum, 43*(1), 38-47. https://doi.org/10.1002/1529-0131(200001)43:1<38::AID-ANR6>3.0.CO;2-L

Tenoever, B. R., Ng, S. L., Chua, M. A., McWhirter, S. M., Garcia-Sastre, A., & Maniatis, T. (2007, Mar 2). Multiple functions of the IKK-related kinase IKKepsilon in interferon-mediated antiviral immunity. *Science, 315*(5816), 1274-1278. https://doi.org/10.1126/science.1136567

Thampatty, B. P., Li, H., Im, H. J., & Wang, J. H. (2007, Jan 15). EP4 receptor regulates collagen type-I, MMP-1, and MMP-3 gene expression in human tendon fibroblasts in response to IL-1 beta treatment. *Gene, 386*(1-2), 154-161. https://doi.org/10.1016/j.gene.2006.08.027

Thankam, F. G., Roesch, Z. K., Dilisio, M. F., Radwan, M. M., Kovilam, A., Gross, R. M., & Agrawal, D. K. (2018, Jun 11). Association of Inflammatory Responses and ECM Disorganization with HMGB1 Upregulation and NLRP3 Inflammasome Activation in the Injured Rotator Cuff Tendon. *Sci Rep, 8*(1), 8918. https://doi.org/10.1038/s41598-018-27250-2

Thiam, H. R., Wong, S. L., Wagner, D. D., & Waterman, C. M. (2020, Oct 6). Cellular Mechanisms of NETosis. *Annu Rev Cell Dev Biol, 36*, 191-218. https://doi.org/10.1146/annurev-cellbio-020520-111016

Thomopoulos, S., Parks, W. C., Rifkin, D. B., & Derwin, K. A. (2015, Jun). Mechanisms of tendon injury and repair. *J Orthop Res, 33*(6), 832-839. https://doi.org/10.1002/jor.22806

Ting, J. P., Lovering, R. C., Alnemri, E. S., Bertin, J., Boss, J. M., Davis, B. K., Flavell, R. A., Girardin, S. E., Godzik, A., Harton, J. A., Hoffman, H. M., Hugot, J. P., Inohara, N., Mackenzie, A., Maltais, L. J., Nunez, G., Ogura, Y., Otten, L. A., Philpott, D., Reed, J. C., Reith, W., Schreiber, S., Steimle, V., & Ward, P. A. (2008, Mar). The NLR gene family: a standard nomenclature. *Immunity, 28*(3), 285-287. https://doi.org/10.1016/j.immuni.2008.02.005

Tohyama, H., Yoshikawa, T., Ju, Y. J., & Yasuda, K. (2009, Mar-Apr). Revascularization in the tendon graft following anterior cruciate ligament reconstruction of the knee: its mechanisms and regulation. *Chang Gung Med J, 32*(2), 133-139. https://www.ncbi.nlm.nih.gov/pubmed/19403002

Touitou, I., Lesage, S., McDermott, M., Cuisset, L., Hoffman, H., Dode, C., Shoham, N., Aganna, E., Hugot, J. P., Wise, C., Waterham, H., Pugnere, D., Demaille, J., & Sarrauste de Menthiere, C. (2004, Sep). Infevers: an evolving mutation database for auto-inflammatory syndromes. *Hum Mutat, 24*(3), 194-198. https://doi.org/10.1002/humu.20080

Towne, J. E., Renshaw, B. R., Douangpanya, J., Lipsky, B. P., Shen, M., Gabel, C. A., & Sims, J. E. (2011, Dec 9). Interleukin-36 (IL-36) ligands require processing for full agonist (IL-36alpha, IL-36beta, and IL-36gamma) or antagonist (IL-36Ra) activity. *J Biol Chem, 286*(49), 42594-42602. https://doi.org/10.1074/jbc.M111.267922

Tschopp, J., Martinon, F., & Burns, K. (2003, Feb). NALPs: a novel protein family involved in inflammation. *Nat Rev Mol Cell Biol, 4*(2), 95-104. https://doi.org/10.1038/nrm1019

Tsuzaki, M., Guyton, G., Garrett, W., Archambault, J. M., Herzog, W., Almekinders, L., Bynum, D., Yang, X., & Banes, A. J. (2003, Mar). IL-1 beta induces COX2, MMP-1, -3 and -13, ADAMTS-4, IL-1 beta and IL-6 in human tendon cells. *J Orthop Res, 21*(2), 256-264. https://doi.org/10.1016/S0736-0266(02)00141-9

Tzeng, T. C., Schattgen, S., Monks, B., Wang, D., Cerny, A., Latz, E., Fitzgerald, K., & Golenbock, D. T. (2016, Jul 12). A Fluorescent Reporter Mouse for Inflammasome Assembly Demonstrates an Important Role for Cell-Bound and Free ASC Specks during In Vivo Infection. *Cell Rep, 16*(2), 571-582. https://doi.org/10.1016/j.celrep.2016.06.011

Uchida, H., Tohyama, H., Nagashima, K., Ohba, Y., Matsumoto, H., Toyama, Y., & Yasuda, K. (2005, Apr). Stress deprivation simultaneously induces over-expression of interleukin-1beta, tumor necrosis factor-alpha, and transforming growth factor-beta in fibroblasts and mechanical deterioration of the tissue in the patellar tendon. *J Biomech, 38*(4), 791-798. https://doi.org/10.1016/j.jbiomech.2004.05.009

Uggenti, C., Lepelley, A., & Crow, Y. J. (2019, Apr 26). Self-Awareness: Nucleic Acid-Driven Inflammation and the Type I Interferonopathies. *Annu Rev Immunol, 37*, 247-267. https://doi.org/10.1146/annurev-immunol-042718-041257

Usuelli, F. G., Grassi, M., Maccario, C., Vigano, M., Lanfranchi, L., Alfieri Montrasio, U., & de Girolamo, L. (2018, Jul). Intratendinous adipose-derived stromal vascular fraction (SVF) injection provides a safe, efficacious treatment for Achilles tendinopathy: results of a randomized controlled clinical trial at a 6-month follow-up. *Knee Surg Sports Traumatol Arthrosc, 26*(7), 2000-2010. https://doi.org/10.1007/s00167-017-4479-9

Vabulas, R. M., Ahmad-Nejad, P., da Costa, C., Miethke, T., Kirschning, C. J., Hacker, H., & Wagner, H. (2001, Aug 17). Endocytosed HSP60s use toll-like receptor 2 (TLR2) and TLR4 to activate the toll/interleukin-1 receptor signaling pathway in innate immune cells. *J Biol Chem, 276*(33), 31332-31339. https://doi.org/10.1074/jbc.M103217200

Vajjhala, P. R., Mirams, R. E., & Hill, J. M. (2012, Dec 7). Multiple binding sites on the pyrin domain of ASC protein allow self-association and interaction with NLRP3 protein. *J Biol Chem, 287*(50), 41732-41743. https://doi.org/10.1074/jbc.M112.381228

Valera-Garrido, F., Jiménez-Rubio, S., Minaya-Munoz, F., Estévez-Rodríguez, J. L., & Navandar, A. (2020). Ultrasound-guided percutaneous needle electrolysis and rehab and reconditioning program for rectus femoris muscle injuries: A cohort study with professional soccer players and a 20-week follow-up. *Applied Sciences, 10*(20), 7912.

Valera-Garrido, F., Minaya-Munoz, F., & Medina-Mirapeix, F. (2014, Dec). Ultrasound-guided percutaneous needle electrolysis in chronic lateral epicondylitis: short-term and long-term results. *Acupunct Med, 32*(6), 446-454. https://doi.org/10.1136/acupmed-2014-010619

Valera-Garrido, F., Minaya-Munoz, F., & Medina-Mirapeix, F. (2019). Fundamentos y principios de la electrolisis percutánea musculoesquelética. In F. Valera-Garrido & F. Minaya-Munoz (Eds.), *Fisioterapia Invasiva* (pp. 390-391). Elsevier.

Valera-Garrido, F., Minaya-Munoz, F., Sánchez-Ibáñez, J. M., García-Palencia, P., Valderrama-Canales, F., Medina-Mirapeix, F., & Polidori, F. (2013). Comparison of the acute inflammatory response and proliferation of dry needling and electrolysis percutaneous intratissue (EPI) in healthy rat Achilles tendons. *British journal of sports medicine, 47*(9), e2.

van de Veerdonk, F. L., Netea, M. G., Dinarello, C. A., & Joosten, L. A. (2011, Mar). Inflammasome activation and IL-1beta and IL-18 processing during infection. *Trends Immunol, 32*(3), 110-116. https://doi.org/10.1016/j.it.2011.01.003

van de Veerdonk, F. L., Netea, M. G., Dinarello, C. A., & van der Meer, J. W. (2011, Feb). Anakinra for the inflammatory complications of chronic granulomatous disease. *Neth J Med, 69*(2), 95. https://www.ncbi.nlm.nih.gov/pubmed/21411850

van den Boom, N. A. C., Winters, M., Haisma, H. J., & Moen, M. H. (2020, Apr). Efficacy of Stem Cell Therapy for Tendon Disorders: A Systematic Review. *Orthop J Sports Med, 8*(4), 2325967120915857. https://doi.org/10.1177/2325967120915857

Van Der Kraak, L. A., Schneider, C., Dang, V., Burr, A. H. P., Weiss, E. S., Varghese, J. A., Yang, L., Hand, T. W., & Canna, S. W. (2021, Sep). Genetic and commensal induction of IL-18 drive intestinal epithelial MHCII via IFNgamma. *Mucosal Immunol, 14*(5), 1100-1112. https://doi.org/10.1038/s41385-021-00419-1

Van Opdenbosch, N., Gurung, P., Vande Walle, L., Fossoul, A., Kanneganti, T. D., & Lamkanfi, M. (2014). Activation of the NLRP1b inflammasome independently of ASC-mediated caspase-1 autoproteolysis and speck formation. *Nat Commun, 5*, 3209. https://doi.org/10.1038/ncomms4209

Vandanmagsar, B., Youm, Y. H., Ravussin, A., Galgani, J. E., Stadler, K., Mynatt, R. L., Ravussin, E., Stephens, J. M., & Dixit, V. D. (2011, Feb). The NLRP3 inflammasome instigates obesity-induced inflammation and insulin resistance. *Nat Med, 17*(2), 179-188. https://doi.org/10.1038/nm.2279

Varela-Rodriguez, S., Sanchez-Sanchez, J. L., Velasco, E., Delicado-Miralles, M., & Sanchez-Gonzalez, J. L. (2022, May 20). Endogenous Pain Modulation in Response to a Single Session of Percutaneous Electrolysis in Healthy Population: A Double-Blinded Randomized Clinical Trial. *J Clin Med, 11*(10). https://doi.org/10.3390/jcm11102889

Veres, S. P., Brennan-Pierce, E. P., & Lee, J. M. (2015, Jan). Macrophage-like U937 cells recognize collagen fibrils with strain-induced discrete plasticity damage. *J Biomed Mater Res A, 103*(1), 397-408. https://doi.org/10.1002/jbm.a.35156

Verma, D., Lerm, M., Blomgran Julinder, R., Eriksson, P., Soderkvist, P., & Sarndahl, E. (2008, Mar). Gene polymorphisms in the NALP3 inflammasome are associated with interleukin-1 production and severe inflammation: relation to common inflammatory diseases? *Arthritis Rheum, 58*(3), 888-894. https://doi.org/10.1002/art.23286

Viaud, S., Terme, M., Flament, C., Taieb, J., Andre, F., Novault, S., Escudier, B., Robert, C., Caillat-Zucman, S., Tursz, T., Zitvogel, L., & Chaput, N. (2009). Dendritic cell-derived exosomes promote natural killer cell activation and proliferation: a role for NKG2D ligands and IL-15Ralpha. *PLoS One, 4*(3), e4942. https://doi.org/10.1371/journal.pone.0004942

Vidya, M. K., Kumar, V. G., Sejian, V., Bagath, M., Krishnan, G., & Bhatta, R. (2018, Jan 2). Toll-like receptors: Significance, ligands, signaling pathways, and functions in mammals. *Int Rev Immunol, 37*(1), 20-36. https://doi.org/10.1080/08830185.2017.1380200

Visnes, H., & Bahr, R. (2007, Apr). The evolution of eccentric training as treatment for patellar tendinopathy (jumper's knee): a critical review of exercise programmes. *Br J Sports Med, 41*(4), 217-223. https://doi.org/10.1136/bjsm.2006.032417

Voleti, P. B., Buckley, M. R., & Soslowsky, L. J. (2012). Tendon healing: repair and regeneration. *Annu Rev Biomed Eng, 14*, 47-71. https://doi.org/10.1146/annurev-bioeng-071811-150122

Volker-Touw, C. M., de Koning, H. D., Giltay, J. C., de Kovel, C. G., van Kempen, T. S., Oberndorff, K. M., Boes, M. L., van Steensel, M. A., van Well, G. T., Blokx, W. A., Schalkwijk, J., Simon, A., Frenkel, J., & van Gijn, M. E. (2017, Jan). Erythematous nodes, urticarial rash and arthralgias in a large pedigree with NLRC4-related autoinflammatory disease, expansion of the phenotype. *Br J Dermatol, 176*(1), 244-248. https://doi.org/10.1111/bjd.14757

Wang, B., Tian, Y., & Yin, Q. (2019). AIM2 Inflammasome Assembly and Signaling. *Adv Exp Med Biol, 1172*, 143-155. https://doi.org/10.1007/978-981-13-9367-9_7

Wang, L., Wen, W., Deng, M., Li, Y., Sun, G., Zhao, X., Tang, X., & Mao, H. (2021). A Novel Mutation in the NBD Domain of NLRC4 Causes Mild Autoinflammation With Recurrent Urticaria. *Front Immunol, 12*, 674808. https://doi.org/10.3389/fimmu.2021.674808

Wang, P., Zhu, S., Yang, L., Cui, S., Pan, W., Jackson, R., Zheng, Y., Rongvaux, A., Sun, Q., Yang, G., Gao, S., Lin, R., You, F., Flavell, R., & Fikrig, E. (2015, Nov 13). Nlrp6 regulates intestinal antiviral innate immunity. *Science, 350*(6262), 826-830. https://doi.org/10.1126/science.aab3145

Wang, S., Huang, Z., Li, W., He, S., Wu, H., Zhu, J., Li, R., Liang, Z., & Chen, Z. (2020, Jan). IL37 expression is decreased in patients with hyperhomocysteinemia and protects cells from inflammatory injury by homocysteine. *Mol Med Rep, 21*(1), 371-378. https://doi.org/10.3892/mmr.2019.10804

Wang, W., Hu, D., Feng, Y., Wu, C., Song, Y., Liu, W., Li, A., Wang, Y., Chen, K., Tian, M., Xiao, F., Zhang, Q., Chen, W., Pan, P., Wan, P., Liu, Y., Lan, H., Wu, K., & Wu, J. (2020, Nov 26). Paxillin mediates ATP-induced activation of P2X7 receptor and NLRP3 inflammasome. *BMC Biol, 18*(1), 182. https://doi.org/10.1186/s12915-020-00918-w

Wang, Y., Yin, B., Li, D., Wang, G., Han, X., & Sun, X. (2018, Jan 1). GSDME mediates caspase-3-dependent pyroptosis in gastric cancer. *Biochem Biophys Res Commun, 495*(1), 1418-1425. https://doi.org/10.1016/j.bbrc.2017.11.156

Wang, Y., Zhai, S., Wang, H., Jia, Q., Jiang, W., Zhang, X., Zhang, A., Liu, J., & Ni, L. (2013, Nov). Absent in melanoma 2 (AIM2) in rat dental pulp mediates the inflammatory response during pulpitis. *J Endod, 39*(11), 1390-1394. https://doi.org/10.1016/j.joen.2013.07.003

Watkin, L. B., Jessen, B., Wiszniewski, W., Vece, T. J., Jan, M., Sha, Y., Thamsen, M., Santos-Cortez, R. L., Lee, K., Gambin, T., Forbes, L. R., Law, C. S., Stray-Pedersen, A., Cheng, M. H., Mace, E. M., Anderson, M. S., Liu, D., Tang, L. F., Nicholas, S. K., Nahmod, K., Makedonas, G., Canter, D. L., Kwok, P. Y., Hicks, J., Jones, K. D., Penney, S., Jhangiani, S. N., Rosenblum, M. D., Dell, S. D., Waterfield, M. R., Papa, F. R., Muzny, D. M., Zaitlen, N., Leal, S. M., Gonzaga-Jauregui, C., Baylor-Hopkins Center for Mendelian, G., Boerwinkle, E., Eissa, N. T., Gibbs, R. A., Lupski, J. R., Orange, J. S., & Shum, A. K. (2015, Jun). COPA mutations impair ER-Golgi transport and cause hereditary autoimmune-mediated lung disease and arthritis. *Nat Genet, 47*(6), 654-660. https://doi.org/10.1038/ng.3279

Weaver, L. K., & Behrens, E. M. (2014, Sep). Hyperinflammation, rather than hemophagocytosis, is the common link between macrophage activation syndrome and hemophagocytic lymphohistiocytosis. *Curr Opin Rheumatol, 26*(5), 562-569. https://doi.org/10.1097/BOR.0000000000000093

Weavers, H., Evans, I. R., Martin, P., & Wood, W. (2016, Jun 16). Corpse Engulfment Generates a Molecular Memory that Primes the Macrophage Inflammatory Response. *Cell, 165*(7), 1658-1671. https://doi.org/10.1016/j.cell.2016.04.049

Weavers, H., Liepe, J., Sim, A., Wood, W., Martin, P., & Stumpf, M. P. H. (2016, Aug 8). Systems Analysis of the Dynamic Inflammatory Response to Tissue Damage Reveals Spatiotemporal

Properties of the Wound Attractant Gradient. *Curr Biol, 26*(15), 1975-1989. https://doi.org/10.1016/j.cub.2016.06.012

Weber, A., Wasiliew, P., & Kracht, M. (2010, Jan 19). Interleukin-1 (IL-1) pathway. *Sci Signal, 3*(105), cm1. https://doi.org/10.1126/scisignal.3105cm1

Werman, A., Werman-Venkert, R., White, R., Lee, J. K., Werman, B., Krelin, Y., Voronov, E., Dinarello, C. A., & Apte, R. N. (2004, Feb 24). The precursor form of IL-1alpha is an intracrine proinflammatory activator of transcription. *Proc Natl Acad Sci U S A, 101*(8), 2434-2439. https://doi.org/10.1073/pnas.0308705101

Werner, S., & Grose, R. (2003, Jul). Regulation of wound healing by growth factors and cytokines. *Physiol Rev, 83*(3), 835-870. https://doi.org/10.1152/physrev.2003.83.3.835

Wesche, H., Korherr, C., Kracht, M., Falk, W., Resch, K., & Martin, M. U. (1997, Mar 21). The interleukin-1 receptor accessory protein (IL-1RAcP) is essential for IL-1-induced activation of interleukin-1 receptor-associated kinase (IRAK) and stress-activated protein kinases (SAP kinases). *J Biol Chem, 272*(12), 7727-7731. https://doi.org/10.1074/jbc.272.12.7727

Wiken, M., Hallen, B., Kullenberg, T., & Koskinen, L. O. (2018, Dec). Development and effect of antibodies to anakinra during treatment of severe CAPS: sub-analysis of a long-term safety and efficacy study. *Clin Rheumatol, 37*(12), 3381-3386. https://doi.org/10.1007/s10067-018-4196-x

Willberg, L., Sunding, K., Forssblad, M., Fahlstrom, M., & Alfredson, H. (2011, Apr). Sclerosing polidocanol injections or arthroscopic shaving to treat patellar tendinopathy/jumper's knee? A randomised controlled study. *Br J Sports Med, 45*(5), 411-415. https://doi.org/10.1136/bjsm.2010.082446

Williams, J. W., Giannarelli, C., Rahman, A., Randolph, G. J., & Kovacic, J. C. (2018, Oct 30). Macrophage Biology, Classification, and Phenotype in Cardiovascular Disease: JACC Macrophage in CVD Series (Part 1). *J Am Coll Cardiol, 72*(18), 2166-2180. https://doi.org/10.1016/j.jacc.2018.08.2148

Wittmann, M., Doble, R., Bachmann, M., Pfeilschifter, J., Werfel, T., & Muhl, H. (2012). IL-27 Regulates IL-18 binding protein in skin resident cells. *PLoS One, 7*(6), e38751. https://doi.org/10.1371/journal.pone.0038751

Wojciak, B., & Crossan, J. F. (1993, Jul). The accumulation of inflammatory cells in synovial sheath and epitenon during adhesion formation in healing rat flexor tendons. *Clin Exp Immunol, 93*(1), 108-114. https://doi.org/10.1111/j.1365-2249.1993.tb06505.x

Wojciak, B., & Crossan, J. F. (1994, Sep). The effects of T cells and their products on in vitro healing of epitenon cell microwounds. *Immunology, 83*(1), 93-98. https://www.ncbi.nlm.nih.gov/pubmed/7821974

Wouters, C. H., Maes, A., Foley, K. P., Bertin, J., & Rose, C. D. (2014). Blau syndrome, the prototypic auto-inflammatory granulomatous disease. *Pediatr Rheumatol Online J, 12*, 33. https://doi.org/10.1186/1546-0096-12-33

Wu, Q., Xiao, Z., Pu, Y., Zhou, J., Wang, D., Huang, Z., & Hou, D. (2019, May). TnI and IL-18 levels are associated with prognosis of sepsis. *Postgrad Med J, 95*(1123), 240-244. https://doi.org/10.1136/postgradmedj-2018-136371

Yamaguchi, Y., Kurita-Ochiai, T., Kobayashi, R., Suzuki, T., & Ando, T. (2017, Jan). Regulation of the NLRP3 inflammasome in Porphyromonas gingivalis-accelerated periodontal disease. *Inflamm Res, 66*(1), 59-65. https://doi.org/10.1007/s00011-016-0992-4

Yamamoto, T., Eckes, B., & Krieg, T. (2001, Feb 16). Effect of interleukin-10 on the gene expression of type I collagen, fibronectin, and decorin in human skin fibroblasts: differential regulation by transforming growth factor-beta and monocyte chemoattractant protein-1. *Biochem Biophys Res Commun, 281*(1), 200-205. https://doi.org/10.1006/bbrc.2001.4321

Yamasaki, S., Ishikawa, E., Sakuma, M., Hara, H., Ogata, K., & Saito, T. (2008, Oct). Mincle is an ITAM-coupled activating receptor that senses damaged cells. *Nat Immunol, 9*(10), 1179-1188. https://doi.org/10.1038/ni.1651

Yan, C., Xiong, Y., Chen, L., Endo, Y., Hu, L., Liu, M., Liu, J., Xue, H., Abududilibaier, A., Mi, B., & Liu, G. (2019, Aug 6). A comparative study of the efficacy of ultrasonics and extracorporeal shock wave in the treatment of tennis elbow: a meta-analysis of randomized controlled trials. *J Orthop Surg Res, 14*(1), 248. https://doi.org/10.1186/s13018-019-1290-y

Yang, G., Im, H. J., & Wang, J. H. (2005, Dec 19). Repetitive mechanical stretching modulates IL-1beta induced COX-2, MMP-1 expression, and PGE2 production in human patellar tendon fibroblasts. *Gene, 363*, 166-172. https://doi.org/10.1016/j.gene.2005.08.006

Yang, J., Zhao, Y., Shi, J., & Shao, F. (2013, Aug 27). Human NAIP and mouse NAIP1 recognize bacterial type III secretion needle protein for inflammasome activation. *Proc Natl Acad Sci U S A, 110*(35), 14408-14413. https://doi.org/10.1073/pnas.1306376110

Yao, L., Bestwick, C. S., Bestwick, L. A., Aspden, R. M., & Maffulli, N. (2011, Sep). Non-immortalized human tenocyte cultures as a vehicle for understanding cellular aspects to tendinopathy. *Transl Med UniSa, 1*, 173-194. https://www.ncbi.nlm.nih.gov/pubmed/23905032

Yeretssian, G., Correa, R. G., Doiron, K., Fitzgerald, P., Dillon, C. P., Green, D. R., Reed, J. C., & Saleh, M. (2011, Jun 2). Non-apoptotic role of BID in inflammation and innate immunity. *Nature, 474*(7349), 96-99. https://doi.org/10.1038/nature09982

Yeretssian, G., Labbe, K., & Saleh, M. (2008, Sep). Molecular regulation of inflammation and cell death. *Cytokine, 43*(3), 380-390. https://doi.org/10.1016/j.cyto.2008.07.015

Yipp, B. G., Petri, B., Salina, D., Jenne, C. N., Scott, B. N., Zbytnuik, L. D., Pittman, K., Asaduzzaman, M., Wu, K., Meijndert, H. C., Malawista, S. E., de Boisfleury Chevance, A., Zhang, K., Conly, J., & Kubes, P. (2012, Sep). Infection-induced NETosis is a dynamic process involving neutrophil multitasking in vivo. *Nat Med, 18*(9), 1386-1393. https://doi.org/10.1038/nm.2847

Yoneyama, M., & Fujita, T. (2008, Aug 15). Structural mechanism of RNA recognition by the RIG-I-like receptors. *Immunity, 29*(2), 178-181. https://doi.org/10.1016/j.immuni.2008.07.009

Yoshikawa, T., Tohyama, H., Katsura, T., Kondo, E., Kotani, Y., Matsumoto, H., Toyama, Y., & Yasuda, K. (2006, Dec). Effects of local administration of vascular endothelial growth factor on mechanical characteristics of the semitendinosus tendon graft after anterior cruciate ligament reconstruction in sheep. *Am J Sports Med, 34*(12), 1918-1925. https://doi.org/10.1177/0363546506294469

Zanoni, I., Tan, Y., Di Gioia, M., Broggi, A., Ruan, J., Shi, J., Donado, C. A., Shao, F., Wu, H., Springstead, J. R., & Kagan, J. C. (2016, Jun 3). An endogenous caspase-11 ligand elicits interleukin-1 release from living dendritic cells. *Science, 352*(6290), 1232-1236. https://doi.org/10.1126/science.aaf3036

Zaslona, Z., Wilhelm, J., Cakarova, L., Marsh, L. M., Seeger, W., Lohmeyer, J., & von Wulffen, W. (2009, Jan 16). Transcriptome profiling of primary murine monocytes, lung macrophages and

lung dendritic cells reveals a distinct expression of genes involved in cell trafficking. *Respir Res, 10*, 2. https://doi.org/10.1186/1465-9921-10-2

Zeisig, E., Ohberg, L., & Alfredson, H. (2006, Nov). Sclerosing polidocanol injections in chronic painful tennis elbow-promising results in a pilot study. *Knee Surg Sports Traumatol Arthrosc, 14*(11), 1218-1224. https://doi.org/10.1007/s00167-006-0156-0

Zelensky, A. N., & Gready, J. E. (2005, Dec). The C-type lectin-like domain superfamily. *FEBS J, 272*(24), 6179-6217. https://doi.org/10.1111/j.1742-4658.2005.05031.x

Zhang, C., Xiao, C., Dang, E., Cao, J., Zhu, Z., Fu, M., Yao, X., Liu, Y., Jin, B., Wang, G., & Li, W. (2018, Feb). CD100-Plexin-B2 Promotes the Inflammation in Psoriasis by Activating NF-kappaB and the Inflammasome in Keratinocytes. *J Invest Dermatol, 138*(2), 375-383. https://doi.org/10.1016/j.jid.2017.09.005

Zhang, J. Y., Zhou, B., Sun, R. Y., Ai, Y. L., Cheng, K., Li, F. N., Wang, B. R., Liu, F. J., Jiang, Z. H., Wang, W. J., Zhou, D., Chen, H. Z., & Wu, Q. (2021, Sep). The metabolite alpha-KG induces GSDMC-dependent pyroptosis through death receptor 6-activated caspase-8. *Cell Res, 31*(9), 980-997. https://doi.org/10.1038/s41422-021-00506-9

Zhang, L., Chen, S., Ruan, J., Wu, J., Tong, A. B., Yin, Q., Li, Y., David, L., Lu, A., Wang, W. L., Marks, C., Ouyang, Q., Zhang, X., Mao, Y., & Wu, H. (2015, Oct 23). Cryo-EM structure of the activated NAIP2-NLRC4 inflammasome reveals nucleated polymerization. *Science, 350*(6259), 404-409. https://doi.org/10.1126/science.aac5789

Zhang, X., Bogunovic, D., Payelle-Brogard, B., Francois-Newton, V., Speer, S. D., Yuan, C., Volpi, S., Li, Z., Sanal, O., Mansouri, D., Tezcan, I., Rice, G. I., Chen, C., Mansouri, N., Mahdaviani, S. A., Itan, Y., Boisson, B., Okada, S., Zeng, L., Wang, X., Jiang, H., Liu, W., Han, T., Liu, D., Ma, T., Wang, B., Liu, M., Liu, J. Y., Wang, Q. K., Yalnizoglu, D., Radoshevich, L., Uze, G., Gros, P., Rozenberg, F., Zhang, S. Y., Jouanguy, E., Bustamante, J., Garcia-Sastre, A., Abel, L., Lebon, P., Notarangelo, L. D., Crow, Y. J., Boisson-Dupuis, S., Casanova, J. L., & Pellegrini, S. (2015, Jan 1). Human intracellular ISG15 prevents interferon-alpha/beta over-amplification and auto-inflammation. *Nature, 517*(7532), 89-93. https://doi.org/10.1038/nature13801

Zhang, Z., Meszaros, G., He, W. T., Xu, Y., de Fatima Magliarelli, H., Mailly, L., Mihlan, M., Liu, Y., Puig Gamez, M., Goginashvili, A., Pasquier, A., Bielska, O., Neven, B., Quartier, P., Aebersold, R., Baumert, T. F., Georgel, P., Han, J., & Ricci, R. (2017, Sep 4). Protein kinase D at the Golgi controls NLRP3 inflammasome activation. *J Exp Med, 214*(9), 2671-2693. https://doi.org/10.1084/jem.20162040

Zhao, Y., Yang, J., Shi, J., Gong, Y. N., Lu, Q., Xu, H., Liu, L., & Shao, F. (2011, Sep 14). The NLRC4 inflammasome receptors for bacterial flagellin and type III secretion apparatus. *Nature, 477*(7366), 596-600. https://doi.org/10.1038/nature10510

Zhong, F. L., Mamai, O., Sborgi, L., Boussofara, L., Hopkins, R., Robinson, K., Szeverenyi, I., Takeichi, T., Balaji, R., Lau, A., Tye, H., Roy, K., Bonnard, C., Ahl, P. J., Jones, L. A., Baker, P. J., Lacina, L., Otsuka, A., Fournie, P. R., Malecaze, F., Lane, E. B., Akiyama, M., Kabashima, K., Connolly, J. E., Masters, S. L., Soler, V. J., Omar, S. S., McGrath, J. A., Nedelcu, R., Gribaa, M., Denguezli, M., Saad, A., Hiller, S., & Reversade, B. (2016, Sep 22). Germline NLRP1 Mutations Cause Skin Inflammatory and Cancer Susceptibility Syndromes via Inflammasome Activation. *Cell, 167*(1), 187-202 e117. https://doi.org/10.1016/j.cell.2016.09.001

Zhong, F. L., Robinson, K., Teo, D. E. T., Tan, K. Y., Lim, C., Harapas, C. R., Yu, C. H., Xie, W. H., Sobota, R. M., Au, V. B., Hopkins, R., D'Osualdo, A., Reed, J. C., Connolly, J. E., Masters, S. L., & Reversade, B. (2018, Dec 7). Human DPP9 represses NLRP1 inflammasome and

protects against autoinflammatory diseases via both peptidase activity and FIIND domain binding. *J Biol Chem, 293*(49), 18864-18878. https://doi.org/10.1074/jbc.RA118.004350

Zhong, Y., Yu, K., Wang, X., Wang, X., Ji, Q., & Zeng, Q. (2015). Elevated Plasma IL-38 Concentrations in Patients with Acute ST-Segment Elevation Myocardial Infarction and Their Dynamics after Reperfusion Treatment. *Mediators Inflamm, 2015*, 490120. https://doi.org/10.1155/2015/490120

Zhou, B., & Abbott, D. W. (2021, Apr 13). Gasdermin E permits interleukin-1 beta release in distinct sublytic and pyroptotic phases. *Cell Rep, 35*(2), 108998. https://doi.org/10.1016/j.celrep.2021.108998

Zhou, Q., Aksentijevich, I., Wood, G. M., Walts, A. D., Hoffmann, P., Remmers, E. F., Kastner, D. L., & Ombrello, A. K. (2015, Sep). Brief Report: Cryopyrin-Associated Periodic Syndrome Caused by a Myeloid-Restricted Somatic NLRP3 Mutation. *Arthritis Rheumatol, 67*(9), 2482-2486. https://doi.org/10.1002/art.39190

Zhou, Q., Wang, H., Schwartz, D. M., Stoffels, M., Park, Y. H., Zhang, Y., Yang, D., Demirkaya, E., Takeuchi, M., Tsai, W. L., Lyons, J. J., Yu, X., Ouyang, C., Chen, C., Chin, D. T., Zaal, K., Chandrasekharappa, S. C., Hanson, E. P., Yu, Z., Mullikin, J. C., Hasni, S. A., Wertz, I. E., Ombrello, A. K., Stone, D. L., Hoffmann, P., Jones, A., Barham, B. K., Leavis, H. L., van Royen-Kerkof, A., Sibley, C., Batu, E. D., Gul, A., Siegel, R. M., Boehm, M., Milner, J. D., Ozen, S., Gadina, M., Chae, J., Laxer, R. M., Kastner, D. L., & Aksentijevich, I. (2016, Jan). Loss-of-function mutations in TNFAIP3 leading to A20 haploinsufficiency cause an early-onset autoinflammatory disease. *Nat Genet, 48*(1), 67-73. https://doi.org/10.1038/ng.3459

Zhou, Q., Yang, D., Ombrello, A. K., Zavialov, A. V., Toro, C., Zavialov, A. V., Stone, D. L., Chae, J. J., Rosenzweig, S. D., Bishop, K., Barron, K. S., Kuehn, H. S., Hoffmann, P., Negro, A., Tsai, W. L., Cowen, E. W., Pei, W., Milner, J. D., Silvin, C., Heller, T., Chin, D. T., Patronas, N. J., Barber, J. S., Lee, C. C., Wood, G. M., Ling, A., Kelly, S. J., Kleiner, D. E., Mullikin, J. C., Ganson, N. J., Kong, H. H., Hambleton, S., Candotti, F., Quezado, M. M., Calvo, K. R., Alao, H., Barham, B. K., Jones, A., Meschia, J. F., Worrall, B. B., Kasner, S. E., Rich, S. S., Goldbach-Mansky, R., Abinun, M., Chalom, E., Gotte, A. C., Punaro, M., Pascual, V., Verbsky, J. W., Torgerson, T. R., Singer, N. G., Gershon, T. R., Ozen, S., Karadag, O., Fleisher, T. A., Remmers, E. F., Burgess, S. M., Moir, S. L., Gadina, M., Sood, R., Hershfield, M. S., Boehm, M., Kastner, D. L., & Aksentijevich, I. (2014, Mar 6). Early-onset stroke and vasculopathy associated with mutations in ADA2. *N Engl J Med, 370*(10), 911-920. https://doi.org/10.1056/NEJMoa1307361

Zhou, R., Tardivel, A., Thorens, B., Choi, I., & Tschopp, J. (2010, Feb). Thioredoxin-interacting protein links oxidative stress to inflammasome activation. *Nat Immunol, 11*(2), 136-140. https://doi.org/10.1038/ni.1831

Zhou, Y., & Wang, J. H. (2016). PRP Treatment Efficacy for Tendinopathy: A Review of Basic Science Studies. *Biomed Res Int, 2016*, 9103792. https://doi.org/10.1155/2016/9103792

Zhou, Z., He, H., Wang, K., Shi, X., Wang, Y., Su, Y., Wang, Y., Li, D., Liu, W., Zhang, Y., Shen, L., Han, W., Shen, L., Ding, J., & Shao, F. (2020, May 29). Granzyme A from cytotoxic lymphocytes cleaves GSDMB to trigger pyroptosis in target cells. *Science, 368*(6494). https://doi.org/10.1126/science.aaz7548

Zhu, X., Hu, C., Zhang, Y., Li, L., & Wang, Z. (2001, May-Jun). Expression of cyclin-dependent kinase inhibitors, p21cip1 and p27kip1, during wound healing in rats. *Wound Repair Regen, 9*(3), 205-212. https://doi.org/10.1046/j.1524-475x.2001.00205.x

SPANISH SUMMARY

Introducción

El sistema inmune innato es la primera barrera de defensa del organismo frente a infección o daño tisular. Para ello, el sistema inmune innato está compuesto por un gran y diverso número de células entre las que destacan macrófagos y neutrófilos. Estas células, llevan a cabo su función a través de receptores que reconocen patrones moleculares relacionadas con patógenos o con daño tisular. Una de las familias más importantes de receptores de reconocimiento de patrones que se activan en el sistema inmune innato son los que forman inflamasomas, de entre los que caben destacar los receptores NLRP3 y NLRC4. Los inflamasomas son complejos multiproteicos que activan a caspasa-1, por tanto, tras la activación de estos inflamasomas se secretan diferentes citoquinas que son sustratos proteicos de caspasa-1, como la IL-1β o la IL-18, que promueven la reacción inflamatoria. Estas citoquinas inducen la producción de otras citoquinas como el TGF-β que a su vez están implicadas en la regeneración tisular. Por ello, estos inflamasomas están estrechamente relacionados con diferentes enfermedades inducidas en ausencia de infecciones, como enfermedades autoinflamatorias y lesiones tipo tendinopatías.

Objetivos

Los objetivos principales de esta tesis son el estudio de la activación de estos dos inflamasomas tanto en enfermedades autoinflamatorias como en tendinopatía, así como el estudio del efecto terapéutico de la corriente galvánica en la activación de NLRP3. En concreto, los objetivos planteados han sido:

1. Determinar el efecto de las mutaciones de NLRC4 asociadas a la autoinflamación en la estructura de NLRC4.
2. Evaluar la activación del inflammasoma NLRC4 y NLRP3 mediante microscopía de fluorescencia.
3. Caracterizar el efecto de la aplicación de corriente galvánica en la activación del inflamasoma NLRP3 en macrófagos.
4. Estudiar la implicación del inflammasoma NLRP3 en las respuestas de inflamación y regeneración en el tendón de Aquiles de ratones tras la aplicación de electrólisis con aguja percutánea.
5. Dilucidar el papel del inflammasoma NLRP3 en un modelo de ratón de daño tisular estéril.

Materiales y métodos

Durante este proyecto, se llevaron a cabo estudios *in vitro* realizando cultivos celulares de macrófagos silvestres y deficientes en diferentes componentes del inflamasoma. Estos macrófagos se activaron con LPS como primera señal de activación tanto del inflamasoma NLRP3. Tras 2h de incubación con LPS se aplicó corriente galvánica utilizando diferentes protocolos en los que variaban la intensidad, el tiempo, y el número de pulsos aplicados. Tras la activación de estos macrófagos se determinó la liberación de diferentes citoquinas pro-inflamatorias como la IL-6, el TNF-α, la IL-1β o la IL-18, mediante ELISA. También se medió la liberación de LDH como marcador de viabilidad celular y la captación de YoPro-1 como marcador de la permeabilidad de la membrana citoplasmática. Por otro lado, se utilizó microscopía de fluorescencia, así como la técnica BRET para estudiar la oligomerización y conformación, respectivamente, del inflamasoma. En el caso de NLRP3 solo se estudió la oligomerización tras la aplicación de corriente galvánica, y en el caso de NLRC4 se estudió tanto la conformación como la oligomerización de forma basal, sin estímulos previos. Por otro lado, se llevaron a cabo estudios *ex vivo*, utilizando la sangre de pacientes con enfermedades autoinflamatorias para aislar células mononucleares de sangre periférica. Las células mononucleares de sangre periférica se aislaron mediante centrifugación utilizando el reactivo Ficoll. Una vez aisladas, las células se sembraron en placas de 24 pocillos a una concentración de 500.000 células por pocillos, y se estimularon para activar específicamente el inflamasoma NLRP3 con LPS durante 4h y ATP durante 30 minutos, y NLRC4 con LPS durante 2h y el reactivo FlaTox durante 5h. Tras su activación, se recogieron los sobrenadantes y se

centrifugaron, para, posteriormente, medir la liberación de IL-6, TNF-α, IL-1β e IL-18 por ELISA, y la formación de oligómeros de ASC por citometría. También se realizaron estudios *in vivo* utilizando tanto ratones silvestres, como *Nlrp3*$^{-/-}$ y *Pycard*$^{-/-}$ para medir la expresión de diferentes citoquinas pro-inflamatorias. También se midió el tipo, la orientación y la fuerza de las fibras de colágeno mediante tinción con rojo picrosirio, microscopia de segundo armónico y pruebas biomecánicas, respectivamente. Todos estos estudios se realizaron en muestras de tendón de Aquiles tras aplicar electrolisis percutánea o punción seca, utilizando como controles tendones tratados con salino o sin tratar. El protocolo de corriente galvánica utilizado ha sido de 3 pulsos de 3mA durante 3 segundos cada uno. Además, se realizó la medición de la expresión y la producción de IL-1β, IL-18, TNF-α e IL-6 por qPCR y ELISA, así como la cuantificación de células polimorfonucleares en muestras teñidas con hematoxilina-eosina, tras inducir un daño en el tendón tras la aplicación de la enzima colagenasa. Para ello, se inyectaron por vía subcutánea 20 µl de colagenasa con una concentración de 10 µg/µl. Tras la aplicación de colagenasa se aplicó corriente galvánica o punción seca para comprobar el efecto de ambos tratamientos en el tendón dañado. El protocolo de corriente galvánica utilizado ha sido de 3 pulsos de 3mA durante 3 segundos cada uno.

Resultados

Como resultados se ha obtenido que la corriente galvánica induce la distribución de NLRP3 en un punteado celular, así como ocurre con las mutaciones de NLRC4 asociadas a síndromes autoinflamatorios, cuando ambas se analizan en sistemas recombinantes de expresión. Este aumento de la distribución punteada de NLRC4 en las células se acompaña en algunas mutaciones con un acusado descenso en la señal BRET de NLRC4, siendo p.Ser445Pro y p.His443Pro las mutaciones que más disminuyen la señal BRET de NLRC4. Por otro lado, se estudió la muestra de sangre de una paciente portadora de la mutación p.Ser171Phe en NLRC4, que mostró un aumento en la formación de oligómeros de ASC en los monocitos, así como en la liberación de IL-18, pero no de IL-1β, en condiciones basales o tras el tratamiento con LPS. Esta diferencia entre ambas citoquinas se debe a la falta de inducción de la expresión de *Il1b* con LPS en comparación con *Il18*, que sí que se indujo en las células de esta paciente. La aplicación de corriente galvánica en macrófagos fue capaz de reforzar el fenotipo M1, ya que se observó un aumento en la expresión de los genes pro-inflamatorios al inducir un fenotipo pro-M1 tratando estos macrófagos con LPS durante 2h, así como una reducción de la expresión de genes pro-regenerativos al inducir un fenotipo pro-M2 tratando estos macrófagos con IL-2 durante 4h. Además, se observó que la corriente galvánica activaba de forma específica el inflamasoma NLRP3, promoviendo la liberación de IL-1β e IL-18. La liberación de estas dos citoquinas se observó que era completamente dependiente del inflamasoma NLRP3. Este resultado, se pudo verificar al utilizar un inhibidor específico de este inflamasoma, como fue el MCC950, y un tampón rico en potasio, para inhibir el descenso del potasio intracelular que ocurre al activar específicamente NLRP3, ya que en ambas condiciones no se observó una liberación ni de IL-1β ni de IL-18. Además, al utilizar diferentes protocolos de corriente galvánica se observó que tanto la liberación de IL-1β y de IL-18, como la liberación de LDH, eran dependientes tanto de la intensidad, como del tiempo y del número de pulsos utilizados en el protocolo de activación de corriente galvánica. Por lo que se observó, que las condiciones del protocolo de corriente galvánica pueden ser modificadas para modular la liberación de IL-1β y la muerte celular, siendo más agresivos los protocolos con mayor tiempo y número de pulsos, sin que se relacionen directamente con la producción de IL-1β. Por último, los resultados *in vivo* en tendón de Aquiles de ratón, mostraron que la aplicación de corriente galvánica resultó en un aumento de la expresión de genes que codifican para

diferentes citoquinas proinflamatorias, sin aumentar de forma significativa la expresión de los genes que codifican los diferentes miembros del inflamasoma NLRP3. También se observó un aumento en el porcentaje de colágeno tipo I en comparación con el colágeno tipo III, en las muestras teñidas con rojo picrosirio. Así como, tanto una mejor orientación de las fibras de colágeno como un aumento de la rigidez del tendón y por ello, una mayor resistencia de los tendones tratados con electrolisis percutánea en comparación con los tratados con punción seca. Cabe destacar, que esta mejora en la resistencia del tendón se observó que era dependiente del inflamasoma NLRP3 ya que en los tendones de ratones *Nlrp3*$^{-/-}$ tratados con electrolisis percutánea no presentaban un aumento en los parámetros comentados previamente. Además, tras la inducción de un daño en el tendón tras tratarlos con colagenasa, se observó un aumento tanto en la expresión del ARN mensajero como en la producción, de las proteínas inflamatorias IL-1β, IL-18, IL-6, TNF-α, y CXCL-10, y que este efecto era parcialmente dependiente del inflamasoma NLRP3. Por último, se observó que la aplicación de electrolisis percutánea no promovía cambios en la expresión de los diferentes genes que codifican citoquinas pro-inflamatorioas a estudio.

Discusión

Los resultados obtenidos en los estudios tanto *in vitro* como *ex vivo* de la activación de NLRC4 desarrollados en esta Tesis apoyan claramente un comportamiento de ganancia de función de la variante p.Ser171Phe de manera similar a otras variantes de NLRC4 previamente reportadas como mutaciones causantes de enfermedades. Además, la paciente a estudio representa el primer caso de enfermedad autoinflamatoria de inicio tardío asociada a NLRC4 como consecuencia de un mosaicismo somático de NLRC4, lo que plantea la cuestión de si las manifestaciones inflamatorias que comienzan durante la edad adulta en otros pacientes pueden ser consecuencia de un defecto genético similar. En conjunto, estos resultados indican que los dominios NBD y WHD, y los últimos aminoácidos del dominio LRR son críticos para la correcta conformación basal inactiva de NLRC4, y las mutaciones que afectan a los aminoácidos contenidos en estos dominios pueden inducir un cambio en la conformación de NLRC4, dando lugar a una estructura autoactiva de NLRC4. En particular, las mutaciones que afectan al dominio NBD pueden desestabilizar la interacción de la proteína con el nucleótido ADP o ATP, las mutaciones que afectan al dominio WHD pueden desestabilizar las interacciones WHD-NBD y las mutaciones que afectan a los últimos aminoácidos del dominio LRR pueden funcionar permitiendo la apertura de la NLRC4 autoinhibida mediante la desestabilización de las interacciones LRR-NBD e induciendo la formación del oligómero NLRC4 al facilitar el reconocimiento y la unión de diferentes monómeros de NLRC4 a través de las interacciones LRR-LRR. Además, encontramos que la distribución de los puntos de NLRC4 también puede correlacionarse con la activación del inflamasoma en el sistema recombinante HEK293T. Este sistema también fue útil para determinar la activación de NLRP3 de tipo salvaje cuando se aplicó corriente galvánica. Por otro lado, a partir de los resultados obtenidos en los estudios *in vitro*, podemos concluir que la aplicación de corriente galvánica activa el inflamasoma NLRP3 e induce una respuesta inflamatoria controlada. Sin embargo, las dosis de alta intensidad de corriente galvánica durante largos periodos de tiempo o los impactos repetidos, que suponen una alta carga total, podrían inducir una alta necrosis tisular, por lo que no se recomiendan para la práctica clínica. Además, tras los estudios *in vivo* utilizando electrolisis percutánea en esta Tesis se ha aportado información sobre cómo la corriente galvánica es una técnica factible aplicada *in vivo* para activar el inflamasoma NLRP3 e inducir una respuesta inflamatoria local para potenciar un proceso de regeneración mediado por colágeno en el tendón, estableciendo el mecanismo molecular de la electrólisis percutánea para

el tratamiento de lesiones crónicas y estableciendo el primer tratamiento dirigido a activar el NLRP3. Por último, los estudios *in vivo* realizados tras la aplicación de colagenasa tanto como tratamiento único como con varios protocolos de dosificación, no indujo cambios en los parámetros estudiados. Estos resultados podrían explicarse con tres posibles teorías: (i) la electrólisis percutánea con aguja no es capaz de interferir en la inflamación de los tendones de Aquiles lesionados de forma crónica, (ii) el modelo de daño inducido por colagenasa no es un buen modelo para inducir el daño crónico del tendón, o (iii) los puntos de tiempo seleccionados o el número de tratamientos aplicados no fueron los óptimos para observar diferencias en los parámetros estudiados. Se necesitan más estudios para validar el valor terapéutico de la electrólisis de aguja percutánea en los tendones lesionados, que podría incluir el desarrollo de tendinopatías fisiológicas en ratones, como por ejemplo al inducir un ejercicio excesivo de las articulaciones.

Conclusiones

A partir de los resultados obtenidos, se han establecidos las siguientes conclusiones:

1. Las mutaciones que afectan al dominio WHD de NLRC4 inducen cambios significativos en la conformación de NLRC4.
2. Diferentes mutantes de NLRC4 descritas en pacientes con síndromes autoinflamatorios inducen una distribución punteada de NLRC4 en las células.
3. La variante p.Ser171Phe de NLRC4 presenta un comportamiento de ganancia de función en el ensamblaje de este inflamasoma.
4. La variante p.Ser171Phe NLRC4 postcigótica es una causa plausible de la enfermedad autoinflamatoria en la paciente estudiada.
5. La aplicación de corriente galvánica en células HEK293T que expresan NLRP3 da lugar a una distribución punteada de NLRP3 en las células.
6. La corriente galvánica aplicada en macrófagos tratados con LPS es capaz de activar el inflamasoma NLRP3.
7. La corriente galvánica aplicada en macrófagos tratados con LPS induce la liberación de las citoquinas IL-1β e IL-18.
8. La corriente galvánica aplicada en macrófagos tratados con LPS no induce la muerte celular por piroptosis.
9. El aumento del tiempo y del número de pulsos en la corriente galvánica aplicada en macrófagos tratados con LPS se relaciona con un aumento de la liberación de IL-1β y también de la muerte celular dependiente de la corriente.
10. La electrólisis percutánea aplicada en el tendón de Aquiles de ratones induce un aumento del colágeno tipo I y de la rigidez del tendón, mejorando su resistencia.
11. La resistencia del tendón tras la electrólisis percutánea es dependiente del inflammasoma NLRP3.
12. La administración de colagenasa en el tendón de Aquiles de ratón induce un daño tisular estéril y una respuesta inflamatoria parcialmente dependiente de NLRP3.
13. El daño inducido por la colagenasa en el tendón de Aquiles de ratón no se ve afectado por la aplicación de electrólisis percutánea utilizando 3 impactos de 3 mA durante 3 segundos.

PUBLICATIONS RESULTING FROM THIS THESIS

1. Published

1. Angosto-Bazarra, D., Molina-Lopez, C., **Penin-Franch, A**., Hurtado-Navarro, L. & Pelegrin, P. (2021, Mar 18). Techniques to Study Inflammasome Activation and Inhibition by Small Molecules. Molecules, *26*(6). doi: 10.3390/molecules26061704. Review.
2. Ionescu, D.*, **Penin-Franch, A**.*, Mensa-Vilaro, A., Castillo, P., Hurtado-Navarro, L., Molina-Lopez, C., Romero-Chala, S., Plaza, S., Fabregat, V., Bujan, S., Marques, J., Casals, F., Yague, J., Oliva, B., Fernandez-Pereira, L. M., Pelegrin, P. & Arostegui, J. I. (2022, Apr). First Description of Late-Onset Autoinflammatory Disease Due to Somatic NLRC4 Mosaicism. Arthritis Rheumatol, *74*(4), 692-699. doi: 10.1002/art.41999. (*Share first autorship).
3. **Penin-Franch, A**., García-Vidal J.A., Martínez, C.M., Escolar-Reina, P., Martínez-Ojeda, R.M., Gómez, A.I., Bueno, J.M., Minaya-Muñoz, F., Valera-Garrido, F., Medina-Mirapeix, F. & Pelegrín, P. (2022, Feb). Galvanic current activates the NLRP3 inflammasome to promote type I collagen production in tendon. Elife *24*(11), e73675. doi: 10.7554/eLife.73675.
4. García-Villalba, J., Hurtado-Navarro, L., **Penin-Franch, A.**, Molina-López, C., Martínez-Alarcón, L., Angosto-Bazarra, D., Baroja-Mazo, A. & Pelegrín, P. (2022, May). Soluble P2X7 receptor is elevated in the plasma of COVID-19 patients and correlates with disease severity. Front Immunol *18*(13), 894470. Doi: 10.3389/fimmu.2022.894470.

2. Under review

1. Martín-Sánchez, F., Compan, V., Tapia-Abellán, A., **Penín-Franch, A**., Gómez-Sánchez, A.I., Baños, M.C., Schmidt, F.I. & Pelegrín, P. ASC oligomer favor caspase-1CARD domain recruitment after intracelluar potassium efflux. Under review in Journal of Cell Biology.
2. Baroja-Mazo, A., **Penín-Franch, A**., Lucas-Ruiz, F., de Torre-Minguela, C., Alarcón-Vila, C., Hernández-Caselles, T. & Pelegrín, P. P2X7 receptor activation impairs antitumor activity of natural killer cells. Under review in British Journal of Pharmacology.

3. Under preparation

1. **Penín-Franch, A**., Hurtado-Navarro, L., Arostegui, J.I. & Pelegrín, P. Characterization of pathogenicity of p.Ser445Pro NLRC4 variant leading to early-onset recurrent panniculitis (under preparation).
2. **Penín-Franch, A**., Tapia-Abellán, A., Arostegui, J.I. & Pelegrín, P. NLRC4 mutations associated to autoinflammatory syndromes results in different structural conformations and inflammasome activation (under preparation).
3. **Peñín-Franch, A**., Pelegrín, P. NLRP3 inflammasome drives inflammation and regeneration in sterile tissue damage (under preparation).